

**ECOLOGY, PHENOLOGY, AND PRESERVATION OF  
RECENT DINOFLAGELLATES CYST FROM THE  
NORTHWEST AFRICAN UPWELLING REGION**

Dissertation to obtain the degree of

*Doctor rerum naturalium*

**(Dr. rer. nat.)**

Submitted to the Department of Geosciences  
University of Bremen

**Surya Eldo Virma Roza**

November 2024



*“The present is the key to the past”*

**Charles Lyell, 1830**

**Reviewers:**

**Prof. Dr. Karin Zonneveld**

MARUM – Center for Marine Environmental Sciences

Department of Geosciences, University of Bremen

Bremen, Germany

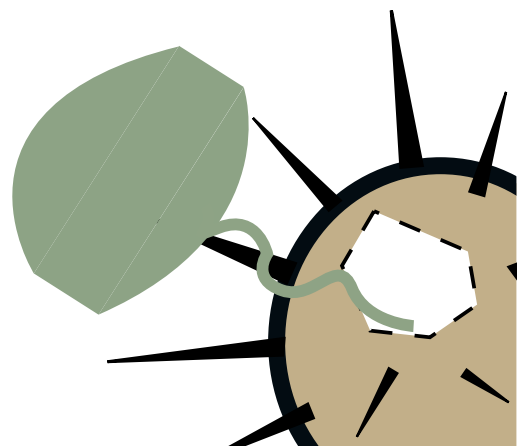
**Asst. Prof. Dr. Ana Amorim**

MARE – Marine and Environmental Sciences Centre

Faculty of Sciences, University of Lisbon

Lisbon, Portugal

**Date of Colloquium:** 6 November 2024





## *Affirmation in lieu of an oath*

*according to § 5 (5) of the Doctoral Degree Rules and Regulations of 28 April, 2022*

I, Surya Eldo Virma Roza, address: [REDACTED] student number:  
[REDACTED]

With my signature, I affirm in lieu of an oath that I prepared the submitted dissertation independently and without illicit assistance from third parties, that I appropriately referenced any text or content from other sources, that I used only literature and resources listed in the dissertation, and that the electronic (PDF) and printed versions of the dissertation are identical.

I affirm in lieu of an oath that the information provided herein to the best of my knowledge is true and complete.

I am aware that a false affidavit is a criminal offence which is punishable by law in accordance with § 156 of the German Criminal Codes (StGB) with up to three years of imprisonment or a fine in case of intention, or in accordance with § 161 of the German Criminal Codes (StGB) with up to one years of imprisonment or a fine in case of negligence.

---

Place, Date

---

Signature



## Acknowledgments

First of all, I would like to thank my Supervisor, Prof. Dr. Karin Zonneveld, who has taught me much knowledge related to my doctoral project and also trained me in many other skills, such as research cruise work, laboratory work, presenting in a scientific meeting, and writing research articles. For almost four years, she guided me to execute three projects successfully and yet gave me some freedom to develop my knowledge and skills outside of the initial plan.

I also want to thank the current and former members of the marine palynology group. Our technician, Nicole Kniebel, has invested her time training me in the laboratory and helping me extract and prepare the samples for my analyses. My gratitude to Dr. Gerard Versteegh and Dr. Iria García-Moreiras, who helped me curate and interpret the data and always spared their time to discuss some difficulties that I dealt with during my doctoral program. To my former fellow PhDs, Katell Alaime and Runa Reuter, with whom I could discuss some things related to work or simply for fun. I wish you succeed in your current or future position. I also would like to show my gratitude to the rest of my project committee (Dr. Karl-Heinz Baumann, Prof. Dr. Gesine Mollenhauer, and Dr. Marina Rillo) and my co-authors (Dr. Vera Pospelova, Prof. Dr. Jan-Berend Stuut, and Dr. Hendrik Wolschke) for their guidance, insight, and support in improving the quality of my doctoral projects.

I express my gratitude to MARUM - Center for Marine Environmental Sciences, the Cluster of Excellence program, Bremen International Graduate School for Marine Sciences (GLOMAR), the Micropaleontology group at MARUM, and the University of Bremen for the resources and support that have allowed me and my team to produce high-quality work in the past four years. I am also grateful for the support that I occasionally received from the International community of dinoflagellate cyst researchers.

I would not be able to handle the pressure during my doctoral program without the intellectual and psychological support of my friends. I thank, Manfred and Selfi, the two persons who are always there during my bright and dark times, despite the great distance between us. I feel incredibly grateful to my friends here in Bremen (Karla, Luis, Lisa, Hana, and many others) for their willingness to hear my joyful, depressing, or upsetting stories. I hope all of you excel in anything that you do or will face in the future.

Finally, I thank my big family for their mental support and belief in my talent and principality. I wish a healthy and joyful life for my parents (Des Enita and Syarifuddin), my numerous siblings (Dilla, Fera, Sony, Hafiv, Lovi, Dio, Dea, and Wandu), my baby nephew (Kleon), and my relatives. Last but not least, I want to dedicate this dissertation to my late grandmother (Anidar Djalil), who, with her wisdom and wit, has taught me to be the person I am until this very day.

## Table of contents

<b>Summary</b> .....	<b>i</b>
<b>Zusammenfassung</b> .....	<b>iv</b>
<b>Ikhtisar</b> .....	<b>vii</b>
<b>Chapter 1 - General Introduction</b> .....	<b>1</b>
1.1. Scientific background .....	1
1.2. Dinoflagellates .....	2
1.3. Northwest African upwelling .....	4
1.4. Aim of the projects.....	5
1.5. Dissertation outline .....	6
<b>Chapter 2 - Methodology</b> .....	<b>9</b>
2.1. Sampling instruments.....	9
2.2. Dinoflagellate cysts extraction, preparation, and identification.....	10
2.3. Environmental factors .....	11
2.4. Multivariate analyses .....	12
2.5. Time series analyses .....	12
2.6. Age model.....	13
<b>Chapter 3 - Environmental control of interannual and seasonal variability in dinoflagellate cyst export flux over 18 years in the Cape Blanc upwelling region (Mauritania)</b> .....	<b>14</b>
Abstract .....	14
3.1. Introduction .....	14
3.2. Materials and Methods .....	16
3.2.1. Oceanography of the study area .....	16
3.2.2. Mooring site and sample treatment .....	17
3.2.3. Dinoflagellate cysts extraction and taxonomic identification .....	18
3.2.4. Environmental parameters.....	18
3.2.5. Statistical analyses.....	20
3.3. Results .....	21
3.3.1. Dinoflagellate cyst flux .....	21
3.3.2. Association of dinoflagellates cysts .....	22
3.3.3. Multivariate analyses.....	23
3.4. Discussion .....	25
3.4.1. Physical condition of the upper water column .....	25
3.4.2. Dinoflagellate cyst export fluxes.....	25
3.4.3. Dinoflagellate cyst groups according to environmental parameters .....	27
3.4.4. Long-term variations in the cyst association .....	34



3.4.5. Cysts of potentially toxic dinoflagellates .....	35
3.5. Conclusions .....	36
3.6. Acknowledgments .....	37
3.7. Data availability statement .....	37
<b>Chapter 4 - Northwest African upwelling ecosystem response to recent climate change reflected by dinoflagellate cyst export production .....</b>	<b>38</b>
Abstract .....	38
4.1. Introduction .....	38
4.2. Methods .....	40
4.2.1. Study site and sampling.....	40
4.2.2. Dinocysts extraction and determination .....	41
4.2.3. Environmental factors time series .....	41
4.2.4. Wavelet time series analysis.....	43
4.3. Results .....	43
4.3.1. Wavelet analysis of the dinocysts .....	43
4.3.2. Wavelet analysis of environmental factors.....	44
4.4. Discussion .....	45
4.4.1. Annual cycle in the time series.....	45
4.4.2. Half-year cycle and other periodicities in the time series .....	47
4.4.3. Ecosystem changes.....	48
4.5. Conclusions .....	49
4.6. Acknowledgments .....	49
4.7. Supplementary materials .....	49
<b>Chapter 5 - How is the export production of dinoflagellate cysts on the ocean surface stored in the sediment? .....</b>	<b>57</b>
Abstract .....	57
5.1. Introduction .....	58
5.2. Oceanography.....	59
5.3. Materials and methods.....	60
5.3.1. Sampling procedures .....	60
5.3.2. Palynological procedures and cysts identification.....	62
5.3.3. Age model and accumulation rates .....	64
5.3.4. Statistics .....	64
5.4. Results .....	64
5.4.1. Dinoflagellate cyst accumulation rates in the sediment trap and down-core .....	64
5.4.2. Dinoflagellate cyst association in the sediment trap and down-core.....	65
5.4.3. Multivariate analyses.....	67
5.5. Discussion .....	69
5.5.1. Production and preservation signals of dinocyst fossils.....	69

5.5.2. Implications for paleoenvironmental studies.....	71
5.6. Conclusions .....	72
5.7. Acknowledgments .....	72
5.8. Supplementary materials .....	73
<b>Chapter 6 - Final remarks .....</b>	<b>75</b>
6.1. Overall conclusions .....	75
6.2. Implication for future research .....	76
<b>References .....</b>	<b>78</b>
<b>Appendix .....</b>	<b>95</b>

## Summary

Marine phytoplankton play a crucial role in ocean and climate sustainability. They are responsible for fixing one-third of atmospheric carbon dioxide and turning it into biomass. Through a biological pump, a fraction of the greenhouse carbon is sequestered in the ocean sediment, while some of the carbon is released back into the atmosphere via respiration. Along with diatoms and coccolithophores, phototrophic dinoflagellates are one of the main eukaryotic phytoplankton in marine ecosystems. This plankton group is highly diverse, distributed worldwide, influenced by certain physical and chemical factors (e.g., nutrients, light, temperature, currents, and salinity), and responds to changes in those limiting factors. In addition, around 15% of dinoflagellates undergo a resting stage during their sexual reproduction cycle, forming a distinctive structure known as dinoflagellate cysts (dinocysts). Many dinocysts are made of resistant organic walls that are highly preservable in the sediment. All of these dinoflagellate aspects make them a valuable proxy for not only ecological, oceanography, and climate studies but also for reconstructing the conditions and changes in past marine ecosystems.

The current fast-changing climate is expected to drive shifts in the atmospheric-oceanic interactions, which influence the bloom dynamics of dinoflagellates and the formation of their cysts. Thus, a multi-year record of in-situ dinocysts and prominent limiting factors are required to create the reconstruction. Unfortunately, such data are scarce, and the available ones cover a short period of time series. In this dissertation, we provide an 18-year time series of organic-walled dinocysts collected by a sediment trap that has been deployed in one of the four eastern boundary upwelling ecosystems (EBUEs) located on the Northwest African coast. The coastal upwelling brings nutrient-rich subsurface waters to nourish the primary producers, such as dinoflagellate, that inhabit the photic zone. The upwelling occurred throughout the year under a seasonal trend controlled by the Inter Tropical Convergence Zone (ITCZ) annual migration. The nutrient-rich waters could reach hundreds of kilometers towards the open ocean in the form of filaments and eddies due to surface water currents in the study area. In addition, Sahara dust increases productivity in this area by providing limiting nutrients and trace elements. The aerosol dust supplies sediment materials, where microfossils could be preserved. The accumulation of the sediments is relatively high, and no hiatus during the Holocene was reported in the area of trap deployment. Consequently, the sediment archive recorded a continuous history of the ocean production in a high time resolution, allowing a comparison of sediment trap dinocysts with the down-core fossils.

To understand the response of dinocyst production to the interannual dynamics in their ecosystem, the dinocyst export flux over 18 years was compared with several environmental parameters such as upwelling wind strength and direction, Saharan dust input, sea surface temperature (SST), sea surface temperature anomaly (SSTa), and sea surface chlorophyll-*a* (Chl*a*) (**Chapter 3**). The results revealed that heterotrophic dinoflagellates contributed to a significant portion of the dinocysts association (ca.94%). Their export flux was usually higher in spring - summer, coinciding with the strongest upwelling wind that blew from the northeast. A few peaks of the high export flux of this dinocysts group in winters of some years aligned with high dust input into the sediment trap area. Stronger inter-annual variability of the export flux was shown by the photo-/mixotrophic dinocysts when their annual highest flux occurred in autumn - winter. Furthermore, Canonical Correspondence Analysis (CCA) confirmed that the upwelling indicator (wind strength and direction) was the most influential parameter, and the SST was the least significant. According to this ordination technique, five dinocyst groups were identified in relation to the environmental parameters. Dinocysts taxa in group 1 (*Echinidinium delicatum/granulatum*, *Echinidinium* spp., *E. transparentum/zonneveldiae*, *Trinovantedinium* spp., and *Protoperidinium latidorsale*) thrived under maximal upwelling intensity. Group 2 (*Archaeoperidinium* spp., *P. americanum*, *P. stellatum*, and *P. subinermis*) consists of taxa favoured by maximal upwelling and dust input. Group 3 (*Gymnodinium* spp. and *L. polyedra*) preferred the upwelling relaxation phase. Dinocyst taxa in group 4 (*Bitectatodinium spongium* and *Protoceratium reticulatum*) occurred when the upper water column was warmer. Lastly, taxa in group 5 (*Brigantedi-*

*nium* spp., *E. aculeatum*, *Impagidinium aculeatum*, *P. conicum*, *P. monospinum*, *Pentaparsodinium dalei*, and *Spiniferites* spp.) did not show a specified correlation to any environmental parameters. In 2009, the dinocyst association shifted from the abundance of various taxa to the abundance of *Echinidinium*, which coincided with the intensification of the dust input. Regarding cysts of potentially toxic dinoflagellates, the sediment trap collected five photo-/mixotrophic taxa of dinocysts affiliated with biotoxin-producing species that threaten the marine ecosystem and human health. Their export flux is low due to the highly mixed water column, which is unfavourable for photo-/mixotrophic dinoflagellates.

To extend our knowledge about the bloom dynamics of the dinocysts and the taxa in the same ecological group that was determined in the previous project, the dinocysts and environmental parameter time series were analysed using Morlet wavelet analysis (**Chapter 4**). This technique allows the visualisation of the periodic or cyclic patterns and their variation throughout the time series by examining the correlation between the wave patterns of the datasets with the Morlet wavelet. Based on the wave spectra representing a high correlation, the total dinocysts time series contained four periodicities: 240-day, 480-day, 180-day interpreted as the half-year cycle, and 360-day interpreted as the annual cycle. The half-year and annual cycles of the total dinocyst export flux coincided with the same cycles in the wind speed, wind direction, aerosol dust time series, and SSTa. The dinocyst winter peak (December - February) aligned with the dust winter peak, whilst the dinocyst spring/summer peak (April - June) aligned with primary upwelling and dust summer peak. The SST wavelet spectra only indicated the annual cycle, but it did not align with months when the annual cycle of the dinocyst was observed. The cycle of total dinocysts indicated variation in three phases, which is in line with changes in the taxa composition. Phase I (2003 - 2008) was indicated by the low significance of 240-day and 480-day periodicities when the dinocyst taxa of maximal upwelling and dust and upwelling relaxation group were abundant. Phase 2 (2009 - 2012) is characterised by the half-year and annual cycles as the product of maximal upwelling group cycles. Phase 3 (2013 -2020) showed the stronger significance of the half-year and annual cycles that were also observed in the upwelling group, plus a slight contribution by the cosmopolite/no relation and upwelling and dust groups. The three phases coincided with the changes in the cycles of the aerosol dust and upwelling wind time series. The results suggested that the stepwise changes in the environments were driven by the southward movement of the ITCZ position that could strengthen the upwelling and dust emission during the time span of our investigation. The dinocyst cycles and taxa composition changes supported this interpretation, indicating that climatic-driven changes in the environment influenced the bloom dynamics and community structure of dinoflagellates.

The information gathered from the sediment trap data in the previous two projects was expected to be preserved in the sediment (paleoarchive), following the long-known hypothesis of uniformitarianism. This theory has allowed microfossils, including dinocysts, to be utilised as past environmental and climatic change proxies. However, some perturbations are known to disrupt the water column signal carried by microfossils in the marine sediment. Therefore, we compared the sediment trap data with sediment core data under the same time span and resolution (**Chapter 5**). The age of every core sample was determined with  $^{210}\text{Pb}$  (lead) half-time decay, which the result stated 1.6 years per 3.1 mm of sediment. After matching the time span and resolution between the trap samples and core samples, the comparison results showed that the dinocyst association in the core resembles a coastal upwelling environment dominated by brown dinocysts mostly affiliated with heterotrophic taxa. The most abundant dinocyst taxa in the sediment trap (e.g., *Archaeperidinium* spp., *Brigantedinium* spp., *Gymnodinium* spp., *P. americanum*, *L. polyedra*, and *Echinidinium* species) are all presented in the core samples. The dinocyst accumulation rates between trap and core samples are comparable; the heterotrophic group ranged in the scale of  $10^6$ , and the photo-/mixotrophic group ranged in the scale of  $10^5$ . However, the relative contribution and accumulation rates of the heterotrophic dinocysts were lower in the core samples, which is the opposite of the photo-/mixotrophic dinocysts. The susceptibility of the brown (coloured) cysts that are mostly produced by the heterotrophic dinoflagellates is suggested to cause the declining rate and contribution of this group in the core samples. In contrast, some

---

heterotrophic taxa (e.g., *P. conica*, *P. monospinum*, and *P. stellatum*) showed an increase in concentration and percentages, indicating foreign materials that were brought to the location of the core. Principal Component analysis (PCA) was applied to the trap samples and core samples, dissecting the trap samples into three groups and the core samples into four groups. The PCA groups of trap samples marked the dinocyst association shift in 2009 to *Echinidinium* abundance (maximal upwelling group) reported in the two previous projects. This shift was detected in the core samples under the same time frame. In addition, the four groups of core samples not only confirmed the association shift but also showed that the four upper samples contained significantly different compositions. These samples are suspected to be the result of a stronger impact of pre and post-depositional processes, such as bioturbation, compaction bias, resuspension, lateral transport, and aerobic microbial degradation.

The knowledge derived from these three projects has enriched our knowledge about the driving factors of dinocyst production, their relation to environmental changes, and the post-depositional processes that potentially disturb the primary signal of preserved dinocysts. Some crucial points, such as inter-annual variability in dinocysts production, a significant shift in the dinocysts association, and how they were influenced by the changing environment and climate, were only made possible due to the availability of 18-year sediment trap series. The high-resolution comparison study between dinocysts produced from the water column with the embedded ones was the first investigation done, aiming to confirm the role of dinocysts as a reliable tool for reconstructing the condition and changes in the past environment and climate.

## Zusammenfassung

Marines Phytoplankton spielt eine wesentliche Rolle für die Nachhaltigkeit von Ozean und Klima. Es ist verantwortlich für die Bindung eines Drittels des Kohlenstoffdioxids in der Atmosphäre und wandelt dieses in Biomasse um. Durch die biologische Pumpe wird ein Teil des Kohlenstoffs in marinen Sedimenten gebunden, während ein anderer Teil durch Atmung zurück in die Atmosphäre entlassen wird. Neben Diatomeen und Coccolithophoriden sind phototrophische Dinoflagellate eine der Hauptgruppen des eukaryotischen Phytoplanktons im marinen Ökosystem. Diese Planktongruppe ist höchst divers, weltweit verbreitet, wird beeinflusst von bestimmten physischen und chemischen Faktoren (z.B. Nährstoffe, Licht, Temperatur, Strömungen und Salinität) und reagiert auf Änderungen dieser limitierenden Faktoren. Hinzukommt, dass 15% aller Dinoflagellate ein Ruhestadium während ihres sexuellen Reproduktionszyklus durchlaufen, in dem sie ein markantes Gebilde formen bekannt als Dinoflagellatenzysten (Dinozysten). Viele Dinozysten sind aus resistenten organischen Wänden aufgebaut, welche sich im Sediment sehr gut erhalten. All diese Aspekte machen Dinoflagellate zu einem wertvollen Anzeiger für nicht nur ökologische, ozeanographische und klimatische Studien, sondern auch für die Rekonstruktion von Umweltbedingungen und Änderungen in ehemaligen marinen Ökosystemen.

Es wird erwartet, dass das aktuell sich schnell ändernde Klima Verschiebungen in die atmosphärisch-ozeanischen Interaktionen bringt, was wiederum die Dynamik von Planktonblüten der Dinoflagellaten und die Bildung von Zysten beeinflussen. Folglich ist ein mehrjähriger Datensatz von in-situ Dinozysten und den wichtigsten limitierenden Faktoren notwendig, um eine Rekonstruktion zu erstellen. Unglücklicherweise ist ein solcher Datensatz selten und die, die vorhanden sind, decken nur einen kurzen Zeitraum ab. In dieser Dissertation präsentieren wir eine 18-jährige Zeitreihe von organisch-wandigen Dinozysten, die von einer Sedimentfalle gesammelt wurden, die in einem der vier östlichen "Eastern Boundary Upwelling Ecosystem" (EBUEs) stationiert ist, welche vor der nordwestafrikanischen Küste gelegen ist. Der litorale Auftrieb bringt nährstoffreiche tiefere Wässer mit sich, welche Primärproduzenten wie Dinoflagellate ernähren, die die photische Zone bewohnen. Der Auftrieb tritt während des ganzen Jahres auf, beeinflusst durch einen jahreszeitlichen Trend, der jährlichen Migration der "Inter Tropical Convergence Zone" (ITCZ). Die nährstoffreichen Wässer können bis zu hunderten Kilometern in den offenen Ozean reichen, in Form von Filamenten und Wirbeln, infolge von Oberflächenströmungen im Studiengebiet. Zusätzlich erhöht Saharastaub durch das Bereitstellen von limitierenden Nährstoffen und Spurenelementen die Produktivität in diesem Gebiet. Der Aerosol Staub liefert Sedimentmaterial, in dem Mikrofossilien erhalten werden können. Die Akkumulation von Sediment ist relativ hoch und außerdem wurde kein Hiatus innerhalb des Holozäns dokumentiert. Folglich stellt das Sediment Archiv eine kontinuierliche Aufzeichnung der Ozean Produktion mit einer hohen Auflösung dar, was einen Vergleich der Dinozysten der Sedimentfalle mit den Fossilien der Kernproben erlauben.

Um die Reaktion der Dinozysten Bildung in Bezug auf die jährlichen Dynamiken ihres Ökosystems zu verstehen, wurde der Dinozysten Export-Flux über 18 Jahre mit verschiedenen Umweltparametern wie Auftrieb Windstärke und Windrichtung, Sahara Staub Eintrag, Meeresoberflächentemperaturen (SST), Meeresoberflächentemperatur Anomalien (SSTa) und Chlorophyll- *a* der Meeresoberfläche (Chl*a*) verglichen (**Kapitel 3**). Die Ergebnisse enthüllen, dass heterotrophische Dinoflagellate zu einem signifikanten Teil zur Dinozysten Vergesellschaftung beisteuern (ca. 94%). Ihr Export-Flux war normalerweise im Frühling/Sommer höher, übereinstimmend mit dem stärksten Auftrieb Wind aus Nordost. Ein paar Höhepunkte des hohen Export-Flux dieser Dinozysten Gruppe im Winter einiger Jahre stimmt mit dem hohen Staub Eintrag im Gebiet der Sedimentfalle überein. Eine starke zwischenjährliche Variabilität des Export-Flux zeigen photo-/mixotrophische Dinozysten, wenn ihr jährlicher höchster Flux im Herbst/Winter auftaucht. Des Weiteren bestätigt die "Canonical Correspondence Analysis" (CCA), dass der Auftriebsindikator (Windstärke und -richtung) der einflussreichste Parameter ist und

der SST der geringste. Nach dieser Anordnungsmethode werden fünf Dinozysten Gruppen in Bezug auf die Umweltparameter identifiziert. Dinozistentaxa der Gruppe 1 (*Echinidinium delicatum/granulatum*, *Echinidinium* spp., *E. transparentum/zonneveldiae*, *Trinovantedinium* spp., and *Protooperidinium latidorsale*) gedeihen unter maximaler Intensität des Auftriebs. Gruppe 2 (*Archaeperidinium* spp., *P. americanum*, *P. stellatum*, and *P. subinermis*) setzt sich aus Taxa zusammen, die vom maximalen Auftrieb und Staub Eintrag begünstigt werden. Gruppe 3 (*Gymnodinium* spp. and *L. polyedra*) bevorzugt die nachlassende Auftriebsphase. Dinozistentaxa der Gruppe 4 (*Bitectatodinium spongium* and *Protoceratium reticulatum*) treten bei wärmerer oberer Wassersäule auf. Taxa der Gruppe 5 (*Brigantedinium* spp., *E. aculeatum*, *Impagidinium aculeatum*, *P. conicum*, *P. monospinum*, *Pentapharsodinium dalei*, and *Spiniferites* spp.) zeigen keine spezifische Korrelation zu irgendeinem Umweltparameter. Im Jahr 2009 verschob sich die Dinozysten Vergesellschaftung von der Dominanz verschiedener Taxa hin zur Dominanz von *Echinidinium*, was mit der Verstärkung des Staub Eintrags einhergeht. Bezüglich Zysten potentiell toxischer Dinoflagellate sammelte die Sedimentfalle fünf photo-/mixotrophische Taxa an Dinozysten, die mit Biotoxin produzierenden Arten in Verbindung gebracht werden, die eine Gefahr für das marine Ökosystem und die menschliche Gesundheit darstellen. Ihr Export-Flux ist gering wegen der stark gemischten Wassersäule, die unvorteilhaft für photo-/mixotrophische Dinoflagellate ist.

Um unser Wissen über die Dynamik von Planktonblüten der Dinozysten und der Taxa der gleichen ökologischen Gruppe, die im vorherigen Projekt bestimmt wurden, zu erweitern, wurde die Zeitreihe der Dinozysten und Umweltparameter im Rahmen einer „Morlet wavelet analysis“ analysiert (**Kapitel 4**). Diese Technik erlaubt die Darstellung von periodischen und zyklischen Mustern und ihre Änderung durch die Zeitreihe unter der Betrachtung der Korrelation zwischen den Wellenmustern des Datensatzes mit den Morlet Wavelets. Basierend auf dem warmen Spektrum, welches eine hohe Korrelation darstellt, enthält die gesamte Zeitreihe der Dinozysten vier Perioden: 240 Tage, 480 Tage, 180 Tage Zyklen, die als halbjähriger Zyklus interpretiert werden und einen 360 Tage Zyklus, der als jährlicher Zyklus verstanden wird. Der halbjährliche und jährliche Zyklus des gesamten Dinozysten Export-Flux stimmt mit den Zyklen der Windgeschwindigkeit, der Windrichtung, der Aerosol Staub Zeitreihe und des SSTa überein. Das Dinozysten Winterhoch (Dezember - Februar) korreliert mit dem Staub Winterhoch, während das Dinozysten Frühling/Sommer Hoch (April - Juni) mit dem primären Auftrieb und dem Staub Sommer Hoch korreliert. Das SST Wavelet Spektrum deutet nur den jährlichen Zyklus an, korreliert aber nicht mit den Monaten, in denen der jährliche Zyklus der Dinozysten beobachtet wurde. Der Zyklus der gesamten Dinozysten deutet Variationen in drei Phasen an, welche mit Änderungen in der Taxa Zusammensetzung übereinstimmen. Phase 1 (2003 - 2008) wird durch die geringe Ausprägung der 240 Tage und 480 Tage Zyklen abgegrenzt, wenn sich die Dinozysten Taxa häufen, die typisch für den maximalen Auftrieb und für die Gruppe des Staubs und des nachlassenden Auftriebs sind. Phase 2 (2009 - 2012) ist durch halbjährliche und jährliche Zyklen charakterisiert, ein Ergebnis der maximalen Auftriebs Gruppen Zyklen. Phase 3 (2013 - 2020) zeigt eine stärkere Ausprägung des halbjährlichen und jährlichen Zyklus, der auch in der Auftriebs Gruppe beobachtet wurde, und zusätzlich einen geringen Anteil der Gruppen der kosmopolitischen/beziehungslosen und der Auftrieb und Staub Gruppe. Die drei Phasen stimmen mit den Änderungen der Aerosol Staub und Auftrieb Wind Zyklen der Zeitreihe überein. Die Ergebnisse legen nahe, dass die schrittweisen Änderungen der Umwelt von der südwärts Bewegung der Lage des ITCZ angetrieben werden, welche sowohl den Auftrieb als auch die Staub Emission während des Zeitraums der Untersuchung verstärkte. Die Dinozysten Zyklen und Änderungen der Taxa Zusammensetzung unterstützen diese Interpretation, darauf hinweisend, dass klimatisch verursachte Änderungen in der Umwelt die Dynamik der Planktonblüten und Zusammensetzung der Gemeinschaft der Dinoflagellate beeinflusst.

Basierend auf der altbekannten Hypothese des Aktualismus Prinzips wird erwartet, dass die Informationen, die in den zwei vorherigen Projekten aus den Proben der Sedimentfalle gewonnen wurden, auch im Paläoarchiv enthalten sind. Das Aktualismus Prinzip erlaubt es Mikrofossilien, wie Dinozysten, als Anzeiger für vergangene Umwelt- und Klimaänderungen zu nutzen. Jedoch sind manche Störungen bekannt, die das Anzeigen der Wassersäulen Signale der Mikrofossilien im Sediment stören.

Deshalb vergleichen wir die Daten der Sedimentfalle mit denen des Sedimentbohrkerns unter der gleichen Zeitspanne und Auflösung (**Kapitel 5**). Das Alter jeder Kernprobe wurde durch das Radionuklid  $^{210}\text{Pb}$  (Blei) bestimmt, was zu einem Ergebnis von 1,6 Jahre pro 3,1 mm Sediment führt. Der Vergleich der Zeitspanne und Auflösung zwischen den Proben der Sedimentfalle und der Kernproben zeigt, dass die Dinozysten Vergesellschaftung im Kern einem Küsten Auftriebs Milieu gleicht, dominiert von braunen Dinozysten, die meist heterotrophischen Taxa zugeordnet werden können. Die häufigsten Dinozysten Taxa in der Sedimentfalle (z.B. *Archaeoperidinium* spp., *Brigantedinium* spp., *Gymnodinium* spp., *P. americanum*, *L. polyedra*, and *Echinidinium*) kommen alle in den Kernproben vor. Die Akkumulationsraten der Dinozysten der Proben der Sedimentfalle und der Kernproben sind vergleichbar. Die heterotrophische Gruppe bewegt sich in der Größenordnung von  $10^6$  und die photo-/mixotrophische Gruppe bewegt sich in der Größenordnung von  $10^5$ . Jedoch ist der relative Anteil und die Akkumulationsraten der heterotrophischen Dinozysten in den Kernproben geringer, im Gegenteil zu den photo-/mixotrophischen Dinozysten. Die Anfälligkeit der braunen (gefärbten) Zysten, die größtenteils von den heterotrophischen Dinoflagellaten erzeugt werden, wird als Grund vermutet für die geringere Akkumulationsrate und relativen Anteil dieser Gruppe in den Kernproben. Im Gegensatz dazu zeigten manche heterotrophischen Taxa (z.B. *P. conica*, *P. monospinum*, and *P. stellatum*) einen Anstieg der Konzentration und des relativen Anteils, was auf einen Eintrag fremden Materials in den Standort des Kerns hindeutet. Eine "Principal Component analysis" (PCA) wurde auf die Proben der Sedimentfalle und die Kernproben angewandt, die die Proben der Sedimentfalle in drei Gruppen und die Kernproben in vier Gruppen aufteilt. Die PCA Gruppen der Sedimentfallen Proben markieren die Verschiebung der Dinozysten Vergesellschaftung im Jahr 2009 hin zur *Echinidinium* Häufigkeit (maximale Auftriebs Gruppe), wie in den zwei vorherigen Projekten berichtet. Diese Verschiebung wurde in den Kernproben im gleichen Zeitraum ermittelt. Hinzukommt, dass die vier Gruppen der Kernproben nicht nur die Verschiebung in der Vergesellschaftung bestätigen, sondern auch, dass die vier oberen Proben signifikant verschiedene Zusammensetzungen zeigen. Dies ist vermutlich das Ergebnis eines stärkeren Einflusses von prä- und postablagerungs Prozessen, wie Bioturbation, Kompaktion, Resuspension, lateraler Transport und aerobisch mikrobieller Abbau.

Die Ergebnisse dieser drei Projekte bereichern unser Wissen über die Einflussfaktoren der Dinozysten Produktion, ihre Beziehung zu Umweltänderungen und den Prozessen nach der Ablagerung, die das primäre Signal der erhaltenen Dinozysten potentiell verfälscht. Einige wesentliche Ergebnisse, wie die zwischenjährliche Variabilität der Dinozystenproduktion, eine signifikante Verschiebung der Dinozysten Vergesellschaftung und wie sie durch die sich ändernde Umwelt und das Klima beeinflusst werden, waren nur durch die Verfügbarkeit von Sedimentfallen Proben über einen Zeitraum von 18 Jahre möglich. Die Studie mit dem hoch auflösenden Vergleich zwischen Dinozysten, die in der Wassersäule produziert wurden, mit denen, die eingebettet wurden, war die erste Untersuchung, die darauf abzielt die Rolle der Dinozysten als verlässliches Werkzeug für die Rekonstruktion der Bedingungen und Änderungen der vergangenen Umwelt und des Klimas zu bestätigen.



## Ikhtisar

Fitoplankton laut memiliki peran yang penting dalam pelestarian lautan dan iklim bumi. Organisme tersebut bertanggung jawab untuk mengekstrak sepertiga dari total karbon dioksida di atmosfer and merubahnya dalam bentuk biomassa. Melalui *biological pump*, sebagian kecil dari karbon dilepaskan kembali ke atmosfer melalui proses pernafasan (respirasi). Bersama dengan diatom dan *coccolithophores*, dinoflagelata yang dapat berfotosintesis adalah salah satu dari fitoplankton eukariotik utama di dalam ekosistem laut. Kelompok plankton ini sangat beragam, tersebar di seluruh dunia, dipengaruhi oleh faktor fisik and kimia tertentu (contohnya nutrisi, cahaya matahari, suhu, arus, dan salinitas), dan juga merespon perubahan yang terjadi pada faktor-faktor tersebut. Selain itu, sekitar 15% dari dinoflagelata melalui tahap *resting* selama siklus reproduksi seksualnya, membentuk struktur khas yang dikenal sebagai *dinoflagellate cysts (dinocysts)*. Banyak dari *dinocysts* terbentuk dari dinding organik yang dapat terfosilkan di dalam sedimen. Aspek-aspek inilah yang menjadikan dinoflagelata sebagai proksi yang berguna tidak hanya untuk studi ekologi, oseanografi, dan iklim tapi juga untuk merekonstruksi kondisi dan perubahan lingkungan di masa lampau.

Perubahan iklim yang cepat saat ini diperkirakan akan mendorong perubahan pada interaksi antara atmosfer dan lautan, yang mempengaruhi dinamika pertumbuhan dinoflagelata dan pembentukan *dinocysts*. Oleh karena itu, diperlukan data dari in-situ *dinocysts* selama beberapa tahun dan faktor-faktor pendukung diperlukan untuk menciptakan sebuah rekonstruksi. Sayangnya, data jenis tersebut cukup langka, dan data yang tersedia hanya mencakup periode waktu yang singkat. Dalam disertasi ini, kami memaparkan sebuah data dalam rangkain waktu 18 tahun dari *organic-walled dinocysts* yang dikumpulkan dengan menggukan *sediment trap* yang telah diposisikan di salah satu dari empat daerah bernama *eastern boundary upwelling ecosystems (EBUEs)* yang terletak di paitani Afrika Barat Laut. *Upwelling* membawa kolom air di bawah permukaan yang kaya nutrisi untuk memberi nutrisi pada produsen laut utama, seperti dinoflagelata, yang hidup di zona fotik. *Upwelling* terjadi sepanjang tahun di bawah siklus musiman yang dikendalikan oleh migrasitahunan *Inter Tropical Convergence Zone (ITCZ)*. Kolom air produktif ini bias mencapai ratusan kilometer ke arah laut lepas dalam bentuk filamen dan pusaran air akibat arus permukaan di wilayah penelitian. Selain itu, debu Sahara meningkatkan produktivitas di area ini dengan menyediakan nutrisi dan elemen tambahan. Debu aerosol memasok material sedimen, dimana mikrofosil dapat terawetkan. Akumulasi sedimen di sini relatif tinggi, dan tidak ada laporan tentang hiatus selama zaman Holosen di area penempatan *sediment trap*. Akibatnya, arsip sedimen mencatat sejarah produksi laut yang berkesinambungan dalam resolusi waktu yang tinggi, memungkinkan perbandingan *dinocysts* pada *sediment trap* and fosilnya di dalam *sediment core*.

Untuk memahami respon dari produksi *dinocysts* terhadap dinamika antar tahunan di ekosistemnya, produksi *dinocysts* selama 18 tahun dibandingkan dengan beberapa parameter lingkungan seperti kecepatan dan arah angin penyebab *upwelling*, pasokan debu Sahara, suhu permukaan air laut, anomali dari suhu permukaan air laut, dan konsentrasi klorofil di permukaan air laut (**Bab 3**). Hasilnya menunjukkan bahwa dinoflagelata heterotrofik berkontribusi terhadap sebagian besar kumpulan *dinocysts* (sekitar 94%). Produksi kelompok dinoflagelata ini biasanya meningkat pada musim semi dan musim panas bertepatan dengan waktu angin tercepat yang bertiup dari timur laut. Beberapa puncak dari produksinya tercatat pada saat musim dingin selama beberapa tahun sejalan dengan tingginya pasokan debu dari Sahara ke area *sediment trap*. Keberagaman tingkat produksi dalam beberapa tahun yang lebih signifikan ditunjukkan oleh dinoflagelata fototrofik ketika produksi tahunan tertingginya terjadi pada musim gugur dan musim dingin. Selanjutnya, *Canonical Correspondence Analysis (CCA)* menegaskan bahwa indikator *upwelling* (kecepatan dan arah angin) merupakan factor yang paling berpengaruh, dan suhu permukaan air laut adalah parameter yang paling tidak signifikan. Berdasarkan metode statistik ini, lima kelompok *dinocysts* teridentifikasi yang di dasarnya pada hubungannya dengan parameter lingkungan. Takson-takson *dinocysts* di kelompok 1 (*Echinidinium delicatum/granulatum*,

*Echinidinium* spp., *E. transparantum/zonneveldiae*, *Trinovante-dinium* spp., and *Proto-peridinium latidorsale*) berkembang pada keadaan intensitas maksimal dari *upwelling*. Kelompok 2 (*Archaeoperidinium* spp., *P. americanum*, *P. stellatum*, and *P. subinermis*) terdiri dari takson-takson yang berkembang pada keadaan maksimal dari *upwelling* dan pasokan debu. Kelompok 3 (*Gymnodinium* spp. and *L. polyedra*) lebih memilih fase relaksasi dari *upwelling*. Takson-takson *dinocysts* di kelompok 4 (*Bitectatodinium spongium* and *Protoceratium reticulatum*) bermunculan ketika kolom air lebih hangat. Dan takson-takson *dinocysts* di kelompok 5 (*Brigantidinium* spp., *E. aculeatum*, *Impagidinium aculeatum*, *P. conicum*, *P. monospinum*, *Pentapharsodinium dalei*, and *Spiniferites* spp.) tidak menunjukkan korelasi tertentu dengan parameter lingkungan apa pun. Pada tahun 2009, kumpulan *dinocysts* berubah dari dominasi berbagai takson menjadi dominasi spesies-species *Echinidinium*, yang bertepatan dengan peningkatan pasokan debu Sahara. Mengenai *cysts* dinoflagelata yang menghasilkan biotoksin, *sediment trap* mengumpulkan lima takson *dinocysts* fototrofik yang berafiliasi dengan spesies penghasil biotoksin yang dapat mengancam ekosistem laut dan kesehatan manusia. Tingkat produksi mereka sangat rendah karena kolom air yang terus-menerus bergerak, dimana keadaan ini tidak menguntungkan bagi dinoflagelata fototrofik.

Untuk memperluas pengetahuan kita tentang dinamika produksi *dinocysts* beserta *cysts* dari takson-takson di dalam satu kelompok ekologi yang telah ditentukan proyek sebelumnya, *time series* dari *dinocysts* dan parameter lingkungan telah dianalisis menggunakan *Morlet wavelet analysis* (Bab 4). Teknik ini memungkinkan visualisasi dari pola-pola periodik atau siklus dan variasinya sepanjang *time series* yang ditentukan dengan menganalisa korelasi antara pola gelombang dari data yang tersedia dengan *Morlet Wavelet*. Berdasarkan spektrum warna hangat (merah) yang mewakili korelasi tinggi, data dari total *dinocysts* memiliki empat periode: 240 hari, 480 hari, 180 hari yang diinterpretasikan sebagai siklus setengah tahun, dan 360 hari yang diinterpretasikan sebagai siklus tahunan. Siklus setengah tahun dan tahunan dari total produksi *dinocysts* beretepatan dengan siklus-siklus yang sama yang terdeteksi pada data kecepatan angin, arah angin, debu aerosol, dan anomali suhu permukaan air. Puncak produksi *dinocysts* pada musim dingin (Desember - Februari) berkesinambungan dengan puncak pasokan debu aerosol dari Sahara pada musim dingin, sedangkan puncak produksi *dinocysts* pada musim semi/panas (April - Juni) bersamaan dengan waktu kemunculan *primary upwelling* dan puncak pasokan debu aerosol dari Sahara pada musim panas. Spektra wavelet dari suhu permukaan air hanya menunjukkan siklus tahunan, namun waktu kemunculannya tidak bersamaan dengan siklus tahunan dari produksi *dinocysts*. Siklus tahunan dari *total dinocysts* juga menunjukkan variasi dalam tiga fase, yang waktunya bersamaan dengan perubahan komposisi takson. Fase I (2003 -2008) ditandai dengan spektra yang tidak signifikan dari periode 240 dan 480 hari, ketika *dinocyst* dari kelompok maksimal *upwelling* dan debu serta relaksasi *upwelling* melimpah. Fase 2 (2009 - 2012) ditandai dengan siklus setengah tahun dan tahunan sebagai produk dari siklus kelompok *upwelling* maksimal. Fase 3 (2013 - 2020) memaparkan bahwa siklus setengah tahun dan tahunan menjadi semakin signifikan yang juga termati pada pola siklus kelompok *upwelling* maksimal, ditambah sedikit kontribusi dari kelompok kosmopolit serta maksimal *upwelling* dan debu. Perubahan pada ketiga fase tersebut bersamaan dengan dengan perubahan siklus pada debu aerosol dan angin penyebab *upwelling*. Hasil ini menunjukkan bahwa perubahan bertahap yang terjadi di lingkungan disebabkan oleh perubahan posisi ITCZ ke arah selatan yang dapat memperkuat *upwelling* dan pasokan debu selama rentang waktu penelitian kami. Siklus produksi *dinocysts* dan komposisi taksonnya mendukung interpretasi ini, yang mengindikasikan perubahan lingkungan yang disebabkan oleh perubahan iklim mempengaruhi dinamika pertumbuhan dan struktur dari komunitas dinoflagelata.

Informasi yang telah dikumpulkan dari data *sediment trap* pada dua proyek sebelumnya diharapkan dapat dianalisis pada arsip paleontologi. Mengikuti hipotesis Uniformitarianisme yang telah lama diketahui. Teori ini memungkinkan mikrofosil, termasuk *dinocysts*, digunakan sebagai proksi perubahan lingkungan dan iklim di masa lampau. Namun, beberapa aspek diketahui dapat mengganggu informasi tentang kolom air laut yang dibawa oleh mikrofosil ke sedimen. Oleh karena itu, kami membandingkan data *sediment trap* dengan *sediment core* dalam rentang waktu dan resolusi yang sama (Bab 5). Umur setiap sampel *core* ditentukan oleh peluruhan paruh waktu dari  $^{210}\text{Pb}$  (timbang), yang

hasilnya menyatakan 1.6 tahun pada setiap 3.1 mm sampel sedimen. Setelah mencocokkan rentang waktu dan resolusi dari sampel *sediment trap* dan *sediment core*, hasil perbandingan menunjukkan bahwa kumpulan *dinocysts* dalam sampel *core* menunjukkan lingkungan pantai khas *upwelling* yang di dominasi oleh *dinocysts* dengan dinding berwarna kecoklatan yang sebagian besar berafiliasi dengan dinoflagelata heterotrofik. Takson *dinocysts* yang paling melimpah dalam sampel *sediment trap* (misalnya *Archaeoperidinium* spp., *Brigantedinium* spp., *Gymnodinium* spp., *P. americanum*, *L. polyedra*, and berbagai spesies *Echinidinium*) semuanya dapat ditemukan pada sampel *core*. Tingkat akumulasi *dinocysts* antara sampel *sediment trap* dan *sediment core* relative sebanding: kelompok heterotrofik berkisar pada skala  $10^6$ , dan kelompok fototrofik berkisar pada skala  $10^5$ . Namun, kontribusi relatif dan akumulasi dari *dinocysts* heterotrofik lebih rendah pada sampel *core*, yang meruoakan hasil berkebalikan untuk kelompok fototrofik. Kerentanan *cysts* berwarna coklat yang sebagian besar dihasilkan oleh dinoflagelata heterotrofik diduga menyebabkan penurunan akumulasi dan kontribusi relatif kelompok ini dalam sampel *core*. Sebaliknya, beberapa takson heterotrofik (contohnya *P. conica*, *P. monospinum*, and *P. stellatum*) menunjukkan peningkatan konsentrasi dan persentase, yang mengindikasikan adanya material asing yang di bawa ke lokasi *core*. *Principal Component analysis (PCA)* yang telah diterapkan pada sampel *trap* dan *core*, mengelompokkan sampel *sediment trap* menjadi tiga kelompok dan sampel *core* menjadi empat kelompok. Kelompok-kelompok PCA pada sampel *trap* menandai perubahan kumpulan *dinocysts* pada tahun 2009 menjadi dominasi *Echinidinium* yang telah dipaparkan di dua proyek sebelumnya. Perubahan ini terdeteksi pada sampel *core* pada waktu yang sama. Selain itu, keempat kelompok PCA pada sampel *core* tidak hanya mengkonfirmasi perubahan pada kumpulan *dinocysts* tetapi juga menunjukkan bahwa empat sampel teratas mengandung kumpulan berbeda yang signifikan. Sampel-sampel ini diduga merupakan dampak yang signifikan dari proses sebelum dan setelah pengendapan seperti bioturbasi, bias yang disebabkan pepadatan sediment, transport lateral dari partikel-partikel, dan degradasi yang disebabkan oleh mikroba aerob.

Informasi yang diperoleh dari ketiga proyek ini telah menambah pengetahuan tentang faktor pendorong produksi *dinocysts*, kaitannya dengan perubahan lingkungan, dan proses-proses yang dapat merubah informasi primer yang terendapkan bersama *dinocysts*. Beberapa poin penting seperti keberagaman pada produksi *dinocysts* dalam beberapa tahun, perubahan signifikan dalam kumpulan *dinocysts*, dan bagaimana perubahan tersebut dipengaruhi oleh perubahan lingkungan dan iklim sekitar hanya mungkin bisa dianalisa karena ketersediaan data *sediment trap* yang mencakup kurun waktu 18 tahun. Studi perbandingan dengan resolusi waktu yang tinggi antara *dinocysts* yang dihasilkan dari kolom air dengan yang terakumulasi di dalam sedimen merupakan investigasi pertama yang dilakukan, bertujuan untuk mengkonfirmasi peran *dinocysts* sebagai alat yang dapat diandalkan untuk merekonstruksi kondisi dan perubahan lingkungan serta iklim di masa lampau.



# Chapter 1 – General introduction

## 1.1. Scientific background

The earth's oceans consist of various ecosystems, from coastal to open oceans and pelagic to benthic. They play a crucial role in engineering a substantial portion of biogeochemical processes that are vital to sustaining the global ecosystem and its climate (Petihakis et al., 2018; Visbeck, 2018). The key players regulating these processes are phytoplankton in the photic zone, which holds the key position as carbon-fixing organisms via photosynthesis, taking around 30% of atmospheric carbon dioxide (CO<sub>2</sub>) and turning it into biomass (**Figure 1.1**) (Worden et al., 2015; Juranek et al., 2020; Cohen et al., 2021). Through this process, phytoplankton not only provides the energy source for other organisms at higher trophic levels but also controls the greenhouse gas concentration in the atmosphere (Falkowski, 2012; Worden et al., 2015; Juranek et al., 2020). Besides sheltering the most biodiverse ecosystem of the planet, oceans offer various resources that support recent and ancient human societies, such as providing food, energy, routes for transportation, and tourism (Visbeck, 2018; Winther et al., 2020). Unfortunately, the overexploitation of ocean resources, notably since industrialisation, has put significant pressure on the ocean, its biochemical properties, and eventually, Earth's climate (Mora et al., 2007; Montero-Serra et al., 2019). Although naturally driven factors have continuously triggered changes in the ocean and climate, increasing anthropogenic CO<sub>2</sub> in the atmosphere leads to an unstable climate, ocean warming, ocean acidification, and biodiversity loss (Francis et al., 2012; Poloczanska et al., 2016; Henson et al., 2021). Therefore, we would like to investigate the influence of the current fast-changing climate on the ecosystem by monitoring changes in long records of marine plankton and various limiting factors that impact plankton production.

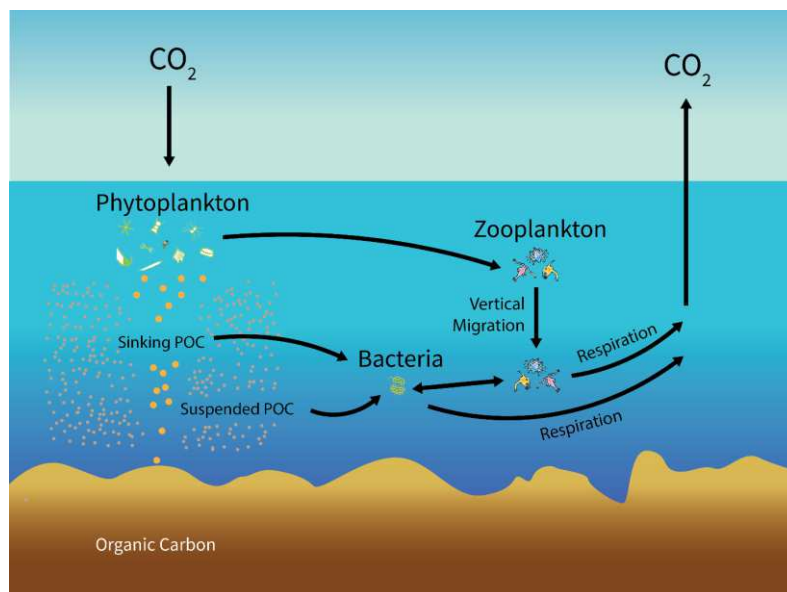


**Figure 1.1.** The simplified scheme of the marine carbon cycle, including photosynthesis, the pelagic food chain, and the biological pump performed by phytoplankton, zooplankton, and the microbial community. The figure was taken from Fowles, 2020.

Eukaryotic marine plankton, such as dinoflagellates, diatoms, coccolithophores, and foraminifera, have been used as environmental and climate proxies due to their crucial role in the marine ecosystem and their worldwide distribution (e.g., Zonneveld et al., 2013; de Garidel-Thoron et al., 2022). Furthermore, the living cells of these plankton bear hard body parts that can be fossilised in the sediment archive. However, this situation is slightly different for dinoflagellates. A dinoflagellate cell is surrounded by a degradable organic wall, leading to a rare chance for them to be fossilised (Dale and Dale, 1992). Fortunately, around 15% of extant species are known to produce preservable cysts during

their reproduction cycle, and the most common type of dinoflagellate cysts (dinocysts) are formed by a polysaccharid-based wall called dinosporin (e.g., Gray et al., 2017; Zonneveld et al., 2019b; Versteegh and Zonneveld, 2022; Meyvisch et al., 2023; Ando et al., 2024). Organic-walled dinocysts were produced by phototrophic, mixotrophic, or heterotrophic species, which means their records contain signals carried by primary and secondary producers (Schnepf and Elbrächter, 1992; Taylor et al., 2008; Jeong et al., 2010). Preserved dinocysts in paleontological archives reflect the production dynamic of their living organisms that were controlled by various factors in the upper water (e.g., nutrient input, temperature, and salinity), making them useful tools for investigating the present and past ocean (e.g., Head, 1996; Dale et al., 2002; Kremp et al., 2016; Brosnahan et al., 2020).

To establish a high-quality observation of climate change influence on the recent dinoflagellate population, we obtained a time series of dinocysts over 18 years in a productive region called the Canary Current upwelling system in Northwest Africa. Herein, the high growth of primary producers, including phototrophic dinoflagellates, is triggered by nutrient-rich subsurface water carried through the upwelling system (Mittelstaedt, 1991; Cropper et al., 2014). The sampling device was placed in an area characterised by permanent upwelling with changing seasonal intensity controlled by the strength and direction of the surface wind trades (Hagen, 2001; Cropper et al., 2014; Faye et al., 2015). Additional micronutrients reach the surface ocean of this region via aerosol dust from the Sahara, which is also controlled by the wind system (Lohan and Tagliabue, 2018; Yu et al., 2019). Changing wind direction and intensity leads to seasonality in dust emissions, similar to the upwelling intensity that is orchestrated by the annual migration of the Inter Tropical Convergence Zone (ITCZ) (Mittelstaedt, 1991; Skonieczny et al., 2013; Prospero, 2014). Saharan dust is the primary source of the lithogenic flux on the Atlantic coast of northwest Africa (van der Does et al., 2021). It provides approximately 7.3 million tons of dust globally each year, which ends up as sediments on the ocean floor (Wang et al., 2023; van der Does et al., 2021). The rate of accumulated sediment is relatively fast, and the region experienced minimal tectonic activity in the Holocene, which minimizes a hiatus in the sediment stratification (Seibold and Fütterer, 1982; Hanebuth and Henrich, 2009). This favorable setting opens an opportunity to compare the records of dinocysts produced from the upper water column to those that accumulated in the sediment floor within the same time span and in a high resolution. Therefore, we hypothesise that the impact of (local) climate change shall be recorded in the multi-year time series of dinocysts from the upper water column and ocean floor due to dinocyst formation relationship to their environments and minimum post-depositional perturbations.

## 1.2. Dinoflagellates

Dinoflagellates are eukaryotic single-celled plankton with more than 2000 species have been described (Gómez, 2012). Their cell sizes usually range between 15 and 150  $\mu\text{m}$ , with a few species that can grow to 2 mm in diameter (Taylor and Pollinger, 1987). The dinoflagellate cell is enveloped by a distinctive structure called amphiesmal vesicles that can contain cellulosic thecal plates (thecate/armoured) (**Figure 1.2A**) or are empty (athecate/naked) (Morrill and Loeblich, 1983). The arrangement of the theca plates or hollow amphiesmal vesicles (tabulation) are important aspects in identifying dinoflagellate lineages such as dinophysoid, gonyauloid, gymnodinoid, peridinioid, prorocentroid, suessoid, etc (Taylor, 1987; Matthiessen et al., 2005). A significant number of dinoflagellate species live in the ocean, with a major part of them adapted phototrophic/mixotrophic or heterotrophic life strategy (e.g., Schnepf and Elbrächter, 1992; Taylor et al., 2008; Jeong et al., 2010). Besides playing the role of primary and secondary producers in the marine food chain, some dinoflagellates live within other organisms as symbionts or parasites (e.g., Stat et al., 2008; Skovgaard et al., 2012). The availability of light and nutrients has a big impact on the photosynthetic dinoflagellates to fix atmospheric  $\text{CO}_2$ . Dinoflagellates themselves are prey for the zooplankton, including the heterotrophic dinoflagellates, fish, and marine mammals (Jeong et al., 2010; Hansen, 2011). The optimum condition of water temperature, salinity, and currents also contributes to the survival rates of dinoflagellates (Smayda, 2002; Smayda and Reynolds, 2003). Since a significant number of

dinoflagellates perform photosynthesis, they inhabit the photic zone by swimming using their two flagella, while less than 10% live in the substrate (Fraga et al., 2012; Gómez, 2012). The ribbon-like flagella enable the planktonic dinoflagellates to migrate vertically in the water column (Taylor and Pollinger, 1987). Those two flagella are the transverse flagellum (horizontally encircling the theca) and longitudinal flagellum (the vertical one located in the sulcus) (**Figure 1.2A**). The wide range of dinoflagellate contributions and responses to their environment makes them one of the key organisms for ecological studies. Moreover, some species secrete various types of biotoxin and cause harmful algal blooms (HAB) when they bloom uncontrollably (e.g., Amorim et al., 2001; Quijano-Scheggia et al., 2012; Liu et al., 2020; Terenko and Krakhmalnyi, 2021). HABs are a threat to marine organisms, human health, and socioeconomic aspects of the coastal population (e.g., Holmes and Teo, 2002; Starr et al., 2017).

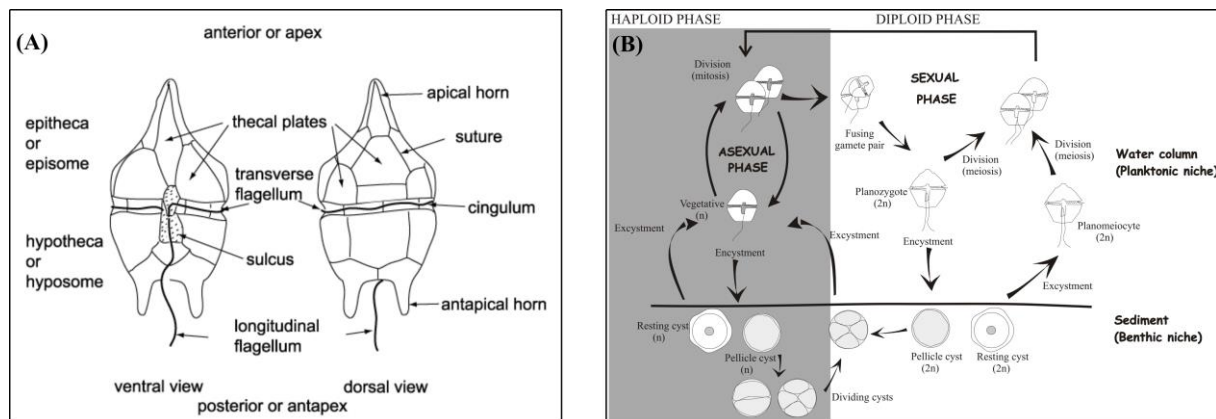


**Figure 1.2.** The biological aspect of dinoflagellates: (A) the terms used to describe the exterior morphology of theca/armoured dinoflagellate. The figure was taken from Fensome et al., 1996. (B) The simplified scheme of dinoflagellates reproduction cycles in asexual and sexual phases. The figure was obtained from Bravo and Figueroa, 2014.

Dinoflagellates can reproduce in asexual and sexual phases to optimise their life cycle (**Figure 1.2B**). This plankton reproduction cycle is complex and still in a debatable stage. However, the asexual phase is generally performed by cell division (mitosis), and the sexual phase is through the fusion of two parental cells (Bravo and Figueroa, 2014). The fusion product known as planozygote ( $2n$ ) can divide through the meiosis process into two daughter cells (Figueroa and Bravo, 2005; Bravo and Figueroa, 2014). For some dinoflagellate species, the planozygote can form a certain structure called cysts that completely surround the specimen (hypnozygote). Many cyst walls are made from resistant organic materials, some are calcareous, and rarely are siliceous, which results in their perseverance against degradation, mechanical, and thermal pressure (Dale and Dale, 1992; Zonneveld et al., 2005; Bravo and Figueroa, 2014). During cyst formation or encystment, the motile cell terminates its flagella that turns it completely immobile/dormant. The encystment is triggered by various environmental factors or driven by the endogenous rhythm, which is also applied to the duration of the dormancy stage for a species or between different species (Anderson and Lindquist, 1985; Anderson and Kaefer, 1987; Taylor, 1987). The cyst morphology is unique to the motile cells that produce them. Organic-walled cysts are usually spherical or reminisce the theca/cell membrane shape and also develop various features such as different colours, wall ornamentations, and spiny structures (processes) (Wall and Dale, 1968; Fensome et al., 1993). The daughter cell emerges out of the cyst (germination) via certain plates called archeophyle, which is an additional feature to determine a dinoflagellate cyst taxonomy (Matsuoka, 1985). The cyst cycle can be completed before reaching a great depth, allowing the new cells to stay in the photic zone (Dale and Dale, 1992; Zonneveld et al., 2022b). In some cases, cysts can accumulate in the sediment on a large scale, creating a seed bank (e.g., Head, 1996; Matsuoka and Head, 2013; Bravo and Figueroa, 2014). They can remain viable for up to a century before being resuspended back to the photic zone via subsurface water currents (Lundholm et al., 2011; Ellegaard and Ribeiro, 2018; Delebecq et al., 2020).

Due to their high preservation rate in sediment, dinocysts have been used in paleontology to investigate the condition of the past environment as well as determine the geological age of sedimentary

rocks (e.g., Dale 1996; McRae et al., 1996; Bijl 2022). Among all dinocyst types, the organic-walled groups are the most commonly applied as paleoenvironmental proxies due to their large diversity and distribution (Marret and Zonneveld, 2003; Zonneveld et al., 2013; de Vernal et al., 2020). Those cysts are produced by gonyauloid, perionoid, and a few species of gymnodinioid dinoflagellates. They encompass species in various trophic levels, and some are known to produce biotoxin. Similar to other shell-bearing plankton, the link of dinocysts with their environment is built according to the correlation of environmental factors to the concentration or distribution of certain taxa in time and space (e.g., Dale and Dale, 1992; Zonneveld et al., 2013; de Vernal et al., 2020; Bringué et al., 2019; Roza et al., 2024). Through dinocyst fossils, we can also estimate ocean productivity, carbon sequestration, and climate change in the past hundred to million years ago (e.g., Radi and de Vernal, 2008; Pospelova et al., 2015; Boyd et al., 2018). In contrast, dinocyst fossil association also provides perturbation signals after deposition, which could mislead the interpretation of past environment or estimation of carbon storage (e.g., Zonneveld et al., 2008; Matthiessen et al., 2018; Nooteboom et al., 2019).

### 1.3. Northwest African upwelling

The study area is one of the four eastern boundary upwelling ecosystems (EBEUs), called the Canary Current upwelling ecosystems. Although only covering approximately 10% of the ocean surface, these four regions contribute to around 25% of global fishery stock and are the biodiversity hot spots in the ocean (Pauly and Christensen, 1995; Carr, 2001; Aristegui et al., 2009;). The Canary Current Upwelling is situated off the Atlantic coast of Northwest Africa in the easternmost part of the North Atlantic subtropical gyres (Mittelstaedt, 1983; Hagen, 2001; Aristegui et al., 2009). Along this coast, subsurface waters containing high nutrients and colder temperatures rise as a result of the wind trade that blows the surface waters offshore (Mittelstaedt, 1991; Cropper et al., 2014). Depending on the coastal wind trade mechanisms and the topography of the ocean floor, three upwelling zones were classified (**Figure 1.3A**). The northernmost zone (26° - 33° N) is called the weak permanent upwelling zone, where the upwelling occurs throughout the year and covers a relatively small surface area (Lathuilière et al., 2008; Cropper et al., 2014). In the southmost (13° - 19° N), the upwelling occurs seasonally within a year (Lathuilière et al., 2008; Cropper et al., 2014). In the middle zone, where the materials for this dissertation were obtained, the upwelling stretches from 20° - 25° N and appears all year long with intensity variation driven by the strength and direction of the wind (Hagen, 2001; Lathuilière et al., 2008; Cropper et al., 2014; Faye et al., 2015). The upwelling reaches its maximum intensity when the Intertropical Convergence Zone (ITCZ) migrates south in boreal winter and becomes weaker in boreal summer as ITCZ moves north (Mittelstaedt, 1991; Maloney and Shaman, 2008). The shelf topography, surface ocean currents, and wind systems facilitate a large coverage of the upwelling filaments in this zone, transporting nutrient-rich waters farther to the open ocean (Mittelstaedt, 1991; van Camp et al., 1991; Hagen, 2001).

The surface waters of the study area are influenced by the Canary Current (CC) from the north and the Mauritanian Current (MC) from the south (**Figure 1.3B**). CC brings cooler water to the North Equator Current alongside the coastline until it turns towards the open ocean between 21° - 25° N (Mittelstaedt, 1983; Mittelstaedt, 1991). In contrast, MC carries warm water from the equator realm parallel to the Mauritanian shelf until 20° N. The MC influence fades in autumn when it is replaced by the southward-moving current (Mittelstaedt, 1983; Mittelstaedt, 1991). The opposing movements of CC and MC form a converge zone in the surface water called the Cape Verde Frontal Zone (CVFZ). This zone creates a separation between the North Atlantic Central Water (NACW) and South Atlantic Central Water (SACW) that supplies the upwelled waters in the study area (Zenk et al., 1991; Sarmiento et al., 2004).



Extra micronutrients and trace elements are brought to the North Atlantic surface waters by the Sahara dust, the world largest aerosol source (Kolber et al., 1994; Jickells et al., 2005; Lohan and Tagliabue, 2018). Sahara dust provides limited nutrients such as iron (Fe) and phosphorus (P) to marine plankton, supporting them to fix carbon and also nitrogen from the atmosphere (Langlois et al., 2012; Krupke et al., 2015). The dust transport mechanism is driven by the surface winds, which show similar seasonality with the coastal upwelling. When the ITCZ is at its southern position, the winds transport relatively large dust particles to the proximal area (North Atlantic) at low altitudes (0 - 3 km) (Skonieczny et al., 2013; Yu et al., 2019; Gutleben et al., 2022). During the ITCZ boreal summer position, the fine dust particles were carried to distal positions (e.g., Caribbean and West Atlantic) through the Sahara Air Layer (SAL) at higher altitudes (Prospero and Carlson, 1972; Doherty et al., 2014; Prospero et al., 2014).

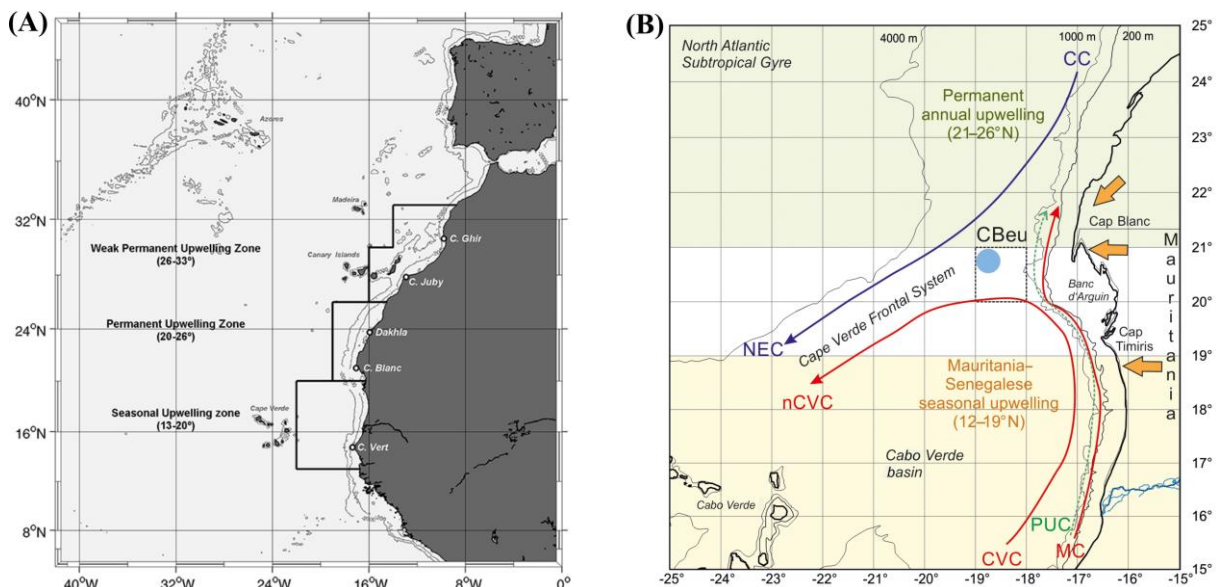


**Figure 1.3.** The regional setting of the study area: (A) the three zones of Canary Current upwelling systems. The figure was obtained from Gómez-Letona et al., 2017. (B) the surface water currents of the study area are represented by the red and blue arrows, which are located between permanent upwelling and seasonal upwelling zones. The figure was taken from Romero et al., 2020, showing the same sediment trap (CBeu) used to collect sinking particles from the upper water column.

#### 1.4. Aims of the projects

Many published reports have answered important questions regarding organic-walled dinocyst taxa ecology and their application for paleoenvironmental reconstructions. However, some knowledge gaps remain to be filled in this discipline. The dinocyst production records in the modern ocean lack in-situ observations, and a long record is extremely limited to better analyse interannual production trends and variations. The same challenge is present in interpreting the dinocyst taxa ecology. Therefore, we provided a study of a high-resolution sediment trap record over 18 years (2003 -2020), which collected dinocyst export flux off Cape Blanc, Northwest Africa. This record was compared and analysed with several prominent environmental factors in the study area to determine dinocyst formation drivers and the ecology of various key taxa. This information is essential for paleoenvironmental and paleoceanography studies using dinocyst fossils. The availability of these multi-proxies from the modern ocean motivated us to apply time series analysis to test dinocyst record potential detecting environmental shifts driven by recent climate change. As mentioned earlier, dinocysts have been used to reconstruct the past environment in accordance with the hypothesis that fossilisable remains of pelagic microorganisms in the sediment records represented the environmental condition when the cell was alive. However, existing studies only compared their sediment trap records to surface sediments, which are temporally incomparable. The study area indicated high sedimentation rates, which allowed for a high resolution of age dating. It allowed a comparison of dinocyst time series from the trap and the core under the same time interval. This method aimed to fill the knowledge gap about the impact of post-

depositional processes on dinocyst records while confirming the role of dinocysts as a reliable paleoenvironment indicator. In detail, ten questions were addressed in this dissertation:

*What does the 18-year sediment trap time series of organic-walled dinocyst export flux tell us about the productivity in the study area?* (Chapter 3)

*What were the driving factors of the dinocyst export flux in the upper water column?* (Chapter 3)

*Which dinocyst species or taxa occurred in the study area, and what environmental aspects induced their export fluxes?* (Chapter 3)

*Were there cysts of potential toxic dinoflagellates found in the trap record, and what were their environmental preferences?* (Chapter 3)

*Did dinocyst export flux time series show cyclicities, and did those cycle patterns change over time?* (Chapter 4)

*Did the dinocyst cycles and the changes correlate to the environmental factors cyclicities, and how did the environmental changes impact the dinocyst community?* (Chapter 4)

*Were the ecosystem changes driven by climatic shifts in the study area between 2003 and 2020?* (Chapter 4)

*Are dinocyst records from the upper water column (sediment trap) comparable to those stored on the ocean floor (down-core)?* (Chapter 5)

*Were some alterations observed in the down-core dinocyst association, and which factors caused these alterations?* (Chapter 5)

*How can we improve paleoenvironmental reconstructions based on the fossil association of organic-walled dinocysts?* (Chapter 5)

## 1.5. Dissertation outline

This dissertation follows the format of a cumulative doctoral thesis, which means it compiled three projects in the form of three manuscripts in different stages of the publishing process. Three manuscripts are listed in this dissertation as Chapters 3, 4, and 5, respectively.

### **Chapter 3 - Environmental control of interannual and seasonal variability in dinoflagellate cyst export flux over 18 years in the Cape Blanc upwelling region (Mauritania)**

Surya Eldo V. Roza, Gerard G. M. Versteegh, Vera Pospelova, and Karin A. F. Zonneveld

*Published in Frontiers in Marine Science*

#### **Research highlights**

- Described high intra- and inter-annual variations in dinoflagellate cysts (dinocysts) export flux and taxa composition over 18 years offshore Cape Blanc, North West Africa.
- Discussed the main environmental drivers of the dinocysts and various dinocysts taxa export fluxes.
- Briefly discussed a significant change in the dinocyst association over time and its possible causal factor.
- Described the potential toxic dinoflagellates ecology and their socio-economy risk in the study area.

### **Authors contribution**

SER counted the dinoflagellate cyst specimens, subtracted information on environmental parameters from several databases, analysed and interpreted the data, performed the statistical analysis, created the graphs, and wrote the manuscript. GV subtracted information on environmental parameters from several databases, was involved in the analyses and interpretation of the data, and contributed to manuscript editing. VP counted dinoflagellate cysts in a set of samples and contributed to the data interpretation and manuscript editing. KZ counted some parts of the association of dinoflagellate cysts, guided the reconstruction, analysis, and interpretation of the data, and contributed to the manuscript construction.

### **Detailed contribution of the lead author**

In the first project, I counted, identified, and documented most of the dinocysts in the sediment trap samples. I also extracted dinocysts and prepared the microscope slide from some samples following the procedure of non-acid treatment used by the University of Bremen marine palynology laboratory. I downloaded the data of environmental parameters (upwelling wind, dust input, sea surface temperature, and sea surface Chlorophyll-a) from the database and reconstructed their graphs. I conducted multivariate analyses and interpreted the results of many dinocyst taxa ecological functions with the help of my supervisor. I gathered the results of other sediment traps, drifting traps, and surface sediment regarding the ecology of those taxa. I wrote the original manuscript and created the tables and graphs. I led the manuscript's submission, revision, and final correction to *Frontiers in Marine Science*. I presented the results of this project at the Status Conference for Research Vessels 2022 (online) in February 2022, the 12th International Conference on Modern and Fossil Dinoflagellates in July 2022, and the 1st Ocean Floor Symposium in October 2022.

## **Chapter 4 - Northwest African upwelling ecosystem response to current climate change reflected by dinoflagellate cyst export production**

Surya Eldo V. Roza, Runa Reuter, Jan-Berend Stuut, Gerard J. M. Versteegh, and Karin A. F. Zonneveld

*To be submitted to Global Change Biology*

### **Research highlights**

- Determined and analysed cyclic patterns in the upwelling wind, Sahara dust, and sea surface temperature using wavelet analysis and their correlations to dinocyst production cycles.
- Discussed different phases in the time series of environmental factors and how they impacted the dinocyst production and community.
- Analysed the climatic driving factors of ecosystem changes in the study area.

### **Authors contribution**

SER conceptualized the project, curated the original datasets, generated the time series, did the formal analysis, created the graphs, and wrote the original manuscript. RR assisted with the time series curation and was involved in the data interpretation. JBS provided the original AOD dust data and was involved in the data interpretation. GV assisted with the original dataset curation and contributed to reviewing and editing the manuscript. KZ assisted with the project conceptualization, curated some of the original datasets, was involved in the data interpretation, and contributed to reviewing and editing the manuscript.

### **Detailed contribution of the lead author**

In the second project, I calculated the mean of the time interval variations and conducted the interpolation method to create a new time series suitable for wavelet analysis. I conducted the wavelet analysis on the time series of dinocyst production and the environmental parameters derived from the first project. I determined and interpreted the cycles of each time series out of wavelet power bands and analysed the different phases that occurred in some of the time series with the assistance of my co-authors. I led the discussion of the driving factor for the significant change in the study area. I wrote the original manuscript and created the graphs. I presented the results of this project at the 20th International Conference on Harmful Algae in November 2023 and the International Seminar Series on Dinophytes (online) in February 2024.

### **Chapter 5 - How is the export production of dinoflagellate cysts on the ocean surface stored in the sediment?**

Surya Eldo V. Roza, Karin A. F. Zonneveld, Gerard J. M. Versteegh, and Hendrik Wolschke

*In preparation for submission to Biogeosciences*

#### **Research highlights**

- Described the similarities and disparities between dinocyst association and accumulation from the sediment trap (upper water column) and down-core (ocean floor).
- Discussed the potential driving factors of the alteration found in the core dinocyst association.
- Identified the production and preservation signals in the time series of trap and core samples assisted by multivariate analyses.
- Provided new information to improve the interpretation quality of dinocyst fossils for paleoenvironmental studies.

#### **Authors contribution**

SER curated the original datasets, compiled supporting data for the analyses, calculated the age of the samples, analysed and interpreted the data, created the graphs and tables, and wrote the original draft. KZ conceptualized the project, obtained the samples from the study area, calculated the age model of the cores, supported the analyses and interpretation of the data, and contributed to reviewing and editing the manuscript. GV collected the samples from the study area and supported the analyses and interpretation of the data. HW conducted the core dating and provided a preliminary age model.

### **Detailed contribution of the lead author**

In the third project, I participated in the research cruise in the study area to collect the cores for the comparison study with the sediment trap data. My colleagues and I sliced, prepared, and stored the core samples for the age dating and palynological procedure. Using the acid treatment, I extracted dinocyst from the sliced sediment core and prepared the material for microscopic work. I counted, identified, and documented the dinocyst from the down-core samples. I calculated the time resolution of each sample based on the determined age model. I calculated the dinocyst accumulation rates in trap and core samples. I conducted the ordination analyses, interpreted the results with the guidance of my supervisor, created the tables and the figures, and wrote the original manuscript. I presented the results of this project at the 15th Bremen PhD days in Marine Sciences in April 2023, the International Conference for Young Marine Researchers in September 2023, and the International Workshop on dinoflagellate cysts in June 2024.

## Chapter 2 – Methodology

### 2.1. Sampling instruments

Two instruments were used to obtain samples for the three projects in this dissertation. To obtain information on the export flux of dinocysts that were initially produced in the upper water column and sinking down in the form of aggregates, fecal pellets, and marine snow, Honjo-type sediment traps located between 20° 44.6' N - 20° 53.0' N and 18° 41.9' W - 18° 45.4' W were used. The traps were deployed by the faculty of Geoscience (GeoB) and the MARUM at the University of Bremen. During material collection, they were deployed at 1249 - 1364 m below the ocean surface es from June 2003 until March 2020. Detailed information on the sediment trap deployments and recoveries can be found in **Table 3.1** in Chapter 3. The sediment trap consists of a cone-shaped funnel equipped with a filter net on the top opening and sampling cups at the lower end (**Figure 2.1A**). The filter net prevents large organisms or other materials from entering the funnel, whereas the sampling cups store the sinking particles entering the funnel through a 0.5 m<sup>2</sup> aperture. There are several procedures applied to the sampling cups before every trap deployment: (1) the cups were filled with poisonous mercury chloride (HgCl<sub>2</sub>) to preserve the materials collected by the funnel, (2) the liquid density inside the cups was concentrated to 40‰ by adding pure sodium chloride (NaCl), and (3) the cup set was programmed to switch from one cup to the next for specific intervals (3 - 22 days). The recovered samples were shipped to the GeoB repository and MARUM and kept in storage at a cold temperature (4° C) before they were filtered with a 1 mm pore size sieve, while larger plankton were carefully removed with a tweezer. The samples were split into 1/125 fractions for various research purposes and stored in a freezer, preserving the organic materials under -20° C.

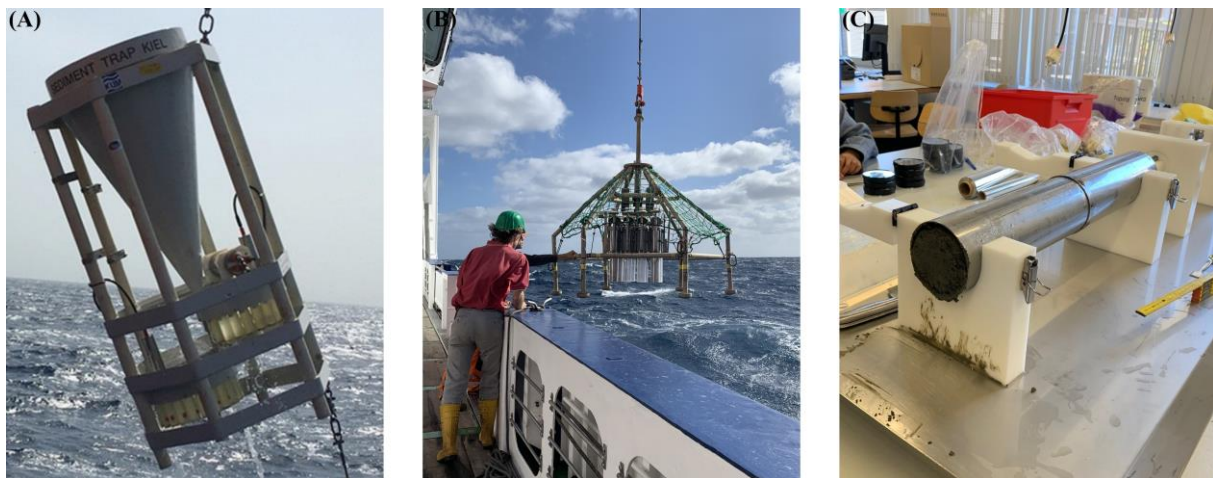


**Figure 2.1.** The following sampling instruments were used to obtain materials for the projects in this dissertation: (A) an Honjo-type sediment trap with sampling cups below the funnel recovered from the ocean depth. The picture was taken by K. Zonneveld; (B) a multicore device to sample short sediment cores from the ocean floor; and (C) the obtained GeoB core was sliced on a core platform.

To collect ocean floor sediment at the trap position, a multicore device was deployed in August 2020 (ca. 18 years after the first trap deployment) (**Figure 2.1B**). Upon sampling, the oxygen concentration in the core sediment was measured with a clarc-type FIBOX3 sensor. The core was sealed and kept in the vessel freezer before it was shipped to MARUM to be stored in the freezer under -20° C. The frozen core was sliced every 3.1 mm (**Figure 2.1C**), transferred to a respective petri dish, and sealed with tape. The core samples were put back into the freezer before the extraction of the dinocysts and <sup>210</sup>Pb analyses for dating purposes.

## 2.2. Dinoflagellate cysts extraction, preparation, and identification

The extraction procedures for sediment trap samples and core samples were slightly different. For the sediment trap samples, the  $\text{HgCl}_2$  poison was removed by sieving the material through a Stork Veco high-precision metal sieve (20  $\mu\text{m}$  pore size) with distilled water (**Figure 2.2A**). This step was repeated three to four times in a laminar flow hood.

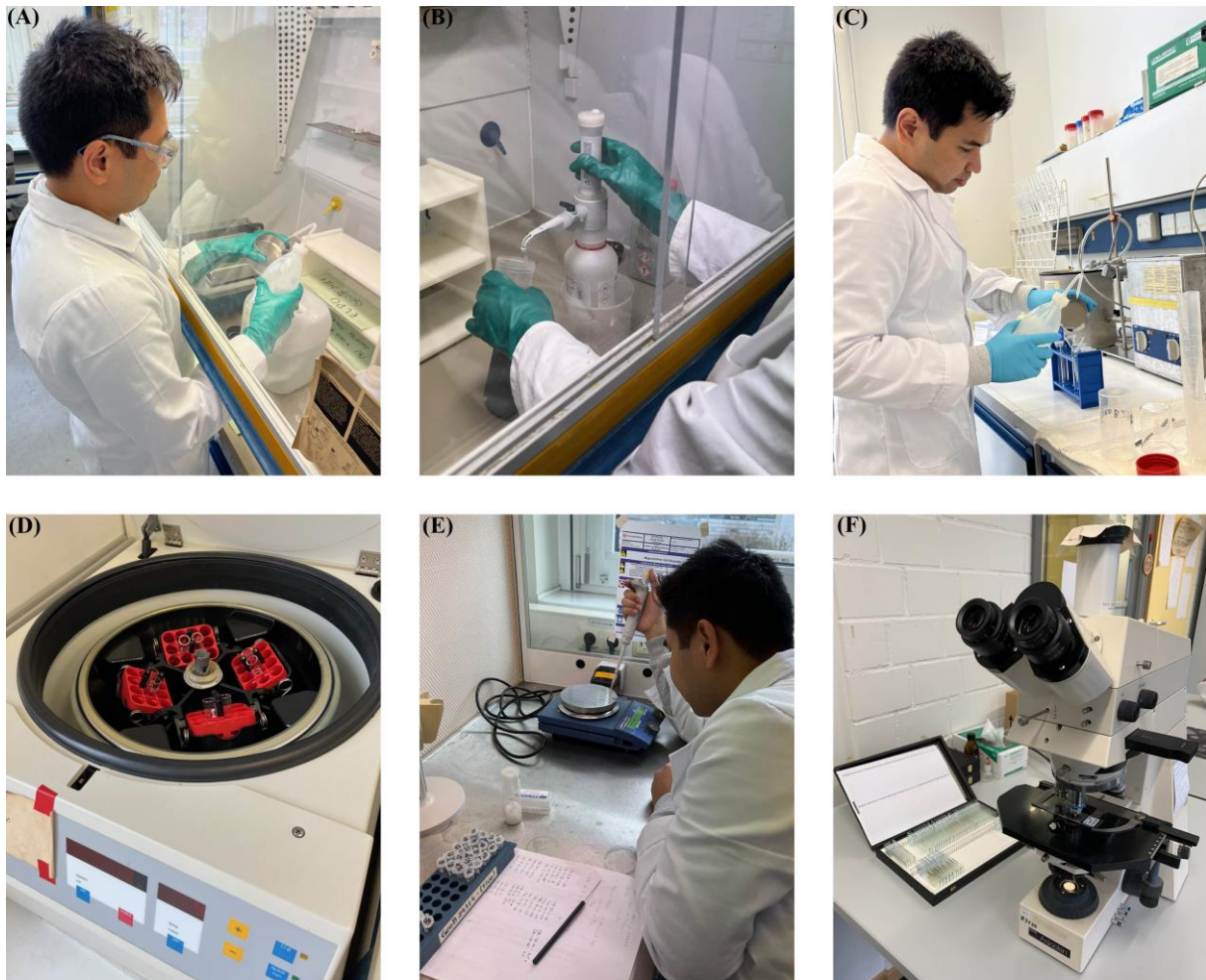


**Figure 2.2.** Several implemented procedures to extract and prepare dinocyst samples in the marine palynology laboratory of the University of Bremen: (A) washing the poisonous  $\text{HgCl}_2$  off the sediment trap samples inside the laminar flow hood, (B) applying HF to the core samples to dissolve siliceous materials, the acid was pumped out through a secured dispenser inside the hood, (C) transferring filtered particles to respective tubes before the sonication procedure, (D) positioning the tube samples equally in the centrifuge tray, (E) transferring an aliquot material to an object glass placed on a heating plate, and (F) identifying dinocysts using a light microscope with 400x magnification.

Sediment samples were thawed, and 1 mL of wet sediment from every sample was transferred to PVC beakers to be dried over two nights at 60° C. After drying, the samples were treated with 10% hydrochloric acid (HCl) to dissolve calcareous materials, after which the samples were left in a fume hood for ca. two hours to enable the dissolution process to complete. The samples were neutralised with 10% kalium hydroxide (KOH) until pH 7. Successively, tap water was added to stabilise the pH. After about 4 hours, the samples were decanted through the 20  $\mu\text{m}$  to be refilled with tap water. After this, 40% hydrofluoric acid (HF) was added to each sample to dissolve siliceous materials (**Figure 2.2B**). For an optimal reaction, the samples were placed on a shaker device to evenly spread the acid within 100 motions per minute for two hours, after which the samples were left for two days for the reaction to complete. The samples were neutralised to pH neutral using 40% KOH before being successively decanted three times.

The samples were filtered using a 20 µm sieve before they were transferred to reagent test tubes and gently sonicated in an ultrasonic bath to clean the dinocysts to be filtered again over a 20 µm sieve (**Figure 2.2C**). This procedure was repeated until no more fine particles were observed during the sonication. The filtered samples were transferred to Eppendorf tubes, centrifuged at 3000 r/min for 10 minutes, and concentrated to 1 ml for the trap samples and 1.5 ml for the core samples (**Figure 2.2D**). A known aliquot of each sample was embedded into glycerine gelatine placed on an objective glass that was placed on a heating plate of 90°C (**Figure 2.2E**). After all the water was evaporated, the sample was covered with a cover slip and sealed using paraffin wax to prevent oxygenation of the organic materials in the sample.

The dinoflagellate cysts were identified using a light microscope (Zeiss Axiovert) under 400x magnification (**Figure 2.2F**). The determination mostly followed the online catalogue of recent organic-walled dinocysts by Zonneveld and Pospelova (2015) based on the cyst morphological features such as colour, shape, processes, tabulation, archeophyle, and wall ornamentation. Some rare dinocysts that were not featured in the online catalogue were identified based on the descriptions reported by Mertens et al. (2020) and van Nieuwenhove et al. (2020). When certain cyst features needed careful observation, the cyst was examined under 1000x magnification using some immersion oil to prevent damage to the objective. The dinocysts were determined at the species level when possible. Various cyst types were grouped into genera. For instance, brown spherical cysts with a smooth wall were grouped as *Brigantedinium* spp., while those with micro-reticulate ornamentation were grouped as *Gymnodinium* spp. *Echinidinium* spp. contained all unidentifiable spiny brown cysts. Transparent cysts that featured septa reflecting tabulation were grouped into *Impagidinium* spp., while those with furcated processes located on the triple junctions were grouped into *Spiniferites* spp. All dinocysts in a sample were counted. The export flux calculation can be found in the methodology sections of Chapters 3, 4, and 5.

### 2.3. Environmental factors

To obtain insight into the environmental factors that influence dinoflagellate cyst export production, the dinocyst export flux has been compared to environmental data of key parameters that are likely to influence dinocyst production. These datasets were wind direction and wind speed, aerosol dust input, sea surface temperature (SST), anomaly of sea surface temperature between the sediment trap location and an area 200 km offshore and the same latitude (SSTa), and the sea surface Chlorophyll-*a* concentration (Chla). The wind system and dust storm events data were obtained from the daily weather report from an airport in Nouadhibou (20°56' N and 17°2' W), a coastal city on the peninsula of Cape Blanc (**Figure 2.1B**). The dust storm event intensity was represented by the difference between the reported visibility distance at the airport with a standardised clear visibility distance of 60 km. A larger negative value indicated higher dust storm intensity. The data from Nouadibhou airport are available from January 2003 until December 2017 with a resolution of 3 hours. Additional data reflecting aerosol dust input was extracted from NASA AERONET (Aerosol Robotic Network), which aerosol particles estimated using various approaches such as the Aerosol Optical Depth (AOD). This algorithm estimated various light wavelengths reflected by aerosol particles in the atmosphere area around Cabo Verde (16° 43.9' N and 22° 56.1' W).

The ocean surface data (SST and Chla) were obtained from the ERDDAP database provided by the National Center for Environmental Information (NCEI) in the vicinity area of the trap at 20° 22.5' N and 18° 22.5' W. Both datasets were available from June 2003 to March 2020 in daily resolution. A lag of 10 days was implemented in each environmental data, correcting for an estimated sinking rate of dinocysts from the upper water column to the collection depth (Fischer and Karakaş, 2009; Iversen and Ploug, 2013). Details with respect to the calculation and access of these data are given in Chapters 3 and 4.

## 2.4. Multivariate analyses

The ordination technique is one of the most commonly used multivariate analyses in ecology. This method visualises the relationship of several variables in multi-dimensional axes (ter Braak et al., 1988). Ordination can elucidate the relationship between the same types of variables, known as the unconstrained method (e.g., species against species), and different types of variables or the constrained method (e.g., species against environmental factors) (ter Braak and Prentice, 1988). Initially, the data trend is tested with detrended correspondence analysis (DCA) to determine the best model to execute the data. The test result is expressed as the length of gradient scores. Scores  $<2$  indicated a linear response of species distribution to environmental gradients, while scores  $\geq 2$  indicate a unimodal response (ter Braak and Prentice, 1988; ter Braak and Šmilauer, 2002). In case the dataset shows a linear a principal component analysis (PCA) is executed for unconstrained analyses and redundancy analysis (RDA) for the constrained analyses. In case the dataset showed a unimodal character, detrended correspondence analysis (DCA) is performed for unconstrained analyses and canonical correspondence analysis (CCA) for the constrained analyses. Regardless of the method used, species, samples, and environmental variables are ordinated along the two most prominent ordination axes (axes 1 and 2). In this dissertation, CCA was applied in Chapter 3 to determine the relationship between key dinocyst species or species groups with environmental parameters. Furthermore, PCA was used in Chapter 5 to determine dinocyst composition shifts in the trap and core data.

## 2.5 Time series analyses

Advanced time series analyses, such as wavelet analysis, were applied to the multi-year sediment trap record to determine cyclic patterns and variations in the dinocyst record and environmental data. Any time series analysis requires a consistent interval throughout the data series. Therefore, the datasets were standardized by interpolating the data for constant time intervals between the data points before conducting further analyses (Lepot et al., 2017). For instance, obtained geoscience records, such as cores, have naturally inconsistent intervals due to variations in sedimentation rates. This latter also occurred in the sediment trap record. Different scientific purposes in each research cruise, malfunctioning of the device, and gaps created by the cruise absence contributed to the high variability of the sampling intervals. For standardisation of the records, the mean of the trap sample interval was calculated, and the result determined the new interval of the environmental data. Interpolated time series were generated using the newly calculated interval with the Piecewise Cubic Hermite Interpolation Polynomial (PCHIP) method (Fritsch and Carlson, 1980). This method was preferred because it represented the original trap time series better than linear and cubic spline methods.

Wavelets have various wave types that can be applied to examine a time series. Among all wave types, the Morlet Wavelet transform was used to analyse the cyclic pattern in our time series (**Figure 2.3A**). Morlet Wavelet fits to analyse climate and ecological time series due to high-resolution frequency and ability to examine patterns in a non-stationary record (Cazelles et al., 2008; Cohen, 2019). The analysed time series will be presented in various colour spectra plotted in two-dimensional axes, period in the y-axis against time in the x-axis (**Figure 2.3B**). The colour spectra range from warm, suggesting a high coefficient correlation between the Morlet Wavelet and the time series, to cold colours that indicate low correlation (Torrence and Compo, 1998; Jensen et al., 2014). More information are available in Chapter 4 regarding the application of wavelet transform in time series.



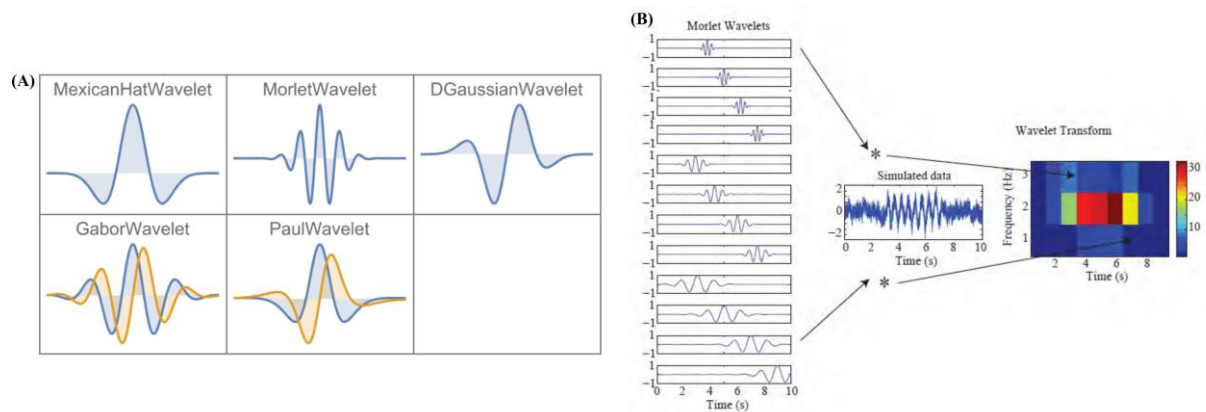


**Figure 2.3.** Technical aspects of wavelet analysis: (A) multiple types of wavelets that can be applied for wavelet transform analyses. The figure was downloaded from the Wolfram website (<http://reference.wolfram.com>) (B) procedures of Morlet Wavelet analysing simulated time series that translated to various colour spectra. The figure was obtained from Jensen et al., 2014.

## 2.6 Age model

Determining the core age was critical for the comparison study between the dinocysts collected by the sediment trap and those in the core. This aspect was needed to calculate the dinocyst accumulation rate in the core similarly to the sampling cup intervals for the export flux estimation in the trap samples. Hanebuth and Henrich (2009) estimated that 1 cm of sediment layer in the vicinity of the study area contains a record of nine years. Thus, six representative sample points were sent to the Chemistry Laboratory of Helmholtz Hereon for a core dating procedure using  $^{210}\text{Pb}/^{137}\text{Cs}$ . The short  $^{210}\text{Pb}$  half-time decay (22.2 years) within the last 100 - 150 years and the high sedimentation rate in the area allowed a high resolution of the core age estimation (Appleby and Oldfield, 1978; Hanebuth and Henrich, 2009). The age dating followed the constant rate of supply (SR) model of the unsupported  $^{210}\text{Pb}$  in the sediments (Appleby and Oldfield, 1978). The linear model of age-depth was applied to determine the sedimentation rates and temporal resolution of every core sample. The resolution of the trap samples was standardised with the resolution of the core samples to allow an adequate comparison. Finally, the unit of cyst accumulation rates in both datasets was calculated as  $\text{cyst m}^{-2} \text{ year}^{-1}$ . More details of this procedure are stated in Chapter 5.

## Chapter 3 - Environmental control of interannual and seasonal variability in dinoflagellate cyst export flux over 18 years in the Cape Blanc upwelling region (Mauritania)

Surya Eldo V. Roza<sup>1</sup>, Gerard G. M. Versteegh<sup>2,3</sup>, Vera Pospelova<sup>4</sup>, Karin A. F. Zonneveld<sup>1,2</sup>

<sup>1</sup>MARUM - Center for Marine Environmental Sciences, University of Bremen, Bremen, Germany

<sup>2</sup>Department of Geosciences, University of Bremen, Bremen, Germany

<sup>3</sup>Department of Physics and Earth Sciences, Constructor University, Bremen, Germany

<sup>4</sup>Department of Earth and Environmental Sciences, University of Minnesota, Minneapolis, United States

*Published in Frontiers in Marine Science*

### Abstract

The increasing threat of anthropogenic environment and climate change amplifies the urgency to investigate the effect of these changes on marine ecosystems. We provide information about the export flux of organic-walled dinoflagellate cysts between 2003 and 2020 in the upwelling ecosystem off Cape Blanc (Mauritania), one of the world's most productive regions. We compared the cyst export flux with variability in environmental parameters, such as wind speed, wind direction, dust emission, sea surface temperature (SST), SST difference between trap location and open ocean (SSTa), and chlorophyll-*a* concentration. This information is valuable to determine the ecological signal of dinoflagellate cysts that could be applied in recent and paleo records. The total export production of dinoflagellate cysts fluctuated between 0 - 1.18 x 10<sup>5</sup> cysts m<sup>-2</sup> d<sup>-1</sup> for the heterotrophs and 0 - 1.06 x 10<sup>4</sup> cysts m<sup>-2</sup> d<sup>-1</sup> for the photo-/mixotrophs. The export productions of both groups were in line with changes in upwelling intensity, which in most years, intensified in spring - summer. Dinoflagellate cyst association was dominated by heterotrophic taxa that formed an average of 94% of the association throughout the sediment trap record. A strong interannual variation in the cyst export fluxes, as well as the association composition, was observed in the record. We identified five groups that showed comparable variability in export production with changes in environmental conditions: (1) maximal upwelling; *Echinidinium delicatum/granulatum*, *E. transparentum/zonneveldiae*, *Echinidinium* spp., *Trinovantedinium* spp., and *Protoperidinium latidorsale*, (2) combined maximal upwelling and dust input; *Archaeoperidinium* spp., *P. americanum*, *P. stellatum*, and *P. subinermis*, (3) upwelling relaxation; *Gymnodinium* spp. and *L. polyedra*, (4) warm surface waters; *Bitectatodinium spongium* and *Protoceratium reticulatum*, and (5) species with no specific relationship to the studied environmental variables; *Brigantedinium* spp., *E. aculeatum*, *Impagidinium aculeatum*, *P. conicum*, *P. monospinum*, *Pentapharsodinium dalei*, and *Spiniferites* spp. The sediment trap record documented a gradual shift in the cyst taxa association that co-occurred with the gradual increase of Saharan dust input to the region, notably after 2008. The cyst association contained five photo-/mixotrophic taxa formed by potentially toxic dinoflagellates. The latter could cause threats to the socio-economy of coastal communities.

**Keywords:** dinoflagellate cysts, ecology, coastal upwelling, Saharan dust, interannual variability, ecosystem change

### 3.1. Introduction

Along with diatoms and coccolithophorids, dinoflagellates are among the major eukaryotic primary producers in marine environments (e.g., Dale and Dale, 1992; Rochon et al., 1999). Dinoflagellates include species with various feeding strategies: some are photosynthetic, heterotrophic, and many are mixotrophic (e.g., Schnepf and Elbrächter, 1992; Taylor et al., 2008; Jeong et al., 2010).

The composition of the dinoflagellate community is strongly influenced by the upper water column environmental and oceanographic conditions (Rochon et al., 1999; Taylor et al., 2008; Gómez, 2012). Within the scope of the concern about the anthropogenic impact on climate and marine ecosystems, changes in the dinoflagellate community can be used as a key indicator to study the impact of these changes on marine ecosystems (e.g., Kremp et al., 2016; Brosnahan et al., 2020).

Around 15% of the extant dinoflagellate species are known to produce fossilisable cysts that have a species-specific morphology (e.g., Dale, 1976; Head, 1996; Dale et al., 2002; Bravo and Figueroa, 2014; Luo et al., 2019). After production in the upper water column, cysts sink to the ocean floor, where they can form a seed bank (e.g., Head, 1996; Matsuoka and Head, 2013; Bravo and Figueroa, 2014). Cysts of some species can remain viable in the sediment for up to a century (Lundholm et al., 2011; Ellegaard and Ribeiro, 2018; Delebecq et al., 2020). Dinoflagellate cysts in sedimentary archives are widely used for environmental, oceanographic, and climatic reconstruction and provide insight into past dinoflagellate bloom dynamics (e.g., Matsuoka and Head, 2013; Zonneveld et al., 2018; Sala-Pérez et al., 2020). To establish an adequate reconstruction of past environmental conditions, detailed information about cyst-forming dinoflagellates ecology is essential. Several dinoflagellate species can produce biotoxins or can form Harmful Algal Blooms (HAB), which can be a significant threat to marine ecosystems and human health (e.g., Balech 1985; Amorim et al., 2001; Figueroa et al., 2018; Anderson et al., 2021). To understand the bloom dynamics of dinoflagellate species, including potentially toxic ones, information about the relationship between upper water column conditions and long-term variability in cyst export production of these species is required.

The number of studies on the ecology of dinoflagellate cysts has increased notably over the last decades (e.g., de Vernal et al., 2020; García-Moreiras et al., 2021; Likumahua et al., 2021; Rodríguez-Villegas et al., 2022; Zonneveld et al., 2022b; Obrezkova et al., 2023). However, only limited information is available about the seasonal, intra-, and interannual variability in dinoflagellate cyst production and their species composition. A method to investigate these aspects is to study sediment trap records (e.g., Dale and Dale, 1992; Harland and Pudsey, 1999; Zonneveld and Brummer, 2000; Fujii and Matsuoka, 2006; Pitcher and Joyce, 2009; Pospelova et al., 2010; Price and Pospelova, 2011; Bringué et al., 2013; Pospelova et al., 2018; Romero et al., 2020). Previous sediment trap studies showed highly variable cyst production and taxa composition over time. Studying a long time series is essential to obtain a better insight into the interannual variability. Until now, decade-long studies are limited, with only one record from the Cariaco Basin covering 12.5 years (Bringué et al., 2019). Here, we enhance the information about the ecology and long-term variability of dinoflagellate cysts by providing a record of cyst export production in the Cape Blanc upwelling region over 18 years.

Cape Blanc in the Canary-Current upwelling system is one of the world's most noteworthy marine ecosystems, forming part of the Eastern Boundary Upwelling Ecosystems (EBUEs). Although covering a small portion of the Earth's ocean surface (ca. 10%), EBUEs are marine diversity hotspots and contribute significantly to marine primary production (e.g., Pauly and Christensen, 1995; Arístegui et al., 2008). In the study area, primary production is enhanced by permanent upwelling and import of trace elements by Saharan dust (e.g., Mittelstaedt, 1983; van Camp et al., 1991; Hagen, 2001). Upwelling on the Atlantic Coast of Mauritania is supported by the coastal wind system, favourable shelf morphology, and surface currents that can transport nutrient-rich water farther offshore (e.g., Mittelstaedt, 1983; Hagen, 2001). Although upwelling occurs all year long, its strongest intensity is observed during boreal winter (winter and spring seasons) (e.g., Lathuilière et al., 2008; Cropper et al., 2014). A similar trend is shown by the dust emission from the Sahara into the Cape Blanc oceanic area by the winds at low altitudes (0 - 3 km) (Stuut et al., 2005; Adams et al., 2012; Skonieczny et al., 2013). The strength of upwelling and dust emission in winter and spring is influenced by the Inter Tropical Convergence Zone (ITCZ), which migrates southward to the equator realm during boreal winter and northward during boreal summer (Mittelstaedt, 1991; Ben-Ami et al., 2009; Adams et al., 2012; Yu et al., 2019).

Here, we present records of the export flux of organic-walled dinoflagellate cysts in the Cape Blanc upwelling area collected by a sediment trap covering the time span from 2003 until 2020 with temporal resolution between 3.5 and 22 days. The trap was moored close to the position of active upwelling cells at a location where upwelling filaments frequently pass the upper waters. We expanded the five years (2003-2008) dataset of Romero et al. (2020) with data from the following 13 years (**Table 3.1**). To obtain insight into abiotic factors that influence the export production of the photo-/mixotrophic and heterotrophic cyst species we compared dinoflagellate cyst fluxes and the association composition with wind speed, wind direction, atmospheric dust concentration, sea surface temperature (SST), SST difference between trap location and open ocean (SSTa), and sea surface chlorophyll-*a* concentration (Chl-*a*) at or in the vicinity of the trap location.

**Table 3.1.** Detailed information of CBeu sediment trap deployments and recoveries during multiple research expeditions off Cape Blanc (Mauritania, NW Africa).

Mooring CBeu	Coordinates	GeoB code and cruise	Trap depth (m)	Ocean depth (m)	Number of samples	Sample interval (sample size x days)	Sampling duration
1	20°45.0' N 18°42.0' W	-/POS 310	1296	2714	20	1x10.5; 19x15.5	05/06/2003 - 05/04/2004
2	20°45.0' N 18°42.0' W	9630-2/M 65-2	1296	2714	20	2x22; 18x23	18/04/2004 - 20/07/2005
3	20°45.5' N 18°41.9' W	11404-3/POS 344	1277	2693	20	20x21.5	25/07/2005 - 28/09/2006
4	20°45.7' N 18°42.4' W	11835-2/MSM 04b	1256	2705	20	1x3.5; 19x7.5	28/10/2006 - 23/03/2007
5	20°44.9' N 18°42.7' W	12910-2/POS 365-2	1263	2709	38	2x6.5; 36x9.5	28/03/2007 - 17/03/2008
6	20°45.1' N 18°41.9' W	13612-1/MSM 11-2	1263	2699	40	2x3.5; 38x8.5	26/04/2008 - 22/03/2009
7	20°44.6' N 18°42.7' W	14202-4/POS 396	1364	2761	37	37x9	01/04/2009 - 28/02/2010
8	20°44.6' N 18°42.7' W	15703-2/MSM 18-1	1322	2720	18	17x10; 1x4	06/03/2010 - 27/08/2010
9	20°46.7' N 18°44.1' W	16103-1/POS 425	1362	2770	16	15x17; 1x10.5	01/05/2011 - 21/01/2012
10	20°46.6' N 18°44.2' W	17108-3/POS 445	1318	2712	35	1x4; 1x7.1; 33x10.75	26/01/2012 - 26/01/2013
11	20°46.4' N 18°44.4' W	18006-2/POS 464	1299	2800	18	17x21; 1x20.5	29/01/2013 - 10/02/2014
12	20°46.6' N 18°44.5' W	19402-1/POS 481	1249	2750	20	1x12.5; 1x10.9; 18x19.5	14/02/2014 - 23/02/2015
13	20°53.0' N 18°43.9' W	20702-1/POS 495	1346	2739	20	1x14; 19x18	27/02/2015 - 18/02/2016
14	20°52.5' N 18°44.7' W	22101-1/POS 508	1356	2749	16	1x18.5; 14x21.5; 1x14.9	25/02/2016 - 24/01/2017
15	20°52.1' N 18°45.4' W	22416-1/M 140	1309	2751	20	20x10.5	26/01/2017 - 24/08/2018
16	20°50.7' N 18°44.6' W	23318-1/MSM 79	1253	2694	20	1x20; 18x22; 1x24	02/09/2017 - 16/11/2011
17	20°50.7' N 18°44.6' W	24104-1/M 165	1252	2694	20	1x21; 19x25	20/11/2018 - 30/03/2020

## 3.2. Materials and Methods

### 3.2.1. Oceanography of the study area

The current research was carried out in the Canary Current Eastern Boundary Upwelling Ecosystem (CC-EBUEs) located at the eastern border of the North Atlantic Subtropical Gyre (e.g., Arístegui et al., 2009; Cropper et al., 2014). The region is characterised by permanent upwelling driven by the equatorward wind trade system and frequent input of Saharan dust. Both upwelling and dust fertilize the upper ocean with the input of nutrients and trace elements, resulting in the CC-EBUEs being one of the most productive oceanic regions in the world (Mittelstaedt, 1983; van Camp et al., 1991; Hagen, 2001; Lathuilière et al., 2008). The surface currents in this area consist of the Canary Current (CC) and Mauritanian Current (MC) (**Figure 3.1**). The CC flows southwards along the northern coast of NW Africa, where it detaches from the shelf between 7° - 20° N, supplying cool coastal upwelled water to the North Equator Current (NEC) (Mittelstaedt, 1991; Alves et al., 2002). The MC gradually flows northward parallel to the Mauritanian coast towards 20° N, transporting warm waters of southern origin northwards (Mittelstaedt, 1983). MC intensifies in summer when it is pushed to the shelf by the North Equatorial Counter Current but weakens and is gradually replaced by the CC in late autumn due to increasing trade wind intensity south of 20° N (Zenk et al., 1991). The movement of both surface currents creates a substantial horizontal shear in the surface layer, forming a convergence zone called the Cape Verde Frontal Zone (CVFZ) (Zenk et al., 1991).

Although coastal upwelling off Cape Blanc is a permanent feature, its maximal southward extension and intensity vary depending on the strength and direction of the surface winds (Lathuilière et al., 2008; Cropper et al., 2014). Maximal upwelling intensity is mainly observed in winter and spring, whereas lower intensity is often observed in summer and autumn (Fischer et al., 2016). The annual trend of the surface wind trade system variation is orchestrated by the seasonal migration of the Inter-Tropical Convergence Zone (ITCZ) (Mittelstaedt, 1991).

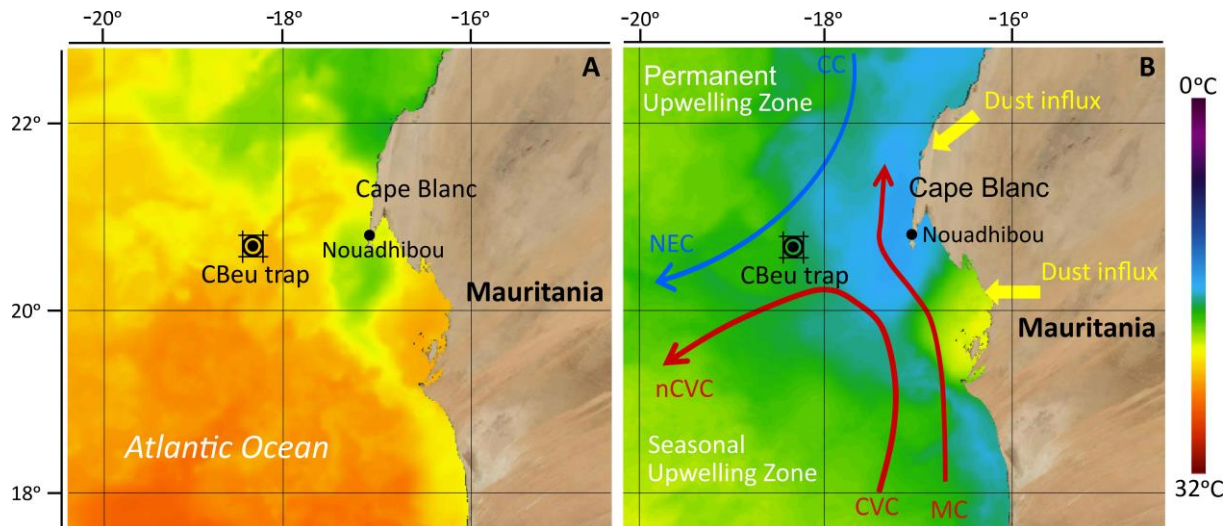


**Figure 3.1.** The location of the CBeu sediment trap (double black circle) and the surface currents in the studied area adapted after Mittelstaedt (1983, 1991) and Zenk et al. (1991). Blue arrow: relatively cold waters of the Canary Current (CC) and North Equatorial Current (NEC). Red arrows: warm waters of the Mauritanian Current (MC), Cape Verde Current (CVC), and north Cape Verde Current (nCVC). Satellite image depicted from NASA “State Of The Ocean (SOTO)” showing sea surface temperature during (A) low upwelling intensity in autumn 2020 and (B) high upwelling intensity in spring 2021.

Upwelled water in the region is sourced from subsurface waters, either from the southward-flowing North Atlantic Central Water (NACW) or the northward-flowing South Atlantic Central Water (SACW) (Mittelstaedt, 1991; Meunier et al., 2012; Olivar et al., 2016). NACW originates from the North Atlantic carrying warmer, more saline, and nutrient-poorer water compared to SACW (Sarmiento et al., 2004). SACW originates from the Southern Ocean, moving north (Sarmiento et al., 2004). Upwelled waters north of Cape Blanc mainly consist of NACW, south of Cape Blanc they are mainly formed by SACW. Off Cape Blanc, NACW forms the major source of upwelling waters at times of maximal upwelling intensity, whereas larger amounts of SACW form the upwelled waters at times of low upwelling intensity (Sarmiento et al., 2004).

Dust emission also plays an important role in the vast growth of plankton in the region. Sahara, as the world’s largest contributor of aeolian mineral dust, influences the studied area by providing essential elements, such as iron and phosphorus (Kolber et al., 1994; Jickells et al., 2005; Huneus et al., 2011). The maximum dust emission in this research area occurs in winter, with dust transported by surface winds at altitudes between 0 - 3 km (Stuut et al., 2005; Adams et al., 2012; Skonieczny et al., 2013; Fomba et al., 2014; Fischer et al., 2016). In summer, dust emissions mainly occur at more distal locations (e.g., the Caribbean) due to Saharan Air Layer (SAL), transporting dust at higher altitudes (5 - 7 km) (Prospero, 1990; Stuut et al., 2005; Adams et al., 2012; Prospero et al., 2014). The occurrence and intensity of dust storms in the Sahara are strongly influenced by the ITCZ, which controls the aridity of the continent and the direction and strength of the wind as an aerosol-carrier to the ocean (Ben-Ami et al., 2009; Adams et al., 2012; Yu et al., 2019).

### 3.2.2. Mooring site and sample treatment

Dinoflagellate cysts were collected between June 2003 and March 2020 at the Cape Blanc eutrophic mooring (CBeu) station (**Figure 3.1**). The trap was located between 20°44.6' - 20°53.0' N and 18°41.9' - 18°45.4' W at water depths between 1249 – 1364 m (**Table 3.1**). Samples were collected by a classical cone-shaped trap with a surface opening area of 0.5 m<sup>2</sup> (Kiel SMT 230/234, Kremling

1998). Particle collection time varied between 3.5 and 22 days. The sampling cups contained mercury chloride ( $\text{HgCl}_2$ ) to prevent biochemical degradation and alteration of the captured organic material. More details on the sample processing were given by Mollenhauer et al. (2015), Romero and Fischer (2017), and Fischer et al. (2019). A total of 369 samples were collected and used throughout the 18 years of study.

Upon recovery, the materials were evenly divided into 1/125 fractions for various purposes using a Mc Lane splitter (Romero and Fischer, 2017; Fischer et al., 2019; Romero et al., 2020). Initially, the larger nektonic plankton, such as the copepods, were manually removed. Samples were filtered with a sieve of 1 mm pore size to isolate the target protists from coarser particles. The samples were transferred into sampling bottles and stored in the dark at the MARUM core repository for further treatment. They were kept at 4°C to prevent degradation of the organic content.

### 3.2.3. Dinoflagellate cysts extraction and taxonomic identification

For every sample, a 1/125 fraction of the material was sieved with distilled water over a 100  $\mu\text{m}$  and a 20  $\mu\text{m}$  high-precision metal sieve (Storck-Veco) to remove the remaining poisonous  $\text{HgCl}_2$ . The washed samples were ultrasonically treated and sieved successively over a high-precision sieve with a pore size of 20  $\mu\text{m}$ . The remaining material was transferred to Eppendorf tubes, diluted to 1 mL, and homogenized. A known volume of the well-mixed sample was embedded in glycerin gelatin that was placed on a microscope slide, covered with a cover slip, and isolated from the air with wax (Zonneveld et al. 2010, 2022b). Organic dinoflagellate cysts were studied by light microscopy (Zeiss Axiovert, 400x magnification). The dinoflagellate export flux ( $\text{cyst m}^{-2} \text{ day}^{-1}$ ) was calculated by dividing the counted specimens with the initial split fraction (1/125), the volume of the counted sample, the trap collection area, and the sampling collecting duration. Taxonomic identification of dinoflagellate cysts and the motile affinity were based on Zonneveld and Pospelova (2015), Mertens et al. (2020), and van Nieuwenhove et al. (2020). Cysts identified at the species level with well-established cyst-theca relationships were referred to by their theca names following the statement of Elbrächter et al. (2023). For the motile affinity of cysts produced by toxin-producing dinoflagellates, see Wall and Dale (1968), Sarjeant (1970), Anderson et al. (1988), Dodge (1989), Head (1996), and Ellegaard and Moestrup (1999).

### 3.2.4. Environmental parameters

Dinoflagellate cyst fluxes and associations composition were compared to wind speed, wind direction, atmospheric dust concentration, sea surface temperature (SST), SST difference between trap location and open ocean (SSTa), and sea surface chlorophyll-*a* concentration (Chl-*a*). Wind speed ( $\text{m s}^{-1}$ ), wind direction, and occurrences of dust input were derived from Nouadhibou Airport (20°56' N and 17°2' W) meteorological report, the land-based location near the sediment trap (**Figure 3.1**). The decoded synoptic values were calculated to determine vector values of wind strength relative to the measured wind direction according to the equations below (Grange, 2014):

$$\vec{u} = -u_i \times \sin \left[ 2\pi \times \frac{\theta_i}{360} \right] \quad \text{calculated vector wind from north}$$

$$\vec{v} = -u_i \times \cos \left[ 2\pi \times \frac{\theta_i}{360} \right] \quad \text{calculated vector wind from east}$$

$$\bar{\theta}_{RV} = \arctan \left( \frac{\vec{u}}{\vec{v}} \right) + \text{flow} \quad \text{calculated resultant vector average of the wind direction}$$

$$\text{flow} = +180 \text{ for } \arctan \left( \frac{\vec{u}}{\vec{v}} \right) < 180^\circ \text{ and } -180 \text{ for } \arctan \left( \frac{\vec{u}}{\vec{v}} \right) > 180^\circ$$

where  $u_i$  is wind speed ( $\text{m s}^{-1}$ ) and  $\theta_i$  is wind direction ( $^\circ$ ). Atmospheric dust concentration was defined by the minimal distance of horizontal visibility. Enhanced atmospheric dust concentration was detected when the visibility distance values were below 60 km.

**Table 3.2.** The list of identified heterotrophic dinoflagellate cyst (paleontological) taxa in the studied area corresponds to their respective motile cell (biological) names and grouping of cysts used in statistical analysis.

Cyst name	Motile name	Taxon used in multivariate analysis
<i>Brigantedinium</i> spp. Reid, 1977 ex Lentini and Williams, 1993	<i>Protoperidinium</i> sp.	<i>Brigantedinium</i> spp.
Cyst of <i>Archaeperidinium constrictum</i> Mertens et al., 2015	<i>Archaeperidinium constrictum</i> Mertens et al., 2015	<i>Archaeperidinium</i> spp.
Cyst of <i>Archaeperidinium minutum</i> Yamaguchi et al., 2011	<i>Archaeperidinium minutum</i> Yamaguchi et al., 2011	
Cyst of <i>Archaeperidinium saanichi</i> Mertens et al., 2012	<i>Archaeperidinium saanichi</i> Mertens et al., 2012	
Cyst of <i>Polykrikos kofoidii</i> Chatton, 1914	<i>Polykrikos kofoidii</i> Chatton, 1914	<i>Polykrikos</i> spp.
Cyst of <i>Polykrikos schwartzii</i> Bütschli, 1873	<i>Polykrikos schwartzii</i> Bütschli, 1873	
Cyst of <i>Polykrikos quadratus</i> Kunz-Pirrung, 1998 - informally described	<i>Polykrikos quadratus</i> Kunz-Pirrung, 1998 - informally described	
Cyst of <i>Protoperidinium americanum</i> (Gran and Braarud, 1935) Balech, 1974	<i>Protoperidinium americanum</i> (Gran and Braarud, 1935) Balech, 1974	<i>P. americanum</i>
Cyst of <i>Protoperidinium monospinum</i> (Paulsen, 1907) Zonneveld and Dale, 1984	<i>Protoperidinium monospinum</i> (Paulsen, 1907) Zonneveld and Dale, 1984	<i>P. monospinum</i>
Cysts of <i>Protoperidinium stellatum</i> (Wall in Wall and Dale, 1968) Head in Rochon et al., 1999	<i>Protoperidinium stellatum</i> (Wall in Wall and Dale, 1968) Head in Rochon et al., 1999	<i>P. stellatum</i>
<i>Echinidinium aculeatum</i> Zonneveld 1997 ex Mertens et al., 2020	Unknown	<i>E. aculeatum</i>
<i>Echinidinium delicatum</i> Zonneveld 1997 ex Head, 2003	Unknown	<i>E. delicatum/granulatum</i>
<i>Echinidinium granulatum</i> Zonneveld 1997 ex Head, 2001	Unknown	
<i>Echinidinium transparentum</i> Zonneveld 1997 ex Mertens et al., 2020	Unknown	<i>E. transparentum/zonneveldiae</i>
<i>Echinidinium zonneveldiae</i> Head, 2003	Unknown	
Unidentified spiny brown cysts	Unknown	<i>Echinidinium</i> spp.
<i>Lejeunecysta paratenella</i> Benedek, 1972	<i>Protoperidinium</i> sp.	<i>L. paratenella</i>
<i>Quinquecuspis concretum</i> (Reid, 1977) Harland, 1977	<i>Protoperidinium leonis</i> Reid, 1977	<i>P. leonis</i>
<i>Selenopemphix nephroides</i> Benedek, 1972	<i>Protoperidinium subinermis</i> (Paulsen, 1904) Loeblich III, 1970	<i>P. subinermis</i>
<i>Selenopemphix quanta</i> (Bradford, 1975) Matsuoka, 1985	<i>Protoperidinium conicum</i> (Gran, 1900) Balech, 1974	<i>P. conicum</i>
<i>Trinovantedinium applanatum</i> (Bradford, 1977) Bujak and Davies, 1983	<i>Protoperidinium shanghaiense</i> Gu et al., 2015	<i>Trinovantedinium</i> spp.
<i>Trinovantedinium pallidifolium</i> Mertens et al., 2017	<i>Protoperidinium louisianense</i> Mertens et al., 2017	
<i>Votadinium calvum</i> (Reid, 1977)	<i>Protoperidinium latidorsale</i> (Dangeard, 1927) Balech, 1974	<i>P. latidorsale</i>
Cyst of <i>Diplopelta symmetrica</i> Dale et al., 1993	<i>Diplopelta symmetrica</i> Dale et al., 1993	Excluded from the analysis
Cyst of <i>Dubridinium</i> sp. Reid, 1977	<i>Preperidinium</i> sp.?	
Cyst of <i>Islandinium</i> spp. Head et al., 2001 emend. Potvin et al., 2013	<i>Islandinium</i> spp. Head et al., 2001 emend. Potvin et al., 2013	
Cyst of <i>Polykrikos hartmanii</i> (Matsuoka and Fukuyo, 1986) Radi et al., 2013	<i>Polykrikos hartmanii</i> (Matsuoka and Fukuyo, 1986) Radi et al., 2013	
Cruciform cyst	Unknown	
Cyst type A	Unknown	
Cyst type B	Unknown	
<i>Echinidinium bispiniformum</i> Zonneveld 1997 ex Mertens et al., 2020	Unknown	
<i>Echinidinium karaense</i> Head et al., 2001	Unknown	
<i>Leipokatium invisitatum</i> (Bradford, 1975)	Unknown	
<i>Lejeunecysta oliva</i> (Bradford, 1975) Turon and Londeix, 1988	<i>Protoperidinium</i> sp.	
<i>Lejeunecysta sabrinum</i> (Reid, 1977) Bujak, 1984	<i>Protoperidinium leonis?</i> (Pavillard, 1916) Balech, 1974	
<i>Selenopemphix undulata</i> Verleye et al., 2011	Unknown	
Unidentified peridinioid-form	<i>Protoperidinium</i> sp.?	
<i>Votadinium spinosum</i> (Reid, 1977)	<i>Protoperidinium claudicans</i> (Paulsen, 1907) Balech, 1974	
<i>Xandarodinium xanthum</i> (Reid, 1977)	<i>Protoperidinium divaricatum</i> (Meunier, 1919) Parke and Dodge, 1976	

SST and Chlorophyll-*a* data were obtained from ERDDAP daily optimum interpolation (OI), AVHRR dataset (Dataset ID ncdcOisst21Agg\_Lon PM 180), from the database of the National Oceanic and Atmospheric Administration (NOAA) for a 4 km grid at the trap location (20° 22.5' N and 18° 22.5' W). Sea surface temperature anomaly (SSTa) represents the difference between the daily values of SST at the trap location and 200 km offshore at the same latitude located outside the influence of upwelling and offshore drifting upwelling filaments (Cropper et al., 2014). More negative SSTa values represent the presence of colder waters at the trap site, which in the region is caused by the presence of upwelled water, as such SSTa represents the upwelling intensity. The daily values of all environmental parameters were calculated as lag and an average of 10 days for the region's estimated sinking duration of the dinoflagellate cyst in the water column (Fischer and Karakaş, 2009; Iversen and Ploug, 2013).

**Table 3.3.** The list of identified photo-/mixotrophic dinoflagellate cyst (paleontological) taxa in the studied area corresponds to their respective motile cell (biological) names and grouping of cysts used in statistical analysis.

Cyst name	Motile name	Taxon used in multivariate analysis
<i>Bitectatodinium spongium</i> (Zonneveld, 1997) Zonneveld and Jurkschat, 1999	Unknown	<i>B. spongium</i>
Cyst of <i>Gymnodinium nolleri</i> Ellegaard and Moestrup, 1999	<i>Gymnodinium nolleri</i> Ellegaard and Moestrup, 1999	<i>Gymnodinium</i> spp.
Cyst of <i>Gymnodinium microreticulatum</i> Bolch, Negri and Hallegraeaf, 1999	<i>Gymnodinium microreticulatum</i> Bolch, Negri and Hallegraeaf, 1999	
Cyst of <i>Pentaparsodinium dalei</i> Indelicato and Loeblich III, 1986	<i>Pentaparsodinium dalei</i> Indelicato and Loeblich III, 1986	<i>P. dalei</i>
<i>Impagidinium aculeatum</i> (Wall 1967) Lentin and Williams, 1981	<i>Gonyaulax</i> sp.	<i>I. aculeatum</i>
<i>Impagidinium paradoxum</i> (Wall 1967) Stover and Evitt, 1978	<i>Gonyaulax</i> sp.	<i>Impagidinium</i> spp.
<i>Impagidinium patulum</i> (Wall 1967) Stover and Evitt, 1978	<i>Gonyaulax</i> sp.	
<i>Impagidinium plicatum</i> Versteegh and Zevenboom, 1995	<i>Gonyaulax</i> sp.	
<i>Impagidinium sphaericum</i> (Wall 1967) Lentin and Williams, 1981	<i>Gonyaulax</i> sp.	
<i>Impagidinium striatum</i> (Wall 1967) Stover and Evitt, 1978	<i>Gonyaulax</i> sp.	
<i>Impagidinium variaseptum</i> Marret and de Vernal, 1997	<i>Gonyaulax bohaisensis</i> Gu et al., 2022	
Unidentified <i>Impagidinium</i>	<i>Gonyaulax</i> sp.	
<i>Lingulodinium machaerophorum</i> (Deflandre and Cookson, 1955) Wall, 1967	<i>Lingulodinium polyedra</i> (Stein, 1883) Dodge, 1989	<i>L. polyedra</i>
<i>Operculodinium centrocarpum</i> sensu Wall and Dale, 1966	<i>Protoceratium reticulatum</i> (Claparède and Lachmann, 1859) Bütschli, 1885	<i>P. reticulatum</i>
<i>Operculodinium israelianum</i> (Rossignol, 1962) Wall, 1967	<i>Protoceratium</i> sp.?	<i>O. israelianum</i>
<i>Spiniferites membranaceus</i> (Rossignol, 1964) Sarjeant, 1970	<i>Gonyaulax membranacea</i> (Rossignol, 1964) Ellegaard et al., 2003	<i>Spiniferites</i> spp.
<i>Spiniferites mirabilis</i> (Rossignol, 1964) Sarjeant, 1970	<i>Gonyaulax spinifera</i> (Claparède and Lachmann, 1859)	
<i>Spiniferites pachydermus</i> (Rossignol, 1964) Reid, 1974	<i>Gonyaulax ellegaardiae</i> Mertens et al., 2015	
<i>Spiniferites ramosus</i> (Ehrenberg, 1838) Mantell, 1854	<i>Gonyaulax spinifera</i> complex	
Unidentified <i>Spiniferites</i>	<i>Gonyaulax</i> sp.	
<i>Ataxiodinium choane</i> Reid, 1974	<i>Gonyaulax spinifera</i> complex	Excluded from the analysis
<i>Biecheleria</i> sp.	Unknown	
<i>Dalella chathamensis</i> McMinn and Sun, 1994	Unknown	
<i>Nematospaeropsis labyrinthus</i> (Ostenfeld, 1903) Reid, 1974	<i>Gonyaulax</i> sp.	
<i>Polysphaeridium zoharyi</i> (Rossignol, 1962) Bujak, 1980	<i>Pyrodinium bahamense</i> Plate, 1906	
<i>Pyxidinopsis psilata</i> Wall and Dale, 1973	Unknown	
<i>Pyxidinopsis reticulata</i> McMinn and Sun, 1994 emend. Marret and de Vernal, 1997	Unknown	
<i>Tectatodinium pellitum</i> Wall, 1967 emend. Head, 1994	Unknown	

### 3.2.5. Statistical analyses

Dinoflagellate cysts and environmental parameter data were analysed by multivariate analyses that can independently explain the relationship between multiple variables, using the software package



Canoco-5 (Šmilauer and Lepš, 2014). For the analyses, species occurring only sporadically in low numbers in the dataset were excluded from this analysis (**Table 3.2 and 3.3**). Multivariate analyses were performed on the relative abundances by excluding samples that contained less than 100 specimens. Detrended Correspondence Analysis (DCA) was carried out to analyse the length of the gradient to verify the species response curves in the dataset (ter Braak et al., 1988; ter Braak and Šmilauer, 2002). Additionally, a Canonical Correspondence Analysis (CCA) was used to determine the relationship between the cyst distribution patterns and the above-described environmental parameters.

### 3.3. Results

#### 3.3.1. Dinoflagellate cyst flux

Throughout 18 years, the cyst export flux of heterotrophic dinoflagellates largely exceeded the photo-/mixotrophic dinoflagellates. On average, heterotrophic taxa formed ca. 94% of the total cyst record. The export flux of heterotrophic dinoflagellate cysts showed large interannual fluctuations with minimal fluxes occurring in spring - summer 2018 when no export flux was observed and maximal flux in winter 2011/2012 ( $1.18 \times 10^5$  cysts  $m^{-2} d^{-1}$ ) (**Figure 3.2B**). A malfunctioning of the sediment trap led to these minimal fluxes, but the samples could still be recovered from the cups. Over the years, the flux showed a trend from relatively low values between 2003 and 2005 to higher values between 2006 – 2013 and declined again after 2014. Exceptions were noted in 2009 and 2010, characterised by lower export fluxes than in the previous and later years. Throughout the years, the flux showed a more or less regular seasonal pattern, with maximal flux occurring in spring at times of maximal wind speed (**Figure 3.2A**). The duration of the high flux period varied; sometimes, it started in late winter or extended to summer. In other years, it was restricted to spring. Few exceptions occurred in 2005 and 2018, where the maximal fluxes occurred in autumn.

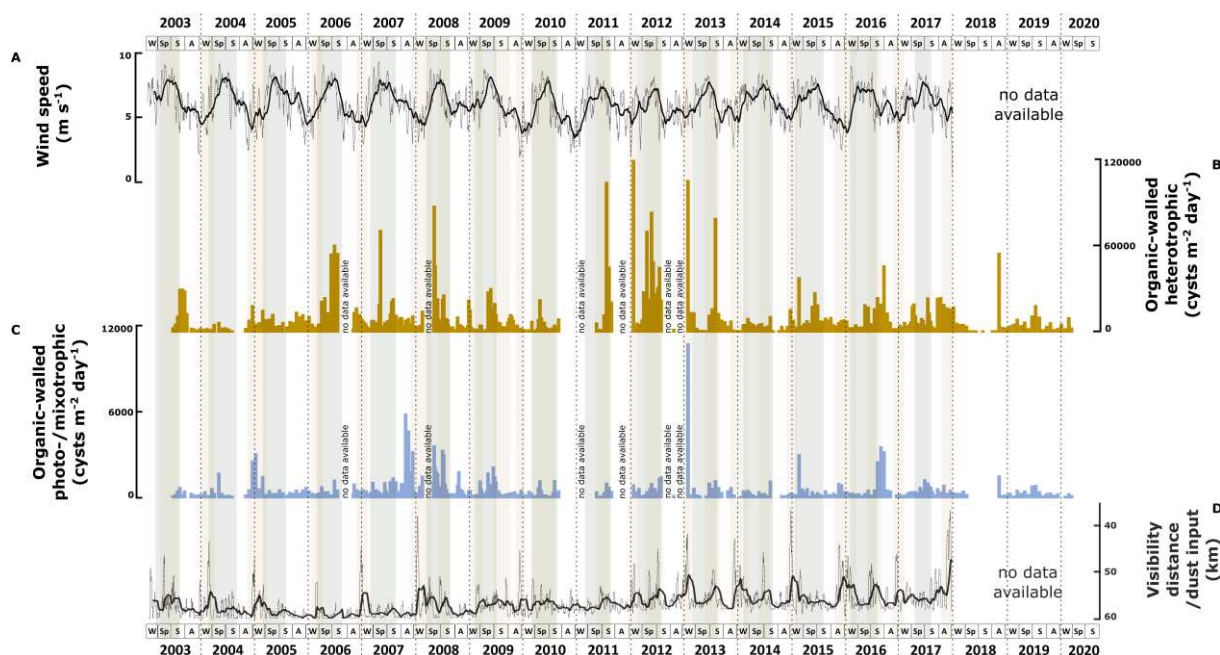


**Figure 3.2.** Correlation of environmental parameters with the total export fluxes of organic-walled dinoflagellate cysts based on 18 years CBeu sediment trap study: (A) daily wind speed in 10-running point average (the background grey line connects daily data points and the thicker black line represents the 10-point mean); (B) heterotrophic dinoflagellate cysts (cysts  $m^{-2} d^{-1}$ , dark yellow bars); (C) photo-/mixotrophic dinoflagellate cysts (cysts  $m^{-2} d^{-1}$ , blue bars). (D) daily visibility distance indicating dust input in 10-running point average (the background grey line connects the daily data points, and the thicker black line represents the 10-point mean). The boxes in the lower panels refer to seasons (W: winter, Sp: spring, S: summer, A: autumn). Grey shades indicate maximal upwelling intensity, brown shades indicate maximum dust input, and the horizontal dashed lines indicate calendar year separation.

The export flux of cysts produced by photo-/mixotrophic dinoflagellates also showed strong interannual variability varying from no observed export flux in spring - summer 2018 to a maximal flux of  $1.06 \times 10^4$  cysts  $m^{-2} d^{-1}$  in winter 2012/2013 (**Figure 3.2C**). The flux was relatively low in 2003 and increased steadily until 2008. From 2008 on, the photo-/mixotrophic cyst export flux decreased except for 2013, 2015, and 2016, when high export fluxes occurred. In contrast to the heterotrophic taxa, the cyst fluxes of photo-/mixotrophic dinoflagellates did not show a clear seasonal pattern. In several years, such as in 2008, 2009, 2016, and 2017, the highest fluxes occurred in spring - summer with intervals of intensified wind speed. In 2004 and 2007, the highest export fluxes occurred during weakened wind speed. In 2013 and 2015, the maximal export flux of cysts of photo/mixotrophic species occurred in winter during maximal Saharan dust input into the North Atlantic (**Figure 3.2D**).

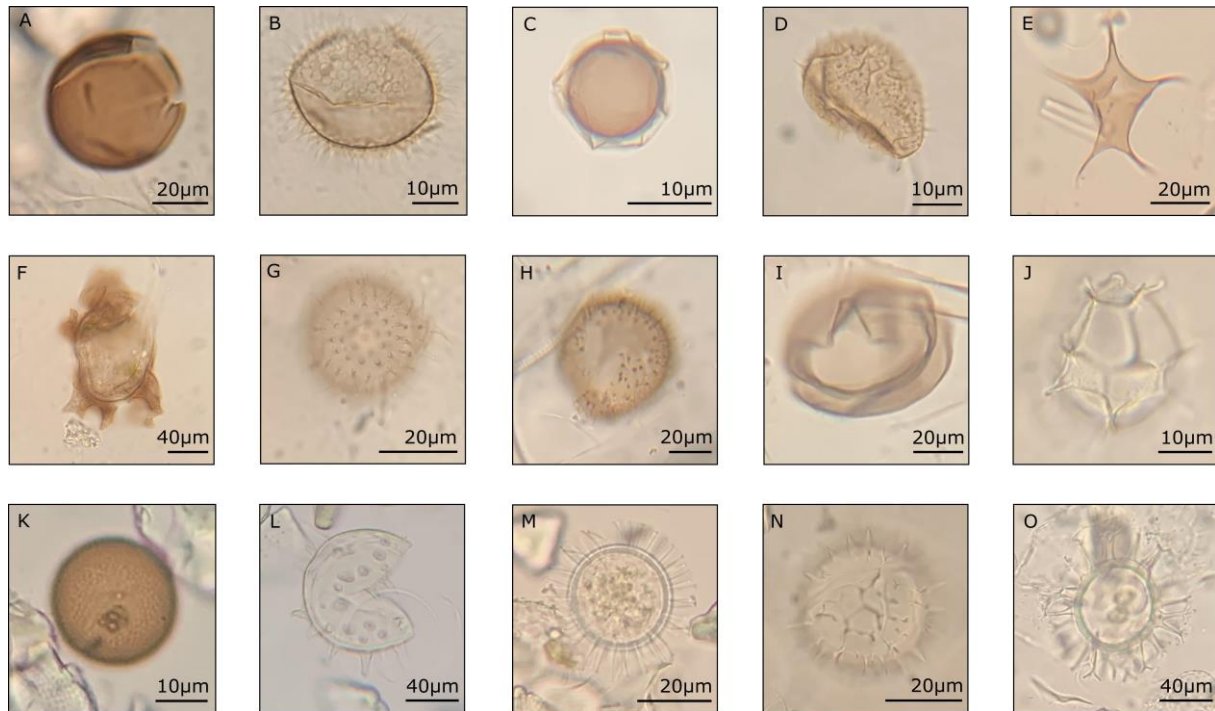


**Figure 3.3.** Some of the identified dinoflagellate cysts taxa from the CBeu trap. Heterotrophic taxa: (A) *Brigantedinium* spp., (B) *Archaeoperidinium constrictum* (uploaded to modern dinocyst key by Zonneveld and Pospelova (2015) online catalogue), (C) *Protoperidinium americanum*, (D) *P. monospinium*, (E) *P. stellatum*, (F) *Polykrikos quadratus*, (G) *Echinidinium granulatum*, (H) *E. zonneveldiae*, and (I) *P. subinermis*. Photo-/mixotrophic taxa: (J) *Impagidinium aculeatum*, (K) *Gymnodinium* spp., (L) *Lingulodinium polyedra*, (M) *Protoceratium reticulatum*, (N) *Pyrodinium bahamense*, and (O) *Spiniferites mirabilis*.

### 3.3.2. Association of dinoflagellates cysts

In the analysed samples, 67 cyst taxa were identified, of which 39 belonged to heterotrophic species (**Figure 3.1A - I**). The most dominant taxon was *Brigantedinium* spp., accounting for ca. 60% of the cyst association (**Figure 3.1A**). This genus was present in the majority of samples throughout the time series, even when cyst recovery was extremely low. The annual and seasonal export flux of *Brigantedinium* spp. followed the trend of the total cyst export flux. Species of *Echinidinium* were the second most abundant, forming an average of 15% of the association (**Figure 3.3G, H**). Of this genus, *Echinidinium transparentum/zonneveldiae* was the most abundant species (5.9%), followed by *E. aculeatum* (4.3%), and *E. delicatum/granulatum* (4.3%). The relative abundance of *Echinidinium* species increased at times of increased total cyst export flux that usually occurred in spring. However, the *Echinidinium* association composition varied between the years (**Figure 3.4A**). *E. aculeatum* dominated in spring-summer 2009 and 2016, *E. delicatum/granulatum* was abundant in spring 2011 and

2019, and spring-summer 2012 and 2017. *E. transparentum/zonneveldiae* dominated in spring-summer 2010 and from 2013 to 2015.

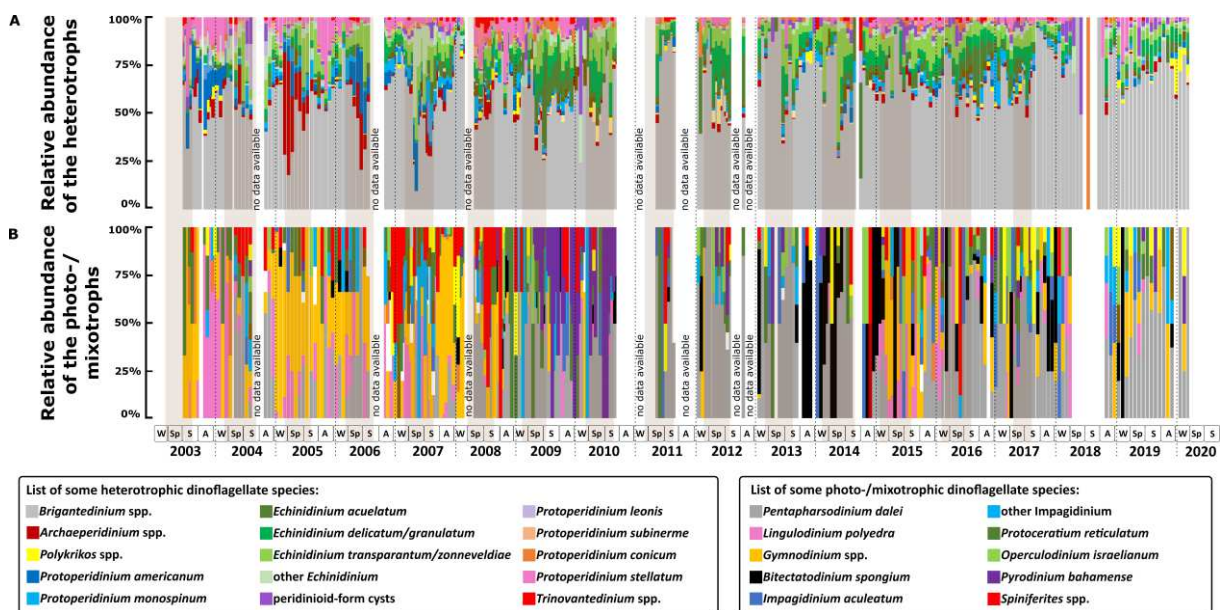


**Figure 3.4.** Relative abundance of dinoflagellate cyst species: (A) heterotrophic dinoflagellate taxa; (B) photo-/mixotrophic dinoflagellate taxa. Two boxes below the graphs show the name of important species found in Cape Blanc, one colour indicates one taxon. The gradation of colours indicates several species in the same genus/group. The squares in the lower panels refer to seasons (W: winter, Sp: spring, S: summer, A: autumn). Brown shades indicate maximal upwelling intensity, and the vertical dashed lines indicate calendar year separation.

Other cyst taxa observed in most samples were *Protoperidinium stellatum* (2.7%), *P. americanum* (2.2%), *Archaeoperidinium* spp. (2.2%), and *P. monospinum* (2.2%) (**Figure 3.3B - E**). The maximal relative abundance of these species varied strongly over the years (**Figure 3.4A**). *P. stellatum* had the highest relative abundance in summer 2003, winter 2003/2004, autumn 2005, and spring to autumn 2008. *Archaeoperidinium* spp. peaked once in spring-summer 2006, while *P. monospinum* peaked in summer 2007. *P. americanum* had the highest relative abundance in autumn 2003, winter 2003/2004, and spring 2006. The irregular abundance of these species documented a strong inter-annual variability of the cyst association in the studied area.

Cysts of photo-/mixotrophic dinoflagellates formed only about 6.8% on average of the total association (**Figure 3.3J - O**). Of this group, *Pentaparsodinium dalei* showed the highest relative abundance (2.1%), followed by *Gymnodinium* spp. (1.3%). Prior to 2008, *Gymnodinium* spp. was the association most common photo/mixotrophic taxon. From then on, *P. dalei* showed an increased relative abundance and sustained its abundance until the end of the time series in 2020. *P. dalei* were observed almost every year with maximal relative abundances in spring - summer. Relative abundance of *Gymnodinium* spp. peaked in 2003 and from 2005 to 2007, mainly in autumn – winter association. Other photo-/mixotrophic cyst species that were commonly observed were *Lingulodinium polyedra* (*Lingulodinium machaerophorum*) (0.8%), *Protoceratium reticulatum* (*Operculodinium centrocarpum*) (0.5%), species of *Spiniferites* (0.3%), *Bitectatodinium spongium* (0.3%), and *Impagidinium aculeatum* (0.2%). *L. polyedra* was observed in higher relative abundances in autumn - winter 2003. *B. spongium* had high relative abundances from autumn 2013 until spring 2014, winter 2015, and autumn 2017. High relative abundances of *Spiniferites* species were observed in spring 2004, winter 2006/2007, spring 2008, and autumn-winter 2009. *P. reticulatum*, *I. aculeatum*, and the other photo-/mixotrophic dinoflagellate taxa were sporadically present throughout the 18-year record and formed a minor part of the total association (**Figure 3.4B**).

### 3.3.3. Multivariate analyses

The DCA ordination revealed a gradient length of 2.2, indicating a unimodal structure of the dataset. Therefore, CCA was the preferred method to study the relationship between cyst taxa and

studied environmental parameters. The CCA analysis indicated that the wind system was the dominant factors influencing cyst export production. Wind speed explained 23.5% of the total variance, followed by Chl-*a* (22.8%), wind direction (18.8%), dust input (15.6%), and SSTa (9.2%). The least prominent parameter (SST) corresponded to 8.4% of the variance (**Table 3.5**). The CCA analysis identified five cyst groups based on similar taxa responses to the analysed environmental parameters (**Figure 3.5**).

**Table 3.4.** Result values of detrended correspondence analysis (DCA) and canonical correspondence analysis (CCA) executed with the software package Canoco 5 (ter Braak and Šmilauer, 2012; Šmilauer and Lepš, 2014). Length of gradient determined if the model response was linear (<2.0) or unimodal (≥2.0). Eigenvalues indicated the rate explained variance of each axis.

Analysis	Method	Length of gradient	Eigenvalue axis 1	Eigenvalue axis 2	Eigenvalue axis 3	Eigenvalue axis 4
1	DCA	2.2	0.548	0.089	0.079	0.056
2	CCA	2.1	0.035	0.023	0.015	0.009

Group 1: *Echinidinium* spp., *Echinidinium delicatum/granulatum*, *Echinidinium transparentum/zonneveldiae*, *Trinovantedinium* spp., and *Protoperidinium latidorsale* (*Votadinium calvum*). These taxa were ordinated on the positive side of the wind speed and SSTa and the negative side of the wind direction (northeastern origin).

Group 2: *Archaeoperidinium* spp., *Lejeunecysta paratenella*, *Polykrikos* spp., *Protoperidinium americanum*, *Protoperidinium leonis* (*Quinquecuspis concretum*), *Protoperidinium subinermis* (*Selenopemphix nephroides*), and *Protoperidinium stellatum* as well as the two photo-/mixotrophic taxa; *Impagidinium* spp. and *Operculodinium israelianum*. These taxa were ordinated on the positive side of the dust input and Chl-*a* concentration, the intermediate value of wind direction, and the negative side of the SST.

Group 3: *Gymnodinium* spp. and *Lingulodinium polyedra* were ordinated on the most positive side of the wind direction and negative side of the wind speed and SSTa.

Group 4: *Bitectatodinium spongium* and *Protoceratium reticulatum*. Taxa of this group were ordinated on high SST values, intermediate wind direction values, and negative side of Chl-*a* and dust input.

Group 5: *Brigantedinium* spp., *Echinidinium aculeatum*, *Protoperidinium monospinum*, and *Protoperidinium conicum* (*Selenopemphix quanta*), as well as three photo-/mixotrophic taxa (*Pentaparsodinium dalei*, *Impagidinium aculeatum*, and *Spiniferites* spp.). These taxa were ordinated on intermediate values of all studied environmental parameters.

**Table 3.5.** Result of canonical correspondence analysis (CCA) measuring contribution values of environmental parameters in the studied area. p-value determined if a variable is statistically significant (<0.05) or not.

Parameter	% variance	p-value
Wind speed	23.5	0.002
Chlorophyll - <i>a</i>	22.8	0.002
Wind direction	18.8	0.002
Dust input	15.6	0.008
SSTa	9.2	0.042
SST	8.4	0.07

### 3.4. Discussion

#### 3.4.1. Physical condition of the upper water column

In the studied area, coastal upwelling was driven by surface winds from the north and northeast with intensities that were strongly related to the wind speed (Cropper et al., 2014; Fischer et al., 2016; Romero et al., 2020) (Figure 3.6C, D). Coastal upwelling transported colder, nutrient-rich intermediate water to the upper water column and successively carried them offshore toward the sediment trap area via large filaments (Fischer et al., 2009). When these filaments crossed the trap mooring site, local surface water temperatures decreased compared to the surrounding offshore waters, causing enhanced sea surface temperature anomaly (SSTa) (Figure 3.6A, B). In contrast, at times of a weakened upwelling intensity (upwelling relaxation), surface waters at the trap were unaffected by upwelling filaments, resulting in the SST of the trap location being similar to that of more offshore waters (low SSTa). We observed enhanced crossing of upwelling filaments at the trap sites, mainly in spring until early summer. The upwelling relaxation at the location mainly occurred in late summer and autumn. Besides upwelling fertilization of the upper water, additional micronutrients were carried into this region by aerosol dust from the Sahara (Jickells et al., 2005; Skonieczny et al., 2013; Fischer et al., 2016). Throughout the record, we observed enhanced dust input mainly in winter to early spring in this studied area, coinciding with the surface winds from the northeast. From 2008, the maximum dust emission increased in winter and summer (Figure 3.6H).

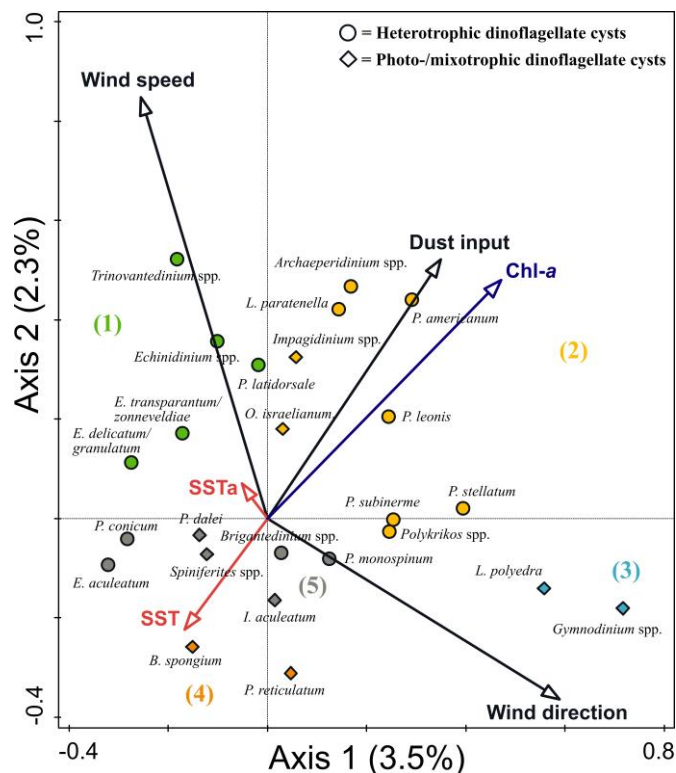


**Figure 3.5.** Result of Canonical Correspondence Analysis (CCA) of dinoflagellate cyst species at the CBeu trap from June 2003 and March 2020. Ordination assigned five species groups: (1) upwelling indicators, (2) upwelling and dust indicators, (3) upwelling relaxation indicators, (4) eutrophic and warm water indicators, and (5) species with no specific indication.

#### 3.4.2. Dinoflagellate cyst export fluxes

The strong dominance of heterotrophic taxa in the organic-walled dinoflagellate cyst export flux was also reported from sediment trap observations in other upwelling ecosystems such as Somali Basin (Northwest Arabian Sea), Benguela (Southwest Africa), NE Pacific, and Cariaco Basin (Caribbean Sea) (Zonneveld and Brummer, 2000; Pitcher and Joyce, 2009; Pospelova et al., 2010; Bringué et al., 2013; Bringué et al., 2018 and 2019). In all of these regions, upwelled nutrient-rich waters stimulated phytoplankton production in surface waters, which in turn formed the food source of heterotrophic dinoflagellates (Jacobson and Anderson, 1986; Jeong, 1999; Pitcher et al., 2010; Anderson et al.,

2018). We also observed that the export fluxes of dinoflagellate cysts in our studied area were in the same range as those in the other upwelling ecosystems, for instance, the Arabian Sea (Zonneveld and Brummer, 2000), off Southern California (Bringué et al., 2013) and the Caribbean Sea (Bringué et al., 2018 and 2019). An exception was formed by the Benguela upwelling region, where the cyst fluxes were assumed to be a factor of 100 higher (Pitcher and Joyce, 2009). The latter might be a calculation error in the study of Pitcher and Joyce as compared to all other studies from the upwelling area; not only the maximal flux but also the variation in fluxes between upwelling and upwelling relaxation phases was similar to our study even though the temporal occurrence and duration of active or strong upwelling varied across different upwelling regions.

To compare the dinoflagellate cyst data with environmental parameters in the upper water column, we have considered a time lag between cyst production in the upper water column and the time of recovery in the sediment trap. Around the mooring site, the sinking velocities of particles in the water column have been estimated between 75 - 150 m day<sup>-1</sup> (Fischer and Karakaş, 2009; Iversen and Ploug, 2013). Iversen and Ploug (2013) showed that sinking velocities of diatoms increased linearly to the size of aggregated diatoms, resulting in a mean sinking velocity of about 150 m day<sup>-1</sup>. Dinoflagellate cysts and diatoms sank down to the ocean floor as part of aggregates or concentrated in fecal pellets. In the upwelling area off East Africa in the Arabian Sea, cyst associations changed simultaneously in sediment trap material collected at 1030 and 3045 m depth within 14 days collection intervals, leading to a minimal sinking velocity of 140 m day<sup>-1</sup> (Zonneveld and Brummer, 2000). Higher sinking velocities of up to 274 m day<sup>-1</sup> were estimated in Cape Blanc by comparing the cyst associations in sediment trap samples collected at 730 and 3557 m depths at a location more offshore to the present trap site (Zonneveld et al., 2010). Based on the results of 140 m day<sup>-1</sup> and 274 m day<sup>-1</sup> sinking velocities and deployment depths between 1249 – 1364 m, a time lag of 4.6 to ten days was estimated. When a maximal time lag of ten days was applied, the cyst export flux was enhanced when upwelling filaments crossed the trap location, and enhanced dust input was observed in the trap samples, increasing the upper water nutrient concentrations (**Figure 3.6E**). Furthermore, the highest export flux of dinoflagellate cysts in the winter of 2012 coincided with a long period of strong upwelling in the region during the years 2011 and 2012 and enhanced lithogenic influx in the trap samples related to increased Saharan dust emissions recorded in 2012 and 2013 (Fischer et al., 2019). This finding agreed with earlier observations of increased cyst production during high nutrient concentrations in upper waters supporting the assumption that of cyst sinking rates are the same order of magnitude as those of diatoms (e.g., Zonneveld et al., 2022a).

Lateral transport of particulate organic matter in the water column can occur in the region in nepheloid layers of subsurface and intermediate water depths as well as just above the sea floor (e.g., Karakaş et al., 2006; Karakaş et al., 2009; Zonneveld et al., 2018). Lateral transport of particles can alter the rate and composition of the export flux collected by the sediment traps (Inthorn et al., 2006; Asper and Smith, 2019; Romero et al., 2021; Romero and Ramondenc, 2022). Dinoflagellate cysts laterally transported in intermediate and bottom water nepheloid layers extended up to 130 km off the Cape Blanc shelf break (Zonneveld et al., 2018). As such, part of the observed cysts collected in the traps did not originate from the upper waters at the trap site. However, recent investigations showed that the resuspension of shelf material and the position of nepheloid layers in the region were not permanent (Zonneveld et al., 2022a; 2022b). Clear nepheloid layers were observed in the water column in November 2015 and 2018 and were almost absent in the summer of 2020 and November 2021 (see cruise reports of Zonneveld et al., 2016, 2019a, 2020, 2022c). Romero and Ramondenc (2022) investigated the diatom export flux in the same sediment trap. They documented that throughout the time series, benthic diatoms from the shelf sediments formed a considerable part of the association. However, microscopic observations of upper water plankton samples collected in November 2018 revealed that many benthic diatoms could have colonized larger pelagic diatoms (Zonneveld and Versteegh, pers. obs). Therefore, it was unclear if the observed benthic diatoms collected in the sediment trap originated from the shelf or local sources. Unfortunately, we have no method to determine the ratio between the autochthonous and allochthonous association recovered in our trap samples. Nevertheless,

we observed a strong correlation of cyst fluxes and association composition variabilities with changing environmental conditions in the upper waters at the trap site with a time lag of ten days. Therefore, we assumed that most of the recovered dinoflagellate cysts in the trap represented cysts originating from the upper water column in the vicinity of the trap site.

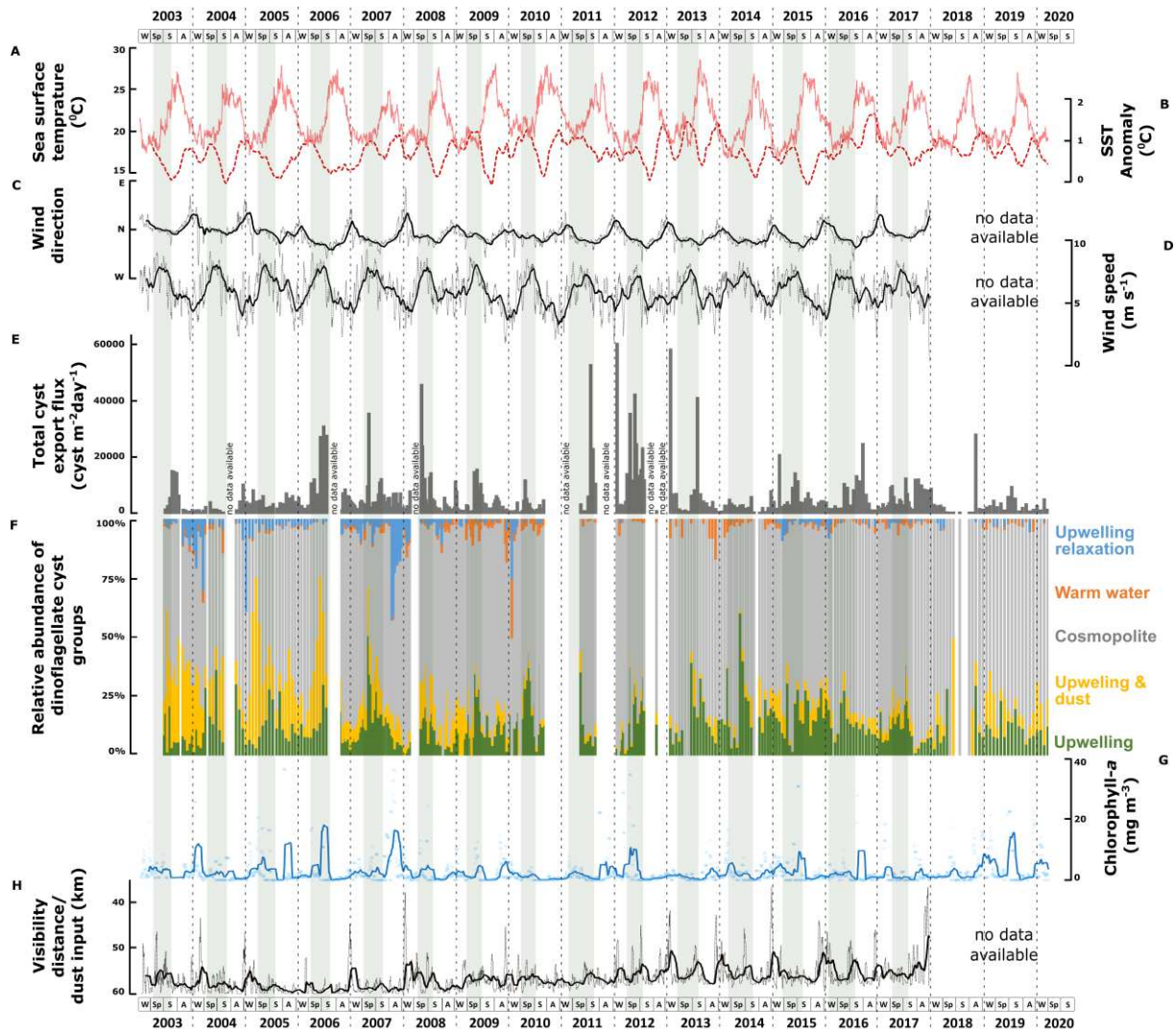


**Figure 3.6.** Comparison between several environmental parameters and the concentration as well as the relative contributions of six dinoflagellate cyst species groups. (A) sea surface temperature (SST); (B) sea surface temperature anomaly (SSTa); (C) wind direction; (D) wind speed; (E) total export fluxes (cysts  $\text{m}^{-2} \text{d}^{-1}$ ) of dinoflagellate cysts; (F) relative contribution (%) of each dinoflagellate species group according to CCA analysis; (G) concentration of Chlorophyll-*a*; (H) visibility distance indicating dust input. Grey shades in the background indicate maximal upwelling intensity.

### 3.4.3. Dinoflagellate cyst groups according to environmental parameters

Based on the CCA analyses mentioned in the result and the visual observation of the absolute abundances of the main contributor species, five groups of dinoflagellate cysts that showed similar relationships to the studied environmental parameters could be distinguished:

#### 3.4.3.1. Species group 1 (maximal upwelling)

CCA group 1 consisted of heterotrophic taxa that were ordinated on the positive side of the wind speed and SSTa. In the region, strong northwestern winds triggered maximal upwelling intensity with the filaments reaching far into the open ocean. These filaments were characterised by relatively stratified surface waters with high nutrient availability. This condition correlated with the highest relative and absolute abundances of *Echinidinium delicatum/granulatum*, *Echinidinium* spp., *Echinidinium transparantum/zonneveldiae*, *Trinovantedinium* spp., and *Protoperidinium latidorsale* (Figure 3.6F, 3.7).

This result was also observed in drifting trap studies in our study area, which revealed that a higher export flux of *Echinidinium* species occurred in and at the rim of active upwelling cells (Zonneveld et al., 2022b). Furthermore, sediment trap and surface sediment studies reported high concentrations of *E. delicatum/granulatum* and *E. transparantum/zonneveldiae* at times of enhanced active upwelling at a more offshore position compared to our trap site (Zonneveld et al., 2010) and in other areas with a similar system such as the Arabian Sea, the Benguela upwelling area, along the North American Pacific coast, along the southwest Mexican coast, the Cariaco Basin, the Portugal Bay, and off the west coast of Iberian Peninsula (Zonneveld and Brummer, 2000; Radi and de Vernal, 2004; Pospelova et al., 2008; Ribeiro and Amorim, 2008; Bouimetarhan et al., 2009; Limoges et al., 2010; Zonneveld et al., 2010; Bringué et al., 2019; García-Moreiras et al., 2021). *E. zonneveldiae* was described by Head (2003) and successively documented in the upwelling regions of the Santa Barbara Basin, Cariaco Basin, and off Cape Blanc. Bringué et al. (2019) reported that *E. granulatum* was more abundant at the weaker stage of upwelling. However, this species was recorded during maximal upwelling in the other regions. Seasonal production of *Echinidinium* was also observed in areas with stratified upper water columns where the high nutrient concentrations were provided by river discharge or transported coastal upwelling waters (Pospelova et al., 2010; Price and Pospelova, 2011). The ambient water conditions of these regions were often characterised by some variability in the water column stratification. A strong stratification appeared when fresh (river) waters covered the salty marine waters while turbulence occurred at the freshwater - saltwater interface.

*Trinovantedinium* spp. was observed only sporadically in our record, and the connection of high concentration of this genus with maximal upwelling was recorded for a few years only. In other upwelling regions, this genus was often grouped with other peridinioid cysts because of its low export flux or its sporadic occurrence showed no clear temporal pattern (Zonneveld and Brummer, 2000; Ribeiro and Amorim, 2008). The same holds for *P. latidorsale*. Nevertheless, in the Santa Barbara Basin sediment traps, an enhanced flux of *P. latidorsale* showed a positive correlation to the active upwelling phase (Bringué et al., 2013). In the Northwest Arabian Sea, Saanich Inlet, and Cariaco Basin, the cyst export production of this species was not strictly linked to the presence of an active upwelling phase but could be linked to the availability of its food source (Zonneveld and Brummer, 2000; Price and Pospelova, 2011; Bringué et al., 2019). Therefore, we assume these species were related to upwelled waters in the research area.

#### 3.4.3.2. Species group 2 (maximal upwelling and dust input)

CCA group 2 consisted of heterotrophic and photo-/mixotrophic taxa that were ordinated on the positive side of dust input, Chl-*a* concentration, and intermediate wind speed values. Throughout the years, the relative abundance and export fluxes of group 2 increased when dust input and upwelling intensified (**Figure 3.6F, 3.7**). Dust contains several trace elements, and although the exact ways in which dust input fertilizes the ocean are not well understood, high dust input can enhance phytoplankton production (Erickson et al., 2003; Stuetz et al., 2005; Duarte et al., 2006; Skonieczny et al., 2013; Fischer et al., 2016). This latter was supported by our observation of a close relationship between Chl-*a* concentration and enhanced dust input in CCA analyses (**Figure 3.5**). Group 2 contained the heterotrophic taxa; *Archaeperidinium* spp., *Lejeunecysta paratenella*, *Polykrikos* spp., *Protoperidinium americanum*, *Protoperidinium stellatum*, and *Protoperidinium subinermis*, and the photo-/mixotrophic species; *Impagidinium* spp. and *Operculodinium israelianum* (**Figure 3.7**).

The seasonal production of *Archaeperidinium* species has not been well investigated, except in Price and Pospelova (2011), where *A. saanichi* was listed as Cyst type L. This condition could be caused by taxonomic difficulties and often low concentrations of this genus in sediment trap samples from other regions. In this study, the cyst export production of this genus, notably *A. saanichi* and *A. constrictum* had relatively high export production until 2008, after which it declined. A similar trend was observed in *P. americanum*. This species seasonal export flux was more pronounced in the first half of the trap time series and declined after 2007. A strong positive correlation between the production of *P.*



*americanum* and seasonal upwelling was observed in the NW Arabian Sea (Zonneveld and Brummer, 2000). However, a relation to enhanced dust input was not reported before the present study.

The overall trend of these species export flux seemed contradictory to the enhanced dust input. The long-term trend of dust input showed a gradual increase rather than a decrease. A possible explanation for this is that the dust composition changed over the years, which could influence the composition of the phytoplankton community (Lu et al., 2017; Friese et al., 2017; Yang et al., 2019). Shifts in prey availability might lead to the declining production of these cyst taxa. Unfortunately, no record was available to show if the dust composition in this location has changed over the trap time series. Future assessments of the dust composition from these sediment trap samples are required to clarify this hypothesis.

A positive relationship between the export fluxes of *P. stellatum* and *P. subinermis* (**Figure 3.3I**) with the presence of upwelling has also been observed in sediment trap samples from the Northwest Arabian Sea and Cariaco Basin (Zonneveld and Brummer, 2000; Bringué et al., 2019). However, the influence of dust input on the respective cyst fluxes had not yet been recorded. This latter holds as well for the other species within this group. It might be caused by taxonomic problems (some species generally being grouped) and the lack of studies investigating the role of terrestrial mineral input on the production of cysts. Therefore, this study proposes implementing terrestrial minerals as potential steering factors for cyst production in future studies.

#### 3.4.3.3. Species group 3 (upwelling relaxation)

CCA group 3 was formed by the photo-/mixotrophic taxa *Lingulodinium polyedra* and *Gymnodinium* spp. (**Figure 3.6F, 3.8**). These taxa were ordinated on the positive side of the wind direction and the negative side of the wind speed and SSTa (**Figure 3.5**). This represents northwestern winds, which led to weaker upwelling in the region, mainly in late summer - autumn. The overall export flux of both species was higher from 2003 to early 2009, strongly fell in the following years, and mildly recovered in 2015.

The increased cyst flux of *L. polyedra* and *Gymnodinium* spp. during less intense upwelling, in line with previous studies in the region and other upwelling areas. Sediment trap studies in the Santa Barbara and Cariaco Basins showed higher export production of *L. polyedra* during phases of upwelling relaxation (Bringué et al., 2013 and 2019). A drifting trap survey in an upwelling cell off Cape Blanc demonstrated that *L. polyedra* was formed during the transition from active upwelling towards more stratified conditions in offshore drifting filaments (Zonneveld et al., 2020b). Sediment surface studies in Northeast Brazil, Northeast Pacific, West Africa, Black Sea corridor and the West Coast of Iberian Peninsula documented that cyst production of this species increased under warm, stratified, and nutrient-rich waters (e.g., Vink et al., 2000; Pospelova et al., 2008; Radi and de Vernal, 2008; Bouimtarhan et al., 2009; Leroy et al., 2013; Mudie et al., 2017; García-Moreiras et al., 2021, 2023). In our record, the export flux of *L. polyedra* was not restricted to upwelling relaxation phases. We observed enhanced export flux of *L. polyedra* during maximal upwelling in a few years. At times of maximal upwelling of this area, the upper water conditions, such as the rate of stratification, can change fast in small spatial and temporal scales. Studies on the life cycle of *L. polyedra* have shown that this species can produce both asexual and sexual cysts (Figueroa and Bravo, 2005). Although the possible role of sexual and asexual cysts has not been established, asexual cysts have often been linked to the ability of the species to adapt quickly to fast-changing environments (Figueroa and Bravo, 2005). In river plume areas and fjord systems that are characterised by a strong variability in upper water stratification, high concentrations of *L. polyedra* were observed (e.g., Lewis, 1988; Blanco, 1995; Smayda and Trainer, 2010; Zonneveld et al., 2013; García-Moreiras et al., 2023). Therefore, we assume that in our research area, *L. polyedra* benefited from the changing environmental conditions in upper water at transition phases from active upwelling to more stratified conditions.

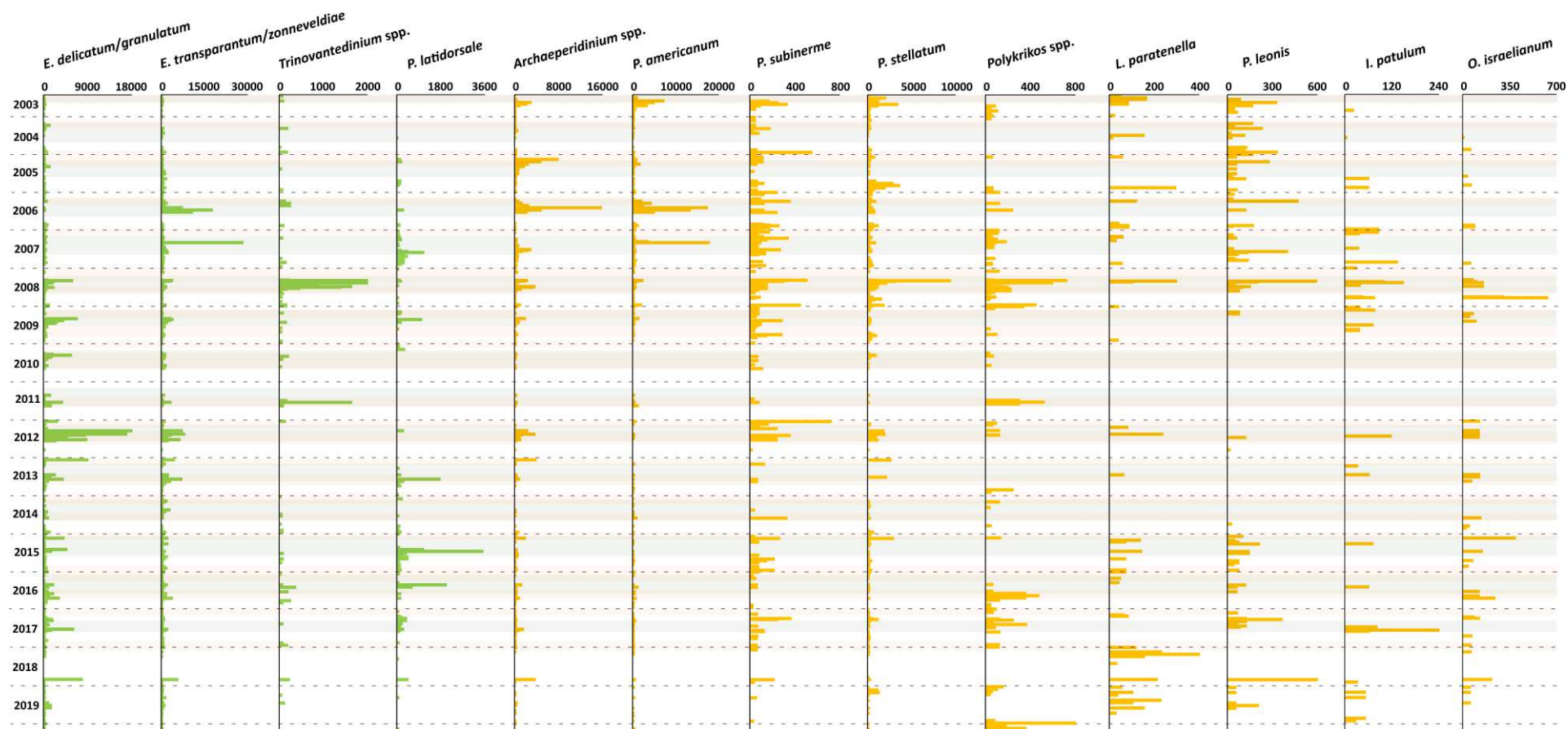


**Figure 3.7.** Flux rate of dinoflagellate cyst species (cysts  $m^{-2} d^{-1}$ ). Fluxes in green bars are species group 1, and fluxes in yellow bars are species group 2. Grey shades indicate maximal upwelling intensity, brown shades indicate maximum dust input, and the horizontal dashed lines indicate calendar year separation.

Unfortunately, it was not possible to differentiate unequivocally between cysts of *G. catenatum*, *G. microreticulatum*, and *G. nolleri* as the size of all brown microreticulate cysts observed in the Cape Blanc region fell in the overlapping size range of the three species. Furthermore, it was generally difficult to identify the exact number of cingular vesicles in the observed specimens. Consequently, we had to group these species as *Gymnodinium* spp. The export fluxes of *Gymnodinium* spp. were higher during the weaker upwelling phases in most of the years but comparable to *L. polyedra*, the enhanced cyst export flux of *Gymnodinium* spp. was not completely restricted to phases of upwelling weakening. Nevertheless, our observations are largely in line with surface sediments studies conducted in NW Iberian Peninsula, where *G. catenatum* had a positive relationship with more stratified upper water conditions (Bravo et al., 2010; Pitcher et al., 2010; Ribeiro et al., 2012; García-Moreiras et al., 2021). In the Cariaco Basin sediment trap study, the concentration of *G. nolleri* cysts increased during "secondary upwelling" marked by the weakening of upwelling winds (Bringué et al., 2018). A 7-day in-situ observation of cyst production in an active upwelling cell offshore Cape Blanc also documented that *L. polyedra* and *Gymnodinium* spp. were generally produced when the water column became more stratified due to upwelled waters forming an offshore drifting upwelling filament (Zonneveld et al., 2022b). Therefore, we suggest that the species of group 3 can be used as indicators for the upwelling relaxation in our studied area.

#### 3.4.3.4. Species group 4 (warm surface waters)

CCA group 4 was formed by species that ordinated on high values of the SST, intermediate values of the wind direction, and negative values of the dust input and Chl-*a* concentration. Despite the insignificant impact of the SST (p-value <0.05) in this system (**Table 3.5**), the relative abundance of this group showed a higher percentage at times of warmer SST that was usually observed during upwelling relaxation (**Figure 3.6F**). The main contributors of this group are *Protoperidinium reticulatum* and *Bitectatodinium spongium* (**Figure 3.8**).

Although *P. reticulatum* was observed in the majority of our samples, its occurrences still showed a positive relationship with warm surface waters at times of weaker upwelling. This result suggested that this species could tolerate variable environmental conditions, which was corroborated by the global geographic distribution of *P. reticulatum* in surface sediment samples, showing that it has a cosmopolitan distribution (e.g., Zonneveld et al., 2013; Marret et al., 2020). The sediment trap study from the Cariaco Basin, *P. reticulatum* showed higher export flux during upwelling relaxation when surface waters were more stratified (Bringué et al., 2018 and 2019). Furthermore, in the Northeast Pacific and Southwest/West African surface sediments, high relative abundances of these cysts were observed in the more offshore regions of the coastal upwelling areas (Radi and de Vernal, 2004; Holzwarth et al., 2007; Pospelova et al., 2008; Bouimetarhan et al., 2009).

In contrast, *B. spongium* is distributed strictly in tropical and sub-tropical regions (e.g., Zonneveld et al., 2013; Marret et al., 2020). In the Cariaco Basin, the highest production of *B. spongium* was observed during active upwelling (Bringué et al., 2018; 2019). However, in other regions, the production of *B. spongium* was not restricted to the presence of upwelling. Although in the Northwest Arabian Sea, the highest export flux was observed during the southwest monsoon at times of active upwelling, cysts of this species were observed as well in samples collected during the northeast monsoon when warm stratified upper waters were present (Zonneveld and Brummer, 2000). The highest absolute and relative abundances of *B. spongium* were found in the Indus Fan (Northwest Arabian Sea), a region without upwelling but with warm and nutrient-rich surface waters (Zonneveld and Jurkschat, 1999). Therefore, we interpret that warm eutrophic surface waters are required for the occurrence of *B. spongium* rather than the mixing of upper waters.

#### 3.4.3.5. Species group 5 (no relationship with local environmental conditions)

CCA group 5 consisted of heterotrophic and photo-/mixotrophic taxa that were ordinated on the intermediate values of all studied parameters. The main contributors in this group were *Brigantodinium* spp., *Echinidinium aculeatum*, *Pentapharsodinium dalei*, *Protoperidinium conicum*,

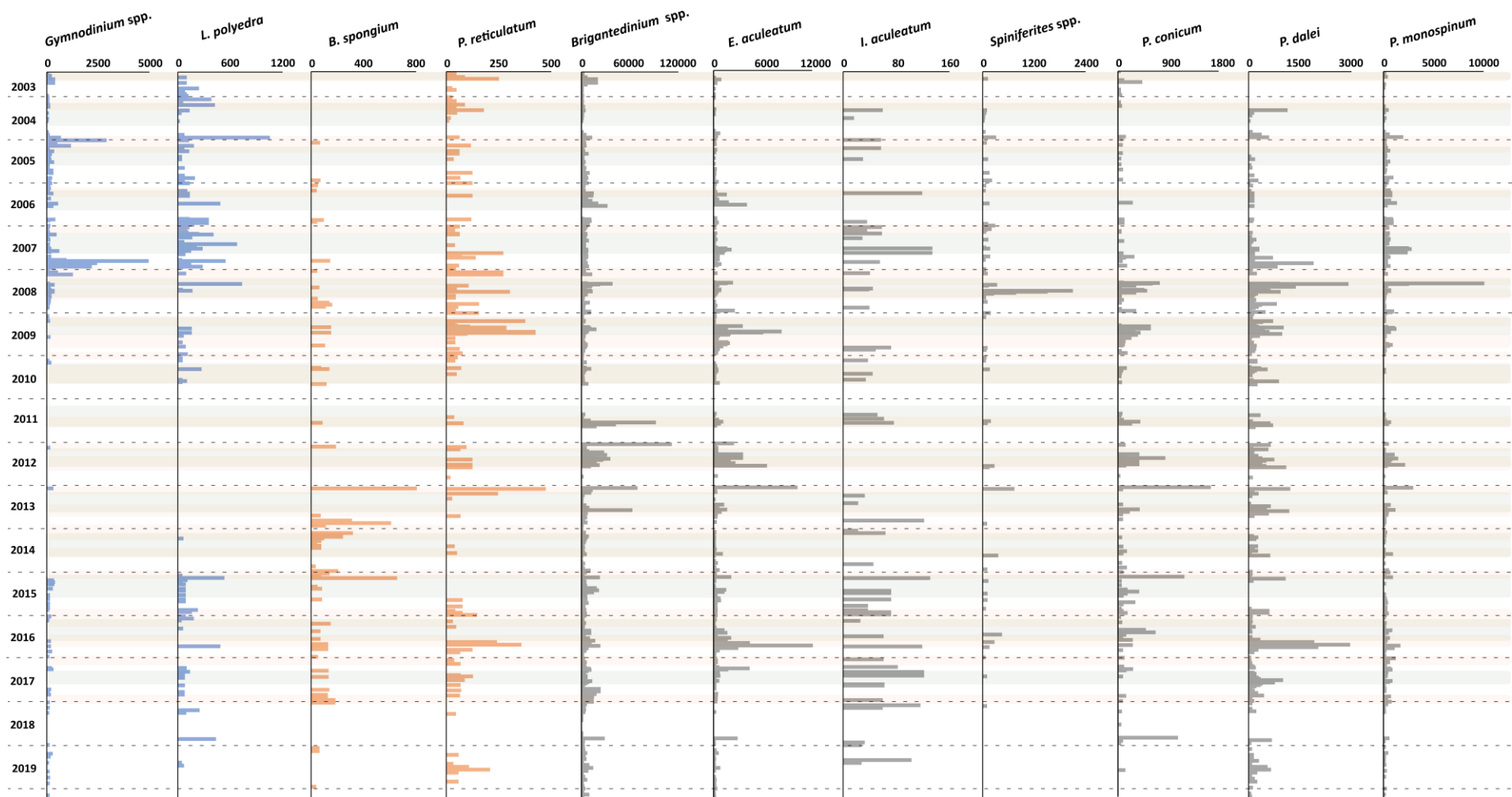


**Figure 3.8.** Flux rate of dinoflagellate cyst species (cysts  $\text{m}^{-2}\text{d}^{-1}$ ). Blue bars represent the species of group 3, orange bars represent the species of group 4, and gray bars represent the species of group 5. Grey shades indicate maximal upwelling intensity, brown shades indicate maximum dust input, and the horizontal dashed lines indicate calendar year separation.

and *Protoperidinium monospinum* (**Figure 3.8**). Additionally, this group includes two taxa that occurred sporadically in the record: *Impagidinium aculeatum* and *Spiniferites* spp.

*Brigantedinium* spp. dominated the dinoflagellate cyst association in most samples. Although its concentration followed the upwelling intensity, its relative abundance remained high during upwelling relaxation. The accumulation rate of *Brigantedinium* spp. was related to enhanced upwelling in many regions such as the Arabian Sea, Benguela upwelling, Canary Current Upwelling, West Coast of Iberian Peninsula, and Northeast Pacific (e.g., Zonneveld and Brummer, 2000; Radi and de Vernal, 2004; Sprangers et al., 2004; Holzwarth et al., 2007; Pospelova et al., 2008; Bouimetarhan et al., 2009; Limoges et al., 2010; García-Moreiras et al., 2021). Sediment trap studies in Omura Bay (Japan), Saanich Inlet (Canada), and the Mauritanian upwelling region (NW Africa) documented a positive correlation between export production of *Brigantedinium* spp. with several primary producers such as diatoms, coccolithophores, and photo-/mixotrophic dinoflagellates (Fujii and Matsuoka, 2006; Pospelova et al., 2010; Zonneveld et al., 2010; Price and Pospelova, 2011; Bringué et al., 2013). These results indicated that the cyst export flux of *Brigantedinium* spp. is strongly related to the abundance of their prey.

Although the relative abundance of *E. aculeatum* did not show a positive relationship with specific environmental parameters, the highest annual export fluxes of *E. aculeatum* usually occurred at times of maximal upwelling and sometimes during high dust input and when upwelling weakened (indicated by higher SST). The export flux of *E. aculeatum* was not always higher during enhanced upwelling or dust input. However, our data still suggested that enhanced availability of nutrients in the upper water might increase its cyst export production. In surface sediments from the Benguela upwelling area and off Southwest Mexico, a higher abundance of *E. aculeatum* was observed in regions characterised by coastal upwelling (Zonneveld et al., 2001; Holzwarth et al., 2007; Limoges et al., 2010). In the sediment traps of the Santa Barbara and Cariaco Basins, *E. aculeatum* showed increased export production during the later stages of active upwelling until upwelling relaxation set in (Bringué et al., 2013, 2018, 2019). The combination of this information and our results indicated that export production of *E. aculeatum* might be positively influenced by the availability of nutrients in the upper water column that was not always triggered by upwelling as observed in Saanich Inlet (Price and Pospelova, 2011).

A similar pattern was observed for *P. dalei*, the most dominant photo-/mixotrophic species in our dataset. However, Li et al. (2020) reported another species (*Pentapharsodinium imarense*) with similar morphology features. It is possible that *P. imarense* was identified as *P. dalei* since they are better distinguished through molecular identification. Although no significant annual trend was observed in the export flux of *P. dalei*, its high cyst flux was observed at maximal upwelling intensity and enhanced dust input, notably in winter. In Northeast Pacific, Portugal Bay, and Red Sea surface sediments, high concentrations of cysts of *P. dalei* were observed in regions characterised by colder upper waters (Radi and de Vernal, 2004; Pospelova et al., 2008; Ribeiro and Amorim, 2008; Elshanawany and Zonneveld, 2016). Also, sediment trap observation in the Cariaco Basin documented increased *P. dalei* export flux during low SST and active upwelling (Bringué et al., 2018; 2019). However, it was argued that lower temperatures rather than upwelling enhanced export fluxes of *P. dalei* in this region. In our record, the occurrence of *P. dalei* could not be linked to low temperatures but rather to nutrient availability.

Even though the overall export flux of *I. aculeatum* was low, it occurred in the samples throughout the trap time series. *I. aculeatum* was generally observed in high relative abundances in surface sediment samples of oligotrophic regions and was often interpreted as a typical oligotrophic species (Vink et al., 2000; Sprangers et al., 2004; Pospelova et al., 2008; Radi and de Vernal, 2008; Bouimetarhan et al., 2009; Elshanawany et al., 2010; Zumaque et al. 2017). However, cyst degradation studies showed that this species is more resistant to aerobic degradation than many other dinoflagellate cysts (Zonneveld et al., 2019b). This species high relative abundance in oligotrophic areas was generally the result of the high bottom water oxygen concentrations that prevail in oligotrophic regions, leading

to the post-depositional degradation of the other cyst species (e.g., Zonneveld et al., 2019b). Upwelling is a permanent feature and dust reaches this region regularly, leading to the upper water column trophic states never becoming oligotrophic. Thus, our results suggested that *I. aculeatum* could tolerate limited nutrient availability but was not restricted to it.

Only little information has been obtained on the relation between the export production of *P. monospinum* and environmental conditions. It could be that this species was often combined with the other spiny peridinioid cysts due to its rarity and low concentration in other locations. Sediment trap studies in the distal extension of the upwelling filaments of Cape Blanc showed that cyst production of *P. monospinum* increased when filaments reached the trap location (Susek et al., 2005; Zonneveld et al., 2010). However, at our trap location, the export production of this species could not be linked to any variation in environmental conditions. This was also the case for *P. conicum*, with a positive relationship between increasing upwelling and increasing export flux of *P. conicum* only reported in the Cariaco Basin (Bingué et al., 2019). In Omura Bay (Japan), Lisbon Bay (Portugal), and the central Strait of Georgia (Canada), the production of *P. conicum* was high throughout the year with no clear seasonal trend (Susek et al., 2005; Fujii and Matsuoka 2006; Ribeiro and Amorim, 2008; Pospelova et al., 2010; Price and Pospelova, 2011). Therefore, our result implies that strong upwelling was not the only driving factor influencing the cyst production of *P. conicum*.

#### 3.4.4. Long-term variations in the cyst association

The result of the CBeu sediment trap study in the Mauritanian upwelling system provided a long and almost continuous record of the seasonal, annual, and multi-annual variability in the dinoflagellate cyst association. As expected, the upwelling intensity was triggered by the strength of upwelling winds that control the annual seasonality of dinoflagellate cyst export flux. However, we observed that each upwelling episode showed differences in the dominance and composition of the species (**Figure 3.4A**). Since the beginning of the record, no species, except for *Brigantedinium* spp., could sustain its dominance during maximal upwelling throughout all years. Sporadic occurrences and irregular increases of some species added to the complexity of dinoflagellate response to episodes of more intense upwelling in the studied area. For instance, the short-term occurrence of *Protoperidinium lousianense* (*Trinovantedinium pallidifulvum*) in 2008 and increased export fluxes of many *Spiniferites* species in 2008 and *B. spongium* in 2014/2015, demonstrated this heterogeneity (**Figure 3.8**). The Chl-*a* concentration was the only parameter that showed strong inter-annual variations similar to the dinoflagellate cyst association composition and export flux (**Figure 3.6G**). These findings suggested that biological factors such as intra- and inter-species interactions were responsible for the changes in this ecosystem, coherent with changes found in other ecosystems (Daly and Smith, 1993; Naujokaitis-Lewis et al., 2016; Rollwagen-Bollens et al., 2020). Inter-species and group competition, predation, and variation of prey might have determined the dominance and composition of dinoflagellate cysts taxa in every upwelling episode (Daly and Smith, 1993; Rollwagen-Bollens et al., 2020). This outcome agreed with observations from in-situ pump and drifting trap surveys in the region. Here, it was observed that the export flux of cysts in individual active upwelling cells contained different unique species associations (Zonneveld et al., 2022a, 2022b).

The 18-year sediment trap record also documented a significant change in the composition of dinoflagellate cyst association. A turnover was marked by the shift in dominance from *Archaeperidinium* and *Protoperidinium* in favour of *Echinidinium* species in the maximum upwelling phase of 2007. The dominance of *Echinidinium* species became more pronounced after 2009 (**Figure 3.4A**). Around the same time, a shift in dominance of the photo-/mixotrophic association was observed from *Gymnodinium* spp. to *Pentapharsodinium dalei* (**Figure 3.4B**). These changes in the association coincided with the enhancement of the frequency of dust input and a shift in its seasonality recorded since 2008. The dust transported offshore in the Cape Blanc area has different sources in different seasons (Friese et al., 2017). In the summer of 2013 - 2015, dust contained ferroglaucophane and zeolite were transported from Mauritania, Mali, and Libya. In the winter, the dust contained fluellite, indicating that it had been transported from Western Sahara. Furthermore, the aerosol dust carried not only

micronutrients but also toxic metals such as Cadmium (Cd), Copper (Cu), and Zinc (Zn). A high concentration of those heavy metals in seawater could threaten phytoplankton growth and alter their community; for instance, cyanobacteria (*Synechococcus*), haptophytes (*Emiliania huxleyi*), chrysophytes (*Hymenomonas corterae*) and dinoflagellates (*Alexandrium* sp. *Gonyaulax* sp. and *Protocentrum* sp.) (Lu et al., 2017; Yang et al., 2019; Zhou et al., 2021). Cyst production of *L. polyedra* was more resistant to metal contamination, but there was a threshold that negatively influenced the cyst production of this species (Lu et al., 2017). A shift in diatoms association was detected from the same sediment trap in 2006 but was not linked to dust input or upwelling changes (Romeo and Ramondenc, 2022). The shifts in phytoplankton would eventually influence the zooplankton, in this case, heterotrophic dinoflagellates. However, no report has specified the prey selections of *Archaeperidinium* and *Protoperidinium* species identified in this study, and the motile affinities of *Echinidinium* species are still unknown (see **Table 3.2**). There is also limited information about the potential influence of dust input and its composition on the dinoflagellate cyst community and production. However, our results suggested that the mineral composition of aerosol dust might be a factor influencing the cyst export production of several dinoflagellate taxa in this study. Consequently, more research is needed to study the effect of terrestrial mineral particle input on the production of dinoflagellate cysts. This new information is valuable to interpret changes in the dinoflagellate cyst association throughout time, such as in sediment cores, since the source or changes of nutrient composition have not often been addressed as driving factors.

### 3.4.5. Cysts of potentially toxic dinoflagellates

Several marine cyst-forming dinoflagellates can produce toxins, with their blooms sometimes accompanied by discoloration of the upper water column (e.g., Amorim et al., 2001; Quijano-Scheggia et al., 2012; Liu et al., 2020; Terenko and Krakhmalnyi, 2021). Blooms of these species can cause severe health problems and/or can have a large economic impact (e.g., Holmes and Teo, 2002; Starr et al., 2017; Pitcher and Louw, 2021). As their cysts can form a seed bank in sediments, the upper water population can be revived, it is important to obtain insight into their cyst export production dynamics (Anderson et al., 2021). We recovered cysts of five potentially toxic dinoflagellates (**Figure 3.3L - O**), they were cysts of *Gymnodinium* spp., *Lingulodinium polyedra*, *Protoceratium reticulatum*, *Pyrodinium bahamense*, and members of the *Gonyaulax spinifera* complex.

*G. spinifera*, *L. polyedra*, and *P. reticulatum* produce yessotoxins, whereas species of *Gymnodinium* (notably *G. catenatum*) and *P. bahamense* secrete saxitoxins (Costa et al., 2015; Liu et al., 2017; Morquecho, 2019). These toxins are the primary cause of high mortality in marine organisms and can cause human health problems as well, such as Diarrhetic Shellfish Poisoning (DSP) and Paralytic Shellfish Poisoning (PSP) (Holmes and Teo, 2002; Starr et al., 2017). So far, only minimal information was available about the impact of these species off Cape Blanc (e.g., Hernández et al., 1998; Reyero et al., 1999). In our study, these species either occurred only in a few years or were present in a certain time interval. For instance, *Gymnodinium* spp. and *L. polyedra* occurred in the association before 2009 and after 2015, while *P. bahamense* was notably present between 2009 and 2012. However, north of this region, on the Atlantic coast in the region north off Cape Yubi, frequent recordings of red tides and high toxin concentrations in mussels and oysters were documented, as well as high concentrations of these cysts in surface sediments (Taleb et al., 2003; Holzwarth et al., 2010; Pitcher and Fraga 2015). Even further north in the upwelling region off the Iberian Peninsula, occurrences of *L. polyedra* were typically observed in sediments of transitional environments between coastal upwelling water and warmer offshore waters whereas cysts of *G. catenatum* were typically observed below the mid-shelf upwelling fronts (Garcia-Moreiras, 2021).

Compared to our study region, the upwelling in these northern regions was not permanent but intensified in summer/fall, and waters were more stratified in boreal winter (Aristegui et al., 2009; Cropper et al., 2014). Our study showed a correlation with earlier observations; these potentially toxic species thrive best at times of upwelling relaxation, where the water column becomes more stratified but still shows high nutrient availability (Smayda, 2002; Smayda and Trainer, 2010). Due to the non-

permanent character of the upwelling episodes in the regions north of Cape Blanc, it was likely that these conditions occurred more frequently, which might explain the higher abundance of these species in these areas. In the sediment trap record, *Gymnodinium* spp. and *L. polyedra* were among the taxa that went down in production after the dust input enhancement in 2008 (**Figure 3.8**). The cause might be the composition and intensity of dust emitted in the upper water column, as explained in the previous section. The methodology applied in this study could not detect a significant change in the upwelling wind speed or direction. therefore, no conclusion could be made from this parameter. However, this study still provided information about the ecology of these harmful species and the potential driving factor of their production dynamics. Hopefully, it will enrich our knowledge about future toxic blooms in the Cape Blanc area and nearby fishing grounds off Mauritania or another location with a similar environmental setting.

### 3.5. Conclusions

The dinoflagellate cyst export flux recovered by a sediment trap off Cape Blanc, Mauritania, between 2003 and 2020 was dominated by heterotrophic species. Throughout this period, the upper water environment was influenced by permanent upwelling, the intensity of which was controlled by the speed of the coastal wind originating from the north and northeast. Stronger upwelling occurred in most years in spring – summer, resulting in large offshore drifting filaments transporting cool and nutrient-rich across the location of our sediment trap. By estimating a phase lag of maximal ten days, the annual high export production of dinoflagellate cysts correlated to the maximum upwelling phase even though the intensities varied over 18 years. Enhanced export fluxes of dinoflagellate cysts were also observed when the Saharan dust input to the Atlantic Ocean intensified in the winter prior to 2008 as well as in both winter and summer after 2008. Indication of laterally transported dinoflagellate cysts could not be confirmed in the trap samples. However, the variations of dinoflagellate cyst export fluxes indicated a positive relationship with the environmental parameters.

Results of Canonical Correspondence Analysis (CCA) demonstrated the strong impact of wind systems on the dinoflagellate cysts export production. On this basis, taxa with similar export flux patterns were grouped. These groups consisted of taxa that had their maximal export flux during (1) maximal upwelling intensity: *Echinidinium* spp., *E. delicatum/ granulatum*, *E. transparentum/zonneveldiae*, *Trinovantedinium* spp., and *Protoperidinium latidorsale*; (2) maximal upwelling and times of increased dust input: *Archaeperidinium* spp., *P. americanum*, *P. stellatum*, *P. subinermis*, *Impagidinium* spp., and *Operculodinium israelianum*; (3) upwelling relaxation: *Gymnodinium* spp. and *Lingulodinium polyedra*; (4) warm surface waters: *Bitectatodinium spongium* and *Protoceratium reticulatum*; (5) dinoflagellate cysts with no specific relation to all studied parameters: *Brigantedinium* spp., *E. aculeatum*, *I. aculeatum*, *Pentapharsodinium dalei*, *P. conicum*, *P. monospinum*, and *Spiniferites* spp.

Although *Brigantedinium* spp. dominated the association throughout the entire sediment trap time series, the composition and total flux of every species varied strongly between episodes of enhanced upwelling. We suggest that biological factors such as intra- and inter-species interactions might have caused this strong variation in the cyst export flux. A long-term variation occurred in 2007 and became more pronounced in 2009. It was indicated by a domination shift from *Archaeperidinium*, *Protoperidinium*, to *Echinidinium* species in the heterotrophic species association as well as a change in domination from *Gymnodinium* spp. to *P. dalei* the photo-/mixotrophic species association. These changes coincided with the increase of dust input and the shift of dust seasonality since 2008, suggesting that different dust compositions due to changes in dust sources might have influenced the cyst export flux off Cape Blanc.

We observed cysts of five potentially toxic dinoflagellate species in our trap material: *Gymnodinium* spp., *L. polyedra*, *Protoceratium reticulatum*, *Pyrodinium bahamense*, and members of the *Gonyaulax spinifera* complex. Although the concentration of these cysts was low and their



---

occurrence was infrequent, their presence in our sediment trap suggests a potential risk for future toxic blooms in the Cape Blanc area and nearby fishing grounds off Mauritania.

### **3.6. Acknowledgments**

The authors thank the captains and crew members of RV Poseidon, RV METEOR, and RV Maria S. Merian, the MARUM sediment trap team for deploying and recovering the sediment trap, and all institutions and individuals who have participated and contributed throughout this research. The authors are also thankful of the support from German, Moroccan, and Mauritanian authorities. The work was supported by the Hanse-Wissenschaftskolleg (HWK) senior research fellowship in marine and climate research to Dr. Pospelova during her 2016 sabbatical at the Institute for Advanced Study (Germany) with Prof. Zonneveld group at the University of Bremen.

### **3.7. Data availability statement**

Supplementary data of this study is available in PANGAEA repository data, access to the dataset: [doi.pangaea.de/10.1594/PANGAEA.963113](https://doi.org/10.1594/PANGAEA.963113)

## Chapter 4 - Northwest African upwelling ecosystem response to recent climate change reflected by dinoflagellate cyst export production

Surya Eldo V. Roza<sup>1</sup>, Runa Reuter<sup>1</sup>, Jan-Berend Stuu<sup>2,3</sup>, Gerard J. M. Versteegh<sup>4</sup>, Karin A. F. Zonneveld<sup>1,5</sup>

<sup>1</sup>MARUM - Center for Marine Environmental Sciences, University of Bremen, Bremen, Germany

<sup>2</sup>Department of Ocean Systems, NIOZ Royal Netherlands Institute for Sea Research, Texel, Netherlands

<sup>3</sup>Faculty of Earth and Life Sciences, Vrije Universiteit (VU) Amsterdam, Amsterdam, Netherlands

<sup>4</sup>Department of Physics and Earth Sciences, Constructor University Bremen, Bremen, Germany

<sup>5</sup>Department of Geosciences, University of Bremen, Bremen, Germany

*To be submitted to Global Change Biology*

### Abstract

In order to better understand the impact of climate change on the Northwest African upwelling ecosystem, the export flux of dinoflagellate cysts (dinocyst) of an 18-year high-temporal resolution sediment trap time series was compared to changes in environmental steering parameters. Environmental parameters, such as upwelling intensity, wind speed and direction, aerosol dust, and sea surface temperature, were obtained from airport synoptic weather reports and satellite databases. To obtain insight into the cyclic character of the datasets, both dinocyst and environmental parameter time series were analyzed by wavelet analysis after being standardized to a resolution of 15 days. Over the whole studied time interval, half-year and annual cycles of the total dinocyst export flux coincided with those of upwelling wind dynamic and aerosol dust input. The cycles in the dinocyst time series showed three distinct phases: phase 1 (2003 – 2008), phase 2 (2009-2012), and phase 3 (2013 – 2020). The composition of the dinocyst taxa differed in each phase. The cycles in the three phases could be related to the changes in upwelling intensity and dust input into the area. This indicates that the ecosystem reacted to changes in these environmental parameters that, in turn, can be related to climate change, driven by the southward movement of the Inter Tropical Convergence Zone during the period of this study.

**Keywords:** dinocysts, upwelling, Saharan dust, Northwest Africa, wavelet analysis, ecosystem changes

### 4.1. Introduction

There has been growing concern about the influence of human activities on climate and the environment, including marine ecosystems and the organisms inhabiting them (Telesh et al., 2021; Ratnarajah et al., 2023). One of the key organisms of the plankton community is dinoflagellates. Due to their strong relationship with the environment, dinoflagellates are often used as a proxy to study modern and past ecosystems (Brosnahan et al., 2020; Zonneveld et al., 2024). Approximately 11 - 16% of living dinoflagellate species produce (resting) cysts during their reproductive cycle (**Figure 4.1**) (Head, 1996; Dale et al., 2002; Bravo and Figueroa, 2014). The morphology of the dinoflagellate cysts, or dinocysts, is species-specific. After their production in the upper water column, they sink to the ocean floor, where they can be fossilized. Dinocysts, particularly those with organic walls, are produced by phototrophic/mixotrophic or heterotrophic species (Schnepf and Elbrächter, 1992; Taylor et al., 2008; Jeong et al., 2010). Several dinocysts are also formed by biotoxin-producing dinoflagellates, capable of creating harmful algal blooms (HABs) that can have a massive impact on their ecosystem and societal community concerning fishery, tourism, and human health (Starr et al., 2017; Pitcher and Louw, 2021).

HABs form a threat to various ocean regions with no exception of the high-productive regions such as the Eastern Boundary Upwelling Ecosystems (EBUEs), which are home to biodiversity hotspots and contribute to around 25% of the global fishery (Pauly and Christensen, 1995). Upwelling systems are propelled by surface wind systems and, as such, are sensitive to changes in atmospheric wind patterns. Moreover, they are major features in the global ocean system, having a strong impact on the global carbon cycle by bringing cool and nutrient-rich deeper waters to the ocean surface, stimulating primary production that takes up large amounts of CO<sub>2</sub> from the ocean surface and transports it to the deeper ocean via the biological pump (Beaulieu, 2002; Jiao et al., 2014). One of the four EBUEs is the Canary Current upwelling system in Northwest Africa, where we conducted this study. The upwelling system is highly dynamic, with strong annual, inter-annual, and decadal variation (Romero et al., 2020; Romero et al., 2021; Roza et al., 2024). Therefore, it is highly relevant to understand the dynamics of upwelling regions in the context of changing abiotic factors and bioproduction to understand the influence of climate change on this ecosystem.

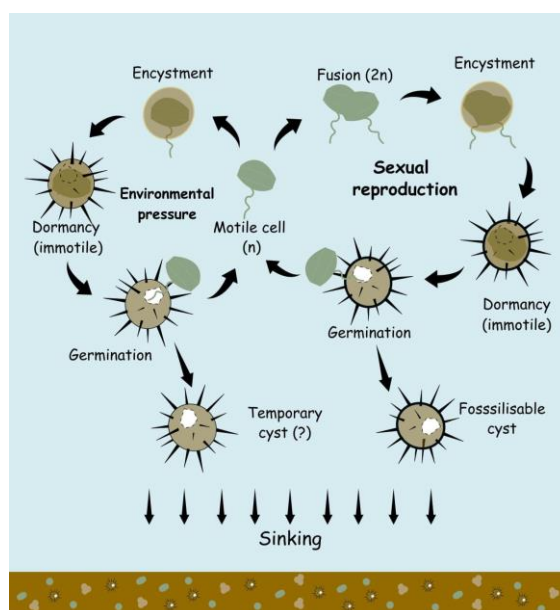


**Figure 4.1.** The simplified scheme of dinoflagellate cysts creation (encystment) shows fossilisable cysts through sexual reproduction and potentially temporary cysts. The scheme was adapted from Bravo and Figueroa (2014).

For an adequate use of dinocysts as a climate proxy, the relationship between oceanographic conditions in the upper ocean with the relative and absolute abundance of dinocyst taxa in surface sediments, as well as their qualitative and quantitative export production reflected by short-term drifting trap and in-situ pump samples have been studied (e.g., de Vernal et al., 2020; García-Moreiras et al., 2021; Likumahua et al., 2021; Rodríguez-Villegas et al., 2022; Zonneveld et al., 2022; Obrezkova et al., 2023). Unfortunately, most studies focusing on the dinocyst export out of the photic zone in relationship to changing environmental conditions only cover short time intervals. Exceptions are the sediment trap studies covering 12.5 years in the Cariaco Basin and 18 years in the upwelling area off Cape Blanc (Bringué et al., 2019; Roza et al., 2024). However, these two studies only reported the relationship between the annual and seasonal variation of dinocyst export production with upper ocean environmental factors. These studies did not focus on the underlying climatic forces that may have steered this change. This information gap inspired us to investigate the environmental driving factors of cyclic changes in total dinocyst export flux to determine how (local) climate change affected the export production of dinocysts as a reflection of changes in the upper ocean ecosystem.

To gain information on the cyclic character of the dinocyst export flux and the potential forcing factors, we performed wavelet analysis on the long-term dinocyst record of sediment trap CBeu located off Cape Blanc, covering a period from June 2003 to March 2020. We compared this record to cyclic variations in the time series of oceanic and atmospheric climate and environmental forcing parameters that were obtained from satellite data (sea surface temperature and aerosol dust) and recordings at the

Nouadhibou airport, which is located in the vicinity of the study site (e.g., wind speed, wind direction, and aerosol dust).

## 4.2. Methods

### 4.2.1. Study site and sampling

We executed this study on the dinocyst export production time series of Roza et al., 2024, covering a period of 18 years. Dinocysts were collected with a sediment trap (CBeu) deployed in the upwelling region off Cape Blanc. This upwelling is part of the Canary Current System, one of the Eastern Boundary Upwelling Ecosystems (EBEUs) (Mittelstaedt, 1983; Hagen, 2001). In this region, the upper ocean production is predominantly fertilized by the nutrients from the upwelled waters and extra micronutrient input from the Sahara (van Camp et al., 1991; Cropper et al., 2014; Chouza et al., 2016). Upwelling can be observed along the shelf break of the northwestern African shelf, with permanent year-round upwelling in the region off Cape Blanc, Mauritania. Here, the local topography, atmospheric, and oceanic factors facilitate the unique character of this upwelling zone, which also supports the distribution of nutrient-rich waters farther to the open ocean via large filaments (**Figure 4.2**) (Mittelstaedt, 1991; van Camp et al., 1991; Hagen, 2001). Although the upwelling is a permanent feature, its intensity differs through the year as a result of the annual migration of the Inter Tropical Convergence Zone (ITCZ) (Hagen, 2001; Faye et al., 2015). Stronger upwelling is forced by winds blowing in winter and spring when ITCZ has migrated south, whereas upwelling is less strong in summer/autumn when the ITCZ has its northernmost position (Hagen, 2001; Faye et al., 2015). The ITCZ also controls the transport of Saharan dust into the region by influencing the strength of the trade winds that carry the dust particles from the Sahara into the open ocean. High dust input to the East Atlantic occurs in winter and spring, while dust is transported at higher altitudes, reaching more distal locations in summer and autumn (Ben-Ami et al., 2009; Skonieczny et al., 2013; Prospero et al., 2014).

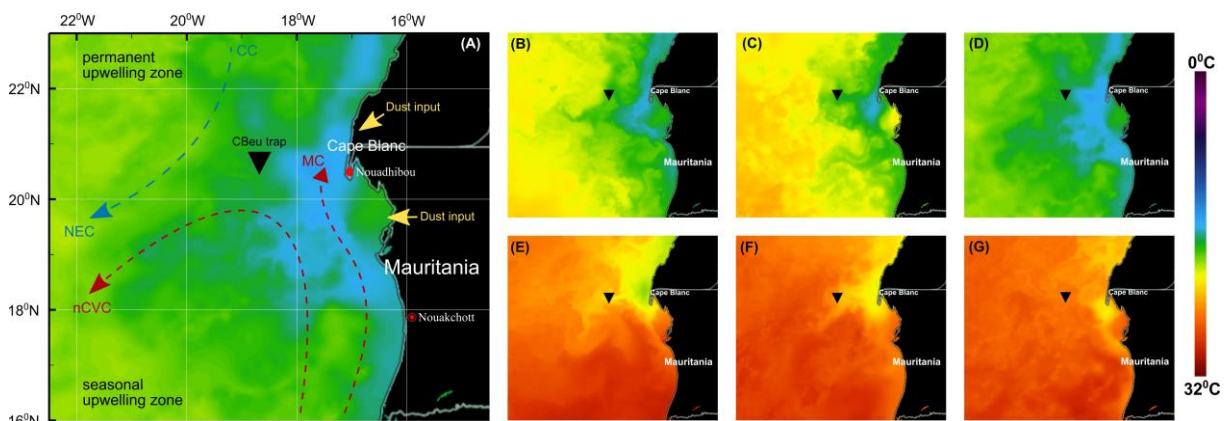


**Figure 4.2.** Location of the moored sediment trap and the temperature of the upper water column extracted from NASA “State Of The Ocean (SOTO)”: (A) the hydrography of the Atlantic coast of Mauritania depicted after Mittelstaedt (1983, 1991) and Zenk et al. (1991) showing Canary Current (CC) and North Equatorial Current (NEC) in the blue arrow as well as Cape Verde Current (CVC), north Cape Verde Current (nCVC), and Mauritania Current (MC) in red arrows. (B-D) conditions of sea surface temperature (SST) at maximum upwelling phases in 2005, 2010, and 2015 respectively. (E-G) conditions of SST at minimum upwelling phases in 2005, 2010, and 2015, respectively.

The studied samples were collected by a Kiel and Honjo type of sediment trap located between 20° 44.6' - 20° 53.0' N and 18° 41.9' - 18° 45.4' W. The trap drifted in the water column at depths around 1300 m. Below the trap funnel, sampling cups were connected to a computer-driven carousel. Sampling cups were filled with a mercury chloride (HgCl<sub>2</sub>) solution that functioned as a poison to stop biochemical processes. Pure Sodium Chloride (NaCl) was added to increase salinity and density in the sampling cups to 40‰. This procedure followed the protocol of the trap research program at MARUM that was applied by Romero and Fischer (2017), Romero et al. (2020), and Romero and Ramondenc (2022). The trap funnels had a sampling surface of 0.5 m<sup>2</sup> and were equipped with a baffle comb (Kremling et al., 1996). The deployment and recovery at the mooring site have been conducted since

2003, with sampling intervals that varied between one and three weeks. The time series of our sediment trap covered June 2003 until March 2020, which was almost continuous, with some small gaps due to the arrival schedules of the research cruises and a few longer gaps that were caused by several reasons, such as (1) malfunctioning of the trap in summer and autumn of 2006, spring of 2008, autumn of 2011, summer of 2012, and winter of 2012/2013, (2) the absence of a research cruise from autumn of 2010 until early spring of 2011. After recovery, the samples were stored in the MARUM repository at 4°C. The samples were split into 1/125 fractions using the McLane wet splitter system. Before the materials were sieved with a 1mm pore size, larger swimmer plankton, such as crustaceans, were picked out of the samples. The sampling and laboratory treatment mentioned above followed the instructions reported by Mollenhauer et al. (2015), Romero and Fischer (2017), and Fischer et al. (2019). Lastly, the materials were transferred into the respective bottles and stored in the University of Bremen freezer for further treatment. A total of 369 samples were collected and prepared for palynological analyses.

#### 4.2.2. Dinocysts extraction and determination

Every sample representing a 1/125 split from the original trap samples was washed with tap water to remove the poisonous  $HgCl_2$  and filtered using a high-precision metal sieve (Stork Veco) with a pore size of  $20\mu m$ . The samples were not treated with acid to preserve the calcareous materials. The filtered sample was sonicated in an ultrasonic bath to resuspend the fine particles. These steps were repeated until no more floating fine particles were observed in the tube. The residue samples were transferred to Eppendorf cups, centrifuged at 3000 r/min for 10 minutes, and successively concentrated to 1 ml. An assigned aliquot (50 or 100  $\mu l$ ) was placed into glycerine gelatine on a microscopic slide, enclosed with a cover slip, and sealed with paraffin wax to protect the organic component from oxidation. This standard procedure refers to Romero et al. (2020) and Roza et al. (2024) sample preparation. The organic dinoflagellate cysts were counted and identified under light microscopy (Zeiss Axiovert) with 400x magnification. The minimum number of individuals per sample was 100; when a sample did not reach this number, a maximum of two slides were added to confirm the low cyst concentration. Cyst taxa were identified based on the morphological features documented in Zonneveld and Pospelova (2015) and van Nieuwenhove et al. (2020). The dinocyst export production was calculated using the equation below:

$$Exportflux(cystm^{-2}day^{-1}) = \frac{(CC) \times (S) \times (F)}{(SS) \times (SI)}$$

Where CC is the cyst concentration (cysts  $\mu L^{-1}$ ), S is the split fraction, F is a fraction ( $\mu L^{-1}$ ), SS is the sampling surface ( $m^2$ ), and SI is the sampling interval ( $day^{-1}$ ).

#### 4.2.3. Environmental factors time series

The environmental data included in this study consist of atmospheric and sea surface parameters. The atmospheric parameters comprise wind speed, wind direction, and dust input obtained from the daily report of Nouadhibou Airport, located on the peninsula of Cape Blanc, Mauritania (**Figure 4.2**). Information about the surface wind system and Saharan dust emission was reported in the form of decoded synoptic values every day in intervals of three hours. For the wind direction, the synoptic values were transformed into the vector values of wind speed relative to its direction. The equations of wind direction vectors were adapted from a report by Grange, 2014, stating that:

$$\vec{u} = -u_i \times \sin \left[ 2\pi \times \frac{\theta_i}{360} \right] \quad \text{calculated vector wind from the north}$$

$$\vec{v} = -u_i \times \cos \left[ 2\pi \times \frac{\theta_i}{360} \right] \quad \text{calculated vector wind from the east}$$

$$\theta_{RV} = \arctan \left( \frac{\vec{u}}{\vec{v}} \right) + flow \quad \text{calculated resultant vector average of the wind direction}$$

$$flow = +180 \text{ for } \arctan\left(\frac{u}{v}\right) < 180^\circ \text{ and } -180 \text{ for } \arctan\left(\frac{u}{v}\right) > 180^\circ$$

where  $u_i$  is wind speed (m/s) and  $\theta_i$  is wind direction ( $^\circ$ ). Meanwhile, the aerosol dust data was transcribed from the horizontal visibility distance at the same airport, which was limited when the dust-storm activity from the Sahara intensified. The time series of the surface wind and dust input in daily resolution were available from January 2003 until December 2017. Additional aerosol dust data was obtained from NASA AERONET through Aerosol Optical Depth (AOD) level 2.0 at various altitudes near Cabo Verde. AERONET (Aerosol Robotic Network) is a ground-based sun photometer that measures aerosol properties through several approaches, including aerosol optical depth (AOD). The AOD algorithm records various light wavelengths reflected by the aerosol particles, providing a relative indication of dust concentration in the atmosphere. This data, particularly the reflected light at 440nm wavelength, generated the aerosol dust time series observed at 16 $^\circ$  43.9' N and 22 $^\circ$  56.1' W. The website for the NASA AERONET database is [https://aeronet.gsfc.nasa.gov/new\\_web/units.html](https://aeronet.gsfc.nasa.gov/new_web/units.html).

**Table 4.1.** The taxa list of dinocyst groups according to their relationship to the environmental parameters.

Group name	Ecological preference	Dinocysts taxa
A	Maximum upwelling+dust	<i>Archaeperidinium</i> spp.
		<i>Impagidinium</i> spp.
		<i>Lejeunecysta paratenella</i>
		<i>Operculodinium israelianum</i>
		<i>Polykrikos</i> spp.
		<i>Protoperidinium americanum</i>
		<i>P. stellatum</i>
		<i>Quinquecuspis concreta</i> ( <i>P. leonis</i> ) <i>Selenopemphix nephroides</i> ( <i>P. subinermis</i> )
B	Maximum upwelling	<i>Echinidinium</i> spp.
		<i>E. delicatum/granulatum</i>
		<i>E. transparentum/zonneveldiae</i>
		<i>Trinovantedinium</i> spp.
		<i>Votadinium calvum</i> ( <i>P. dorsale</i> )
C	Cosmopolite	<i>Brigantedinium</i> spp.
		<i>E. aculeatum</i>
		<i>I. aculeatum</i>
		<i>P. monospinum</i>
		<i>Pentapharsodinium dalei</i>
		<i>S. quanta</i> ( <i>P. conicum</i> ) <i>Spiniferites</i> spp.
D	Upwelling relaxation	<i>Gymnodinium</i> spp.
		<i>Lingulodinium machaerophorum</i> ( <i>L. polyedra</i> )

The environmental data of the sea surface encompassed sea surface temperature (SST) and sea surface temperature anomaly (SSTa) in daily resolution covering the period from January 2003 until March 2020. The SSTa time series represents the SST difference between the trap location and 200 km further offshore at the same latitude (Cropper et al., 2014). These time series were obtained from the ERDDAP data server provided by the National Center for Environmental Information (NCEI) at the vicinity area (4km grid) of the CBeu trap. Those data can be accessed through the griddap page of ERDAPP, which lists detailed information regarding the data type, resolution, sources, locations,

available time span, etc. For example, the downloaded dataset for this study is titled SST, daily optimum interpolation (OI), AVHRR Only, version 2.1, Final, Global, 0.25°, 1981-present, Lon +/-180. Furthermore, the Data Access Form can address the specification of the time span, depth, and coordinates of the desired dataset. For this study, the sea surface temperature dataset was downloaded from 01 June 2003 until 30 March 2020, located at 20° 22.5' N and 18° 22.5' W. This database link is <https://coastwatch.pfeg.noaa.gov/erddap/griddap/index.html>. A time lag of 10 days was estimated for all environmental parameters to account for the sinking duration of the dinocysts (Fischer and Karakaş, 2009; Iversen and Ploug, 2013).

#### 4.2.4. Wavelet time series analysis

Wavelet analysis can decompose one or more time series in the dimension of period and time. Wavelet requires an evenly spaced time resolution, but the time series of the dinocysts export flux had inconsistent resolution ranging from 3.5 to 25 days. In addition, gaps in the cyst flux time series contributed to the variation of the time resolution with a maximum interval of 255 days. To transform the data to evenly spaced time intervals, the mean values of dinocyst species and the environmental parameters of a time interval of 15 days have been calculated. Values for missing data of both the time series of the dinoflagellate cysts export flux and environmental data were interpolated using the Piecewise Cubic Hermite Interpolating Polynomial (PCHIP) method (Fritsch and Carlson, 1980). This method was selected as its outcome data reflected the original data better than the linear and cubic-spline methods. We performed this interpolation using MATLAB version R2019a. Morlet wavelet transform was performed using the Paleontological Statistics "PAST" software version 4.03 with the "Timeseries - Wavelet transform" package (Hammer et al., 2001) on the time series data of all studied environmental parameters, the total flux of dinocysts, and some groups of species with similar ecological preferences. Morlet wavelet displayed the coherence coefficient between the wavelet method and the data time series in different color spectra. On the color scale, coherency increases from blue to red.

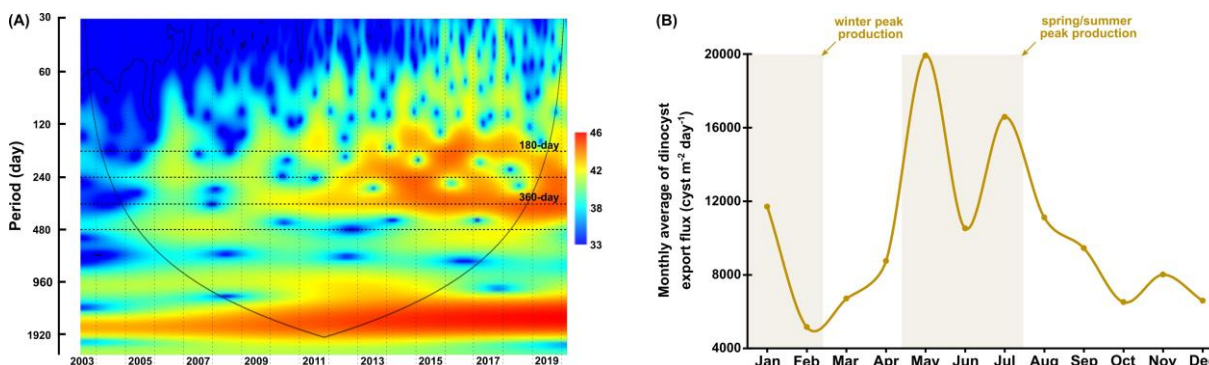


**Figure 4.3.** The time series analyses of total dinocyst export flux in the studied area were obtained by the CBeu trap. (A) The wavelet power spectra. The colour spectra indicate the different degrees of variance (ranging from high significance in red to low significance in blue), solid lines indicate regions with a high level of significance ( $p=0.05$ ), cone of influence surrounds the significant region of time and frequency that is not affected by the edges of the time series. (B) The monthly average flux of total dinocysts.

### 4.3. Results

#### 4.3.1. Wavelet analysis of the dinocysts

The wavelet power spectrum of the dinocyst export flux indicated four significant power bands reflecting different periods: 180-day (half-year cycle), 240-day, 360-day (annual cycles), and 480-day (**Figure 4.3A**). However, the expression of these periods was different over time and for the total cyst flux and four species groups with similar ecological preferences as defined by Roza et al., 2024 (**Table 4.1**). These four groups were (A) species that increased export flux during intensive upwelling and enhanced dust input (**Figure 4.4A**), (B) species that enhanced export flux during intensive upwelling only (**Figure 4.4B**), (C) species that showed no relationship with specific environmental conditions

(Figure 4.4C), and (D) species that enhanced export flux during upwelling relaxation (Figure 4.4D). In the total cyst flux time series, three phases can be distinguished:

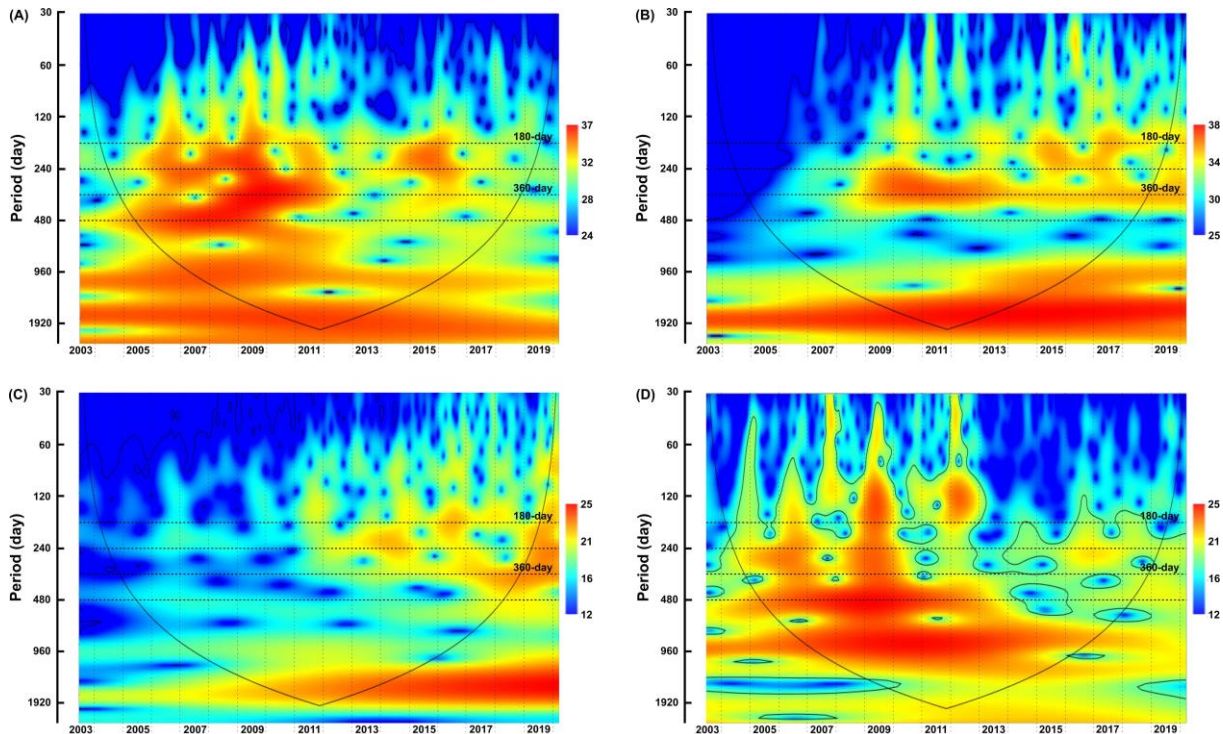


**Figure 4.4.** The wavelet power spectra of dinocyst groups with similar ecological traits: (A) upwelling+dust group, (B) upwelling group, (C) cosmopolite group, (D) upwelling relaxation group. Spectra of colours indicate the differing degree of variance (ranging from high significance in red to low significance in blue), solid lines indicate regions with a high level of significance ( $p=0.05$ ), cone of influence surrounds the significant region of time and frequency that is not affected by the edges of the time series.

**Phase 1 (2003 - 2008):** This phase is characterized by more pronounced power bands of 240 and 480 days in the total cyst export flux time series. These two periods were also observed in the time series of group A (upwelling + dust) and group D (upwelling relaxation).

**Phase 2 (2009 - 2012):** The total cyst export production visualised the strong power bands of half-year and annual cycles (180 and 360 days) during this phase. The cyst export production of groups A and B (upwelling) indicated a strong annual cycle during this phase. The cyst export production of group D showed a 480-day period in this phase.

**Phase 3 (2013 - 2020):** In the third phase, the total cyst export production shows stronger and intertwined half-year and annual cycles. The cyst export production of group A indicated a brief occurrence of half-year and annual cycles as well as the 240-day period, whereas cysts of group C (cosmopolites) showed these three periods throughout the third phase. Cysts of group B showed half-year and annual cycles, whereas cysts of group D showed weakly the 240-day period.

### 4.3.2. Wavelet analysis of environmental factors

The time series of environmental factors showed significant power bands of 180- and 360-day periods interpreted as half-year and annual cycles. The distribution of these cycle bands was different across various studied environmental factors. In the time series of wind speed and aerosol dust observed by the AOD satellite in Cabo Verde, the annual cycle was much more significant than the half-year cycle indicated by the colour of the power band and the marking of the significant lines ( $p = 0.05$ ). The combination of the two aspects also hinted at three different phases of the annual cycle in an 18-year period: phase 1 (2003 - 2008), phase 2 (2009 - 2012), phase 3 (2013 - 2020). The significant lines highlighted the three phases in the wind speed time series with the transition occurring in 2008 and 2013 (Figure 4.5A), whereas narrower and weaker annual power bands during the same transition years



indicated the three phases in the aerosol dust (AOD) time series (**Figure 4.6A**). Meanwhile, the sea surface temperature (SST) and wind direction time series displayed undisturbed annual cycle bands, showing no phase differences in these time series. The half-year cycle band was not significant in the SST time series (**Figure 4.6C**) but expressed stronger in the wind direction time series (**Figure 4.5C**). The half-year cycle showed more significant and consistent power bands in the time series of dust storms observed from the Nouadhibou Airport and sea surface temperature anomaly (SSTa). The half-year dust storm intensity (Nouadhibou) intensified during phase 3, whereas the annual cycle became less pronounced in phase 2 (**Figure 4.5E**). The annual and half-year cycles in the SSTa time series showed high variability, but the temporal variation did not match the distribution of the three phases mentioned earlier (**Figure 4.6E**).

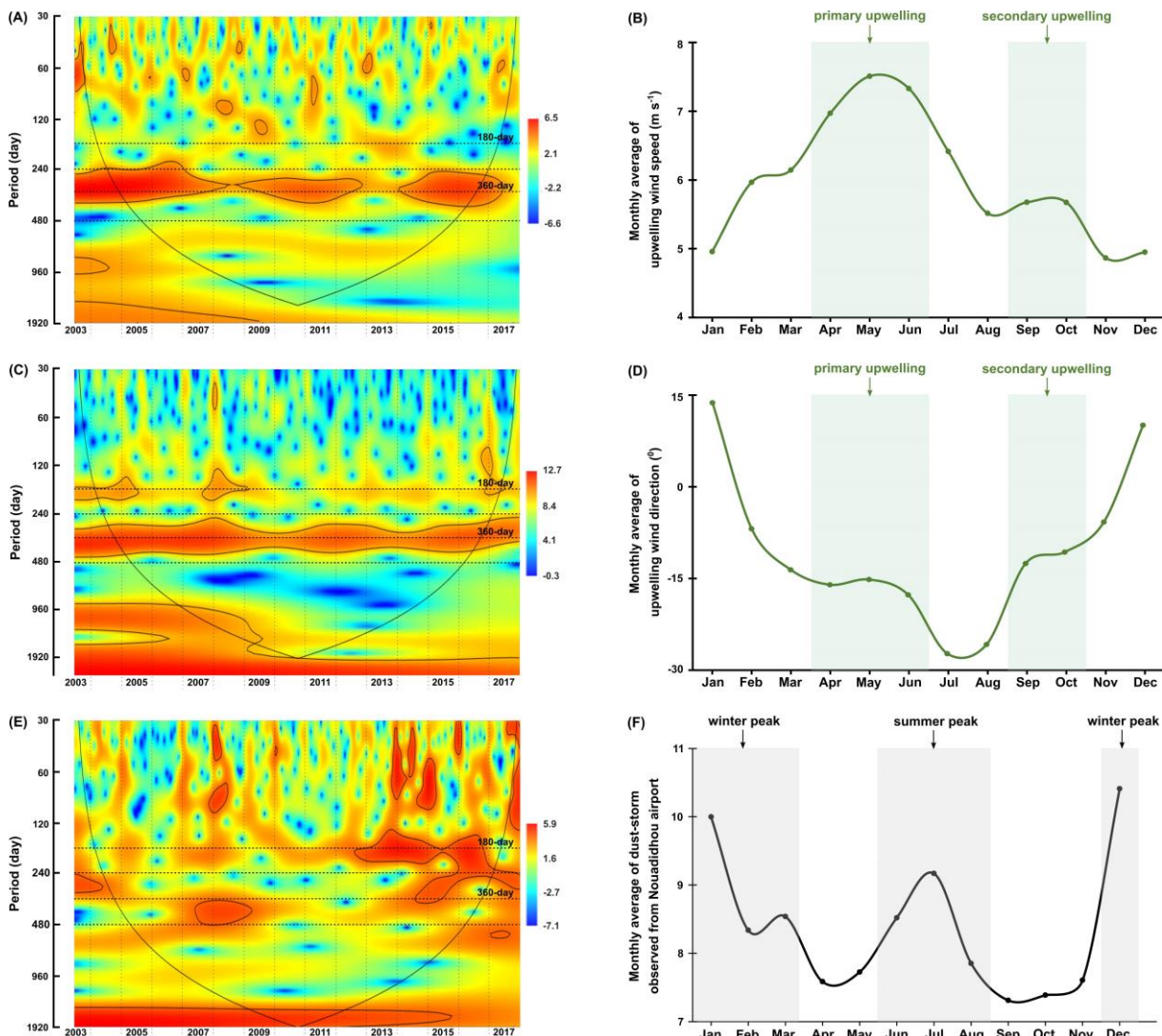


**Figure 4.5.** The wavelet power spectra (left) and the monthly average values (right) of (A-B) wind speed, (C-D) wind direction, and (E-F) dust storm events observed at Nouadhibou airport. The wavelet colour spectra indicate the different degrees of variance (ranging from high significance in red to low significance in blue), solid lines in the colour spectra indicate regions with a high level of significance ( $p=0.05$ ), cone of influence surrounds the significant region of time and frequency that is not affected by the edges of the time series.

## 4.4. Discussion

### 4.4.1. Annual cycles in the time series

The wavelet analysis showed a significant spectrum of annual cycles in all environmental factors and total dinocyst export production time series. The annual cycle in the wind system represented the

highest intensity of the wind speed coming from the north to northwest of our trap location, which was usually detected in spring (April - June) (**Figure 4.5B, D**), even though sometimes it started from late winter or stretched into early summer (Cropper et al., 2014; Fischer et al., 2016; Roza et al., 2024). The temporal occurrence of this wind speed maximum was driven by the annual boreal winter position of the Inter Tropical Convergence Zone (ITCZ), allowing the northeast trade winds to blow stronger along the northwest African coast (Faye et al., 2015; Sylla et al., 2019). This coastal wind mechanism accommodated the upwelling events in this region, bringing up nutrient-rich subsurface waters that nourished the bloom of phytoplankton, including dinoflagellates (Chen et al., 2021; Picado et al., 2023). Although most of the dinocysts collected by the sediment trap were produced by heterotrophic dinoflagellates, the rise of their concentration was in line with the concentration of their preys (such as phytoplankton) as suggested by the results of diatom and coccolithophore export productions from the same sediment trap (e.g., Romero et al., 2021; Romero and Ramondenc, 2022). Therefore, we could also see the significant spectra of the annual cycle in the dinocyst time series observed from May until July (**Figure 4.3**).

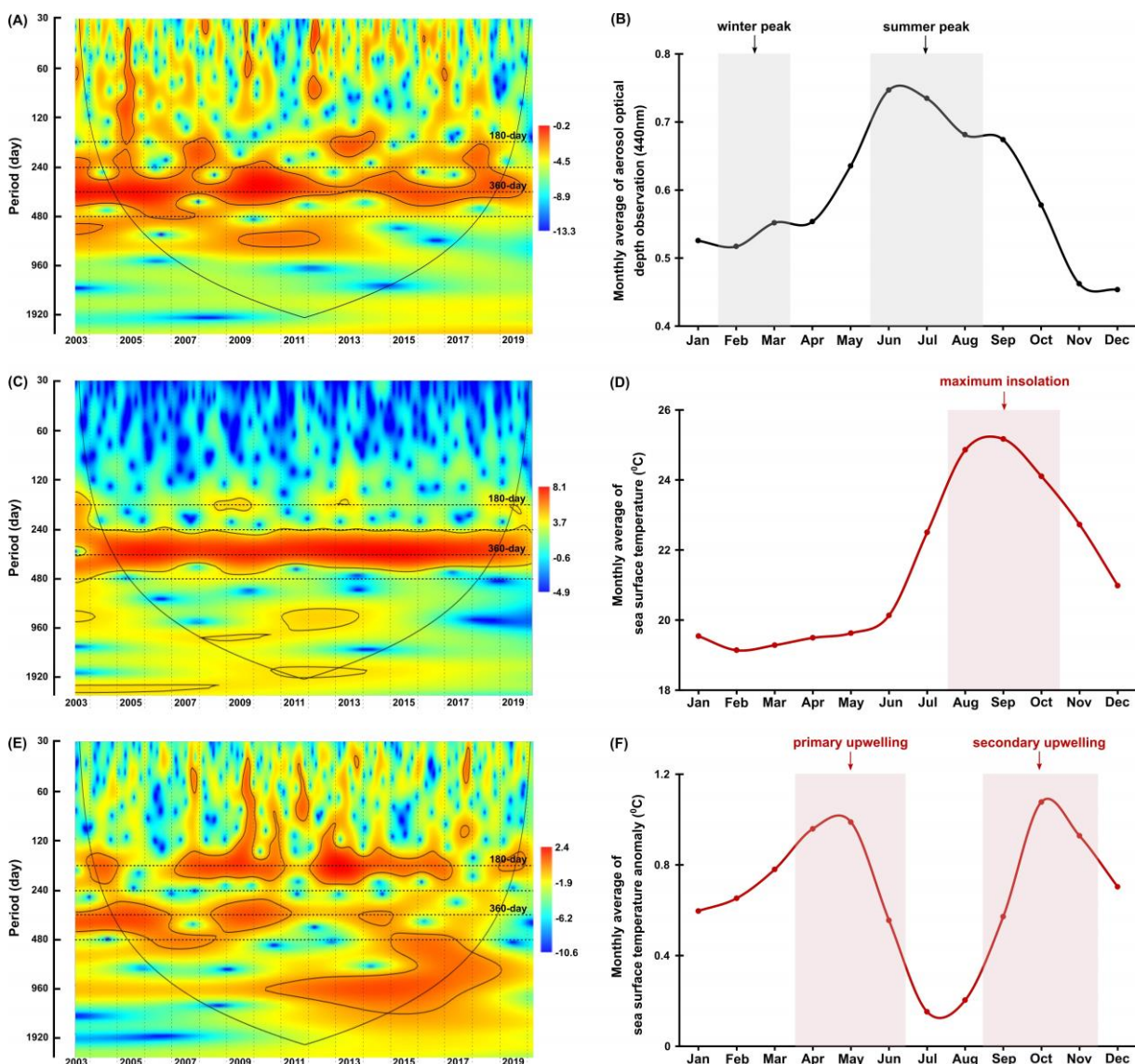


**Figure 4.6.** The wavelet power spectra (left) and the monthly average values (right) of (A-B) aerosol dust observed by NASA AERONET, (C-D) sea surface temperature, and (E-F) sea surface temperature. The wavelet colour spectra indicate the different degrees of variance (ranging from high significance in red to low significance in blue), solid lines in the colour spectra indicate regions with a high level of significance ( $p=0.05$ ), cone of influence surrounds the significant region of time and frequency that is not affected by the edges of the time series.

Surface winds also transported dust particles from the Sahara, resulting in a strong annual cycle in the dust time series observed from the AOD at Cabo Verde and Nouadhibou airport. The maximum

dust emission in the studied area was usually in winter (December - February) and extended sometimes to spring (Fischer et al., 2016; Roza et al., 2024). Despite a slight phase difference with the surface wind, this relationship still explains the influence of ITCZ on dust transport. The contribution of Saharan dust-derived nutrients to the export production of dinocysts is relatively similar to that of the coastal upwelling with dust containing essential elements for cell growth and photosynthesis (Lohan and Tagliabue, 2018; Wyatt et al., 2023). However, the annual cycles of both dust records (Cabo Verde and Nouadhibou) showed different patterns over time. The dust time series from the Nouadhibou airport showed a weak annual cycle from 2005 to 2006 and 2010 to 2013 but strongly expressed the half-year cycle (**Figure 4.5E**). Conversely, the annual cycle in the Cabo Verde dust time series was significant every year (**Figure 4.6A**). We assume that this difference might be due to the differences in dust mobilization at various locations and observation altitudes. Cabo Verde is situated further to the southwest of Nouadhibou airport, so sources of emitted dust in boreal winter and summer could differ depending on the wind trade distribution in these two locations (van Der Does et al., 2016; Yu et al., 2019). In addition, dust emission in Cabo Verde was observed by a satellite that combined dust concentrations at various altitudes, resulting in a higher peak in summer (**Figure 4.6B**). In comparison, the dust storm events were estimated from lower altitudes at the Nouadhibou airport, where the dust load displayed the highest peak in winter (**Figure 4.5F**).

The annual sea surface temperature (SST) at the trap location is driven by the sun's insolation into the ocean surface, with the maximum insolation usually occurring during boreal summer (June - August) in the northern hemisphere (Bae et al., 2022). In the studied area, the highest SST was observed in autumn (September and October), sometimes already starting in late summer (**Figure 4.6D**) (Fischer et al., 2016; Roza et al., 2024). The region impacted by high solar insolation has higher precipitation rates and lower air pressure that changes in time with the movement of the ITCZ (Vindel et al., 2020; Bae et al., 2023). Consequently, when this area experienced maximum SST, the intensity of upwelling and dust input was lowest. This resulted in significant disparities between SST in boreal winter (low insolation plus colder upwelled water reached the sea surface) and summer, explaining why the annual SST cycle appeared the strongest among the time series (**Figure 4.6C**). It can be concluded that the annual peak production of dinocysts in the studied area thrived under strong upwelling, high dust input, and low SST (**Figure 4.3B**).

#### 4.4.2. Half-year cycle and other periodicities in the time series

Besides the annual cycle, there were 240- and 480-day periods, and the half-year cycle was shown by the wavelet power bands. Unfortunately, the 240- and 480-day periods were only detected in the dinocyst time series, and none of the environmental factors showed this cyclicity pattern. Therefore, no relationship between these period occurrences in the total dinocyst export flux and the studied environmental parameters could be drawn, and further study is required to investigate the possible driving factors. On the contrary, the half-year cycle only displayed strong and consistent results in a few time series, such as wind direction, dust storm (Nouadhibou airport), SSTa, and dinocyst export production. The half-year cycle in the wind direction was observed when the trade winds blew from a northwest direction ( $-10^{\circ}$  to  $-15^{\circ}$ ), which coincided with the time of most active upwelling (April - June) and secondary upwelling (September - October) (**Figure 4.5D**). The half-year cycle in the dust records showed two annual peaks. The first was the maximum emission during winter, as mentioned earlier, and the second usually occurred in summer with a lower peak (**Figure 4.5F, 3.6B**). In the SSTa (caused by the temperature differences between areas influenced by upwelling and offshore) time series, the most significant appearance of the half-year cycle coincided with the maximum upwelling in spring (April - June) and once more in autumn (September - November) (**Figure 4.6E, F**). This result indicated the existence of the second period of upwelling with weaker intensity in the area that was not clearly reflected in the wind speed time series (**Figure 4.5A, B**). The half-year cycle was also observed in the dinocyst time series, coinciding with the high winter dust emission (January - February) as well as a combination of intensive upwelling and summer dust emission (May - July) (**Figure 4.3B**). This latter suggests again the positive relationship between upwelling and dust emission to dinocyst export flux.

#### 4.4.3. Ecosystem changes

The advantage of wavelet analysis is that it can visualise changes in the strength of cycles in the time series. As mentioned earlier, the annual and half-year cycles of the dinocyst export flux hinted at three phases that showed changes from one phase to the other (**Figure 4.3A**). The first phase (2003 - 2008) was specified by insignificant annual and half-year cycles of dinocysts production, and most of the cysts during this phase were produced by cysts of group A (upwelling+dust) (**Figure 4.4A**). The annual and half-year cycles emerged in the second phase (2009 - 2012) when the upwelling group dominated the dinocysts association (**Figure 4.4B**). The final interval (2013 - 2020) showed an intensification for both cycles that was also seen in the upwelling group. In the third phase, a brief emergence of both cycles was displayed in the cosmopolite group as well. These phases could also be observed in the annual cycle of wind speed and dust emission (AOD), with the spectra of the annual cycle of both time series weakened in 2008 and 2012, the transition years between the phases (**Figure 4.5A, 3.6A**). According to the wavelet spectra, dinocyst cycles were more pronounced in the second phase and stronger in the third phase, in which their cycles strongly correlated to the upwelling wind and dust emission. Therefore, we interpret that the influence of these two factors on dinocyst export flux increased with time in this area. Although the annual cycle in the dust storm (Nouadhibou airport) did not reflect the exact same pattern, the weakened spectra between 2010 – 2012 correspond to most of the interval of phase 2. Coinciding with the start of phase three, a strong half-year cyclicity appeared in this parameter from 2013 onwards (**Figure 4.5E**).

Since the intensity of upwelling and dust transport is strongly related to the position of Inter Tropical Convergence Zone (ITCZ), the observed shifts in the cyclic pattern of the wind speed and aerosol dust time series suggest that long-term changes in the ITCZ position occurred. Mamalakis et al. (2021) conducted a reconstruction of the global mean position of ITCZ from 1983 to 2005 (baseline), and they established a model to predict the movement of this zone in the future to 2100. Their model suggested that the ITCZ in the East Pacific-Atlantic sector will move southward by  $0.7^{\circ} \pm 0.9^{\circ}$  from its original baseline from 2007 onwards. Furthermore, Rodríguez et al. (2015) measured an increase in the atmospheric pressure differences from the summer of 2008, where the subtropics (Morocco) indicated maximum high pressure and the tropics (Bamako region) showed minimum low pressure. This latter supported the scenario of an ITCZ southward shift because this convergence belt moves to areas with lower atmospheric pressures (Arbuszewski et al., 2013; Rodríguez et al. (2015); Mamalakis et al., 2021). A southward shift of the ITCZ position would lead to stronger westerly trade winds and more aridity in the Sahara regions (North Africa), which would lead to more intensified upwelling and more dust emission to the (sub)tropical part of the North Atlantic Ocean (Rodríguez et al., 2015). This hypothesis is supported by the dinocyst time series reflecting more pronounced occurrences of the annual and half cycles in phase 2 (2009 - 2012) and even stronger in phase 3 (2013 - 2020). In addition, upwelling taxa (group B) showed more pronounced cyclicities in phases 2 and 3, and the cyst of the upwelling relaxation group showed insignificant half-year and annual cycles in phase 3. According to the result of Roza et al. 2024, the dinocyst export flux increased during most of phase 2. However, this trend did not continue in phase 3, as indicated by the cyclic pattern of the dinocyst time series. It indicated that other abiotic and biotic factors could also influence the concentration of dinocyst export flux over time.

We suggest that the observed changes in the dinocyst export flux composition can be correlated to upwelling wind and dust dynamics consistent with a southward movement of ITCZ position from phase 1 to phase 3 (June 2003 - March 2020). This shift could be driven by lowering air pressure and warming temperatures south of the Northwest Africa upwelling region, which is the climatic condition where ITCZ will migrate. The three-step change in dinocyst association composition suggests that the change in the upper ocean ecosystem of this upwelling area reacted stepwise on the climate change-induced southward movement of the ITCZ. Our results demonstrate that a long record of dinocyst (plankton) production is essential to investigate an indication of climatic changes in a certain area through their relationship with the environment.

## 4.5. Conclusions

Wavelet analysis demonstrates a strong annual cycle in all records of total dinocyst export flux and environmental factors from 2003 - 2020 off Cap Blanc. Additionally, the analyses show a prominent half-year cycle in dinocyst export flux, wind speed, and dust. The dinocyst export flux maximized during the winter dust peak in January - February combined with intensive upwelling. A second high in cyst production occurs during the summer dust peak in April - June. In 18 years, the pattern of half-year and annual cycles in dinocyst export flux showed variations divided into three phases, which were also detected in upwelling wind speed and Saharan dust input. Phase 1 (2003 - 2008): half-year and annual cycles were insignificant, and the upwelling+dust group mostly represented the total dinocyst export flux cycles. Phase 2 (2009 -2012): both cycles were observed and were most pronounced visible in the upwelling group. Phase 3 (2013 – 2020): both cycles were more strongly pronounced in the spectra of the upwelling and cosmopolite groups. These findings indicated that the upwelling wind and dust emission showed increasingly pronounced half-year and annual cyclicity from phase 1 to phase 3, which could be related to the southward movement of the ITCZ position. The three-phase change in reaction of the dinocyst community suggests that the upwelling ecosystem off Cape Blanc reacted to the climate-induced changes in forcing parameters.

## 4.6. Acknowledgements

This study was financially supported by the German Research Foundation (DFG) through the MARUM Cluster of Excellence (EXC): The Ocean Floor – Earth’s Uncharted Interface, in the research unit Recorder and Receiver. The research would not have been possible without the support of the authorities of Germany, Morocco, and Mauritania. Sampling with the sediment trap was made possible with the help of the captain and the ship crews of RV Poseidon, RV Sonne, and RV Maria S. Merian, as well as the MARUM sediment trap team. The authors are thanking Dr. Pospelova, who acquired support from the Hanse-Wissenschaftskolleg (HWK) fellowship for her contribution to this project during her 2016 sabbatical at the Institute for Advance Study (Germany) with Prof. Zonneveld at the University of Bremen. The authors also thank all individuals and institutions that have directly contributed to the implementation of this study.

## 4.7. Supplementary materials

**Supplementary table 4.1.** Multi-year sediment trap datasets containing the original temporal resolution with the respective export fluxes of total dinocyst, upwelling, upwelling dust, cosmopolite, and upwelling relaxation groups.

Sample ID	Sampling duration	Julian day	Total dinocyst flux	Upwelling group	Upwelling+dust group	Cosmopolite group	Upwelling relaxation group
CBi1-1	05/06/2003 - 16/06/2003	161.75	1306.45	112.90	177.42	967.74	0.00
CBi1-2	16/06/2003 - 01/07/2003	174.75	2338.71	423.39	181.45	1673.39	20.16
CBi1-3	01/07/2003 - 17/07/2003	190.25	4919.35	80.65	2983.87	1693.55	161.29
CBi1-4	17/07/2003 - 01/08/2003	205.75	10645.16	2258.06	2096.77	5887.10	241.94
CBi1-5	01/08/2003 - 17/08/2003	221.25	29516.13	1048.39	8629.03	19274.19	322.58
CBi1-6	17/08/2003 - 01/09/2003	236.75	28870.97	1774.19	9032.26	17903.23	80.65
CBi1-7	01/09/2003 - 17/09/2003	252.25	27983.87	1612.90	6774.19	19193.55	403.23
CBi1-8	17/09/2003 - 02/10/2003	267.75	12016.13	725.81	5322.58	5967.74	0.00
CBi1-9	02/10/2003 – 18/10/2003	283.25	0.00	0.00	0.00	0.00	0.00
CBi1-10	18/10/2003 - 02/11/2003	298.75	2157.26	181.45	826.61	907.26	221.77
CBi1-11	02/11/2003 - 18/11/2003	314.25	1713.71	120.97	483.87	967.74	60.48
CBi1-12	18/11/2003 - 03/12/2003	329.75	806.45	20.16	302.42	423.39	60.48
CBi1-13	03/12/2003 - 19/12/2003	345.25	745.97	40.32	241.94	342.74	80.65
CBi1-14	19/12/2003 - 03/01/2004	360.75	2016.13	181.45	423.39	1270.16	120.97

CBi1-15	03/01/2004 - 19/01/2004	376.25	1088.71	20.16	302.42	604.84	141.13
CBi1-16	19/01/2004 - 03/02/2004	391.75	1774.19	201.61	483.87	725.81	362.90
CBi1-17	03/02/2004 - 19/02/2004	407.25	1733.87	80.65	524.19	1048.39	40.32
CBi1-18	19/02/2004 - 05/03/2004	422.75	564.52	20.16	100.81	403.23	40.32
CBi1-19	05/03/2004 - 21/03/2004	438.25	1612.90	161.29	161.29	725.81	483.87
CBi1-20	21/03/2004 - 05/04/2004	453.75	241.94	1169.35	362.90	2258.06	80.65
Gap time	05/04/2004 - 18/04/2004	467.75	0.00	0.00	0.00	0.00	0.00
CBi2-1	18/04/2004 - 10/05/2004	485.00	7386.36	1250.00	1022.73	4715.91	113.64
CBi2-2	10/05/2004 - 01/06/2004	507.00	2239.13	304.35	456.52	1391.30	43.48
CBi2-3	01/06/2004 - 24/06/2004	529.50	2228.26	815.22	217.39	1195.65	0.00
CBi2-4	24/06/2004 - 17/07/2004	552.50	1345.11	149.46	312.50	828.80	27.17
CBi2-5	17/07/2004 - 09/08/2004	575.50	135.87	8.15	43.48	62.50	5.43
CBi2-6	09/08/2004 - 01/09/2004	598.50	0.00	0.00	0.00	0.00	0.00
CBi2-7	01/09/2004 - 24/09/2004	621.50	0.00	0.00	0.00	0.00	0.00
CBi2-8	24/09/2004 - 17/10/2004	644.50	0.00	0.00	0.00	0.00	0.00
CBi2-9	17/10/2004 - 09/11/2004	667.50	1739.13	529.89	176.63	1005.43	13.59
CBi2-10	09/11/2004 - 02/12/2004	690.50	7934.78	1576.09	760.87	5543.48	108.70
CBi2-11	02/12/2004 - 25/12/2004	713.50	19836.96	2336.96	1467.39	14347.83	1630.43
CBi2-12	25/12/2004 - 17/01/2005	736.50	7554.35	380.43	760.87	3532.61	2934.78
CBi2-13	17/01/2005 - 09/02/2005	759.50	6250.00	434.78	1195.65	4130.43	434.78
CBi2-14	09/02/2005 - 04/03/2005	782.50	15815.22	815.22	8858.70	4728.26	1250.00
CBi2-15	04/03/2005 - 27/03/2005	805.50	7826.09	271.74	5706.52	1793.48	108.70
CBi2-16	27/03/2005 - 19/04/2005	828.50	8478.26	706.52	4076.09	3260.87	380.43
CBi2-17	19/04/2005 - 12/05/2005	851.50	11684.78	1521.74	2065.22	7880.43	163.04
CBi2-18	12/05/2005 - 04/06/2005	874.50	3369.57	516.30	788.04	1875.00	135.87
CBi2-19	04/06/2005 - 27/06/2005	897.50	4211.96	1195.65	815.22	1983.70	163.04
CBi2-20	27/06/2005 - 20/07/2005	920.50	6086.96	1467.39	869.57	3478.26	271.74
Gap time	20/07/2005 - 25/07/2005	934.50	0.00	0.00	0.00	0.00	0.00
CBi3-1	25/07/2005 - 16/08/2005	947.75	2965.12	348.84	232.56	2354.65	58.14
CBi3-2	16/08/2005 - 06/09/2005	969.25	6744.19	1860.47	465.12	4186.05	116.28
CBi3-3	06/09/2005 - 28/09/2005	990.75	6162.79	697.67	1046.51	4186.05	232.56
CBi3-4	28/09/2005 - 19/10/2005	1012.25	13604.65	1046.51	3255.81	8953.49	232.56
CBi3-5	19/10/2005 - 10/11/2005	1033.75	10000.00	639.53	3895.35	5465.12	58.14
CBi3-6	10/11/2005 - 01/12/2005	1055.25	11744.19	1627.91	2209.30	7441.86	348.84
CBi3-7	01/12/2005 - 23/12/2005	1076.75	7558.14	755.81	1162.79	5406.98	174.42
CBi3-8	23/12/2005 - 13/01/2006	1098.25	10348.84	930.23	1337.21	7674.42	290.70
CBi3-9	13/01/2006 - 04/02/2006	1119.75	4806.20	658.91	620.16	3410.85	77.52
CBi3-10	04/02/2006 - 25/02/2006	1141.25	2848.84	232.56	58.14	2383.72	116.28
CBi3-11	25/02/2006 - 19/03/2006	1162.75	5000.00	406.98	552.33	3837.21	145.35
CBi3-12	19/03/2006 - 09/04/2006	1184.25	20697.67	1627.91	4302.33	14418.60	348.84
CBi3-13	09/04/2006 - 01/05/2006	1205.75	23488.37	2790.70	5697.67	14767.44	116.28
CBi3-14	01/05/2006 - 22/05/2006	1227.25	12906.98	1395.35	4883.72	6395.35	116.28
CBi3-15	22/05/2006 - 13/06/2006	1248.75	53372.09	7558.14	33139.53	12674.42	0.00
CBi3-16	13/06/2006 - 04/07/2006	1270.25	60697.67	18488.37	18953.49	22209.30	930.23
CBi3-17	04/07/2006 - 26/07/2006	1291.75	54186.05	11279.07	7790.70	34767.44	232.56
CBi3-18	26/07/2006 - 16/08/2006	1313.25	0.00	0.00	0.00	0.00	0.00
CBi3-19	16/08/2006 - 07/09/2006	1334.75	0.00	0.00	0.00	0.00	0.00
CBi3-20	07/09/2006 - 28/09/2006	1356.25	0.00	0.00	0.00	0.00	0.00
Gap time	28/09/2006 - 28/10/2006	1382.00	0.00	0.00	0.00	0.00	0.00
CBi4-1	28/10/2006 - 01/11/2006	1398.75	1777.78	333.33	185.19	1074.07	111.11
CBi4-2	01/11/2006 - 08/11/2006	1404.25	13666.67	777.78	1000.00	11111.11	666.67
CBi4-3	08/11/2006 - 16/11/2006	1411.75	12416.67	1666.67	1166.67	9250.00	83.33
CBi4-4	16/11/2006 - 23/11/2006	1419.25	16333.33	1250.00	2750.00	12083.33	166.67
CBi4-5	23/11/2006 - 01/12/2006	1426.75	5266.67	333.33	466.67	4333.33	66.67
CBi4-6	01/12/2006 - 08/12/2006	1434.25	10916.67	1000.00	916.67	8750.00	333.33
CBi4-7	08/12/2006 - 16/12/2006	1441.75	11666.67	833.33	916.67	9750.00	83.33
CBi4-8	16/12/2006 - 23/12/2006	1449.25	6666.67	611.11	388.89	5388.89	166.67
CBi4-9	23/12/2006 - 31/12/2006	1456.75	8666.67	250.00	916.67	7333.33	83.33
CBi4-10	31/12/2006 - 07/01/2007	1464.25	7277.78	666.67	444.44	5722.22	166.67

CBi4-11	07/01/2007 - 15/01/2007	1471.75	6333.33	388.89	388.89	5388.89	111.11
CBi4-12	15/01/2007 - 22/01/2007	1479.25	5500.00	444.44	388.89	4611.11	0.00
CBi4-13	22/01/2007 - 30/01/2007	1486.75	4583.33	333.33	125.00	3875.00	125.00
CBi4-14	30/01/2007 - 06/02/2007	1494.25	2766.67	166.67	200.00	2333.33	33.33
CBi4-15	06/02/2007 - 14/02/2007	1501.75	2500.00	166.67	200.00	2033.33	33.33
CBi4-16	14/02/2007 - 21/02/2007	1509.25	2366.67	166.67	200.00	1800.00	133.33
CBi4-17	21/02/2007 - 01/03/2007	1516.75	2333.33	233.33	200.00	1733.33	100.00
CBi4-18	01/03/2007 - 08/03/2007	1524.25	7277.78	1111.11	611.11	5333.33	222.22
CBi4-19	08/03/2007 - 16/03/2007	1531.75	8500.00	1055.56	722.22	5722.22	777.78
CBi4-20	16/03/2007 - 23/03/2007	1539.25	7055.56	1111.11	888.89	4944.44	55.56
Gap time	23/03/2007 - 28/03/2007	1545.50	0.00	0.00	0.00	0.00	0.00
CBi5-1	28/03/2007 - 03/04/2007	1550.75	5913.46	961.54	1105.77	3750.00	48.08
CBi5-2	03/04/2007 - 09/04/2007	1556.75	5144.23	625.00	673.08	3365.38	192.31
CBi5-3	09/04/2007 - 19/04/2007	1564.75	2868.42	315.79	289.47	2263.16	26.32
CBi5-6	19/04/2007 - 28/04/2007	1574.25	18596.49	9473.68	3859.65	5175.44	87.72
CBi5-7	28/04/2007 - 08/05/2007	1583.75	69736.84	43508.77	18508.77	7719.30	0.00
CBi5-10	08/05/2007 - 17/05/2007	1593.25	3815.79	1315.79	447.37	1921.05	52.63
CBi5-11	17/05/2007 - 27/05/2007	1602.75	3322.37	1019.74	493.42	1644.74	0.00
CBi5-12	27/05/2007 - 05/06/2007	1612.25	6973.68	986.84	986.84	4013.16	723.68
CBi5-13	05/06/2007 - 15/06/2007	1621.75	5000.00	986.84	690.79	2927.63	263.16
CBi5-14	15/06/2007 - 24/06/2007	1631.25	7302.63	2894.74	723.68	3486.84	197.37
CBi5-15	24/06/2007 - 04/07/2007	1640.75	3125.00	855.26	361.84	1743.42	65.79
CBi5-17	04/07/2007 - 13/07/2007	1650.25	12894.74	2105.26	3552.63	6842.11	394.74
CBi5-18	13/07/2007 - 23/07/2007	1659.75	21315.79	4078.95	2894.74	13947.37	131.58
CBi5-19	23/07/2007 - 01/08/2007	1669.25	23684.21	4210.53	2500.00	15657.89	657.89
CBi5-20	01/08/2007 - 11/08/2007	1678.75	11842.11	3552.63	789.47	7236.84	131.58
CBi5-21	11/08/2007 - 20/08/2007	1688.25	12236.84	1578.95	657.89	9342.11	0.00
CBi5-22	20/08/2007 - 30/08/2007	1697.75	7434.21	1315.79	394.74	5592.11	65.79
CBi5-23	30/08/2007 - 08/09/2007	1707.25	0.00	0.00	0.00	0.00	0.00
CBi5-24	08/09/2007 - 18/09/2007	1716.75	10131.58	1447.37	789.47	7763.16	131.58
CBi5-25	18/09/2007 - 27/09/2007	1726.25	10526.32	1710.53	657.89	7894.74	131.58
CBi5-26	27/09/2007 - 07/10/2007	1735.75	3834.59	451.13	225.56	3082.71	75.19
CBi5-27	07/10/2007 - 16/10/2007	1745.25	2105.26	184.21	210.53	815.79	894.74
CBi5-28	16/10/2007 - 26/10/2007	1754.75	13421.05	1052.63	1447.37	5263.16	5394.74
CBi5-29	26/10/2007 - 04/11/2007	1764.25	5157.89	157.89	473.68	3421.05	1157.89
CBi5-30	04/11/2007 - 14/11/2007	1773.75	13552.63	1973.68	789.47	8026.32	2500.00
CBi5-31	14/11/2007 - 23/11/2007	1783.25	6105.26	368.42	684.21	3947.37	1157.89
CBi5-32	23/11/2007 - 03/12/2007	1792.75	6368.42	736.84	315.79	4473.68	789.47
CBi5-33	03/12/2007 - 12/12/2007	1802.25	13552.63	657.89	1315.79	9210.53	2368.42
CBi5-34	12/12/2007 - 22/12/2007	1811.75	3157.89	187.97	187.97	2406.02	375.94
CBi5-35	22/12/2007 - 31/12/2007	1821.25	3533.83	150.38	75.19	3233.08	0.00
CBi5-36	31/12/2007 - 10/01/2008	1830.75	657.89	0.00	0.00	605.26	26.32
CBi5-37	10/01/2008 - 19/01/2008	1840.25	2368.42	32.89	98.68	2039.47	32.89
CBi5-38	19/01/2008 - 29/01/2008	1849.75	4605.26	131.58	65.79	3684.21	460.53
CBi5-39	29/01/2008 - 07/02/2008	1859.25	4172.93	150.38	338.35	3270.68	375.94
CBi5-40	07/02/2008 - 17/02/2008	1868.75	15131.58	921.05	657.89	12105.26	1184.21
Gap time	17/02/2008 - 26/04/2008	1908.25	0.00	0.00	0.00	0.00	0.00
CBi6-1	26/04/2008 - 30/04/2008	1944.75	10428.57	1214.29	2214.29	7000.00	71.43
CBi6-2	30/04/2008 - 03/05/2008	1948.25	90000.00	13571.43	14285.71	61428.57	714.29
CBi6-3	03/05/2008 - 12/05/2008	1954.25	46764.71	8088.24	7500.00	30441.18	294.12
CBi6-4	12/05/2008 - 20/05/2008	1962.75	22941.18	3725.49	3431.37	15294.12	0.00
CBi6-5	20/05/2008 - 29/05/2008	1971.25	23823.53	5588.24	3823.53	14411.76	0.00
CBi6-6	29/05/2008 - 06/06/2008	1979.75	8774.51	1813.73	1568.63	5196.08	98.04
CBi6-7	06/06/2008 - 15/06/2008	1988.25	3403.36	504.20	378.15	2478.99	42.02
CBi6-8	15/06/2008 - 23/06/2008	1996.75	5551.47	294.12	551.47	4448.53	183.82
CBi6-9	23/06/2008 - 02/07/2008	2005.25	24852.94	3676.47	4852.94	16029.41	441.18
CBi6-10	02/07/2008 - 10/07/2008	2013.75	27745.10	5000.00	5294.12	16862.75	294.12
CBi6-11	10/07/2008 - 19/07/2008	2022.25	9705.88	1985.29	1397.06	6176.47	147.06
CBi6-12	19/07/2008 - 27/07/2008	2030.75	8823.53	1102.94	2132.35	5514.71	0.00

CBi6-13	27/07/2008 - 05/08/2008	2039.25	8014.71	882.35	882.35	6176.47	73.53
CBi6-14	05/08/2008 - 13/08/2008	2047.75	3860.29	551.47	551.47	2720.59	0.00
CBi6-15	13/08/2008 - 22/08/2008	2056.25	2242.65	110.29	36.76	1948.53	147.06
CBi6-16	22/08/2008 - 30/08/2008	2064.75	1801.47	110.29	110.29	1433.82	110.29
CBi6-17	30/08/2008 - 08/09/2008	2073.25	2977.94	441.18	257.35	2169.12	36.76
CBi6-18	08/09/2008 - 16/09/2008	2081.75	924.37	42.02	84.03	798.32	0.00
CBi6-19	16/09/2008 - 25/09/2008	2090.25	1066.18	110.29	36.76	772.06	110.29
CBi6-20	25/09/2008 - 03/10/2008	2098.75	551.47	0.00	0.00	551.47	0.00
CBi6-21	03/10/2008 - 12/10/2008	2107.25	10504.20	378.15	1092.44	8949.58	84.03
CBi6-22	12/10/2008 - 20/10/2008	2115.75	6029.41	183.82	919.12	5183.82	36.76
CBi6-23	20/10/2008 - 29/10/2008	2124.25	4950.98	294.12	1568.63	2892.16	0.00
CBi6-24	29/10/2008 - 06/11/2008	2132.75	3411.76	147.06	823.53	2382.35	0.00
CBi6-25	06/11/2008 - 15/11/2008	2141.25	3725.49	147.06	49.02	3333.33	49.02
CBi6-26	15/11/2008 - 23/11/2008	2149.75	2279.41	147.06	147.06	1985.29	36.76
CBi6-27	23/11/2008 - 02/12/2008	2158.25	1985.29	36.76	367.65	1544.12	0.00
CBi6-28	02/12/2008 - 10/12/2008	2166.75	1764.71	220.59	110.29	1397.06	0.00
CBi6-29	10/12/2008 - 19/12/2008	2175.25	3529.41	196.08	343.14	2990.20	0.00
CBi6-30	19/12/2008 - 27/12/2008	2183.75	21911.76	2500.00	5294.12	14117.65	0.00
CBi6-31	27/12/2008 - 05/01/2009	2192.25	15000.00	1764.71	1764.71	11176.47	0.00
CBi6-32	05/01/2009 - 13/01/2009	2200.75	2757.35	294.12	735.29	1727.94	0.00
CBi6-33	13/01/2009 - 22/01/2009	2209.25	1544.12	147.06	220.59	1139.71	0.00
CBi6-34	22/01/2009 - 30/01/2009	2217.75	1617.65	0.00	330.88	1250.00	36.76
CBi6-35	30/01/2009 - 08/02/2009	2226.25	1286.76	73.53	183.82	992.65	36.76
CBi6-36	08/02/2009 - 16/02/2009	2234.75	1397.06	0.00	220.59	1029.41	0.00
CBi6-37	16/02/2009 - 25/02/2009	2243.25	1029.41	73.53	73.53	808.82	0.00
CBi6-38	25/02/2009 - 05/03/2009	2251.75	1176.47	147.06	147.06	808.82	0.00
CBi6-39	05/03/2009 - 14/03/2009	2260.25	5294.12	514.71	294.12	4044.12	73.53
CBi6-40	14/03/2009 - 22/03/2009	2268.75	4558.82	808.82	514.71	3235.29	0.00
Gap time	22/03/2009 - 01/04/2009	2277.75	0.00	0.00	0.00	0.00	0.00
CBi7-1	01/04/2009 - 10/04/2009	2287.00	902.78	69.44	0.00	763.89	0.00
CBi7-2	10/04/2009 - 19/04/2009	2296.00	648.15	0.00	92.59	555.56	0.00
CBi7-3	19/04/2009 - 28/04/2009	2305.00	1284.72	104.17	138.89	868.06	0.00
CBi7-4	28/04/2009 - 07/05/2009	2314.00	28750.00	10555.56	3333.33	14166.67	0.00
CBi7-5	07/05/2009 - 16/05/2009	2323.00	22777.78	7916.67	833.33	13888.89	138.89
CBi7-6	16/05/2009 - 25/05/2009	2332.00	30277.78	7638.89	972.22	21250.00	0.00
CBi7-8	25/05/2009 - 03/06/2009	2341.00	8796.30	2500.00	740.74	5462.96	0.00
CBi7-9	03/06/2009 - 12/06/2009	2350.00	17083.33	5138.89	694.44	9722.22	0.00
CBi7-10	12/06/2009 - 21/06/2009	2359.00	20416.67	3888.89	555.56	15138.89	138.89
CBi7-11	21/06/2009 - 30/06/2009	2368.00	12407.41	1296.30	370.37	10648.15	0.00
CBi7-12	30/06/2009 - 09/07/2009	2377.00	6527.78	625.00	208.33	5625.00	0.00
CBi7-13	09/07/2009 - 18/07/2009	2386.00	6296.30	509.26	46.30	5601.85	46.30
CBi7-14	18/07/2009 - 27/07/2009	2395.00	5740.74	1666.67	46.30	3888.89	92.59
CBi7-15	27/07/2009 - 05/08/2009	2404.00	2777.78	486.11	34.72	2222.22	0.00
CBi7-16	05/08/2009 - 14/08/2009	2413.00	3055.56	520.83	69.44	2361.11	0.00
CBi7-17	14/08/2009 - 23/08/2009	2422.00	2604.17	208.33	34.72	2256.94	0.00
CBi7-18	23/08/2009 - 01/09/2009	2431.00	1527.78	173.61	34.72	1250.00	0.00
CBi7-19	01/09/2009 - 10/09/2009	2440.00	3125.00	138.89	69.44	2812.50	34.72
CBi7-20	10/09/2009 - 19/09/2009	2449.00	6458.33	694.44	347.22	5277.78	0.00
CBi7-21	19/09/2009 - 28/09/2009	2458.00	8796.30	740.74	370.37	7685.19	0.00
CBi7-22	28/09/2009 - 07/10/2009	2467.00	11666.67	1574.07	1296.30	8703.70	0.00
CBi7-23	07/10/2009 - 16/10/2009	2476.00	10069.44	2013.89	1250.00	6666.67	69.44
CBi7-24	16/10/2009 - 25/10/2009	2485.00	7708.33	1319.44	486.11	5902.78	0.00
CBi7-25	25/10/2009 - 03/11/2009	2494.00	4111.11	611.11	333.33	3000.00	0.00
CBi7-26	03/11/2009 - 12/11/2009	2503.00	4027.78	370.37	462.96	3240.74	0.00
CBi7-27	12/11/2009 - 21/11/2009	2512.00	4212.96	555.56	231.48	3425.93	0.00
CBi7-28	21/11/2009 - 30/11/2009	2521.00	1215.28	173.61	104.17	937.50	0.00
CBi7-29	30/11/2009 - 09/12/2009	2530.00	1388.89	347.22	34.72	868.06	0.00
CBi7-30	09/12/2009 - 18/12/2009	2539.00	2314.81	46.30	138.89	1712.96	92.59
CBi7-31	18/12/2009 - 27/12/2009	2548.00	1215.28	69.44	34.72	1041.67	0.00



CBi7-32	27/12/2009 - 05/01/2010	2557.00	740.74	138.89	0.00	601.85	0.00
CBi7-33	05/01/2010 - 14/01/2010	2566.00	1064.81	185.19	46.30	740.74	0.00
CBi7-34	14/01/2010 - 23/01/2010	2575.00	138.89	0.00	0.00	69.44	34.72
CBi7-35	23/01/2010 - 01/02/2010	2584.00	138.89	104.17	0.00	34.72	0.00
CBi7-36	01/02/2010 - 10/02/2010	2593.00	1180.56	138.89	34.72	937.50	69.44
CBi7-37	10/02/2010 - 19/02/2010	2602.00	1180.56	173.61	0.00	937.50	34.72
CBi7-38	19/02/2010 - 28/02/2010	2611.00	7152.78	1319.44	0.00	5625.00	138.89
Gap time	28/02/2010 - 06/03/2010	2618.50	0.00	0.00	0.00	0.00	0.00
CBi8-1	06/03/2010 - 16/03/2010	2626.50	281.25	0.00	0.00	250.00	0.00
CBi8-2	16/03/2010 - 26/03/2010	2636.50	250.00	0.00	0.00	250.00	0.00
CBi8-3	26/03/2010 - 05/04/2010	2646.50	1375.00	218.75	156.25	937.50	0.00
CBi8-4	05/04/2010 - 15/04/2010	2656.50	8500.00	2937.50	312.50	4937.50	0.00
CBi8-5	15/04/2010 - 25/04/2010	2666.50	22750.00	6500.00	875.00	14875.00	250.00
CBi8-6	25/04/2010 - 05/05/2010	2676.50	9687.50	3125.00	437.50	5875.00	0.00
CBi8-7	05/05/2010 - 15/05/2010	2686.50	6062.50	2625.00	187.50	3250.00	0.00
CBi8-8	15/05/2010 - 25/05/2010	2696.50	6187.50	2312.50	187.50	3687.50	0.00
CBi8-9	25/05/2010 - 04/06/2010	2706.50	2875.00	916.67	83.33	1875.00	0.00
CBi8-10	04/06/2010 - 14/06/2010	2716.50	1812.50	312.50	62.50	1437.50	0.00
CBi8-11	14/06/2010 - 24/06/2010	2726.50	687.50	156.25	0.00	500.00	0.00
CBi8-12	24/06/2010 - 04/07/2010	2736.50	1125.00	93.75	0.00	1031.25	0.00
CBi8-13	04/07/2010 - 14/07/2010	2746.50	2083.33	41.67	41.67	1958.33	0.00
CBi8-14	14/07/2010 - 24/07/2010	2756.50	2375.00	218.75	62.50	1968.75	31.25
CBi8-15	24/07/2010 - 03/08/2010	2766.50	5250.00	2083.33	83.33	2791.67	83.33
CBi8-16	03/08/2010 - 13/08/2010	2776.50	2937.50	406.25	0.00	2406.25	31.25
CBi8-17	13/08/2010 - 23/08/2010	2786.50	2041.67	250.00	83.33	1666.67	0.00
CBi8-18	23/08/2010 - 27/08/2010	2793.50	8750.00	1145.83	208.33	7187.50	0.00
Gap time	27/08/2010 - 01/05/2011	2919.00	0.00	0.00	0.00	0.00	0.00
CBi9-1	01/05/2011 - 18/05/2011	3051.00	5931.37	2107.84	588.24	3284.31	0.00
CBi9-2	18/05/2011 - 04/06/2011	3068.00	1088.24	147.06	0.00	911.76	0.00
CBi9-3	04/06/2011 - 21/06/2011	3085.00	1088.24	58.82	88.24	1000.00	0.00
CBi9-4	21/06/2011 - 08/07/2011	3102.00	11397.06	735.29	367.65	10220.59	0.00
CBi9-5	08/07/2011 - 25/07/2011	3119.00	103897.06	8970.59	1323.53	93455.88	0.00
CBi9-6	25/07/2011 - 11/08/2011	3136.00	44852.94	1911.76	514.71	42426.47	0.00
CBi9-7	11/08/2011 - 28/08/2011	3153.00	20441.18	1691.18	1102.94	17426.47	0.00
CBi9-8	28/08/2011 - 14/09/2011	3170.00	0.00	0.00	0.00	0.00	0.00
CBi9-9	14/09/2011 - 01/10/2011	3187.00	0.00	0.00	0.00	0.00	0.00
CBi9-10	01/10/2011 - 18/10/2011	3204.00	0.00	0.00	0.00	0.00	0.00
CBi9-11	18/10/2011 - 04/11/2011	3221.00	0.00	0.00	0.00	0.00	0.00
CBi9-12	04/11/2011 - 21/11/2011	3238.00	0.00	0.00	0.00	0.00	0.00
CBi9-13	21/11/2011 - 08/12/2011	3255.00	0.00	0.00	0.00	0.00	0.00
CBi9-14	08/12/2011 - 25/12/2011	3272.00	0.00	0.00	0.00	0.00	0.00
CBi9-15	25/12/2011 - 11/01/2012	3289.00	0.00	0.00	0.00	0.00	0.00
CBi9-16	11/01/2012 - 21/01/2012	3302.75	118928.57	3928.57	1428.57	113571.43	0.00
Gap time	21/01/2012 - 26/01/2012	3310.25	0.00	0.00	0.00	0.00	0.00
CBi10-1	26/01/2012 - 30/01/2012	3314.50	520.83	0.00	0.00	520.83	0.00
CBi10-2	30/01/2012 - 06/02/2012	3320.05	3961.27	88.03	88.03	3521.13	0.00
CBi10-3	06/02/2012 - 17/02/2012	3328.98	5503.88	387.60	465.12	4573.64	77.52
CBi10-4	17/02/2012 - 27/02/2012	3339.73	5116.28	581.40	174.42	4302.33	0.00
CBi10-5	27/02/2012 - 09/03/2012	3350.48	1162.79	116.28	0.00	1046.51	0.00
CBi10-6	09/03/2012 - 20/03/2012	3361.23	7674.42	77.52	155.04	7441.86	0.00
CBi10-7	20/03/2012 - 31/03/2012	3371.98	27209.30	697.67	232.56	26279.07	0.00
CBi10-8	31/03/2012 - 10/04/2012	3382.73	3720.93	523.26	58.14	3139.53	0.00
CBi10-9	10/04/2012 - 21/04/2012	3393.48	69534.88	26162.79	4186.05	39302.33	0.00
CBi10-10	21/04/2012 - 02/05/2012	3404.23	17209.30	697.67	232.56	16279.07	0.00
CBi10-11	02/05/2012 - 13/05/2012	3414.98	22558.14	5000.00	1046.51	16279.07	0.00
CBi10-12	13/05/2012 - 23/05/2012	3425.73	83139.53	25232.56	5813.95	52093.02	0.00
CBi10-13	23/05/2012 - 03/06/2012	3436.48	48255.81	12209.30	2790.70	33255.81	0.00
CBi10-14	03/06/2012 - 14/06/2012	3447.23	20000.00	2790.70	116.28	16860.47	0.00
CBi10-15	14/06/2012 - 25/06/2012	3457.98	25930.23	4651.16	1162.79	20232.56	0.00

CBi10-16	25/06/2012 - 05/07/2012	3468.73	30232.56	7093.02	1511.63	21511.63	0.00
CBi10-17	05/07/2012 - 16/07/2012	3479.48	45348.84	15232.56	2209.30	27325.58	0.00
CBi10-18	16/07/2012 - 27/07/2012	3490.23	22906.98	4418.60	232.56	18023.26	0.00
CBi10-19	27/07/2012 - 07/08/2012	3500.98	0.00	0.00	0.00	0.00	0.00
CBi10-20	07/08/2012 - 17/08/2012	3511.73	0.00	0.00	0.00	0.00	0.00
CBi10-21	17/08/2012 - 28/08/2012	3522.48	0.00	0.00	0.00	0.00	0.00
CBi10-22	28/08/2012 - 08/09/2012	3533.23	0.00	0.00	0.00	0.00	0.00
CBi10-23	08/09/2012 - 19/09/2012	3543.98	0.00	0.00	0.00	0.00	0.00
CBi10-24	19/09/2012 - 29/09/2012	3554.73	0.00	0.00	0.00	0.00	0.00
CBi10-25	29/09/2012 - 10/10/2012	3565.48	0.00	0.00	0.00	0.00	0.00
CBi10-26	10/10/2012 - 21/10/2012	3576.23	1209.30	162.79	58.14	976.74	0.00
CBi10-27	21/10/2012 - 01/11/2012	3586.98	0.00	0.00	0.00	0.00	0.00
CBi10-28	01/11/2012 - 11/11/2012	3597.73	0.00	0.00	0.00	0.00	0.00
CBi10-29	11/11/2012 - 22/11/2012	3608.48	0.00	0.00	0.00	0.00	0.00
CBi10-30	22/11/2012 - 03/12/2012	3619.23	0.00	0.00	0.00	0.00	0.00
CBi10-31	03/12/2012 - 14/12/2012	3629.98	0.00	0.00	0.00	0.00	0.00
CBi10-32	14/12/2012 - 24/12/2012	3640.73	0.00	0.00	0.00	0.00	0.00
CBi10-33	24/12/2012 - 04/01/2013	3651.48	0.00	0.00	0.00	0.00	0.00
CBi10-34	04/01/2013 - 15/01/2013	3662.23	0.00	0.00	0.00	0.00	0.00
CBi10-35	15/01/2013 - 26/01/2013	3672.98	114883.72	13720.93	6279.07	86046.51	232.56
Gap time	26/01/2013 - 29/01/2013	3679.85	0.00	0.00	0.00	0.00	0.00
CBi11-1	29/01/2013 - 19/02/2013	3691.85	12916.67	654.76	59.52	12202.38	0.00
CBi11-2	19/02/2013 - 12/03/2013	3712.85	13214.29	1309.52	476.19	11071.43	0.00
CBi11-3	12/03/2013 - 02/04/2013	3733.85	1904.76	119.05	29.76	1755.95	0.00
CBi11-4	02/04/2013 - 23/04/2013	3754.85	535.71	59.52	0.00	436.51	0.00
CBi11-5	23/04/2013 - 14/05/2013	3775.85	357.14	0.00	0.00	357.14	0.00
CBi11-6	14/05/2013 - 04/06/2013	3796.85	198.41	0.00	19.84	198.41	0.00
CBi11-7	04/06/2013 - 25/06/2013	3817.85	12023.81	4761.90	535.71	6607.14	0.00
CBi11-8	25/06/2013 - 16/07/2013	3838.85	15833.33	3333.33	2500.00	10119.05	0.00
CBi11-9	16/07/2013 - 06/08/2013	3859.85	80773.81	13333.33	892.86	66547.62	0.00
CBi11-10	06/08/2013 - 27/08/2013	3880.85	12976.19	4285.71	178.57	8511.90	0.00
CBi11-11	27/08/2013 - 17/09/2013	3901.85	7976.19	1845.24	59.52	5892.86	0.00
CBi11-12	17/09/2013 - 08/10/2013	3922.85	6607.14	952.38	59.52	5595.24	0.00
CBi11-13	08/10/2013 - 29/10/2013	3943.85	3809.52	476.19	297.62	2857.14	0.00
CBi11-14	29/10/2013 - 19/11/2013	3964.85	7559.52	654.76	297.62	6011.90	0.00
CBi11-15	19/11/2013 - 10/12/2013	3985.85	714.29	39.68	79.37	476.19	0.00
CBi11-16	10/12/2013 - 31/12/2013	4006.85	257.94	39.68	0.00	218.25	0.00
CBi11-17	31/12/2013 - 21/01/2014	4027.85	376.98	59.52	19.84	317.46	0.00
CBi11-18	21/01/2014 - 10/02/2014	4048.60	5000.00	670.73	121.95	3902.44	0.00
Gap time	10/02/2014 - 14/02/2014	4060.60	0.00	0.00	0.00	0.00	0.00
CBi12-1	14/02/2014 - 26/02/2014	4068.60	4950.00	1850.00	50.00	2800.00	0.00
CBi12-2	26/02/2014 - 09/03/2014	4080.30	9174.31	1146.79	229.36	7568.81	0.00
CBi12-3	09/03/2014 - 28/03/2014	4095.50	6282.05	213.68	42.74	5897.44	42.74
CBi12-4	28/03/2014 - 17/04/2014	4115.00	4871.79	384.62	256.41	4102.56	0.00
CBi12-5	17/04/2014 - 06/05/2014	4134.50	3461.54	128.21	64.10	3237.18	0.00
CBi12-6	06/05/2014 - 26/05/2014	4154.00	5032.05	3044.87	64.10	1794.87	0.00
CBi12-7	26/05/2014 - 14/06/2014	4173.50	5256.41	2115.38	256.41	2820.51	0.00
CBi12-8	14/06/2014 - 04/07/2014	4193.00	2820.51	705.13	160.26	1955.13	0.00
CBi12-9	04/07/2014 - 23/07/2014	4212.50	3461.54	811.97	85.47	2521.37	0.00
CBi12-10	23/07/2014 - 12/08/2014	4232.00	11025.64	1346.15	1410.26	8333.33	0.00
CBi12-11	12/08/2014 - 31/08/2014	4251.50	192.31	0.00	0.00	192.31	0.00
CBi12-12	31/08/2014 - 20/09/2014	4271.00	0.00	0.00	0.00	0.00	0.00
CBi12-13	20/09/2014 - 09/10/2014	4290.50	128.21	21.37	21.37	85.47	0.00
CBi12-14	09/10/2014 - 29/10/2014	4310.00	3418.80	341.88	256.41	2905.98	0.00
CBi12-15	29/10/2014 - 17/11/2014	4329.50	534.19	128.21	21.37	384.62	0.00
CBi12-16	17/11/2014 - 07/12/2014	4349.00	3333.33	576.92	64.10	2628.21	0.00
CBi12-17	07/12/2014 - 26/12/2014	4368.50	15128.21	3076.92	1282.05	10576.92	0.00
CBi12-18	26/12/2014 - 15/01/2015	4388.00	7692.31	1474.36	576.92	5512.82	0.00
CBi12-19	15/01/2015 - 03/02/2015	4407.50	2756.41	448.72	256.41	1955.13	32.05

CBi12-20	03/02/2015 - 23/02/2015	4427.00	39871.79	5897.44	5512.82	27564.10	512.82
Gap time	23/02/2015 - 27/02/2015	4438.55	0.00	0.00	0.00	0.00	0.00
CBi13-1	27/02/2015 - 13/03/2015	4447.35	4062.50	401.79	357.14	2946.43	357.14
CBi13-2	13/03/2015 - 31/03/2015	4463.35	5451.39	416.67	486.11	4201.39	347.22
CBi13-3	31/03/2015 - 18/04/2015	4481.35	7430.56	2291.67	486.11	4097.22	347.22
CBi13-4	18/04/2015 - 06/05/2015	4499.35	5173.61	243.06	104.17	4791.67	0.00
CBi13-5	06/05/2015 - 24/05/2015	4517.35	17500.00	347.22	0.00	16805.56	277.78
CBi13-6	24/05/2015 - 11/06/2015	4535.35	27708.33	6180.56	347.22	21180.56	69.44
CBi13-7	11/06/2015 - 29/06/2015	4553.35	21666.67	6111.11	833.33	14930.56	0.00
CBi13-8	29/06/2015 - 17/07/2015	4571.35	7291.67	1111.11	555.56	5486.11	138.89
CBi13-9	17/07/2015 - 04/08/2015	4589.35	7013.89	972.22	694.44	5277.78	69.44
CBi13-10	04/08/2015 - 22/08/2015	4607.35	9722.22	2708.33	486.11	6319.44	138.89
CBi13-11	22/08/2015 - 09/09/2015	4625.35	8194.44	1944.44	347.22	5763.89	69.44
CBi13-12	09/09/2015 - 27/09/2015	4643.35	9513.89	833.33	972.22	7708.33	69.44
CBi13-13	27/09/2015 - 15/10/2015	4661.35	4513.89	694.44	416.67	3229.17	34.72
CBi13-14	15/10/2015 - 02/11/2015	4679.35	3750.00	555.56	208.33	2916.67	69.44
CBi13-15	02/11/2015 - 20/11/2015	4697.35	6840.28	1423.61	277.78	4895.83	243.06
CBi13-16	20/11/2015 - 08/12/2015	4715.35	8194.44	2361.11	347.22	5347.22	138.89
CBi13-17	08/12/2015 - 26/12/2015	4733.35	8125.00	1319.44	1041.67	5625.00	0.00
CBi13-18	26/12/2015 - 13/01/2016	4751.35	7291.67	1736.11	694.44	4583.33	208.33
CBi13-19	13/01/2016 - 31/01/2016	4769.35	2708.33	532.41	138.89	1828.70	208.33
CBi13-20	31/01/2016 - 18/02/2016	4787.35	2523.15	300.93	185.19	1898.15	46.30
Gap time	18/02/2016 - 25/02/2016	4799.85	0.00	0.00	0.00	0.00	0.00
CBi14-1	25/02/2016 - 14/03/2016	4812.60	4549.55	270.27	135.14	4009.01	0.00
CBi14-2	14/03/2016 - 05/04/2016	4832.60	2829.46	271.32	0.00	2519.38	0.00
CBi14-3	05/04/2016 - 26/04/2016	4854.10	2906.98	658.91	38.76	2170.54	38.76
CBi14-4	26/04/2016 - 18/05/2016	4875.60	20290.70	5639.53	1569.77	12906.98	0.00
CBi14-5	18/05/2016 - 08/06/2016	4897.10	17558.14	2790.70	1511.63	13197.67	0.00
CBi14-6	08/06/2016 - 30/06/2016	4918.60	5058.14	697.67	290.70	4127.91	0.00
CBi14-7	30/06/2016 - 21/07/2016	4940.10	15872.09	1976.74	930.23	13023.26	0.00
CBi14-8	21/07/2016 - 12/08/2016	4961.60	25697.67	3720.93	930.23	20697.67	116.28
CBi14-9	12/08/2016 - 02/09/2016	4983.10	22093.02	2558.14	813.95	18372.09	0.00
CBi14-10	02/09/2016 - 24/09/2016	5004.60	48372.09	6627.91	2093.02	39302.33	581.40
CBi14-11	24/09/2016 - 15/10/2016	5026.10	12790.70	1162.79	232.56	11162.79	0.00
CBi14-12	15/10/2016 - 06/11/2016	5047.60	6453.49	755.81	232.56	5174.42	174.42
CBi14-13	06/11/2016 - 27/11/2016	5069.10	1647.29	155.04	116.28	1375.97	0.00
CBi14-14	27/11/2016 - 19/12/2016	5090.60	1666.67	155.04	116.28	1298.45	38.76
CBi14-15	19/12/2016 - 09/01/2017	5112.10	4302.33	319.77	203.49	3750.00	0.00
CBi14-16	09/01/2017 - 24/01/2017	5130.30	2894.30	545.30	41.95	2307.05	0.00
Gap time	24/01/2017 - 26/01/2017	5138.55	0.00	0.00	0.00	0.00	0.00
CBi15-1	26/01/2017 - 05/02/2017	5144.60	6011.90	357.14	238.10	5357.14	0.00
CBi15-2	05/02/2017 - 16/02/2017	5155.10	3452.38	238.10	178.57	3035.71	0.00
CBi15-3	16/02/2017 - 26/02/2017	5165.60	3095.24	297.62	119.05	2559.52	0.00
CBi15-4	26/02/2017 - 09/03/2017	5176.10	4761.90	317.46	238.10	4206.35	0.00
CBi15-5	09/03/2017 - 19/03/2017	5186.60	6746.03	1190.48	238.10	5158.73	238.10
CBi15-6	19/03/2017 - 30/03/2017	5197.10	17500.00	2023.81	1071.43	14285.71	238.10
CBi15-7	30/03/2017 - 09/04/2017	5207.60	18809.52	3095.24	2261.90	13333.33	0.00
CBi15-8	09/04/2017 - 20/04/2017	5218.10	11071.43	2261.90	1190.48	7619.05	119.05
CBi15-9	20/04/2017 - 30/04/2017	5228.60	5654.76	773.81	357.14	4464.29	59.52
CBi15-10	30/04/2017 - 11/05/2017	5239.10	4940.48	833.33	297.62	3690.48	0.00
CBi15-11	11/05/2017 - 21/05/2017	5249.60	5595.24	1011.90	416.67	3869.05	59.52
CBi15-12	21/05/2017 - 01/06/2017	5260.10	9166.67	1666.67	714.29	6666.67	0.00
CBi15-13	01/06/2017 - 11/06/2017	5270.60	7738.10	892.86	476.19	6190.48	59.52
CBi15-14	11/06/2017 - 22/06/2017	5281.10	5317.46	634.92	238.10	4206.35	0.00
CBi15-15	22/06/2017 - 02/07/2017	5291.60	3650.79	793.65	79.37	2698.41	0.00
CBi15-16	02/07/2017 - 13/07/2017	5302.10	24047.62	9285.71	1428.57	13095.24	0.00
CBi15-17	13/07/2017 - 23/07/2017	5312.60	13214.29	3095.24	1071.43	8690.48	0.00
CBi15-18	23/07/2017 - 03/08/2017	5323.10	7440.48	1190.48	535.71	5476.19	0.00
CBi15-19	03/08/2017 - 13/08/2017	5333.60	3333.33	357.14	297.62	2619.05	59.52

CBi15-20	13/08/2017 - 24/08/2017	5344.10	2083.33	178.57	119.05	1726.19	0.00
Gap time	24/08/2017 - 02/09/2017	5353.85	0.00	0.00	0.00	0.00	0.00
CBi16-1	02/09/2017 - 22/09/2017	5368.35	23250.00	312.50	500.00	22125.00	125.00
CBi16-2	22/09/2017 - 14/10/2017	5389.35	23409.09	795.45	284.09	22215.91	113.64
CBi16-3	14/10/2017 - 05/11/2017	5411.35	19261.36	1136.36	284.09	17443.18	170.45
CBi16-4	05/11/2017 - 27/11/2017	5433.35	16193.18	965.91	113.64	14943.18	0.00
CBi16-5	27/11/2017 - 19/12/2017	5455.35	15681.82	1193.18	568.18	13806.82	0.00
CBi16-6	19/12/2017 - 10/01/2018	5477.35	16875.00	1363.64	795.45	14488.64	56.82
CBi16-7	10/01/2018 - 01/02/2018	5499.35	5568.18	170.45	284.09	5170.45	0.00
CBi16-8	01/02/2018 - 23/02/2018	5521.35	4659.09	625.00	681.82	3409.09	56.82
CBi16-9	23/02/2018 - 17/03/2018	5543.35	5000.00	284.09	568.18	3920.45	227.27
CBi16-10	17/03/2018 - 08/04/2018	5565.35	3522.73	303.03	151.52	2916.67	113.64
CBi16-11	08/04/2018 - 30/04/2018	5587.35	198.86	56.82	0.00	142.05	0.00
CBi16-12	30/04/2018 - 22/05/2018	5609.35	142.05	0.00	0.00	142.05	0.00
CBi16-13	22/05/2018 - 13/06/2018	5631.35	56.82	0.00	28.41	28.41	0.00
CBi16-14	13/06/2018 - 05/07/2018	5653.35	0.00	0.00	0.00	0.00	0.00
CBi16-15	05/07/2018 - 27/07/2018	5675.35	28.41	0.00	0.00	28.41	0.00
CBi16-16	27/07/2018 - 18/08/2018	5697.35	0.00	0.00	0.00	0.00	0.00
CBi16-17	18/08/2018 - 09/09/2018	5719.35	0.00	0.00	0.00	0.00	0.00
CBi16-18	09/09/2018 - 01/10/2018	5741.35	28.41	0.00	0.00	28.41	0.00
CBi16-19	01/10/2018 - 23/10/2018	5763.35	142.05	0.00	28.41	113.64	0.00
CBi16-20	23/10/2018 - 16/11/2018	5786.35	55000.00	16458.33	5416.67	32708.33	416.67
Gap time	16/11/2018 - 20/11/2018	5800.35	0.00	0.00	0.00	0.00	0.00
CBi17-1	20/11/2018 - 11/12/2018	5812.85	2648.81	267.86	89.29	2291.67	0.00
CBi17-2	11/12/2018 - 05/01/2019	5835.85	2150.00	175.00	25.00	1875.00	50.00
CBi17-3	05/01/2019 - 30/01/2019	5860.85	3700.00	500.00	500.00	2600.00	0.00
CBi17-4	30/01/2019 - 24/02/2019	5885.85	4700.00	550.00	1150.00	2950.00	0.00
CBi17-5	24/02/2019 - 21/03/2019	5910.85	8450.00	700.00	1500.00	6000.00	200.00
CBi17-6	21/03/2019 - 15/04/2019	5935.85	3900.00	300.00	166.67	3300.00	100.00
CBi17-7	15/04/2019 - 10/05/2019	5960.85	6600.00	1550.00	400.00	4700.00	0.00
CBi17-8	10/05/2019 - 04/06/2019	5985.85	1825.00	150.00	325.00	1300.00	50.00
CBi17-9	04/06/2019 - 29/06/2019	6010.85	11100.00	1650.00	500.00	8800.00	50.00
CBi17-10	29/06/2019 - 24/07/2019	6035.85	18200.00	2600.00	400.00	15000.00	0.00
CBi17-11	24/07/2019 - 18/08/2019	6060.85	9950.00	2000.00	350.00	7350.00	50.00
CBi17-12	18/08/2019 - 12/09/2019	6085.85	975.00	125.00	50.00	775.00	0.00
CBi17-13	12/09/2019 - 07/10/2019	6110.85	3425.00	400.00	175.00	2750.00	75.00
CBi17-14	07/10/2019 - 01/11/2019	6135.85	5950.00	300.00	100.00	5500.00	0.00
CBi17-15	01/11/2019 - 26/11/2019	6160.85	975.00	75.00	0.00	800.00	50.00
CBi17-16	26/11/2019 - 21/12/2019	6185.85	2025.00	175.00	175.00	1550.00	0.00
CBi17-17	21/12/2019 - 15/01/2020	6210.85	4800.00	500.00	1000.00	3300.00	0.00
CBi17-18	15/01/2020 - 09/02/2020	6235.85	1600.00	175.00	175.00	1225.00	0.00
CBi17-19	09/02/2020 - 05/03/2020	6260.85	9500.00	450.00	700.00	8200.00	50.00
CBi17-20	05/03/2020 - 30/03/2020	6285.85	2175.00	275.00	250.00	1650.00	0.00

## Chapter 5 - How is the export production of dinoflagellate cysts on the ocean surface stored in the sediment?

Surya Eldo V. Roza<sup>1</sup>, Karin A. F. Zonneveld<sup>1,2</sup>, Gerard Versteegh<sup>3</sup>, Hendrik Wolschke<sup>4</sup>

<sup>1</sup>MARUM - Center for Marine Environmental Sciences, University of Bremen, Bremen, Germany

<sup>2</sup>Department of Geosciences, University of Bremen, Bremen, Germany

<sup>3</sup>Department of Physics and Earth Sciences, Constructor University Bremen, Bremen, Germany

<sup>4</sup>Helmholtz-Zentrum hereon, Institute of Coastal Environmental Chemistry, Germany

*In preparation for submission to Biogeosciences*

### Abstract

Organic-walled dinoflagellate cysts (dinocysts) are a useful microfossil group for reconstructing past ocean conditions due to the strong relationship between living cells and their environment. Environmental signals can be obtained by analysing dinocyst associations in surface sediments or down-cores. However, multiple processes in the water column and sediments could alter the information that dinocysts carry and store on the ocean floor. Consequently, such processes in the water column and post-depositional processes can alter the primary ecological signals. In this study, we aimed to identify the rate and character of alteration between the environmental signals reflected in the export production and the ultimate ones in the sediments. This is to improve the interpretation of sedimentary dinocyst associations for better paleoenvironmental reconstructions. We compared an 18-year record of dinocyst export flux collected by a sediment trap offshore Cape Blanc, Northwest Africa, with a <sup>210</sup>Pb dated core taken from the same location. The core was sliced every 3.1 mm to enable a high temporal resolution investigation. After matching the sampling interval duration in the traps with that of the sediment core, cyst association composition was compared. Comparable to the trap samples, the core dinocysts were dominated by heterotrophic taxa that are typical for a coastal upwelling environment, and their accumulation rates in the trap and core were more or less in the same range. The accumulation rates of heterotrophic dinocysts in the core samples fluctuated between  $1.0 \times 10^6$  and  $4.4 \times 10^6$  cyst m<sup>-2</sup> year<sup>-1</sup>, and they ranged between  $2.4 \times 10^6$  and  $8.1 \times 10^6$  cyst m<sup>-2</sup> year<sup>-1</sup> in the trap samples. The accumulation rates of photo-/mixotrophic dinocysts in the core ranged from  $1.6 \times 10^5$  to  $9.7 \times 10^5$  cyst m<sup>-2</sup> year<sup>-1</sup>, while their accumulation rates in the trap fluctuated between  $1.2 \times 10^5$  and  $4.6 \times 10^5$  cyst m<sup>-2</sup> year<sup>-1</sup>. However, the association composition appeared to be quite different. The relative abundances and accumulation rates of many heterotrophic dinocysts known to be sensitive to post-depositional degradation were remarkably lower in the core samples, suggesting that selective preservation affected the core sediment post-depositional. Some other taxa, such as *Protoperidinium conicum* (*Selenopemphix quanta*), *P. monospinum*, and *P. stellatum* showed higher absolute and relative abundances in the core sediments, which suggests that allochthonous materials had reached the coring site. The dinocyst composition over time was much more homogenised in the core sediments, suggesting a strong vertical mixing in the ocean sediments through bioturbation. Nevertheless, the results of a Principal Component Analysis (PCA) indicated that the overall association shift over time observed in the trap series was still detected in the core sediments despite the alteration of the initial signal by pre- and post-depositional processes (e.g., particle transport, bioturbation, compaction bias, and microbial degradation).

**Keywords:** dinocysts, paleoenvironment, lateral transport, selective preservation, compaction bias, bioturbation.

## 5.1. Introduction

Marine plankton provides a resourceful record of past climatic and environmental conditions through the concentration, distribution, and chemical composition of their remaining hard parts called microfossils. Unlike other microfossils that bear fossilized shells throughout their life cycle, the dinoflagellate theca is susceptible to mechanical and thermal pressures and degradation (Dale and Dale, 1992). Fortunately, some species (ca. 15%) with various life strategies (phototrophic/mixotrophic, and heterotrophic) produce resistant cysts (dinocysts) during their reproductive phase that sink to the ocean floor, where they can become fossilized (Taylor et al., 2008; Jeong et al., 2010). Dinocysts have diverse morphological features that are species-specific and many types of wall properties, such as organic-walled, a few calcareous-walled, and much rarer containing siliceous parts (Zonneveld et al., 2005; Bravo and Figueroa, 2014). Preserved in bottom sediments, they store information about the upper water condition, carbon sequestration, and can even provide sometimes information about the pelagic food chain (Head, 1996; Dale et al., 2002; Bravo and Figueroa, 2014; Luo et al., 2019). This information can be extracted and analysed from surface sediment and down-core samples and is widely used to establish palaeoenvironmental and paleoceanographic reconstructions (e.g., García-Moreiras et al., 2021; Obrezkova et al., 2023; Zonneveld et al., 2024).

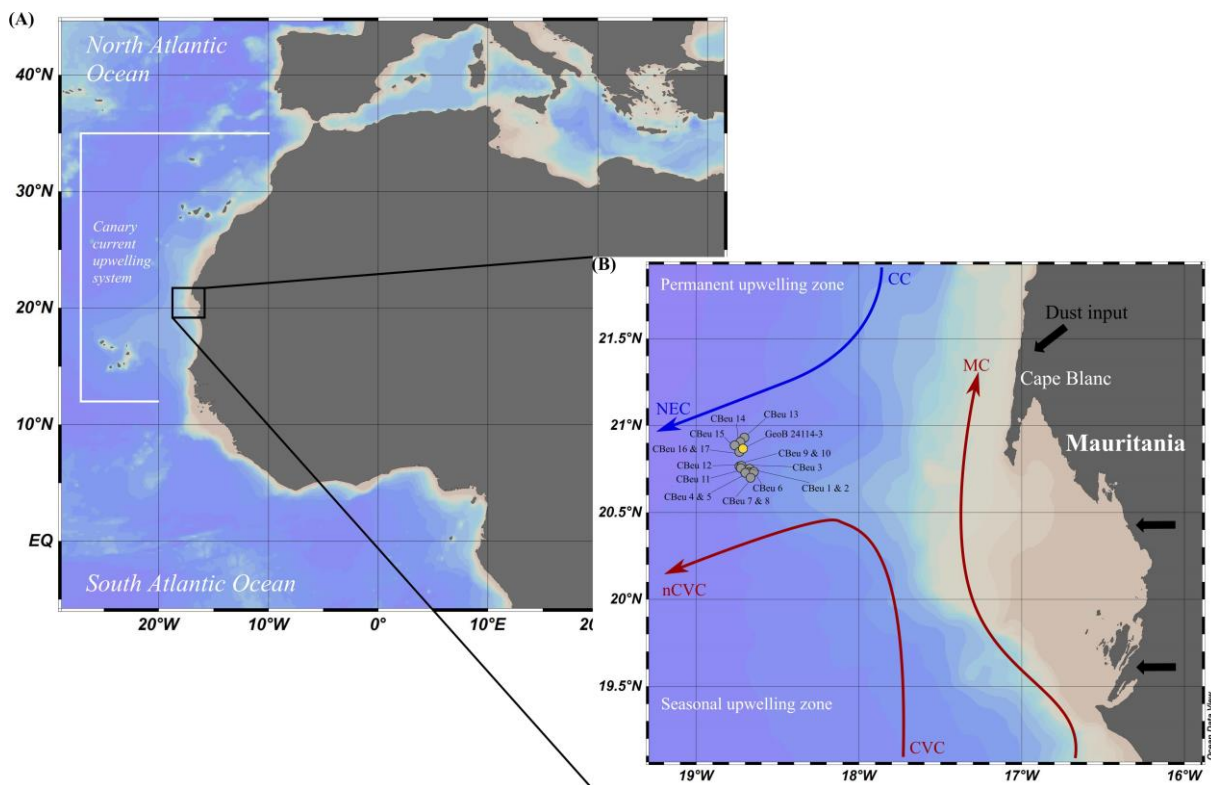


**Figure 5.1.** The map of the study area (A) the region classified as the Canary Current upwelling system on the Atlantic coast of Northwest Africa, (B) the subregion of the annual permanent upwelling zone off Cape Blanc where the CBeu sediment trap has been deployed (grey circles), and the GeoB core was obtained (yellow circle). The thin arrows represented the surface currents drawn after Mittelstaedt (1983, 1991) and Zenk et al. (1991). The blue arrow shows the direction of relatively cold waters of the Canary Current (CC) and North Equatorial Current (NEC), whereas the red arrows represent warmer waters of the Mauritanian Current (MC), Cape Verde Current (CVC), and north Cape Verde Current (nCVC). The thick black arrows show the origin of the Sahara dust.

However, the study of dinocyst association, particularly the organic-walled ones, is not without its challenges. Dinocysts could be deformed after deposition, potentially resulting in misinterpretation of their fossil records for paleoenvironment or paleoceanography applications. Dinocysts in sediments can be resuspended, transported to distal areas, compacted, and vertically redistributed due to bioturbation activity (Loubere, 1989; Piot et al., 2008; Nooteboom et al., 2019). Although the organic-walled dinocysts have a high preservation rate, they are not entirely immune to degradation and diagenesis processes (Kodrans-Nsiah et al., 2008; Gray et al., 2017; Zonneveld et al., 2019b; Versteegh

and Zonneveld, 2022). This complexity underscores the need for further investigation to address questions such as to how well the production signal of organic-walled dinocysts is recorded in the sediment floor, what alterations affect the embedding and fossilisation process, and what is the effect of such perturbations on the fossil record. The existing studies only explained dinocyst flux and taxa composition similarities between cyst association in the water column and the surface sediment (e.g., Pitcher and Joyce, 2009; Prebble et al., 2013; Heikkilä et al., 2016). Other more sophisticated methods focused on solving the impact of lateral transport on the sedimentary dinocysts in three-dimensional distributed transects (e.g., Zonneveld et al., 2018; Zonneveld et al., 2022a; García-Moreiras et al., 2023; García-Moreiras et al., 2024). This study aims to elevate the knowledge of the cyst embedding process and preservation in sediments and investigate its quality as a paleoenvironmental proxy. Therefore, we compared information from a long-time series of dinocyst export flux from the water column collected by sediment traps with those accumulated in the bottom sediments at the trap location.

This study was conducted off Cape Blanc on the Atlantic coast of Northwest Africa as part of the Canary Current upwelling ecosystem (**Figure 5.1A**). This region is known for its high primary production induced by the subsurface nutrient-rich upwelled waters (Carr, 2001; Aristegui et al., 2009). The favourable morphology of the shelf and dynamic surface water currents accommodate a permanent upwelling feature. Upwelled waters can be transported in the surface water layers several hundred kilometers to the open ocean in the form of upwelling filaments (van Camp et al., 1991; Cropper et al., 2014). Saharan dust also contributes to enhanced phytoplankton growth by supplying essential trace elements to the ocean (Kolber et al., 1994; Jickells et al., 2005). In this region, aeolian dust is the primary, if not the only, source of terrigenous sediment materials in the study region (Wynn et al., 2000; Henrich et al., 2008). The productive and dynamic settings of this ecosystem, plus minimum perturbation in the stratification, make this region the most suitable for comparing the export flux and fossilisation of dinocysts in the ocean sediments.

The dinocyst record from the water column was collected by a sediment trap from June 2003 until March 2020 with a sampling interval of one to three weeks. Dinocysts in the bottom sediment were probed with a multicore device, and the core was sliced every 3.1 mm to achieve a high temporal resolution. An interval of 1.63 years per core sample was distinguished based on an age model (linear interpolation) based on the  $^{210}\text{Pb}$  half-year time of 22 years. The time frame and interval of the sediment trap and core samples were matched. The relative abundances and accumulation rates of dinocyst were calculated to produce a high-quality comparison study. Multivariate analyses and a biodiversity index were applied to examine the relationship across sample points in the water column and sediments based on the taxa composition.

## 5.2. Oceanography

The climatic and oceanographic conditions in the study area are strongly influenced by the annual migration of the Inter Tropical Convergence Zone over the African continent (between 8° N and 24° N) and the eastern Atlantic Ocean (between 2° N and 12° N) (Schneider et al., 2014; Nicholson, 2018). Between July and September, the ITCZ reaches its most northern position, resulting in moist air in West Africa (Sultan and Janicot, 2000; Schneider et al., 2014). ITCZ moves to its most southern position from December to February, leaving the West Africa region hot and dry (Sultan and Janicot, 2000; Schneider et al., 2014). The position of the ITCZ strongly influences the strength and position of the surface trade winds blowing from a northeasterly direction, relatively parallel to the coast of Northwest Africa. Due to Eckmann-transport, pumped intermediate waters are brought up to the surface, resulting in a band of upwelling along the Northwest African coast (21 - 35° N) (Cropper et al., 2014). This coastal upwelling off Cape Blanc is part of the Canary Current Eastern Boundary Upwelling System (CC-EBUE), one of the four EBUEs that contribute to a major part of the global marine plankton production despite their small coverage of earth's ocean surface (Carr, 2001; Aristegui et al., 2009; Cropper et al., 2014). The CC-EBUE can be divided into three subregions characterised by a weak

permanent upwelling zone (26° - 33° N), permanent upwelling zone (20° - 25° N), and seasonal upwelling zone (13° - 19° N) within boreal summer and winter respectively (Lathuilière et al., 2008; Cropper et al., 2014). The permanent upwelling zone offshore Cape Blanc shows varying intensities orchestrated by the strength and position of the local winds (Hagen, 2001; Faye et al., 2015). The intensity of this upwelling reaches its maximum strength during winter and spring, coinciding when the ITCZ migrates south and weakening when ITCZ moves up north to the vicinity area of our study (Mittelstaedt, 1991; Maloney and Shaman, 2008).

The hydrography of the Northwest African Coast is influenced by the Canary Current (CC) and Mauritania Current (MC) (**Figure 5.1B**). CC entrains the study area from the northern realm, flowing as a surface current alongside the coastline from 7 - 20° N. CC turns towards the open ocean between 21 and 25° N, providing cooler water to the North Equator Current (NEC). From the equator realm, the poleward MC transports warm water that flows parallel to the Mauritanian coast until 20° N. In autumn, MC influence weakens and is gradually overtaken by a southward-flowing surface current. The opposing directions of CC and MC create the Cape Verde Frontal Zone (CVFZ), a convergence zone that borders the North Atlantic Central Water (NACW) and South Atlantic Central Water (SACW) (Zenk et al., 1991). These two subsurface water masses are the sources of upwelled waters off Cape Blanc, where they mixed (Sarmiento et al., 2004). This ocean circulation compensates for transporting several hundred kilometers of nutrient-rich upwelled subsurface waters into the more oligotrophic open oceans in large filaments and eddies (Mittelstaedt, 1983; van Camp, 1991; Hagen, 2001).

The emission of dust from the Sahara provides some micronutrients and trace elements that can support the growth of phytoplankton (Kolber et al., 1994; Jickells et al., 2005; Lohan and Tagliabue, 2018). The Sahara contributes to up to half a portion of the global aerosol dust, making it the world's primary source of aeolian sediment (Tanaka and Chiba, 2006; Kok et al., 2021). The distribution of dust is accommodated by the surface winds, which transport Saharan dust to far distances such as Europe, the Caribbean, and South America (Stuut et al., 2005; Chouza et al., 2016). The annual migration of ITCZ plays a crucial role in transporting Saharan dust into the Atlantic Ocean (Ben-Ami et al., 2009; Skonieczny et al., 2013; Prospero, 2014; Yu et al., 2019). In boreal winter, dust is transported at low altitudes (0-3 km), causing its deposition at proximal locations such as the Atlantic Ocean (Skonieczny et al., 2013; Yu et al., 2019; Gutleben et al., 2022). When the ITCZ is located in its northern position (boreal summer), surface winds carry dust at higher latitude (5 - 7 km) via Sahara Air Layers (SAL) that enables dust to travel to the western coast of the Atlantic Ocean (Prospero and Carlson, 1972; Doherty et al., 2014; Prospero, 2014).

### 5.3. Materials and methods

#### 5.3.1. Sampling procedures

Dinoflagellate cysts from the upper water column were collected by a Honjo-type sediment trap deployed and recovered during 17 research cruises to the study area. The deployment coordinates ranged between 20° 44.6' N - 20° 53.0' N and 18° 41.9' W - 18° 45.4' W, and the trap drifted in ocean depth between 1249 – 1364 m. The sediment trap is a cone-shaped device with a filter net on the upper end, and the lower end is connected to sampling cups with a 0.5m<sup>2</sup> aperture opening and equipped with a baffle comb (Kremling et al. 1996). Before every deployment, sampling cups were filled with mercury chloride (HgCl<sub>2</sub>) to poison the captured organisms. The sampling cup density was increased to 40‰ by adding pure sodium chloride (NaCl). The pre-deployment procedure was adapted from the MARUM protocol of the trapping research program. The sampling cups were programmed to close and switch in a certain period, creating a sampling interval of 3.5 to 22 days for this study. The sample collection was done continuously except for a cruise absent in September 2010 - April 2011, resulting in relatively long gaps in the time series. Some shorter gaps were also recorded in the series due to device malfunction. The recovered samples were shipped to MARUM repository storage and stored under 4° C. The collected particles were filtered with a 1 mm pore size sieve, but large crustaceans were initially removed



with a tweezer. The filtered samples were split using the McLane wet splitter system into 1/125 fractions each and placed in the University of Bremen freezer to preserve those samples for the following procedures.

**Table 5.1.** Detailed information of the core samples used for age dating and the results derived from the  $^{210}\text{Pb}$  dating experiment.

Core depth (mm)	Dry bulk density (g cm <sup>-3</sup> )	$^{210}\text{Pb}$ unsupported (Bq kg <sup>-1</sup> )	$^{210}\text{Pb}$ uncertainty (Bq kg <sup>-1</sup> )	Age interval (years)	Age of the center depth
0 – 12.4	0.2	727.4	16.9	3.3	2016.7
24.8 – 37.2	0.4	300.9	9.6	16.3	2003.7
49.6 – 62.0	0.4	137.6	4.5	29.3	1990.7
74.4 – 86.8	0.5	151.2	8.4	42.3	1977.7
99.2 – 111.6	0.5	87.8	5.1	55.3	1964.7
151.9 – 164.3	0.6	4.31	2.3	81.4	1938.6

In August 2020, a sediment core (GeoB 24114-3) was obtained with a multi-coring device equipped with twelve core tubes at the deployment location of the sediment trap, more precisely at 20° 50.8' N and 18° 43.5' W (Zonneveld 2020). Each tube probed a ca. 30 cm sediment core at 2681 m from the ocean surface. The sediment cores were characterised by homogenous foraminifera-rich mud from top to bottom and heavily bioturbated, especially within the upper 10 mm with burrows diameter measured up to 1 cm (**Figure 5.2C**). One core was measured for oxygen concentration within the upper sediment layers using a fiber optic oxygen sensor (FIBOX3). This sensor was connected to micromanipulator software to depict the oxygen concentration (mg/l) with the core depth (mm) (**Figure 5.2A**). The core for dinocysts analysis was immediately sealed and stored in the vessel freezer before being shipped to the MARUM/IODP core freezer to be kept under -20° C. The core was sliced every 3.1 mm (12.2 inches) based on a preliminary age assessment assuming a sedimentation rate of 9 years/cm. This value was the highest sedimentation rate calculated by Hanebuth and Henrich (2009) for sediment cores in the upwelling region off Cape Blanc. Each sediment slice was transferred to the respective petri dish, wrapped with tape, and restored in the MARUM/IODP freezer before the cyst extraction.

**Table 5.2.** Corrected intervals of each sediment core and its equivalent to the sediment trap sample. (\*) The day when the GeoB core was obtained in the research area.

Core ID	Core depth (mm)	Sample interval (years)	Sediment trap ID	Date in the sediment trap
GeoB 14-01	0 – 3.1	1.6	CBeu-10	21/08/2020* – 05/01/2019
GeoB 14-02	3.1 – 6.2	1.6	CBeu-09	04/01/2019 – 11/05/2017
GeoB 14-03	6.2 – 9.3	1.6	CBeu-08	10/05/2017 – 15/10/2015
GeoB 14-04	9.3 – 12.4	1.6	CBeu-07	14/10/2015 – 14/02/2014
GeoB 14-05	12.4 – 15.5	1.6	CBeu-06	13/02/2014 – 25/06/2012
GeoB 14-06	15.5 – 18.7	1.6	CBeu-05	24/06/2012 – 12/11/2010
GeoB 14-07	18.7 – 21.8	1.6	CBeu-04	11/11/2010 – 01/04/2009
GeoB 14-08	21.8 – 24.9	1.6	CBeu-03	31/03/2009 – 11/08/2007
GeoB 14-09	24.9 – 28.0	1.6	CBeu-02	10/08/2007 – 23/12/2005
GeoB 14-10	28.0 – 31.1	1.6	CBeu-01	22/12/2005 – 10/05/2004

### 5.3.2. Palynological procedures and cysts identification

A 1/125 fraction of the sediment trap samples were filtered using a 20 $\mu$ m metal high-precision sieve (Stork Veco) while washing the poison with distilled water. This procedure was repeated at least three times. The frozen sediment samples were thawed, and 1 ml of wet sediment was taken from each sample. Every sample was placed in a beaker and weighed before all samples were dried in an oven under 60°C overnight or longer if required. The dried samples were weighed and treated with 10% hydrochloric acid (HCl) to dissolve the calcareous material. The treated samples were left for about two hours or until no more reaction from the acid was observed. Successively, the samples were neutralised using 10% kalium hydroxide (KOH) until pH was 7, water was added to induce neutralisation, and the samples were left for at least four hours before being decanted through a 20 $\mu$ m metal high-precision sieve (Stork Veco). After decanting, additional water was added to be left overnight. The next day, samples were decanted for the second time, treated with 40% hydrofluoric acid (HF) to dissolve siliceous material, and placed on a shaker device set with 100 motion per minute for two hours. After this, the samples were left for two days. The samples were neutralized with 40% KOH and successively washed three times.

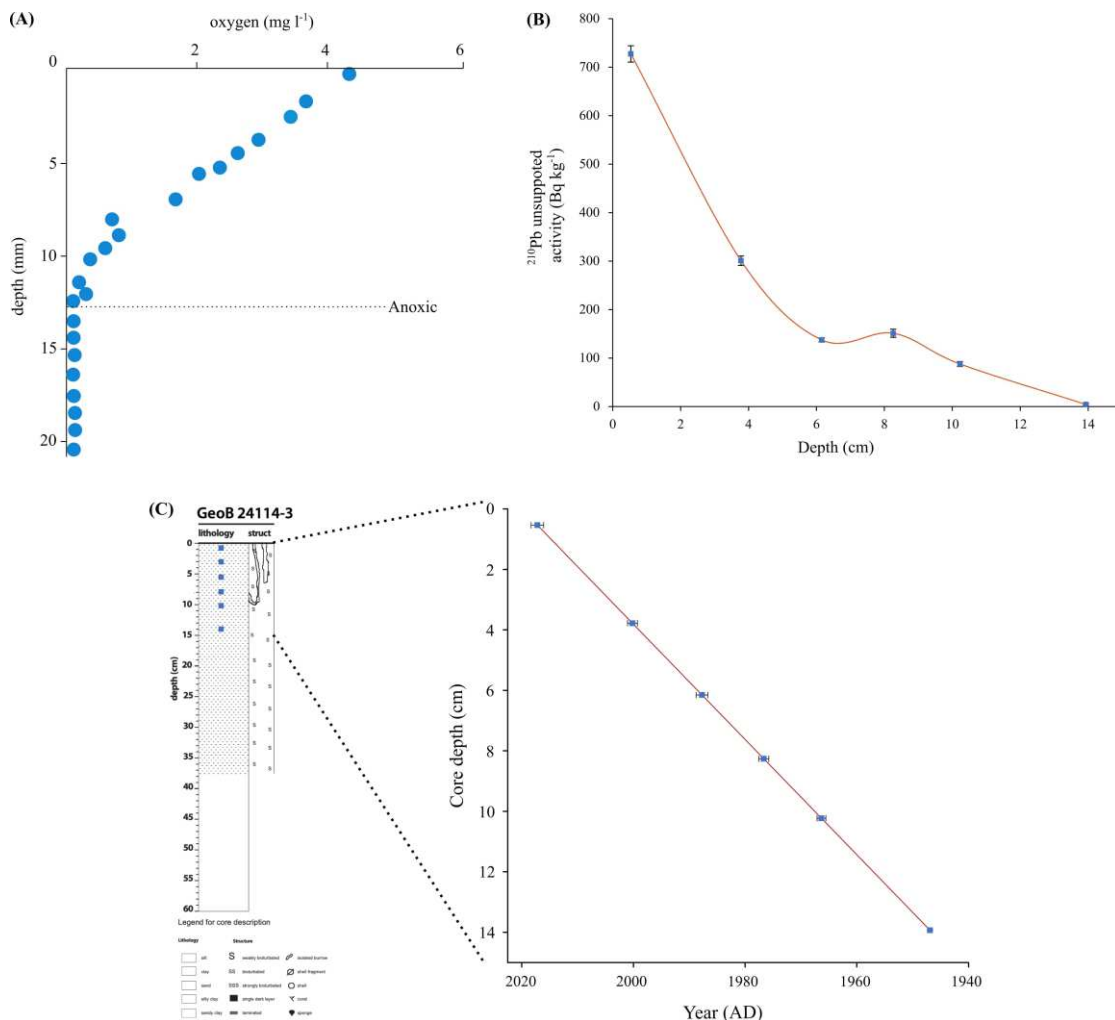


**Figure 5.2.** Several analyses were applied to the GeoB 24114 core: (A) the oxygen concentration profile measured by the FIBOX3 sensor, (B) the profile of <sup>210</sup>Pb unsupported plotted to the depth of dated core samples, (C) the GeoB 24114 (GeoB 14) lithology profile with the sample used for age dating (blue squares) and the profile of liner age model, plotting the depth of the samples over their respective estimated age.

The following procedures were applied to both sediment trap and core samples. They were gently sonicated on an ultrasonic bath to break up the fine particles, and the samples were sieved several times over a 20 $\mu$ m metal high-precision sieve (Stork Veco) until no more fine particles were observed. The residue was transferred to Eppendorf tubes, centrifuged, and concentrated to 1 ml for the trap samples and 1.5 ml for the core samples. A determined aliquot sample was transferred to a palynological

slide, embedded into glycerine gelatine, covered with a cover slip, and enclosed with paraffin wax. Dinoflagellate cysts in every sample were identified at the species or genus level with light microscopy (Zeiss Axiovert) under 400x magnification. Dinoflagellate cyst species that have been linked to their theca were cited by their motile names based on the statement of Elbrächter et al., 2023. The references used for the identification of dinoflagellate cyst taxa are Zonneveld and Pospelova (2015), Mertens et al. (2020), and van Nieuwenhove et al. (2020). Specimens of the respective taxa were counted and documented for further analysis.

**Table 5.3.** The list of dinoflagellate cyst taxa that was identified at the study sites. Taxa with an asterisk (\*) were found only in the sediment trap.

Cyst name (heterotrophs)	Biological affinity	Cyst name (photo-/mixotrophs)	Biological affinity
<i>Brigantedinium</i> spp.	<i>Protoberidinium</i> sp.	<i>Ataxiodinium choane</i> *	<i>Gonyaulax spinifera</i> complex
Cruciform cyst	Unknown	<i>Biecheleria</i> sp.*	Unknown
Cyst of <i>Archaerberidinium constrictum</i>	<i>Archaerberidinium constrictum</i>	<i>Bitectatodinium spongium</i>	Unknown
Cyst of <i>Archaerberidinium minutum</i> *	<i>Archaerberidinium minutum</i>	<i>Dalella chathamensis</i> *	Unknown
Cyst of <i>Archaerberidinium saanichi</i>	<i>Archaerberidinium saanichi</i>	Cyst of <i>Gymnodinium nolleri</i>	<i>Gymnodinium nolleri</i>
Cyst of <i>Diplopelta symmetrica</i>	<i>Diplopelta symmetrica</i>	Cyst of <i>Gymnodinium</i>	<i>Gymnodinium</i>
Cyst of <i>Islandinium</i> spp.	<i>Islandinium</i> spp.	<i>microreticulatum</i>	<i>microreticulatum</i>
Cyst of <i>Polykrikos hartmanii</i> *	<i>Polykrikos hartmanii</i>	<i>Impagidinium aculeatum</i>	<i>Gonyaulax</i> sp.
Cyst of <i>Polykrikos kofoidii</i> *	<i>Polykrikos kofoidii</i>	<i>Impagidinium paradoxum</i>	<i>Gonyaulax</i> sp.
Cyst of <i>Polykrikos quadratus</i> *	<i>Polykrikos quadratus</i>	<i>Impagidinium patulum</i>	<i>Gonyaulax</i> sp.
Cyst of <i>Polykrikos schwartzii</i>	<i>Polykrikos schwartzii</i>	<i>Impagidinium plicatum</i> *	<i>Gonyaulax</i> sp.
Cyst of <i>Protoberidinium americanum</i>	<i>Protoberidinium americanum</i>	<i>Impagidinium sphaericum</i>	<i>Gonyaulax</i> sp.
Cyst of <i>Protoberidinium monospinum</i>	<i>Protoberidinium monospinum</i>	<i>Impagidinium</i> spp.	<i>Gonyaulax</i> sp.
Cyst of <i>Protoberidinium stellatum</i>	<i>Protoberidinium stellatum</i>	<i>Impagidinium striatum</i>	<i>Gonyaulax</i> sp.
Cyst type A*	Unknown	<i>Impagidinium variaseptum</i> *	<i>Gonyaulax bohaiensis</i>
Cyst type B*	Unknown	<i>Nematosphaeropsis labyrinthus</i> *	<i>Gonyaulax</i> sp.
<i>Dubridinium</i> sp.	<i>Preberidinium</i> sp.?	<i>Lingulodinium machaerophorum</i>	<i>Lingulodinium polyedra</i>
<i>Echinidinium aculeatum</i>	Unknown	<i>Operculodinium israelianum</i>	<i>Protoceratium</i> sp.?
<i>Echinidinium bispiniformum</i> *	Unknown	<i>Operculodinium centrocarpum</i>	<i>Protoceratium reticulatum</i>
<i>Echinidinium delicatum</i>	Unknown	Cyst of <i>Pentapharsodinium dalei</i>	<i>P. dalei</i>
<i>Echinidinium granulatum</i>	Unknown	<i>Polysphaerodinium zoharyi</i>	<i>Pyrodinium bahamense</i>
<i>Echinidinium karaense</i> *	Unknown	<i>Pyxididopsis</i> spp.	Unknown
<i>Echinidinium</i> spp.	Unknown	<i>Spiniferites membranaceus</i>	<i>Gonyaulax membranacea</i>
<i>Echinidinium transparentum</i>	Unknown	<i>Spiniferites mirabilis</i>	<i>Gonyaulax spinifera</i> complex
<i>Echinidinium zonneveldiae</i>	Unknown	<i>Spiniferites pachydermus</i>	<i>Gonyaulax ellegaardiae</i>
<i>Leipokatium invisitatum</i>	Unknown	<i>Spiniferites ramosus</i>	<i>Gonyaulax spinifera</i> complex
<i>Lejeunecysta oliva</i> *	<i>Protoberidinium</i> sp.	<i>Spiniferites</i> spp.	<i>Gonyaulax</i> sp.
<i>Lejeunecysta paratenella</i> *	<i>Protoberidinium</i> sp.	<i>Tectatodinium pellitum</i> *	Unknown
<i>Lejeunecysta sabrinum</i> *	<i>Protoberidinium leonis</i> ?		
<i>Quinquecuspis concreta</i>	<i>Protoberidinium leonis</i>		
<i>Selenopemphix nephroides</i>	<i>Protoberidinium subinermis</i>		
<i>Selenopemphix quanta</i>	<i>Protoberidinium conicum</i>		
<i>Selenopemphix undulata</i> *	-		
<i>Trinovantedinium applanatum</i>	<i>Protoberidinium shanghaiense</i>		
<i>Trinovantedinium pallidifulum</i> *	<i>Protoberidinium louisianense</i>		
<i>Votadinium calvum</i>	<i>Protoberidinium latidorsale</i>		
<i>Votadinium spinosum</i> *	<i>Protoberidinium claudicans</i>		
<i>Xandarodinium xanthum</i>	<i>Protoberidinium divaricatum</i>		

### 5.3.3. Age model and accumulation rate

Since the sampling interval of sediment trap samples was already assigned by the sampling cups. Therefore, the cyst accumulation rates in the sediment trap ( $\text{cyst m}^{-2} \text{ day}^{-1}$ ) could be easily calculated by dividing the counted cysts with fraction size (1/125), the surface area of the sampling cup aperture ( $\text{m}^2$ ), and sampling interval (day). Meanwhile, core sediments comprised silty/clays of similar sizes throughout the core. This suggests that no major changes in sediment flux have occurred, and we assume constant sedimentation over time. This hypothesis is supported by sediment trap studies at the core location that show a relatively constant yearly flux of particles since the start of the record in 2003 (e.g., Fischer et al., 2019; Romero et al., 2020). Six representative sample points of the GeoB core were determined for a core dating analysis (**Table 5.1**), and they were sent to the Chemistry laboratory at Helmholtz-Zentrum Hereon, Institute of Coastal Environmental Chemistry in Geesthacht, Germany. The sample ages were measured with  $^{210}\text{Pb}/^{137}\text{Cs}$  by assuming a constant supply rate of unsupported  $^{210}\text{Pb}$  in the sediments, known as the CSR model (Appleby and Oldfield, 1978). The linear model of the age-depth relationship revealed the GeoB 24114-3 core sedimentation rate as  $0.2 \text{ cm year}^{-1}$  (**Figure 5.2C**), which means the average resolution per core sample was 1.6 years with 0.9 years of uncertainty. Finally, the dinoflagellate cyst accumulation rates ( $\text{cyst m}^{-2} \text{ year}^{-1}$ ) could be calculated by multiplying the cyst concentration ( $\text{cyst g}^{-1}$ ), dry bulk density ( $\text{g cm}^{-3}$ ), and sedimentation rate ( $\text{cm year}^{-1}$ ). To enable an adequate comparison, the unit of cyst accumulation rates from the two sources was converted to  $\text{cyst m}^{-2} \text{ year}^{-1}$ .

### 5.3.4. Statistics

Initially, the interval of sediment trap samples was recalibrated to match the sediment core samples resolution, and the accumulation rates of new sediment trap sample points were recalculated. This calibration and the core dating result were conducted to find the equivalent of core sample points in the sediment trap samples (**Table 4.2**). The taxa applied for multivariate analyses were those with average relative abundance exceeding 1% in either sediment trap or sediment core samples, and the rest of the dinocysts taxa were combined as others. A constrained ordination technique was performed to explain the relationship of the sample points based on the dinocyst taxa distribution in two-dimensional axes. Detrended correspondence analysis (DCA) was executed on all samples to distinguish the main response of the taxa, represented by the value of gradient length. A linear response was symbolized by a gradient length lower than 2 (ter Braak and Prentice., 1988; ter Braak and Šmilauer, 2002). Consequently, a Principal component Analysis (PCA) was performed to trap and core samples separately. With the assistance of the Shannon index, the PCA ordination was used to estimate the correlation among samples according to their taxa composition. The statistical analyses were performed using the Canoco5 software package.

## 5.4. Results

### 5.4.1. Dinoflagellate cyst accumulation rates in the sediment trap and down-core

After fitting the corresponding age between the sediment trap and the down-core samples, it was revealed that most dinoflagellate cyst taxa identified in the sediment trap (65 taxa) also occurred in the sediment core (44 taxa). Many of the not recovered taxa in the core were only rarely observed in the material collected by the sediment trap. These species are *Ataxiodinium choane*, *Echinidinium bispiniformum*, *Echinidinium karaense*, *Impagidinium plicatum*, *Impagidinium variaseptum*, *Polykrikos quadratus*, and *Selenopemphix undulata* (**Table 5.3**). Cyst accumulation rates of both heterotrophic and photo-/mixotrophic dinoflagellate increased with depth in the core, whereas the concentration of those groups in the sediment trap did not display the same trend (**Figure 5.4**). Between sediment trap and down-core, the fluctuating pattern of cyst accumulation rates was more different in the heterotrophic group. The accumulation rates of heterotrophic dinoflagellate cysts in the core ranged from  $1.0 \times 10^6$  to  $4.4 \times 10^6 \text{ cyst m}^{-2} \text{ year}^{-1}$  (**Figure 5.4A**). The minimum rate in the core was recorded in sample GeoB 14-01, while the maximum was recorded in sample GeoB 14-08. The minimum heterotrophic dinoflagellate

cyst accumulation rate in the sediment trap was  $2.4 \times 10^6$  cyst  $m^{-2}$  year $^{-1}$ , recorded between January 2019 and August 2020 (CBeu-10). The maximum accumulation rate was  $8.1 \times 10^6$  cyst  $m^{-2}$  year $^{-1}$ , which accumulated from December 2005 to August 2007 (CBeu-02).

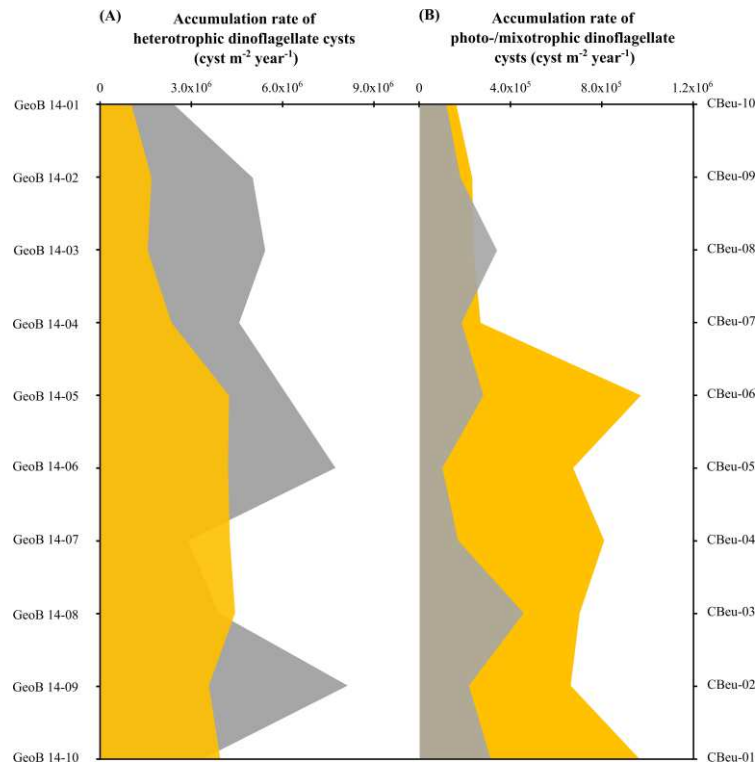


**Figure 5.3.** The dinocyst accumulation rate (cyst  $m^{-2}$  year $^{-1}$ ) comparison between samples collected by CBeu sediment trap (gray area) from approximately 2003 to 2020 and samples of GeoB 24114 core (yellow area) in the same time frame. (A) Heterotrophic dinoflagellate cysts, (B) Photo-/mixotrophic dinoflagellate cysts.

Although the general trend of photo-/mixotrophic dinoflagellate cysts in the core and sediment trap was relatively similar, their actual accumulation rates were much higher in the core. The concentration of photo-/mixotrophic dinoflagellate cysts in the core fluctuated between  $1.6 \times 10^5$  and  $9.7 \times 10^5$  cyst  $m^{-2}$  year $^{-1}$  (**Figure 5.4B**). The lowest concentration was in sample GeoB 14-01, and the highest was recorded in sample GeoB 14-06. Meanwhile, the lowest concentration of photo-/mixotrophic dinoflagellate cysts in the trap was  $1.2 \times 10^5$  cyst  $m^{-2}$  year $^{-1}$ , recorded from November 2010 until June 2012 (CBeu-05). The highest concentration was  $4.6 \times 10^5$  cyst  $m^{-2}$  year $^{-1}$ , which accumulated from August 2007 and March 2009 (CBeu-03).

#### 5.4.2. Dinoflagellate cyst association in the sediment trap and down-core

Comparable to the trap samples, the dinoflagellate cyst associations in the core were dominated by the heterotrophic taxa such as *Brigantedinium* spp., *Protoperidinium americanum*, *P. stellatum*, *P. subinermis* (*Selenopemphix nephroides*), and many spiny brown cyst taxa including, *Archaeperidinium* spp., *E. aculeatum*, *E. delicatum/granulatum*, and *P. monospinum* (**Figure 5.4B**). However, the relative abundance distribution of the important dinoflagellate cysts taxa appeared different, resulting in the abundance disparities of each taxon between the two sample sets (**Figure 5.4A, B**).

The mean relative abundance of the heterotrophic taxa dropped from 88 - 97% in the sediment trap to 81 - 90% in the sediment core, which impacted the composition of the taxa as well (**Figure 5.5**). The most significant decrease in the mean relative abundance appeared in the most common taxa of *Brigantedinium* spp., which fell from 47 - 73% in the sediment trap to only 28 - 43% in the core (**Figure 5.5**). This trend was also observed in other heterotrophic dinoflagellates such as *E. aculeatum*, *Polykrikos* spp., and *P. americanum*. In contrast, several heterotrophic taxa showed an increase in mean relative abundance, with *P. monospinum* and *P. stellatum* displaying the most significant increase in the down core association. *P. monospinum* relative abundance ranged from 0.9 - 4% in the sediment trap

association, but 7 - 16% of this species was discovered in the core samples. *P. stellatum* relative abundance in the sediment trap was between 0.9 - 5%, which rose to 7 - 15% in the core. The relative abundance of photo-/mixotrophic dinoflagellate cysts increased significantly in the core association from 2 - 12 % in the sediment trap to 10 - 20% (**Figure 5.5**). Almost all photo-mixotrophic taxa showed the same results; for instance, *I. aculeatum*, (from 0.1 - 0.9% to 0.5 - 2%), *Lingulodinium polyedra* (from 0.1 - 1% to 0.7 - 7%), *Operculodinium israelianum* (from 0.1 - 0.3% to 0.5 - 2%), and *Spiniferites* spp. (from 0.1 - 0.9% to 0.5 - 3%). *Gymnodinium* spp. was the only taxon that showed a declining trend in the relative abundance from the sediment trap (0.1 - 4%) to down-core (0.5 - 2%).

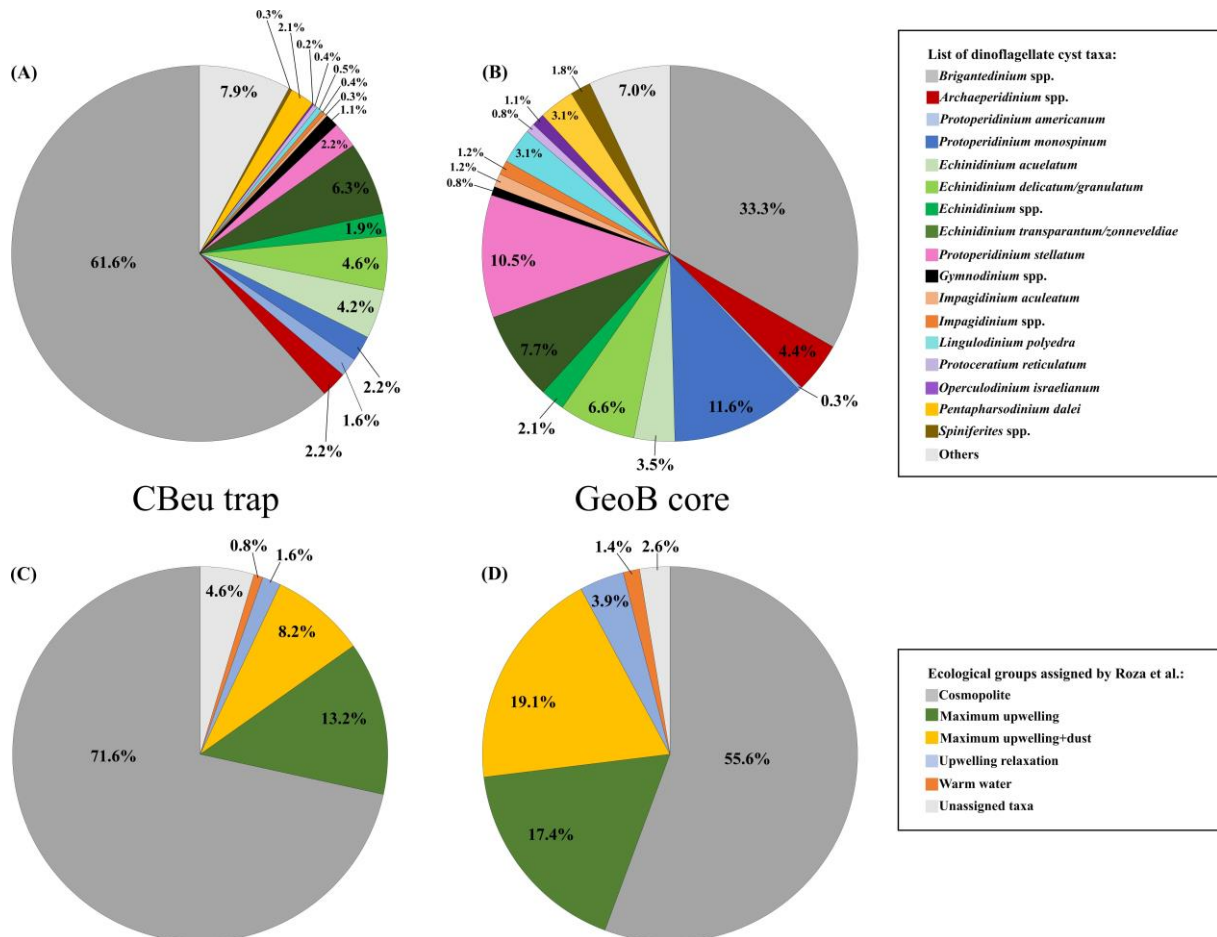


**Figure 5.4.** The pie charts of overall average contribution of (A) the common heterotrophic and photo-mixotrophic dinocyst taxa in the sediment trap samples, (B) the same list of dinocyst taxa found in the core samples, (C) ecological groups according to the relationship between dinocysts taxa in the sediment trap samples with prominent environmental parameters in the study area, and (D) the same list of ecological groups implemented to the dinocysts in the core samples.

In Roza et al.,2024, the most common heterotrophic and photo-/mixotrophic dinocyst taxa were assigned into five groups based on the ordination result of canonical correspondence analysis (CCA). The analysis showed the relationship of each dinocyst taxa to several environmental parameters. The list of taxa in each group was stated in **Table 2.1.** in the previous chapter. Some changes were observed in the overall average contribution of those ecological groups in the sediment trap and down-core data. A significant increase was observed in the average contribution of the upwelling+dust group, from 8.2% in the trap to 19.1% in the core. In contrast, the cosmopolite group contribution strongly dominated in the trap data with 71.6%, but it drastically declined to 55.6% in the core data. The rest of the groups showed an increase from the trap to core data, but they are not as significant as in the upwelling+dust group. The upwelling group accounted for 13.2% of the sediment trap data and 17.4% in the core. The upwelling relaxation contributed around 1.6% in the trap and 3.9% in the core. Lastly, the warm water group accounted for only 0.8% of the trap data and increased to 1.4% in the core.

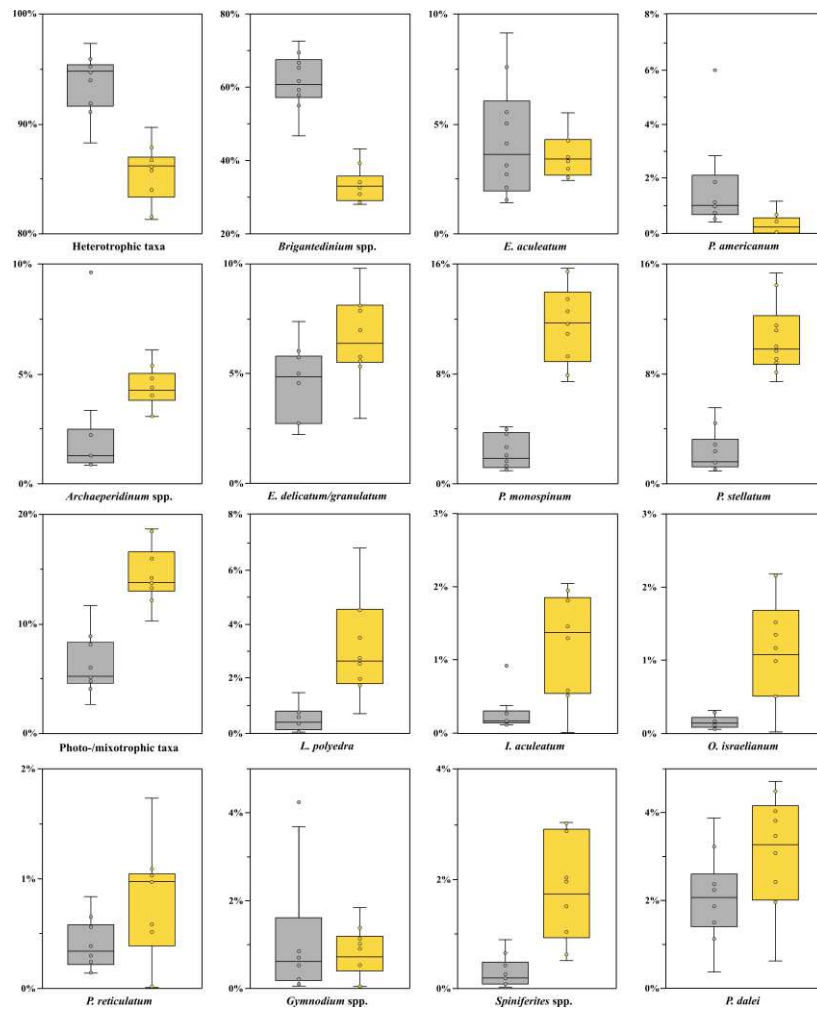


**Figure 5.5.** The boxplot shows the relative abundance of dinoflagellate cyst groups and taxa acquired from the CBeu sediment trap (gray boxes) and Geob 24114 down-core (yellow bars) samples.

### 5.4.3. Multivariate analyses

The gradient length score of detrended correspondence analysis (DCA) performed on the sediment trap samples was 0.7, indicating a linear response (**Table 5.4**). This result means that principal component analysis (PCA) is the fitted model to explain the sample distribution. The main axis of PCA (axis 1) explained 73.4% of the total variance, whereas the PCA axis 2 explained 12.7%. Four groups were determined according to PCA ordination and Shannon index similarity of the sample points (**Figure 5.6A**). Group I consisted of three sample points, ordinated on the positive side of axis 1 and the negative side of axis 2. Group II consisted of two sample points ordinated on the positive sides of both axes. Group III contained five sample points scattered on the negative side of PCA axis 1 and both of axis 2. The sediment trap time series was split into two parts according to the grouping of PCA (**Figure 5.6C**). The first three samples (PCA group I) were dominated by several number of taxa (e.g., *Archaeoperidinium* spp., *Gymnodinium* spp., *Impagidinium* spp., *P. americanum*, *P. stellatum*, and *Spiniferites* spp.). The second part consisted of PCA groups II and III, which were dominated by a few taxa, particularly *Echindinium* species (*E. aculeatum* and *E. delicatum/granulatum*).

**Table 5.4.** Gradient length score determined by detrended correspondence analysis (DCA) and every axis score of principal component analysis (PCA), performed in the software package Canoco 5 (ter Braak and Šmilauer, 2012; Šmilauer and Lepš, 2014).

Sample type	Gradient length	Method	Eigenvalue axis 1	Eigenvalue axis 2	Eigenvalue axis 3	Eigenvalue axis 4
Sediment trap	0.7	PCA	0.734	0.127	0.060	0.033
Down-core	0.6	PCA	0.412	0.295	0.115	0.056

DCA gradient length of the core samples scored 0.6, suggesting a linear response and further executed with PCA (Table 5.4). PCA axis 1 explained 41.2% of the total variance, while PCA axis 2 explained 29.5%. Four groups were assigned based on the ordination and Shannon index of the sample points (Figure 5.6B). Group IV comprises two sample points distributed on the positive side of axis 1 and the negative side of axis 2. Group V also contained two sample points distributed on the positive side of both axes. Group VI consisted of two sample points, ordinated on the negative side of axis 1 and both sides of axis 2. Group VII contained three sample points, ordinated on the negative sides of both axes. These PCA groups separated the sediment core time series into three parts (Figure 5.6D). The first part consisted of PCA group VII, containing high contributions of *Impagidinium* spp., *L. polyedra*, and *P. monospinum*. The middle part is occupied by group VI, with high contributions of *Echindinium* species (*E. aculeatum*, *E. delicatum/granulatum*, and *Echindinium* spp.), *P. dalei*, and *P. reticulatum*. The last part of the time series encompassed PCA groups V and IV and contained high contributions of *Archaeperidinium* spp., *Brigantedinium* spp., *E. transparentum/zonneveldiae*, *Gymnodinium* spp., and *P. americanum*. The dinocyst taxa distribution in the core times series shows less variability throughout the samples compared to the sediment trap taxa distribution. It is supported by the Shannon index score of core samples (2.0 - 2.4) that are higher than those of the sediment trap (1.1 - 2.0) (Figure 5.6A, B). A higher Shannon index score indicated a more even distribution of taxa or species in as sample.

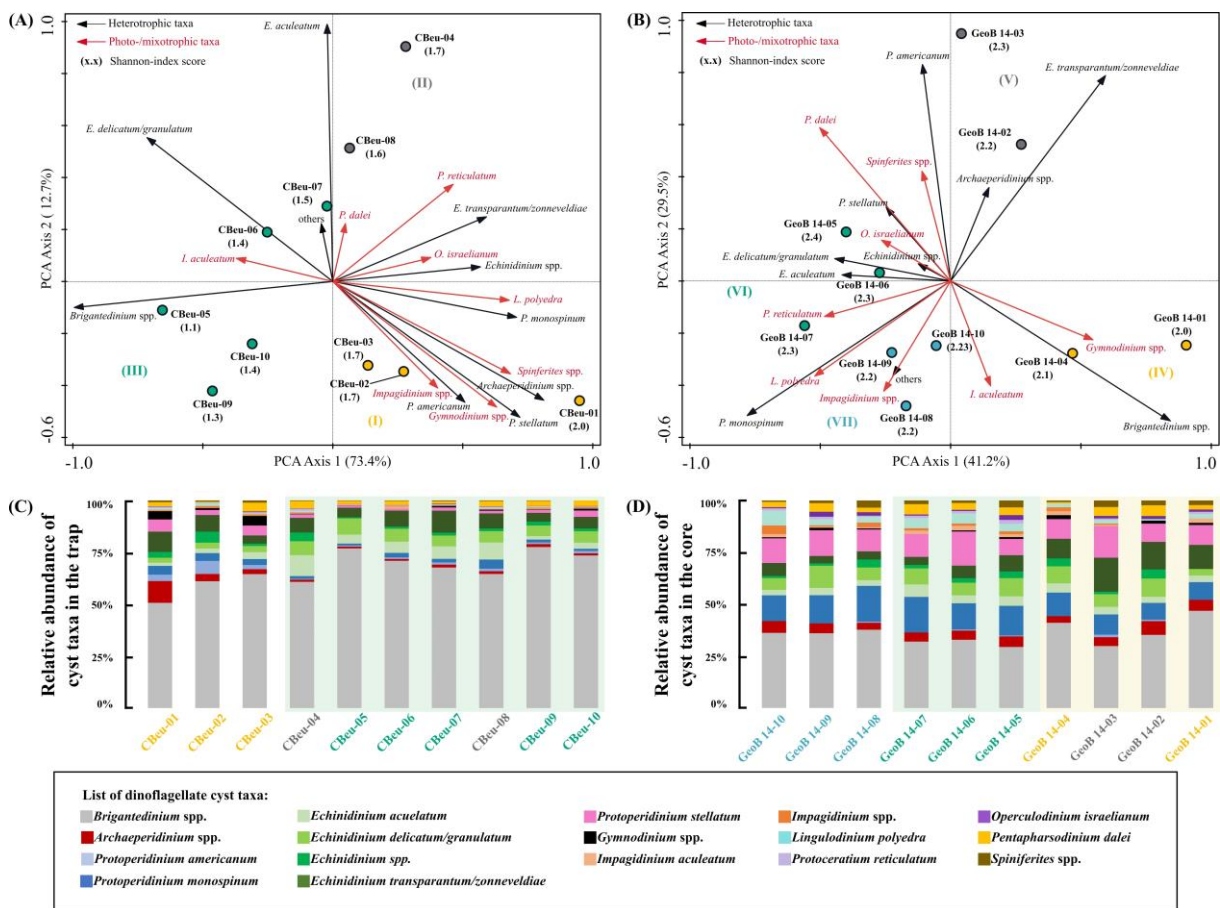


**Figure 5.6.** Comparison analyses of dinoflagellate cyst associations from the CBeu sediment trap and GeoB 24114 core. (A) Principal Component Analysis (PCA) of the trap samples depicted four groups (I: yellow, II: gray, and III: green), (B) PCA of the core samples depicted four groups (IV: yellow, V: gray, VI: green, and VII: blue), (C) Time series of trap samples showing the relative abundance of the abundant taxa. The colour of the label represents the PCA groups, and the green shade marked the association shift from group I to groups II and III, (D) Time series of core samples showing the relative abundance of the abundant taxa. The colour of the label represents the PCA groups. The green shade marked the association shift from group VII to group VI, and the yellow shade marked the association shift from group VI to groups V and IV.



## 5.5. Discussion

### 5.5.1. Production and preservation signals of dinocyst fossils

The identified taxa in the core samples were relatively similar to those in the sediment trap, where heterotrophic taxa, especially *Brigantedinium* spp, still dominated the association. However, considerable differences were observed in the relative abundances of the dinocyst taxa. Initially, it is important to acknowledge that those disparities could be caused by biases that occurred during the sampling and preparation of the materials. (1) The time gap in the sediment trap time series contributed to underestimating the dinocyst flux from the upper water column. (2) Long exposure to hydrofluoric acid could degrade and damage organic-walled dinocysts (Persson and Smith, 2022), decreasing the dinocyst accumulation rates in the down-core samples. Those two aspects are believed to influence the dinocyst taxa equally, yet different signals were observed with higher accumulation rates of photo/mixotrophic cysts found in the core samples compared to the trap, indicating that we have no evidence that process 2 did occur. The absence of rare dinocyst taxa collected in the sediment trap could be caused during the identification and counting procedure. Zonneveld et al. (2019b) found that rarer dinocyst taxa were more easily recognised within the samples in which the abundant dinocysts were highly degraded.

Although the accumulation rates of heterotrophic dinocysts in both trap and core samples were comparable on the scale of  $10^6$ , the overall accumulation rates were higher in the trap. The photo-mixotrophic group accumulation rates showed the opposite trend. The rate values were relatively similar between trap and core samples in the scale of  $10^5$ , but the general concentrations were higher in the core samples. Unfortunately, only two similar comparison studies reported dinocyst trap v. core accumulation rates. In Hudson Bay (Canada), Heikkilä et al. (2016) found more dinocysts in the surface sediments than in the trap. The disparities were relatively small, which is comparable to our result. However, Pitcher and Joyce (2009) conducted the same study in the Namaqua Shelf (Benguela) and reported much higher dinocyst concentration in the surface sediment by factor 2. We assume that a rate calculation error in the trap or sediment data in this latter study led to these large differences.

The photo-/mixotrophic taxa accumulation rate fluctuation is more similar than heterotrophic (**Figure 5.3**). The concentration of heterotrophic dinocysts dropped in the core samples and was depicted by many taxa in this group, for instance, *Archaeperidinium* spp., *Brigantedinium* spp., *Echinidinium aculeatum*, and *E. delicatum/granulatum*. Out of all, *Brigantedinium* spp. indicated the most severe alteration signal in total concentration and rate fluctuation (**Figure 5.7**). Cyst accumulation rate reduction was also shown in the other three taxa, but less extreme. Moreover, their concentration fluctuated more similar to the sediment trap record for each taxon, particularly the species of *Echinidinium* (**Figure 5.7**). On the east coast of New Zealand, Prebble et al., 2013 documented that heterotrophic dinocysts were underrepresented in the surface sediments. The cyst selective degradation can explain the reduction of this group. It has been proposed that this might be caused by the coloured-cyst wall (produced mainly by heterotrophic dinoflagellates) containing a nitrogen-rich glycan that is more susceptible to post-depositional degradation (Bogus et al., 2014; Zonneveld et al., 2019b; Versteegh and Zonneveld, 2022). The degradation impact varies between species or taxa. Zonneveld et al. (2019b) demonstrated that *Brigantedinium* spp. were highly degradable under oxic conditions, while species like *E. aculeatum* are slightly more resistant. These results fit the trend shown in the accumulation rates of respective taxa (**Figure 5.7**).

All photo-/mixotrophic taxa showed an increase in their relative abundance and, more significantly, in their accumulation rates. Most photo-/mixotrophic dinoflagellates produce transparent cyst walls formed by glycans that are more resistant to aerobic post-depositional degradation (Bogus et al., 2014). Interestingly, the relative abundance of *Gymnodinium* spp. indicated the tightest difference between trap and core data (**Figure 5.4A, B**). Since this taxon produced brown cysts like those of the heterotrophic groups, it is suggested they are more vulnerable than the other photo-/mixotrophic taxa (Bogus et al., 2014; Meyvisch et al., 2023). However, we could not entirely confirm this theory due to

the significant concentration difference in accumulation rates in almost all taxa of photo-mixotrophic dinocysts (**Figure 5.7**). *P. dalei* is the only species with comparable signals in trap and core data. *Spiniferites* spp. showed a similar trend in both datasets, but its accumulation rates in the trap were much lower, and this result was shown more significantly in other rarer taxa (e.g., *L. polyedra* and *O. israelianum*). Two aspects that could be the reasons are: (1) a small area of sediment trap probing might underestimate the collected dinocyst export flux and representative taxa, which is more pronounced in the rare taxa such as photo-mixotrophic ones, and (2) dinocysts in the core originated from vertical and lateral transported particles that create the larger difference to the trap signal. Therefore, we suggest applying the same comparison technique as in this study in the area where high photo-/mixotrophic dinocysts are produced from the upper water column to confirm their resistance to degradation.

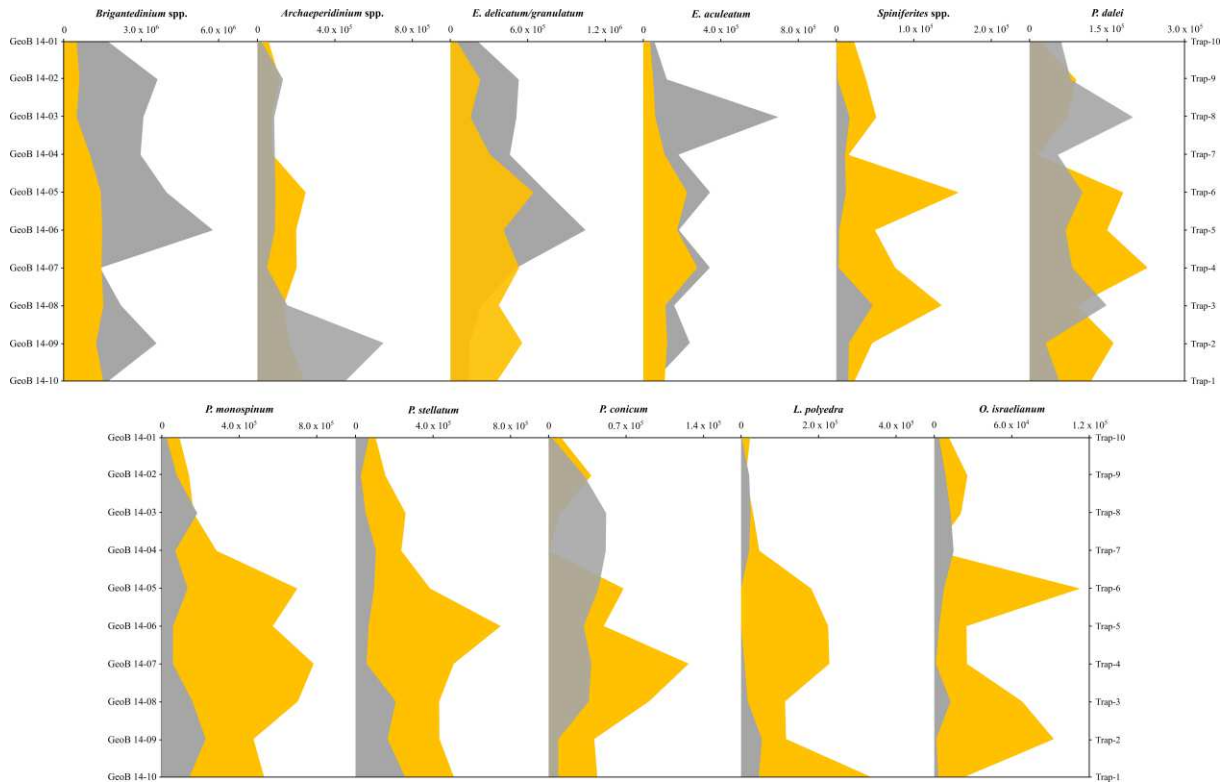


**Figure 5.7.** The cyst accumulation rate (cyst  $m^{-2} year^{-1}$ ) of several taxa between samples collected by CBeu sediment trap (gray area) and GeoB 24114 core (yellow area) in the same time frame.

Similar to many heterotrophic dinocysts, *Protoperidinium monospinum* was also classified as a highly degradable cyst. However, our data showed a significant increase in the percentage and concentration of this species from the trap to the core samples (**Figures 5.3, 5.7**). The same pattern is observed in other heterotrophic taxa, such as *P. stellatum* and *P. conicum*. The only process that in our opinion can explain this discrepancy is that materials from foreign sources (allochthonous materials) reached the core location. There are strong indications that in the research area dinocysts and many other microfossil groups are being laterally transported by ocean currents in surface, subsurface and bottom water layers such as e.g. nepheloid layers (Zonneveld et al., 2018; Nootboom et al., 2019). The water column in the eastern boundary regions is extremely dynamic due to intense and continuous coastal upwelling systems, leading to resuspension and transportation of particles in the bottom nepheloid layer (Zonneveld et al., 2018). The results of several studies conducted at and in the vicinity of the CBeu trap supported our interpretation (e.g., Zonneveld et al., 2022a; García-Moreiras et al., 2023; García-Moreiras et al., 2024). In multiple transects, they obtained samples from the water column, nepheloid layers, and top core. They confirmed that dinocysts in the surface sediments consisted of local and foreign materials. However, those studies did not mention or confirm that certain taxa (e.g., *P. monospinum*, *P. stellatum*) concentrations were enhanced in the sediments due to transport mechanisms from the shelf to greater ocean depths. Since the sampling location is affected by the Canary Current flowing from the north and Cape Verde Current from the south, it opens many possibilities of drivers

for a significant increase of these two taxa in the bottom sediment. Therefore, more comprehensive work covering a larger area is needed.

In the newly adjusted sediment trap data, PCA and Shannon-index marked the association shift from the CBeu-04 sample (**Figure 5.6A, C**). This sample noted the interval between April 2009 and November 2010 (**Table 5.2**). This association shift has been reported by Roza et al., 2024, stating that *Echindinium* species became more consistently abundant since 2009. The statistical analyses confirmed that the core samples recorded higher *Echindinium* relative contribution started from the GeoB 14-07 sample (**Figure 5.6B, D**) that was accumulated in the same time intervals as CBeu-04. Result of PCA group also indicated that the upper layers of the core (GeoB 14-01 to 14-04) was very different from those in the lower layers (**Figure 5.6D**). The core upper layers showed stronger evidence of bioturbation (**Figure 5.2C**), and the sediment might have been resuspended, which could explain the disparate dinocyst composition. The bulk density of sediments sent for age dating listed that the upper layers (0 - 12.4 mm) contained fewer particles than the more compacted ones in the lower depth, which could lead to lower dinocyst concentration in the upper core (**Table 5.1**). Furthermore, the depth of those four samples ranged from 0 to 12.4 mm, coincidentally matching the depth of higher measured oxygen in the core (**Figure 5.2A**). Oxygen worsens the degradation rate of the organic-walled dinocysts, more specifically, the sensitive ones (Zonneveld et al., 2007; Kodrans-Nsiah et al., 2008; Gray et al., 2017). The accumulation rates of many dinocyst taxa supported the effect of those factors mentioned, where the upper sample points showed a severe decline in their concentrations, making a larger difference with the respective trap samples (**Figure 5.3, 5.7**). It is interesting that the statistics demonstrated the signal of production and preservation of dinocyst well in the GeoB core data.

### 5.5.2. Implication for paleoenvironmental studies

As discussed above, lateral transport and selective preservation resulted in considerable alterations to the dinocyst associations in the core samples. Furthermore, other processes were interpreted to alter dinocyst core associations. The distribution of dinocyst taxa relative abundances over time was more homogenised in the core data than in the trap data (**Figure 5.6C, D**). As we visually observed traces of bioturbation activity in the upper part of the core, we assume that the homogenized associations could result from this process (Piot et al., 2008; Pérez-Asensio et al., 2017). Compaction can squeeze several years of ocean history into a thin layer of sediment/rock, inducing homogenisation (Saraswati and Srinivasan, 2016).

Although the dinocyst record in the core showed alteration due to multiple aspects, the signals of their environment can still be extracted. For example, the core association still contained a high number of heterotrophic dinocysts (e.g., *Brigantedinium* spp. and spiny brown cysts) and rare photo-/mixotrophic dinocysts representing a eutrophic upper water column with high turbulence, typical condition of a coastal upwelling ecosystem (Zonneveld and Brummer, 2000; Pitcher and Joyce, 2009; Pospelova et al., 2010; Bringué et al., 2013; Bringué et al., 2018; Bringué et al., 2019; Roza et al., 2024). The multi-year CBeu trap study by Roza et al., 2024 revealed five groups that indicate similar ecological functions: cosmopolite, upwelling, and upwelling+dust, which overnumbered species affiliated with upwelling relaxation and warm water conditions (**Figure 5.4C**). The three dominating groups in the trap were still highly abundant in the core samples, although their relative abundances declined (**Figure 5.4D**). This comparison study confirmed that dinocyst in the core sediment contained information of the upper water condition and perturbations caused by multiple factors. Therefore, understanding the dynamics and perturbation factors in the study area is essential when linking dinocyst association to environmental factors.

Based on our findings, we suggest several tips for interpreting dinocyst fossils for better paleoenvironment or paleoceanography reconstructions. (1) Be more cautious about allochthonous materials brought by the ocean currents in the study area; (2) consider all factors that could alter the core associations, such as transport, bioturbation, oxygenation, compaction, and selective preservation, especially when using surface sediments; (3) reconstruct the environment based on a group of taxa with

the same ecological function instead of using one species, and (4) the trend shown by the accumulation rates of dinocysts or other microfossils should be assisted with other proxies such as isotope or biomarker to ensure their accuracy.

## 5.6. Conclusions

The dinocyst association in the core samples contained most of the taxa collected from the 18-year sediment trap record. Heterotrophic dinocysts such as *Brigantedinium* spp. and spiny brown cysts (e.g., *Archaeoperidinium* spp., *P. monospinum*, and *Echinidinium* species) dominated the association in the trap and core samples, representing the dinocyst community of a coastal upwelling environment. The accumulation rates of dinocysts in the trap and core samples accounted for the comparable values, but considerable differences occurred between the two datasets. Heterotrophic dinocyst taxa relative abundance decreased in the core association, such as *Brigantedinium* spp., *E. aculeatum*, and *P. americanum*. In contrast, almost all taxa of the photo-/mixotrophic group relative abundance increased in the core samples, except for one taxon (*Gymnodinium* spp.). The accumulation rates of the mentioned groups and taxa showed similar results. The heterotrophic group concentration was higher in the trap samples, while the photo-/mixotrophic group concentration was higher in the core samples. This condition could be driven by different resistance of the organic-walled dinocyst to microbial degradation since the coloured cysts (heterotrophic groups and *Gymnodinium* spp.) are more susceptible to post-depositional degradation. However, some heterotrophic dinocysts (e.g., *P. monospinum* *P. stellatum*) showed increases in relative abundance and accumulation rates. It was interpreted as a result of foreign materials brought to the coring site. A similar condition was also observed in many photo-/mixotrophic taxa.

The composition of the dinocyst taxa in the core samples was more homogenous over time than in the trap samples, which indicated vertical mixing in the core stratification induced by bioturbation. PCA analysis applied to the core time series suggested that the upper four sample points showed a significantly different taxa composition, and the accumulation rates of dinocysts were significantly low within these sample points. The depth of these samples coincided with the oxic depth in the core, which can increase the aerobic degradation of organic-walled dinocysts. Furthermore, bioturbation structures were identified within 10 mm in the core upper part, and the dry bulk density indicated fewer sediment particles than in the lower part. Although multiple differences occurred in the core dinocyst association, the ecological groups of upwelling, upwelling+dust, and cosmopolite were still vastly more common than the upwelling relaxation and warm water groups, which will not lead to a core misinterpretation of the area oceanographic conditions. PCA and Shannon's index classified three groups of sediment trap samples that translated to the association shift in 2009 when the groups were plotted in the trap time series. This signal was also observed in the core time series by applying the same technique. Therefore, our result confirmed that organic-walled dinocyst fossils in the sediment core represented the upper water condition. However, pre and post-depositional aspects (e.g., lateral transport, bioturbation, compaction, and selective preservation) need to be considered when reconstructing the paleoenvironment and paleoceanography of certain areas, especially using dinocysts from surface sediments.

## 5.7. Acknowledgements

The financial support for this comparison study was provided by the German Research Foundation (DFG) through MARUM The Cluster of Excellence Project (EXC) in Recorder unit. We would like to thank the authorities of Germany, Morocco, and Mauritania for their support and allowance to obtain the samples. The authors would like to thank the captain and crew of RV Poseidon, RV Sonne, and RV Maria S. Merian, as well as the MARUM sediment trap team. Lastly, we

thank our colleagues (Iria García-Moreiras and Fangzhu Wu) for their assistance during the core samples preparation.

## 5.8. Supplementary data

**Supplementary table 5.1.** The count of identified heterotrophic dinocysts taxa from GeoB 24114-3 core. The abbreviations of the taxa are: Acont (*A. constrictum*), Asaan (*A. saanichi*), Briga (*Brigantedinium* spp.), Dsymm (*Diplopelta symmetrica*), Dubri (*Dubridinium* sp.), Eacul (*Echinidinium aculeatum*), Egran (*E. delicatum*), Echini (*Echinidinium* spp.), Etran (*E. transparentum*), Ezonn (*E. zonneveldiae*), Islan (*Islandinium* spp.), Linvi (*Leipokatium invisitatum*), Pschwa (*Polykrikos schwartzii*), Pamer (*Protoperidinium americanum*), Pcruci (cruciform-cyst), Pmono (*Protoperidinium monospinum*), Pschwa (*Polykrikos schwartzii*), Pshan (*P. shanghaiense*), Pstel (*P. stellatum*), and Psubi (*P. subinermis*).

Sample ID	Acont	Asaan	Briga	Dsymm	Dubri	Eacul	Edeli	Egran	Echin	Etran	Ezonn	Islan
GeoB 14-01	1	4	44	0	1	3	0	3	0	1	10	0
GeoB 14-02	2	7	48	0	0	4	2	10	6	0	18	0
GeoB 14-03	1	6	49	0	0	6	2	8	2	0	27	0
GeoB 14-04	0	5	65	0	3	7	3	10	6	0	15	0
GeoB 14-05	1	10	64	1	0	10	2	17	7	2	15	0
GeoB 14-06	1	7	60	0	2	7	2	9	4	0	11	3
GeoB 14-07	0	8	58	0	1	11	3	11	3	0	7	2
GeoB 14-08	1	5	68	0	1	5	3	8	7	0	7	1
GeoB 14-09	2	6	61	0	1	6	5	13	2	0	6	1
GeoB 14-10	1	10	70	1	1	5	3	8	2	2	10	0

Sample ID	Linvi	Pamer	Pconi	Pcruci	Pdiva	Plati	Pleon	Pmono	Pschwa	Pshan	Pstel	Psubi
GeoB 14-01	0	0	1	0	0	0	1	8	1	1	9	0
GeoB 14-02	1	1	3	0	0	2	1	11	0	1	12	1
GeoB 14-03	0	2	1	0	1	0	2	16	1	0	25	1
GeoB 14-04	0	0	0	0	0	0	0	18	0	0	15	1
GeoB 14-05	0	1	3	1	0	0	1	31	0	1	17	3
GeoB 14-06	0	1	2	0	0	3	2	23	0	1	30	0
GeoB 14-07	0	0	5	0	0	1	1	31	0	4	20	2
GeoB 14-08	0	1	4	1	0	0	1	31	1	5	19	1
GeoB 14-09	0	0	2	0	1	0	2	23	0	3	21	1
GeoB 14-10	0	0	2	0	0	1	1	24	0	2	23	2

**Supplementary table 5.2.** The count of identified photo-/mixotrophic dinocysts taxa from GeoB 24114-3 core. The abbreviations of the taxa are: Bspan (*Bitectatodinium spongium*), Gmicr (*Gymnodinium microreticulatum*), Gnoll (*G. nolleri*), Iacul (*Impagidinium aculeatum*), Impag (*Impagidinium* spp.), Ipara (*I. paradoxum*), Ipatu (*I. patulum*), Ispha (*I. sphaericum*), Istria (*I. strialatum*), Lpoly (*Lingulodinium polyedra*), Oisra (*Operculodinium israelianum*), Pbaha (*Pyrodinium bahamense*), Pdal (*Pentapharsodinium dalei*), Preti (*Protoceratium reticulatum*), Pyxid (*Pyxidopsis* spp.), Smemb (*Spiniferites membranaceus*), Smira (*S. mirabilis*), Spach (*S. pachydermus*), Spini (*Spiniferites* spp.), and Sramo (*Spiniferites ramosus*).

Sample ID	Bspan	Gmicr	Gnoll	Iacul	Impag	Ipara	Ipatu	Ispha	Istria	Lpoly
GeoB 14-01	2	1	0	2	0	0	0	0	0	2
GeoB 14-02	1	2	0	0	0	0	0	0	0	1
GeoB 14-03	2	0	0	1	0	0	0	0	1	3
GeoB 14-04	0	3	0	3	1	1	0	1	0	3
GeoB 14-05	1	0	2	3	3	0	0	0	0	8
GeoB 14-06	0	1	0	4	1	0	1	0	0	9
GeoB 14-07	0	0	0	3	1	0	1	0	0	9
GeoB 14-08	1	1	0	1	2	0	2	0	0	5
GeoB 14-09	1	2	0	1	0	0	1	0	0	5
GeoB 14-10	2	0	1	3	0	1	4	3	0	14

Sample ID	Oisra	Pbaha	Pdal	Preti	Pyxid	Smemb	Smira	Spach	Spini	Sramo
GeoB 14-01	1	0	2	1	1	0	0	1	1	0
GeoB 14-02	2	1	7	0	1	0	0	1	2	0
GeoB 14-03	2	0	7	1	1	2	0	1	2	0
GeoB 14-04	0	1	1	0	2	0	1	0	0	0
GeoB 14-05	5	0	8	4	2	2	1	2	2	0
GeoB 14-06	1	0	6	2	0	0	0	0	1	1
GeoB 14-07	1	0	9	2	3	0	1	0	2	0
GeoB 14-08	3	0	4	1	1	2	1	0	1	2
GeoB 14-09	4	1	7	2	0	0	0	0	0	2
GeoB 14-10	1	1	5	2	0	0	0	0	1	04

## Chapter 6 – Final remarks

### 6.1. Overall conclusions

The multi-year sediment trap series revealed that the dinoflagellate cysts export flux near Cape Blanc, Northwest Africa, contained a large portion (ca. 94%) of heterotrophic taxa, particularly *Brigantedinium* spp., and several spiny brown cysts taxa (e.g., *Archaerperidinium* spp. and *Echinidinium* species). Their export fluxes usually increased in spring-summer, which coincided with the high upwelling intensity. However, a few variations were observed over the years. The photo-/mixotrophic group suggested stronger interannual variability in their export fluxes. Occupying only ca. 6% of the overall association, their export fluxes increased sometime in autumn-winter when the upper water column was more stratified. Besides upwelling, trace minerals from the Saharan dust played an important role in the dinocysts export fluxes. Canonical Correspondence Analysis (CCA) ordination showed five groups in relation to several environmental parameters in the study area. The first two groups encompassed many heterotrophic dinocysts that positively correlated to maximum upwelling conditions (e.g., *E. delicatum/granulatum*, *E. transparantum/zonneveldiae*, *P. latidorsale*, and *Trinovantedinium* spp.) and the combination of strong upwelling and dust input (e.g., *Archaerperidinium* spp., *P. americanum*, *P. stellatum*, and *P. subinermis*). Two groups consisted of only photo-/mixotrophic taxa: upwelling relaxation (*Gymnodinium* spp. and *L. polyedra*) and warm water groups (*B. spongium* and *P. reticulatum*). The fifth group did not align with a specific environmental condition. The group contained a mixture of heterotrophic and photo-/mixotrophic dinocysts (e.g., *Brigantedinium* spp., *E. aculeatum*, *I. aculeatum*, *P. conicum*, *P. dalei*, *P. monospinum*, and *Spiniferites* spp.).

Out of 17 photo-/ mixotrophic dinocysts identified from the trap samples, five cysts were produced by biotoxin-producing dinoflagellates (*Gymnodinium* spp., *L. polyedra*, *P. reticulatum*, *P. bahamense*, and *G. spinifera* complex). Their concentrations were very low due to a lack of stratification in an all-year permanent upwelling ecosystem that disturb their cell growth. However, their occurrence throughout the trap record indicates that they still could be a threat to the ecosystem and fishery industry of the area in the future.

When performed with the Morlet Wavelet transform, the dinocysts export flux time series showed four significant bands, pointing out periods of half-year cycle, annual cycle, 240-day, and 480-day. The cycles in the dinocyst time series were indicated by higher export fluxes during winter (December to February) and spring-summer (April to June), which coincided with the cycles of the upwelling wind system and aerosol dust time series. Across 18 years, those periods indicated strong variations that could be classified into three phases. Phase I (2003 - 2008) was marked by the 240-day and 480-day bands as a result of the upwelling+dust group spectra band. Phase II (2009 - 2012) showed the half-year and annual cycles driven by the cyclic pattern of the upwelling group. Phase III (2013 - 2020) indicated more significant half-year and annual cycles that were also emphasized in the upwelling group cycles. These three phases were also observed in the upwelling wind and Saharan dust time series, solidifying the influence of those factors on the dinocyst export flux. The stepwise changes in the dinocyst time series suggested that upwelling and Saharan dust impacts became stronger in the later phase, which an ITCZ southward movement might have regulated. These findings demonstrated that environmental changes due to recent climatic shifts affected the plankton community, as hinted in the 18-year record of dinocyst export flux.

Many of the results mentioned above were observed when the dinocysts in the trap time series were compared with dinocysts in the core under the same temporal interval. All key dinocyst taxa in the trap samples were identified in the core samples. Heterotrophic dinocysts still dominated the dinocyst association, although their percentage declined to ca. 88%. The accumulation rates of both dinocyst

groups in the core and trap samples were relatively comparable. However, the heterotrophic dinocyst concentration declined in the core sample, while the photo-/mixotrophic dinocyst concentration was higher in the core samples. This might be the result of the heterotrophic dinocyst taxa (e.g., *Brigantedinium* spp., *Archaeoperidinium* spp., *E. aculeatum*, and *E. delicatum/granulatum*) vulnerability to microbial degradation. In contrast, a few species (e.g., *P. monospinum* and *P. stellatum*) accumulation rates increased in the core samples, which was interpreted as an indication of transported materials (allochthonous). Unfortunately, published literature could not confirm the origin of the foreign materials found in the sediment samples of this region, nor was the methodology applied in this study.

The most significant differences in the dinocyst composition and concentration occurred in the upper four sample points of the core. Bioturbation, sediment compaction, resuspension, and higher oxygen concentration contributed to more significant alteration in those samples. Despite the changes observed in the dinocyst core association, the upwelling, upwelling+dust, and cosmopolite groups established in the first project still dominated the core association. Furthermore, Principal Component Analysis (PCA) detected two steps of the taxa composition shift in the core time series. The first shift marked the abundant transition to *Echinidinium* species reported in the first and second projects. The second shift showed the association with the most substantial alteration. In conclusion, the three projects in this dissertation demonstrated the strong correlation between dinocyst production and the upper water column condition. Consequently, a long-time series of in-situ dinocysts provided valuable information about climatic-driven environmental changes in the study area that are transferrable in the sediment archive. However, considering the impact of multiple post-depositional processes is essential to improve our interpretation of dinocyst fossil association in paleoenvironmental and paleoclimate reconstructions.

## 6.2. Implications for future research

Although the three projects presented in this dissertation have successfully addressed multiple interesting questions regarding recent organic-walled dinocyst applications for ecology, oceanography, climate reconstruction, and paleontology, some aspects still need further investigation to provide more and better information. For instance:

- Examining multiple marine plankton groups collected by this sediment trap could support the finding of community shift from 2009.
- The variability of Sahara dust chemical properties over the years seemed to be critical to the shift in dinocyst or the marine plankton communities. Thus, further analysis through a long record of lithogenic particles collected in the same sediment trap or dust bouy near the trap is necessary.
- Establishing the theca-cyst relationship for the unsolved taxa becomes more important, especially for the key taxa in this study area, such as *Echinidinium* species. This latter will help distinguish whether the association shift in 2009 was related to different prey selections.
- Applying a more sophisticated time series analysis or including other potential driving factors could help clarify the existence of the 240- and 480-day periods detected by the wavelet transform in the dinocyst time series.
- Obtaining another core below the trap with a minimum perturbation effect, such as bioturbation, can increase the result of the comparison study.
- Conducting the same comparison technique in an area where the transparent dinocysts are more abundant can confirm the hypothesis of their resistant trait against microbial degradation.
- Obtaining more samples from the water column and the sediment floor in a larger spatial dimension could help track the origin of the allochthonous materials.

Besides the weakness in a few results and analyses of the three projects, the outputs also open multiple intriguing topics for the future of dinocysts and marine geoscience research. They are:



- 
- Analysing the export flux of multiple plankton groups collected by the CBeu trap could shed some light on the biological interaction between different groups and its impact on the plankton community over time. This type of investigation using in-situ environmental data is scarce.
  - This comprehensive observation could also provide a wider perspective of marine productivity and carbon biological pump in the area because various phyto- and zooplankton bear preservable calcareous or organic carbon remains (e.g., coccolithophores, planktonic foraminifera, and dinocysts).
  - Since the linear relationship between stepwise change in the environment and the dinocyst record was only detected in its cyclic pattern but not in its export flux, it is vital to reconsider inducing marine primary production through artificial mechanisms.
  - It is noteworthy to investigate the impact of changing climate (e.g., ITCZ migration) on the past ecosystem (dinocysts and their environment) in the study area deeper in geological time.

## References

- Adams, A. M., Prospero, J. M., and Zhang, C. (2012). CALIPSO-Derived three-dimensional structure of aerosol over the Atlantic Basin and adjacent continents. *J. Clim.* 25, 6862–6879. doi: 10.1175/JCLI-D-11-00672.1
- Alves, M., Gaillard, F., Sparrow, M., Knoll, M., and Giraud, S. (2002). Circulation patterns and transport of the Azores Front-Current system. *Deep Sea Res. Part 2 Top. Stud. Oceanogr.* 49, 3983–4002. doi: 10.1016/S0967-0645(02)00138-8
- Ando, T., Zonneveld, K. A. F., Versteegh, G. J. M., Ishigaki, M., Yamamoto, T., and Matsuoka, K. (2024). Why cysts of *Alexandrium catenella* and/or *A. pacificum* (Gonyaulacales, Dinophyceae) do not remain in sediments as fossils? *Rev. Palaeobot. Palynol.* 329, 105161. doi: 10.1016/j.revpalbo.2024.105161
- Arbuszewski, J. A., deMenocal, P. B., Cléroux, C., Bradtmiller, L., and Mix, A. (2013). Meridional shifts of the Atlantic intertropical convergence zone since the Last Glacial Maximum. *Nat. Geosci.* 6, 959–962. doi: 10.1038/ngeo1961
- Amorim, A., Palma, A. S., Sampayo, M. A., and Moita, M. T. (2001). On a *Lingulodinium polyedrum* bloom in Setúbal bay, Portugal. *Harmful Algal Blooms 2000.*, 133–136.
- Anderson, D. M., Fachon, E., Pickart, R. S., Lin, P., Fischer, A. D., Richlen, M. L., et al. (2021). Evidence for massive and recurrent toxic blooms of *Alexandrium catenella* in the Alaskan Arctic. *Proceedings of the National Academy of Sciences* 118, e2107387118. doi: 10.1073/pnas.2107387118
- Anderson, D. M., Jacobson, D. M., Bravo, I., and Wrenn, J. H. (1988). The unique, microreticulate cyst of the naked dinoflagellate *Gymnodinium catenatum*. *J. Phycol.* 24, 255–262. doi: 10.1111/j.1529-8817.1988.tb04241.x
- Anderson, D. M., and Keafer, B. A. (1987). An endogenous annual clock in the toxic marine dinoflagellate *Gonyaulax tamarensis*. *Nature* 325, 616–617. doi: 10.1038/325616a0
- Anderson, D. M., and Lindquist, N. L. (1985). Time-course measurements of phosphorus depletion and cyst formation in the dinoflagellate *Gonyaulax tamarensis* Lebour. *J. Exp. Mar. Bio. Ecol.* 86, 1–13. doi: 10.1016/0022-0981(85)90039-5
- Anderson, E. E., Wilson, C., Knap, A. H., and Villareal, T. A. (2018). Summer diatom blooms in the eastern North Pacific gyre investigated with a long-endurance autonomous surface vehicle. *PeerJ* 6, e5387. doi: 10.7717/peerj.5387
- Appleby, P. G., and Oldfield, F. (1978). The calculation of lead-210 dates assuming a constant rate of supply of unsupported  $^{210}\text{Pb}$  to the sediment. *Catena* 5, 1–8. doi: 10.1016/S0341-8162(78)80002-2
- Aristegui, J., Barton, E. D., Álvarez-Salgado, X. A., Santos, A. M. P., Figueiras, F. G., Kifani, S., et al. (2009). Sub-regional ecosystem variability in the Canary Current upwelling. *Prog. Oceanogr.* 83, 33–48. doi: 10.1016/j.pocean.2009.07.031
- Asper, V. L., and Smith, W. O., Jr (2019). Variations in the abundance and distribution of aggregates in the Ross Sea, Antarctica. *Elementa (Wash., DC)* 7, 23. doi: 10.1525/elementa.355
- Bae, S. W., Lee, K. E., Ko, T. W., Kim, R. A., and Park, Y.-G. (2022). Holocene centennial variability in sea surface temperature and linkage with solar irradiance. *Sci. Rep.* 12, 15046. doi: 10.1038/s41598-022-19050-6

- Balech, E. (1985). The genus *Alexandrium* or *Gonyaulax* of the *tamarensis* group. *Toxic Dinoflagellates*, 33–38. Available at: <https://ci.nii.ac.jp/naid/10004853601/>
- Beaulieu, S. (2002). Accumulation and fate of phytodetritus on the sea floor. *Oceanogr. Mar. Biol. Annu. Rev.* 40, 171–232. doi: 10.1201/9780203180594.ch4
- Ben-Ami, Y., Koren, I., and Altaratz, O. (2009). Patterns of North African dust transport over the Atlantic: winter vs. summer, based on CALIPSO first year data. *Atmos. Chem. Phys.* 9, 7867–7875. doi: 10.5194/acp-9-7867-2009
- Bijl, P. K. (2022). DINOSTRAT: a global database of the stratigraphic and paleolatitudinal distribution of Mesozoic–Cenozoic organic-walled dinoflagellate cysts. *Earth Syst. Sci. Data* 14, 579–617. doi: 10.5194/essd-14-579-2022
- Blanco, J. (1995). The distribution of dinoflagellate cysts along the Galician (NW Spain) coast. *J. Plankton Res.* 17, 283–302. doi: 10.1093/plankt/17.2.283
- Bogus, K., Mertens, K. N., Lauwaert, J., Harding, I. C., Vrielinck, H., Zonneveld, K. A. F., et al. (2014). Differences in the chemical composition of organic-walled dinoflagellate resting cysts from phototrophic and heterotrophic dinoflagellates. *J. Phycol.* 50, 254–266. doi: 10.1111/jpy.12170
- Bouimetarhan, I., Marret, F., Dupont, L., and Zonneveld, K. A. F. (2009). Dinoflagellate cyst distribution in marine surface sediments off West Africa (17–6 N) in relation to sea-surface conditions, freshwater input and seasonal coastal upwelling. *Marine Micropaleontology* 71, 113–130. doi: 10.1016/j.marmicro.2009.02.001
- Boyd, J. L., Riding, J. B., Pound, M. J., De Schepper, S., Ivanovic, R. F., Haywood, A. M., et al. (2018). The relationship between Neogene dinoflagellate cysts and global climate dynamics. *Earth-Sci. Rev.* 177, 366–385. doi: 10.1016/j.earscirev.2017.11.018
- Bravo, I., and Figueroa, R. (2014). Towards an ecological understanding of dinoflagellate cyst functions. *Microorganisms* 2, 11–32. doi: 10.3390/microorganisms2010011
- Bravo, I., Fraga, S., Isabel Figueroa, R., Pazos, Y., Massanet, A., and Ramilo, I. (2010). Bloom dynamics and life cycle strategies of two toxic dinoflagellates in a coastal upwelling system (NW Iberian Peninsula). *Deep Sea Res. Part 2 Top. Stud. Oceanogr.* 57, 222–234. doi: 10.1016/j.dsr2.2009.09.004
- Bringué, M., Pospelova, V., and Pak, D. (2013). Seasonal production of organic-walled dinoflagellate cysts in an upwelling system: A sediment trap study from the Santa Barbara Basin, California. *Mar. Micropaleontol.* 100, 34–51. doi: 10.1016/j.marmicro.2013.03.007
- Bringué, M., Pospelova, V., Tappa, E. J., and Thunell, R. C. (2019). Dinoflagellate cyst production in the Cariaco Basin: A 12.5 year-long sediment trap study. *Prog. Oceanogr.* 171, 175–211. doi: 10.1016/j.pocean.2018.12.007
- Bringué, M., Thunell, R. C., Pospelova, V., Pinckney, J. L., Romero, O. E., and Tappa, E. J. (2018). Physico-chemical and biological factors influencing dinoflagellate cyst production in the Cariaco Basin. *Biogeosciences* 15, 2325–2348. doi: 10.5194/bg-15-2325-2018
- Brosnahan, M. L., Fischer, A. D., Lopez, C. B., Moore, S. K., and Anderson, D. M. (2020). Cyst-forming dinoflagellates in a warming climate. *Harmful Algae* 91, 101728. doi: 10.1016/j.hal.2019.101728
- Carr, M.-E. (2001). Estimation of potential productivity in Eastern Boundary Currents using remote sensing. *Deep Sea Res. Part 2 Top. Stud. Oceanogr.* 49, 59–80. doi: 10.1016/S0967-0645(01)00094-7
- Cazelles, B., Chavez, M., Berteaux, D., Ménard, F., Vik, J. O., Jenouvrier, S., et al. (2008). Wavelet analysis of ecological time series. *Oecologia* 156, 287–304. doi: 10.1007/s00442-008-0993-2

- Chen, C.-C., Shiah, F.-K., Gong, G.-C., and Chen, T.-Y. (2021). Impact of upwelling on phytoplankton blooms and hypoxia along the Chinese coast in the East China Sea. *Mar. Pollut. Bull.* 167, 112288. doi: 10.1016/j.marpolbul.2021.112288
- Chouza, F., Reitebuch, O., Benedetti, A., and Weinzierl, B. (2016). Saharan dust long-range transport across the Atlantic studied by an airborne Doppler wind lidar and the MACC model. *Atmos. Chem. Phys.* 16, 11581–11600. doi: 10.5194/acp-16-11581-2016
- Cohen, M. X. (2019). A better way to define and describe Morlet wavelets for time-frequency analysis. *Neuroimage* 199, 81–86. doi: 10.1016/j.neuroimage.2019.05.048
- Cohen, N. R., McIlvin, M. R., Moran, D. M., Held, N. A., Saunders, J. K., Hawco, N. J., et al. (2021). Dinoflagellates alter their carbon and nutrient metabolic strategies across environmental gradients in the central Pacific Ocean. *Nat Microbiol* 6, 173–186. doi: 10.1038/s41564-020-00814-7
- Costa, P. R., Robertson, A., and Quilliam, M. A. (2015). Toxin profile of *Gymnodinium catenatum* (Dinophyceae) from the Portuguese coast, as determined by liquid chromatography tandem mass spectrometry. *Mar. Drugs* 13, 2046–2062. doi: 10.3390/md13042046
- Cropper, T. E., Hanna, E., and Bigg, G. R. (2014). Spatial and temporal seasonal trends in coastal upwelling off Northwest Africa, 1981–2012. *Deep Sea Res. Part I* 86, 94–111. doi: 10.1016/j.dsr.2014.01.007
- Dale, B. (1976). Cyst formation, sedimentation, and preservation: Factors affecting dinoflagellate assemblages in recent sediments from Trondheimsfjord, Norway. *Rev. Palaeobot. Palynol.* 22, 39–60. doi: 10.1016/0034-6667(76)90010-5
- Dale, B. (1996). Dinoflagellate cyst ecology: modeling and geological applications. *Palynology: Principles and Applications*, 1249–1275. Available at: <https://ci.nii.ac.jp/naid/10006327854/>
- Dale, B., Dale, A. L., and Jansen, J. H. F. (2002). Dinoflagellate cysts as environmental indicators in surface sediments from the Congo deep-sea fan and adjacent regions. *Palaeogeogr. Palaeoclimatol. Palaeoecol.* 185, 309–338. doi: 10.1016/S0031-0182(02)00380-2
- Dale, B., and Dale, B. (1992). “Dinoflagellate contributions to the open ocean sediment flux,” in *Dinoflagellate contributions to the deep sea*, (Woods Hole Oceanographic Institution Woods Hole), 45–73. Available at: <https://pdfs.semanticscholar.org/df07/b08fc5a00d579ad1da0ef15019b294b834d4.pdf#page=9>
- Daly, K. L., and Smith, W. O. (1993). Physical-biological interactions influencing marine plankton production. *Annu. Rev. Ecol. Syst.* 24, 555–585. doi: 10.1146/annurev.es.24.110193.003011
- de Vernal, A., Radi, T., Zaragosi, S., Van Nieuwenhove, N., Rochon, A., Allan, E., et al. (2020). Distribution of common modern dinoflagellate cyst taxa in surface sediments of the Northern Hemisphere in relation to environmental parameters: The new n= 1968 database. *Mar. Micropaleontol.* 159, 101796. doi: 10.1016/j.marmicro.2019.101796
- de Garidel-Thoron, T., Chaabane, S., Giraud, X., Meilland, J., Jonkers, L., Kucera, M., et al. (2022). The foraminiferal response to climate stressors project: tracking the community response of planktonic foraminifera to historical climate change. *Frontiers in Marine Science* 9. doi: 10.3389/fmars.2022.827962
- Delebecq, G., Schmidt, S., Ehrhold, A., Latimier, M., and Siano, R. (2020). Revival of ancient marine dinoflagellates using molecular biostimulation. *J. Phycol.* 56, 1077–1089. doi: 10.1111/jpy.13010

- Doherty, O. M., Riemer, N., and Hameed, S. (2014). Role of the convergence zone over West Africa in controlling Saharan mineral dust load and transport in the boreal summer. *Tellus B Chem. Phys. Meteorol.* 66, 23191. doi: 10.3402/tellusb.v66.23191
- Duarte, C. M., Dachs, J., Llabrés, M., Alonso-Laita, P., Gasol, J. M., Tovar-Sánchez, A., et al. (2006). Aerosol inputs enhance new production in the subtropical northeast Atlantic. *J. Geophys. Res.* 111. doi: 10.1029/2005jg000140
- Elbrächter, M., Gottschling, M., Hoppenrath, M., Keupp, H., Kusber, W.-H., Streng, M., et al. (2023). (258–260) Proposals to eliminate contradiction between Articles 11.7 and 11.8 and to equate non-fossil with fossil names of dinophytes for purposes of priority. *Taxon* 72, 258–260. doi: 10.1002/tax.12947
- Ellegaard, M., and Moestrup, Ø (1999). Fine structure of the flagellar apparatus and morphological details of *Gymnodinium nolleri* sp. nov. (Dinophyceae), an unarmored dinoflagellate producing a microreticulate cyst. *Phycologia* 38, 289–300. doi: 10.2216/i0031-8884-38-4-289.1
- Ellegaard, M., and Ribeiro, S. (2018). The long-term persistence of phytoplankton resting stages in aquatic “seed banks.” *Biol. Rev. Camb. Philos. Soc.* 93, 166–183. doi: 10.1111/brv.12338
- Elshanawany, R., and Zonneveld, K. A. F. (2016). Dinoflagellate cyst distribution in the oligotrophic environments of the Gulf of Aqaba and northern Red Sea. *Mar. Micropaleontol.* 124, 29–44. doi: 10.1016/j.marmicro.2016.01.003
- Elshanawany, R., Zonneveld, K., Ibrahim, M. I., and Kholeif, S. E. A. (2010). Distribution patterns of recent organic-walled dinoflagellate cysts in relation to environmental parameters in the Mediterranean Sea. *Palynology* 34, 233–260. doi: 10.1080/01916121003711665
- Erickson, D. J., III, Hernandez, J. L., Ginoux, P., Gregg, W. W., McClain, C., and Christian, J. (2003). Atmospheric iron delivery and surface ocean biological activity in the Southern Ocean and Patagonian region. *Geophys. Res. Lett.* 30. doi: 10.1029/2003gl017241
- Falkowski, P. (2012). Ocean Science: The power of plankton. *Nature* 483, S17–20. doi: 10.1038/483S17a
- Faye, S., Lazar, A., Sow, B., and Gaye, A. (2015). A model study of the seasonality of sea surface temperature and circulation in the Atlantic North-eastern Tropical Upwelling System. *Frontiers in Physics* 3. doi: 10.3389/fphy.2015.00076
- Fensome, R. A., MacRae, R. A., Moldowan, J. M., Taylor, F. J. R., and Williams, G. L. (1996). The early Mesozoic radiation of dinoflagellates. *Paleobiology* 22, 329–338. doi: 10.1017/S0094837300016316
- Fensome, R. A., Taylor, F. J. R., Norris, G., Sarjeant, W. A. S., Wharton, D. I., and Williams, D. L. (1993). *A Classification of Living and Fossil Dinoflagellates*. American Museum of Natural History. Available at: <https://play.google.com/store/books/details?id=nG8yRAAACAAJ>
- Figueroa, R. I., and Bravo, I. (2005). Sexual reproduction and two different encystment strategies of *Lingulodinium polyedrum* (Dinophyceae) in culture1. *J. Phycol.* 41, 370–379. doi: 10.1111/j.1529-8817.2005.04150.x
- Figueroa, R. I., Estrada, M., and Garcés, E. (2018). Life histories of microalgal species causing harmful blooms: Haploids, diploids and the relevance of benthic stages. *Harmful Algae* 73, 44–57. doi: 10.1016/j.hal.2018.01.006
- Fischer, G., and Karakaş, G. (2009). Sinking rates and ballast composition of particles in the Atlantic Ocean: implications for the organic carbon fluxes to the deep ocean. *Biogeosciences* 6, 85–102. doi: 10.5194/bg-6-85-2009

- Fischer, G., Reuter, C., Karakas, G., Nowald, N., and Wefer, G. (2009). Offshore advection of particles within the Cape Blanc filament, Mauritania: Results from observational and modelling studies. *Prog. Oceanogr.* 83, 322–330. doi: 10.1016/j.pocean.2009.07.023
- Fischer, G., Romero, O., Merkel, U., Donner, B., Iversen, M., Nowald, N., et al. (2016). Deep ocean mass fluxes in the coastal upwelling off Mauritania from 1988 to 2012: variability on seasonal to decadal timescales. *Biogeosciences* 13, 3071–3090. doi: 10.5194/bg-13-3071-2016
- Fischer, G., Romero, O., Toby, E., Iversen, M., Donner, B., Mollenhauer, G., et al. (2019). Changes in the dust-influenced biological carbon pump in the canary current system: Implications from a coastal and an offshore sediment trap record off cape Blanc, Mauritania. *Global Biogeochem. Cycles* 33, 1100–1128. doi: 10.1029/2019gb006194
- Friese, C. A., van Hateren, J. A., Vogt, C., Fischer, G., and Stuut, J.-B. W. (2017). Seasonal provenance changes in present-day Saharan dust collected in and off Mauritania. *Atmos. Chem. Phys.* 17, 10163–10193. doi: 10.5194/acp-17-10163-2017
- Fomba, K. W., Müller, K., van Pinxteren, D., Poulain, L., van Pinxteren, M., and Herrmann, H. (2014). Long-term chemical characterization of tropical and marine aerosols at the Cape Verde Atmospheric Observatory (CVAO) from 2007 to 2011. *Atmospheric Climate and Physics*. 14, 8883–8904. doi: 10.5194/acp-14-8883-2014
- Fowles, V. (2020). Sea-questration: the effects of marine iron fertilization on phytoplankton carbon uptake in the Southern Ocean. *Canadian Jour. of Undergrad. Research*. 5. Available at: [https://cjur.ca/wp-content/uploads/2020/09/5-1\\_A4.pdf](https://cjur.ca/wp-content/uploads/2020/09/5-1_A4.pdf)
- Fraga, S., Rodríguez, F., Bravo, I., Zapata, M., and Marañón, E. (2012). Review of the main ecological features affecting benthic dinoflagellate blooms. *Cryptogam. Algal.* 33, 171–179. doi: 10.7872/crya.v33.iss2.2011.171
- Francis, T. B., Scheuerell, M. D., Brodeur, R. D., Levin, P. S., Ruzicka, J. J., Tolimieri, N., et al. (2012). Climate shifts the interaction web of a marine plankton community. *Glob. Chang. Biol.* 18, 2498–2508. doi: 10.1111/j.1365-2486.2012.02702.x
- Fritsch, F. N., and Carlson, R. E. (1980). Monotone Piecewise Cubic Interpolation. *SIAM J. Numer. Anal.* 17, 238–246. doi: 10.1137/0717021
- Fujii, R., and Matsuoka, K. (2006). Seasonal change of dinoflagellates cyst flux collected in a sediment trap in Omura Bay, West Japan. *J. Plankton Res.* 28, 131–147. doi: 10.1093/plankt/fbi106
- García-Moreiras, I., Amorim, A., and Zonneveld, K. (2024). Transport and preservation of calcareous and organic-walled dinoflagellate cysts off Cape Blanc (NW Africa) in relation to nepheloid layers. *Mar. Environ. Res.*, 106577. doi: 10.1016/j.marenvres.2024.106577
- García-Moreiras, I., Oliveira, A., Santos, A. I., Oliveira, P. B., and Amorim, A. (2021). Environmental Factors Affecting Spatial Dinoflagellate Cyst Distribution in Surface Sediments Off Aveiro-Figueira da Foz (Atlantic Iberian Margin). *Frontiers in Marine Science* 8. doi: 10.3389/fmars.2021.699483
- García-Moreiras, I., Vila Costas, S., García-Gil, S., and Muñoz Sobrino, C. (2023). Organic-walled dinoflagellate cyst assemblages in surface sediments of the Ría de Vigo (Atlantic margin of NW Iberia) in relation to environmental gradients. *Mar. Micropaleontol.* 180, 102217. doi: 10.1016/j.marmicro.2023.102217
- Gómez, F. (2012). A quantitative review of the lifestyle, habitat and trophic diversity of dinoflagellates (Dinoflagellata, Alveolata). *System. Biodivers.* 10, 267–275. doi: 10.1080/14772000.2012.721021

- Gómez-Letona, M., Ramos, A. G., Coca, J., and Arístegui, J. (2017). Trends in primary production in the Canary Current upwelling system - a regional perspective comparing remote sensing models. *Frontiers in Marine Science* 4. doi: 10.3389/fmars.2017.00370
- Grange, S. K. (2014). Technical report: Averaging wind speeds and directions. 12. doi: 10.13140/RG.2.1.3349.2006
- Gray, D. D., Zonneveld, K. A. F., and Versteegh, G. J. M. (2017). Species-specific sensitivity of dinoflagellate cysts to aerobic degradation: A five-year natural exposure experiment. *Rev. Palaeobot. Palynol.* 247, 175–187. doi: 10.1016/j.revpalbo.2017.09.002
- Gribble, K. E., and Nolan, G. (2007). Biodiversity, biogeography and potential trophic impact of *Protoperdinium* spp. (Dinophyceae) off the southwestern coast of Ireland. *J. Plankton Res.* 29, 931–947. doi: 10.1093/plankt/fbm070
- Gutleben, M., Groß, S., Heske, C., and Wirth, M. (2022). Wintertime Saharan dust transport towards the Caribbean: an airborne lidar case study during EUREC<sup>4</sup>A. *Atmos. Chem. Phys.* 22, 7319–7330. doi: 10.5194/acp-22-7319-2022
- Hagen, E. (2001). Northwest African upwelling scenario. *Oceanol. Acta* 24, 113–128. doi: 10.1016/S0399-1784(00)01110-5
- Hammer, Ø., Harper, D. A. T., and Ryan, P. D. (2001). Paleontological statistics software: package for education and data analysis. *Palaeontol. Electronica*. Available at: <http://www.forskningssdatabasen.dk/en/catalog/2192867784>
- Hanebuth, T. J. J., and Henrich, R. (2009). Recurrent decadal-scale dust events over Holocene western Africa and their control on canyon turbidite activity (Mauritania). *Quat. Sci. Rev.* 28, 261–270. doi: 10.1016/j.quascirev.2008.09.024
- Hansen, P. J. (2011). The role of photosynthesis and food uptake for the growth of marine mixotrophic dinoflagellates. *J. Eukaryot. Microbiol.* 58, 203–214. doi: 10.1111/j.1550-7408.2011.00537.x
- Harland, R., and Pudsey, C. J. (1999). Dinoflagellate cysts from sediment traps deployed in the Bellingshausen, Weddell and Scotia seas, Antarctica. *Mar. Micropaleontol.* 37, 77–99. doi: 10.1016/S0377-8398(99)00016-X
- Head, M. J. (1996). “Modern dinoflagellate cysts and their biological affinities,” in *Palynology: Principles and Applications*, eds. J. Jansonius and D. C. McGregor (American Association of Stratigraphic Palynologists), 1197–1248. Available at: [https://www.researchgate.net/profile/Martin-Head/publication/259866107\\_Modern\\_dinoflagellate\\_cysts\\_and\\_their\\_biological\\_affinities/links/546d02180cf2193b94c57cb2/Modern-dinoflagellate-cysts-and-their-biological-affinities.pdf](https://www.researchgate.net/profile/Martin-Head/publication/259866107_Modern_dinoflagellate_cysts_and_their_biological_affinities/links/546d02180cf2193b94c57cb2/Modern-dinoflagellate-cysts-and-their-biological-affinities.pdf)
- Head, M. J. (2003). *Echinidinium zonneveldiae* sp. nov., a dinoflagellate cyst from the Late Pleistocene of the Baltic Sea, northern Europe. *Journal of Micropalaeontology* 21, 169–173. doi: 10.1144/jm.21.2.169
- Heikkilä, M., Pospelova, V., Forest, A., Stern, G. A., Fortier, L., and Macdonald, R. W. (2016). Dinoflagellate cyst production over an annual cycle in seasonally ice-covered Hudson Bay. *Mar. Micropaleontol.* 125, 1–24. doi: 10.1016/j.marmicro.2016.02.005
- Henrich, R., Hanebuth, T. J. J., Krastel, S., Neubert, N., and Wynn, R. B. (2008). Architecture and sediment dynamics of the Mauritania Slide Complex. *Mar. Pet. Geol.* 25, 17–33. doi: 10.1016/j.marpetgeo.2007.05.008
- Henson, S. A., Cael, B. B., Allen, S. R., and Dutkiewicz, S. (2021). Future phytoplankton diversity in a changing climate. *Nat. Commun.* 12, 5372. doi: 10.1038/s41467-021-25699-w

- Hernández, M., Robinson, I., Aguilar, A., González, L. M., López-Jurado, L. F., Reyero, M. I., et al. (1998). Did algal toxins cause monk seal mortality? *Nature* 393, 28–29. doi: 10.1038/29906
- Holmes, M. J., and Teo, S. L. M. (2002). Toxic marine dinoflagellates in Singapore waters that cause seafood poisonings. *Clin. Exp. Pharmacol. Physiol.* 29, 829–836. doi: 10.1046/j.1440-1681.2002.03724.x
- Holzwarth, U., Esper, O., and Zonneveld, K. (2007). Distribution of organic-walled dinoflagellate cysts in shelf surface sediments of the Benguela upwelling system in relationship to environmental conditions. *Mar. Micropaleontol.* 64, 91–119. doi: 10.1016/j.marmicro.2007.04.001
- Huneeus, N., Schulz, M., Balkanski, Y., Griesfeller, J., Prospero, J., Kinne, S., et al. (2011). Global dust model intercomparison in AeroCom phase I. *Atmos. Chem. Phys.* 11, 7781–7816. doi: 10.5194/acp-11-7781-2011
- Iversen, M. H., and Ploug, H. (2013). Temperature effects on carbon-specific respiration rate and sinking velocity of diatom aggregates – potential implications for deep ocean export processes. *Biogeosciences* 10, 4073–4085. doi: 10.5194/bg-10-4073-2013
- Inthorn, M., Mohrholz, V., and Zabel, M. (2006). Nepheloid layer distribution in the Benguela upwelling area offshore Namibia. *Deep Sea Res. Part I* 53, 1423–1438. doi: 10.1016/j.dsr.2006.06.004
- Jacobson, D. M., and Anderson, D. M. (1986). Thecate heterotrophic dinoflagellates: Feeding behavior and mechanisms. *J. Phycol.* 22, 249–258. doi: 10.1111/j.1529-8817.1986.tb00021.x
- Jensen, O., Spaak, E., and Zumer, J. M. (2014). “Human Brain Oscillations: From Physiological Mechanisms to Analysis and Cognition,” in *Magnetoencephalography: From Signals to Dynamic Cortical Networks*, eds. S. Supek and C. J. Aine (Berlin, Heidelberg: Springer Berlin Heidelberg), 359–403. doi: 10.1007/978-3-642-33045-2\_17
- Jeong, H. J. (1999). The ecological roles of heterotrophic dinoflagellates in marine planktonic community. *J. Eukaryot. Microbiol.* 46, 390–396. doi: 10.1111/j.1550-7408.1999.tb04618.x
- Jeong, H. J., Yoo, Y. D., Kim, J. S., Seong, K. A., Kang, N. S., and Kim, T. H. (2010). Growth, feeding and ecological roles of the mixotrophic and heterotrophic dinoflagellates in marine planktonic food webs. *Ocean Sci. J.* 45, 65–91. doi: 10.1007/s12601-010-0007-2
- Jickells, T. D., An, Z. S., Andersen, K. K., Baker, A. R., Bergametti, G., Brooks, N., et al. (2005). Global iron connections between desert dust, ocean biogeochemistry, and climate. *Science* 308, 67–71. doi: 10.1126/science.1105959
- Jiao, N., Zhang, Y., Zhou, K., Li, Q., Dai, M., Liu, J., et al. (2014). Revisiting the CO<sub>2</sub> “source” problem in upwelling areas – a comparative study on eddy upwellings in the South China Sea. *Biogeosciences* 11, 2465–2475. doi: 10.5194/BG-11-2465-2014
- Juranek, L. W., White, A. E., Dugenne, M., Henderikx Freitas, F., Dutkiewicz, S., Ribalet, F., et al. (2020). The importance of the phytoplankton “middle class” to ocean net community production. *Global Biogeochem. Cycles* 34. doi: 10.1029/2020gb006702
- Karakaş, G., Nowald, N., Blaas, M., Marchesiello, P., Frickenhaus, S., and Schlitzer, R. (2006). High-resolution modeling of sediment erosion and particle transport across the northwest African shelf. *J. Geophys. Res.* 111. doi: 10.1029/2005jc003296
- Karakaş, G., Nowald, N., Schäfer-Neth, C., Iversen, M., Barkmann, W., Fischer, G., et al. (2009). Impact of particle aggregation on vertical fluxes of organic matter. *Prog. Oceanogr.* 83, 331–341. doi: 10.1016/j.pocean.2009.07.047



- Kodrans-Nsiah, M., de Lange, G. J., and Zonneveld, K. A. F. (2008). A natural exposure experiment on short-term species-selective aerobic degradation of dinoflagellate cysts. *Rev. Palaeobot. Palynol.* 152, 32–39. doi: 10.1016/j.revpalbo.2008.04.002
- Kok, J. F., Adebisi, A. A., Albani, S., Balkanski, Y., Checa-Garcia, R., Chin, M., et al. (2021). Contribution of the world's main dust source regions to the global cycle of desert dust. *Atmos. Chem. Phys.* 21, 8169–8193. doi: 10.5194/acp-21-8169-2021
- Kolber, Z. S., Barber, R. T., Coale, K. H., Fitzwater, S. E., Greene, R. M., Johnson, K. S., et al. (1994). Iron limitation of phytoplankton photosynthesis in the equatorial Pacific Ocean. *Nature* 371, 145–149. doi: 10.1038/371145a0
- Kremling, K., Lentz, U., and Zeitzschel, B. (1996). New type of time-series sediment trap for the reliable collection of inorganic and organic trace chemical substances. *Review of Scientific.* doi: 10.1063/1.1147582
- Kremp, A., Oja, J., LeTortorec, A. H., Hakanen, P., Tahvanainen, P., Tuimala, J., et al. (2016). Diverse seed banks favour adaptation of microalgal populations to future climate conditions. *Environ. Microbiol.* 18, 679–691. doi: 10.1111/1462-2920.13070
- Krupke, A., Mohr, W., LaRoche, J., Fuchs, B. M., Amann, R. I., and Kuypers, M. M. M. (2015). The effect of nutrients on carbon and nitrogen fixation by the UCYN-A-haptophyte symbiosis. *ISME J.* 9, 1635–1647. doi: 10.1038/ismej.2014.253
- Langlois, R. J., Mills, M. M., Ridame, C., Croot, P., and LaRoche, J. (2012). Diazotrophic bacteria respond to Saharan dust additions. *Mar. Ecol. Prog. Ser.* 470, 1–14. doi: 10.3354/meps10109
- Lathuilière, C., Echevin, V., and Lévy, M. (2008). Seasonal and intraseasonal surface chlorophyll-a variability along the northwest African coast. *J. Geophys. Res.* 113. doi: 10.1029/2007jc004433
- Lepot, M., Aubin, J.-B., and Clemens, F. H. L. R. (2017). Interpolation in Time Series: An Introductory Overview of Existing Methods, Their Performance Criteria and Uncertainty Assessment. *Water* 9, 796. doi: 10.3390/w9100796
- Leroy, S. A. G., Lahijani, H. A. K., Reyss, J.-L., Chalié, F., Haghani, S., Shah-Hosseini, M., et al. (2013). A two-step expansion of the dinocyst *Lingulodinium machaerophorum* in the Caspian Sea: the role of changing environment. *Quat. Sci. Rev.* 77, 31–45. doi: 10.1016/j.quascirev.2013.06.026
- Lewis, J. (1988). Cysts and sediments: *Gonyaulax machaerophorum* (*Lingulodinium machaerophorum*) in Loch Creran. *J. Mar. Biol. Assoc. U. K.* 68, 701–714. doi: 10.1017/S0025315400028812
- Li, Z., Mertens, K. N., Gottschling, M., Gu, H., Söhner, S., Price, A. M., et al. (2020). Taxonomy and molecular phylogenetics of Ensiculiferaceae, fam. nov. (Peridinales, Dinophyceae), with consideration of their life-history. *Protist* 171, 125759. doi: 10.1016/j.protis.2020.125759
- Likumahua, S., Sangiorgi, F., de Boer, M. K., Tatipatta, W. M., Pelasula, D. D., Polnaya, D., et al. (2021). Dinoflagellate cyst distribution in surface sediments of Ambon Bay (eastern Indonesia): Environmental conditions and harmful blooms. *Mar. Pollut. Bull.* 166, 112269. doi: 10.1016/j.marpolbul.2021.112269
- Limoges, A., Kieft, J.-F., Radi, T., Ruiz-Fernandez, A. C., and de Vernal, A. (2010). Dinoflagellate cyst distribution in surface sediments along the south-western Mexican coast (14.76° N to 24.75°N). *Mar. Micropaleontol.* 76, 104–123. doi: 10.1016/j.marmicro.2010.06.003
- Liu, M., Gu, H., Krock, B., Luo, Z., and Zhang, Y. (2020). Toxic dinoflagellate blooms of *Gymnodinium catenatum* and their cysts in Taiwan Strait and their relationship to global populations. *Harmful Algae* 97, 101868. doi: 10.1016/j.hal.2020.101868

- Liu, L., Wei, N., Gou, Y., Li, D., Liang, Y., Xu, D., et al. (2017). Seasonal variability of *Protoceratium reticulatum* and yessotoxins in Japanese scallop *Patinopecten yessoensis* in northern Yellow Sea of China. *Toxicon* 139, 31–40. doi: 10.1016/j.toxicon.2017.09.015
- Lohan, M. C., and Tagliabue, A. (2018). Oceanic micronutrients: trace metals that are essential for marine life. *Elements* 14, 385–390. doi: 10.2138/gselements.14.6.385
- Loubere, P. (1989). Bioturbation and sedimentation rate control of benthic microfossil taxon abundances in surface sediments: A theoretical approach to the analysis of species microhabitats. *Mar. Micropaleontol.* 14, 317–325. doi: 10.1016/0377-8398(89)90016-9
- Lu, X., Wang, Z., Guo, X., Gu, Y., Liang, W., and Liu, L. (2017). Impacts of metal contamination and eutrophication on dinoflagellate cyst assemblages along the Guangdong coast of southern China. *Mar. Pollut. Bull.* 120, 239–249. doi: 10.1016/j.marpolbul.2017.05.032
- Lundholm, N., Ribeiro, S., Andersen, T. J., Koch, T., Godhe, A., Ekelund, F., et al. (2011). Buried alive – germination of up to a century-old marine protist resting stages. *Phycologia* 50, 629–640. doi: 10.2216/11-16.1
- Luo, Z., Mertens, K. N., Nézan, E., Gu, L., Pospelova, V., Thoha, H., et al. (2019). Morphology, ultrastructure and molecular phylogeny of cyst-producing *Caladoa arcachonensis* gen. et sp. nov. (Peridinales, Dinophyceae) from France and Indonesia. *Eur. J. Phycol.* 54, 235–248. doi: 10.1080/09670262.2018.1558287
- Maloney, E. D., and Shaman, J. (2008). Intraseasonal variability of the West African Monsoon and Atlantic ITCZ. *J. Clim.* 21, 2898–2918. doi: 10.1175/2007JCLI1999.1
- Mamalakis, A., Randerson, J. T., Yu, J.-Y., Pritchard, M. S., Magnusdottir, G., Smyth, P., et al. (2021). Zonally contrasting shifts of the tropical rainbelt in response to climate change. *Nat. Clim. Chang.* 11, 143–151. doi: 10.1038/s41558-020-00963-x
- Marret, F., Bradley, L., de Vernal, A., Hardy, W., Kim, S.-Y., Mudie, P., et al. (2020). From bipolar to regional distribution of modern dinoflagellate cysts, an overview of their biogeography. *Mar. Micropaleontol.* 159, 101753. doi: 10.1016/j.marmicro.2019.101753
- Marret, F., and Zonneveld, K. A. F. (2003). Atlas of modern organic-walled dinoflagellate cyst distribution. *Rev. Palaeobot. Palynol.* 125, 1–200. doi: 10.1016/S0034-6667(02)00229-4
- Matsuoka, K. (1985). Archeopyle structure in modern gymnodinial dinoflagellate cysts. *Rev. Palaeobot. Palynol.* 44, 217–231. doi: 10.1016/0034-6667(85)90017-X
- Matsuoka, K., and Head, M. J. (2013). “Clarifying cyst–motile stage relationships in dinoflagellates,” in *Biological and Geological Perspectives of Dinoflagellates*, eds. J. M. Lewis, F. Marret, and L. Bradley (The Micropalaeontological Society, Special Publications. Geological Society, London), 325–350. Available at: [https://books.google.com/books?hl=en&lr=&id=bu6lt7114NQC&oi=fnd&pg=PA325&dq=Clarifying+cyst+motile+stage+relationships+in+dinoflagellates&ots=kDhA8DaUkO&sig=c3Jgk1Ek47\\_qG8EZ4\\_ZUIDWnQTc](https://books.google.com/books?hl=en&lr=&id=bu6lt7114NQC&oi=fnd&pg=PA325&dq=Clarifying+cyst+motile+stage+relationships+in+dinoflagellates&ots=kDhA8DaUkO&sig=c3Jgk1Ek47_qG8EZ4_ZUIDWnQTc)
- Matthiessen, J., Schreck, M., De Schepper, S., Zorzi, C., and de Vernal, A. (2018). Quaternary dinoflagellate cysts in the Arctic Ocean: Potential and limitations for stratigraphy and paleoenvironmental reconstructions. *Quat. Sci. Rev.* 192, 1–26. doi: 10.1016/j.quascirev.2017.12.020
- McRae, R. A., Fensome, R. A., and Williams, G. L. (1996). Fossil dinoflagellate diversity, originations, and extinctions and their significance. *Can. J. Bot.* 74, 1687–1694. doi: 10.1139/b96-205
- Menden-Deuer, S., Lessard, E. J., Satterberg, J., and Grünbaum, D. (2005). Growth rates and starvation survival of three species of the pallium-feeding, thecate dinoflagellate genus *Protoperidinium*. *Aquat. Microb. Ecol.* 41, 145–152. doi: 10.3354/ame041145

- Mertens, K. N., Gu, H., Gurdebeke, P. R., Takano, Y., Clarke, D., Aydin, H., et al. (2020). A review of rare, poorly known, and morphologically problematic extant marine organic-walled dinoflagellate cyst taxa of the orders Gymnodiniales and Peridinales from the Northern Hemisphere. *Mar. Micropaleontol.* 159, 101773. doi: 10.1016/j.marmicro.2019.101773
- Meunier, T., Barton, E. D., Barreiro, B., and Torres, R. (2012). Upwelling filaments off Cap Blanc: Interaction of the NW African upwelling current and the Cape Verde frontal zone eddy field? *J. Geophys. Res. C: Oceans* 117. doi: 10.1029/2012JC007905
- Meyvisch, P., Mertens, K. N., Gurdebeke, P. R., Sandt, C., Pospelova, V., Vrielinck, H., et al. (2023). Does dinocyst wall composition really reflect trophic affinity? New evidence from ATR micro-FTIR spectroscopy measurements. *J. Phycol.* doi: 10.1111/jpy.13382
- Mittelstaedt, E. (1983). The upwelling area off Northwest Africa—A description of phenomena related to coastal upwelling. *Prog. Oceanogr.* 12, 307–331. doi: 10.1016/0079-6611(83)90012-5
- Mittelstaedt, E. (1991). The ocean boundary along the northwest African coast: Circulation and oceanographic properties at the sea surface. *Prog. Oceanogr.* 26, 307–355. doi: 10.1016/0079-6611(91)90011-A
- Mollenhauer, G., Basse, A., Kim, J.-H., Damste, J. S. S., and Fischer, G. (2015). A four-year record of UK' 37-and TEX86-derived sea surface temperature estimates from sinking particles in the filamentous upwelling region off Cape Blanc, Mauritania. *Deep Sea Res. Part I* 97, 67–79. doi: 10.1016/j.dsr.2014.11.015
- Montero-Serra, I., Garrabou, J., Doak, D. F., Ledoux, J., and Linares, C. (2019). Marine protected areas enhance structural complexity but do not buffer the consequences of ocean warming for an overexploited precious coral. *J. Appl. Ecol.* 56, 1063–1074. doi: 10.1111/1365-2664.13321
- Mora, C., Metzger, R., Rollo, A., and Myers, R. A. (2007). Experimental simulations about the effects of overexploitation and habitat fragmentation on populations facing environmental warming. *Proc. Biol. Sci.* 274, 1023–1028. doi: 10.1098/rspb.2006.0338
- Morquecho, L. (2019). *Pyrodinium bahamense* one the most significant harmful dinoflagellate in Mexico. *Frontiers in Marine Science* 6. doi: 10.3389/fmars.2019.00001
- Morrill, L. C., and Loeblich, A. R., 3rd (1983). Ultrastructure of the dinoflagellate amphiesma. *Int. Rev. Cytol.* 82, 151–180. doi: 10.1016/s0074-7696(08)60825-6
- Mudie, P. J., Marret, F., Mertens, K. N., Shumilovskikh, L., and Leroy, S. A. G. (2017). Atlas of modern dinoflagellate cyst distributions in the Black Sea Corridor: from Aegean to Aral Seas, including Marmara, Black, Azov and Caspian Seas. *Mar. Micropaleontol.* 134, 1–152. doi: 10.1016/j.marmicro.2017.05.004
- Naujokaitis-Lewis, I., and Fortin, M.-J. (2016). Spatio-temporal variation of biotic factors underpins contemporary range dynamics of congeners. *Glob. Chang. Biol.* 22, 1201–1213. doi: 10.1111/gcb.13145
- Naustvoll, L.-J. (2000). Prey size spectra and food preferences in thecate heterotrophic dinoflagellates. *Phycologia* 39, 187–198. doi: 10.2216/i0031-8884-39-3-187.1
- Nicholson, S. E. (2018). The ITCZ and the Seasonal Cycle over Equatorial Africa. *Bull. Am. Meteorol. Soc.* 99, 337–348. doi: 10.1175/BAMS-D-16-0287.1
- Nooteboom, P. D., Bijl, P. K., van Sebille, E., and von der Heydt, A. S. (2019). Transport bias by ocean currents in sedimentary microplankton assemblages: Implications for paleoceanographic reconstructions. *Paleoceanography and Paleoclimatology* 34, 1178–1194. doi: 10.1029/2019PA003606

- Obrezkova, M. S., Pospelova, V., and Kolesnik, A. N. (2023). Diatom and dinoflagellate cyst distribution in surface sediments of the Chukchi Sea in relation to the upper water masses. *Mar. Micropaleontol.* 178, 102184. doi: 10.1016/j.marmicro.2022.102184
- Olivar, M. P., Sabatés, A., Pastor, M. V., and Pelegrí, J. L. (2016). Water masses and mesoscale control on latitudinal and cross-shelf variations in larval fish assemblages off NW Africa. *Deep Sea Res. Part I* 117, 120–137. doi: 10.1016/j.dsr.2016.10.003
- Pauly, D., and Christensen, V. (1995). Primary production required to sustain global fisheries. *Nature* 374, 255–257. doi: 10.1038/374255a0
- Pérez-Asensio, J. N., Aguirre, J., and Rodríguez-Tovar, F. J. (2017). The effect of bioturbation by polychaetes (Opheliidae) on benthic foraminiferal assemblages and test preservation. *Palaeontology* 60, 807–827. doi: 10.1111/pala.12317
- Persson, A., and Smith, B. C. (2022). Preservation of dinoflagellate cysts in different oxygen regimes: Differences in cyst survival between oxic and anoxic natural environments. *Phycology* 2, 384–418. doi: 10.3390/phycolgy2040022
- Petihakis, G., Perivoliotis, L., Korres, G., Ballas, D., Frangoulis, C., Pagonis, P., et al. (2018). An integrated open-coastal biogeochemistry, ecosystem and biodiversity observatory of the eastern Mediterranean – the Cretan Sea component of the POSEIDON system. *Ocean Science* 14, 1223–1245. doi: 10.5194/os-14-1223-2018
- Picado, A., Vaz, N., Alvarez, I., and Dias, J. M. (2023). Modelling coastal upwelling off NW Iberian Peninsula: New insights on the fate of phytoplankton blooms. *Sci. Total Environ.* 874, 162416. doi: 10.1016/j.scitotenv.2023.162416
- Piot, A., Rochon, A., Stora, G., and Desrosiers, G. (2008). Experimental study on the influence of bioturbation performed by *Nephtys caeca* (Fabricius) and *Nereis virens* (Sars) annelidae on the distribution of dinoflagellate cysts in the sediment. *J. Exp. Mar. Bio. Ecol.* 359, 92–101. doi: 10.1016/j.jembe.2008.02.023
- Pitcher, G. C., Figueiras, F. G., Hickey, B. M., and Moita, M. T. (2010). The physical oceanography of upwelling systems and the development of harmful algal blooms. *Prog. Oceanogr.* 85, 5–32. doi: 10.1016/j.pocean.2010.02.002
- Pitcher, G. C., and Fraga, S. (2015). Harmful algal bloom events in the Canary Current large marine ecosystem. Available at: <https://aquadocs.org/handle/1834/9187>
- Pitcher, G. C., and Joyce, L. B. (2009). Dinoflagellate cyst production on the southern Namaqua shelf of the Benguela upwelling system. *J. Plankton Res.* 31, 865–875. doi: 10.1093/plankt/fbp040
- Pitcher, G. C., and Louw, D. C. (2021). Harmful algal blooms of the Benguela eastern boundary upwelling system. *Harmful Algae* 102, 101898. doi: 10.1016/j.hal.2020.101898
- Poloczanska, E. S., Burrows, M. T., Brown, C. J., García Molinos, J., Halpern, B. S., Hoegh-Guldberg, O., et al. (2016). Responses of Marine Organisms to Climate Change across Oceans. *Frontiers in Marine Science* 3, 62. doi: 10.3389/fmars.2016.00062
- Pospelova, V., de Vernal, A., and Pedersen, T. F. (2008). Distribution of dinoflagellate cysts in surface sediments from the northeastern Pacific Ocean (43–25 N) in relation to sea-surface temperature, salinity, productivity and coastal upwelling. *Mar. Micropaleontol.* 68, 21–48. doi: 10.1016/j.marmicro.2008.01.008
- Pospelova, V., Esenkulova, S., Johannessen, S. C., O'Brien, M. C., and Macdonald, R. W. (2010). Organic-walled dinoflagellate cyst production, composition and flux from 1996 to 1998 in the central

- Strait of Georgia (BC, Canada): A sediment trap study. *Mar. Micropaleontol.* 75, 17–37. doi: 10.1016/j.marmicro.2010.02.003
- Pospelova, V., Price, A. M., and Pedersen, T. F. (2015). Palynological evidence for late Quaternary climate and marine primary productivity changes along the California margin. *Paleoceanography* 30, 877–894. doi: 10.1002/2014pa002728
- Pospelova, V., Zonneveld, K. A. F., Heikkilä, M., Bringué, M., Price, A. M., Esenkulova, S., et al. (2018). Seasonal, annual, and inter-annual *Spiniferites* cyst production: a review of sediment trap studies. *Palynology* 42, 162–181. doi: 10.1080/01916122.2018.1465738
- Prebble, J. G., Crouch, E. M., Carter, L., Cortese, G., and Nodder, S. D. (2013). Dinoflagellate cysts from two sediment traps east of New Zealand. *Mar. Micropaleontol.* 104, 25–37. doi: 10.1016/j.marmicro.2013.08.003
- Price, A. M., and Pospelova, V. (2011). High-resolution sediment trap study of organic-walled dinoflagellate cyst production and biogenic silica flux in Saanich Inlet (BC, Canada). *Mar. Micropaleontol.* 80, 18–43. doi: 10.1016/j.marmicro.2011.03.003
- Prospero, J. M. (1990). “Mineral-aerosol transport to the North Atlantic and North Pacific: The impact of African and Asian sources,” in *The Long-Range Atmospheric Transport of Natural and Contaminant Substances*, eds. A. H. Knap, M.-S. Kaiser, and M.-S. Kaiser (Dordrecht: Springer Netherlands), 59–86. doi: 10.1007/978-94-009-0503-0\_4
- Prospero, J. M., Collard, F.-X., Molinié, J., and Jeannot, A. (2014). Characterizing the annual cycle of African dust transport to the Caribbean Basin and South America and its impact on the environment and air quality. *Global Biogeochem. Cycles* 28, 757–773. doi: 10.1002/2013gb004802
- Prospero, J. M., and Carlson, T. N. (1972). Vertical and areal distribution of Saharan dust over the western equatorial north Atlantic Ocean. *Journal of Geophysical Research* 77, 5255–5265. doi: 10.1029/JC077i027p05255
- Quijano-Scheggia, S., Olivos-Ortiz, A., Bustillos-Guzmán, J. J., Garcés, E., Gaviño-Rodríguez, J. H., Galicia-Pérez, M. A., et al. (2012). Bloom of *Gymnodinium catenatum* in Bahía Santiago and Bahía Manzanillo, Colima, Mexico. *Rev. Biol. Trop.* 60, 173–186. doi: 10.15517/rbt.v60i1.2750
- Radi, T., and de Vernal, A. (2004). Dinocyst distribution in surface sediments from the northeastern Pacific margin (40–60°N) in relation to hydrographic conditions, productivity and upwelling. *Rev. Palaeobot. Palynol.* 128, 169–193. doi: 10.1016/s0034-6667(03)00118-0
- Radi, T., and de Vernal, A. (2008). Dinocysts as proxy of primary productivity in mid–high latitudes of the Northern Hemisphere. *Mar. Micropaleontol.* 68, 84–114. doi: 10.1016/j.marmicro.2008.01.012
- Ratnarajah, L., Abu-Alhaja, R., Atkinson, A., Batten, S., Bax, N. J., Bernard, K. S., et al. (2023). Monitoring and modelling marine zooplankton in a changing climate. *Nat. Commun.* 14, 564. doi: 10.1038/s41467-023-36241-5
- Reyero, M., Cacho, E., Martínez, A., Vázquez, J., Marina, A., Fraga, S., et al. (1999). Evidence of saxitoxin derivatives as causative agents in the 1997 mass mortality of monk seals in the Cape Blanc Peninsula. *Nat. Toxins* 7, 311–315. doi: 10.1002/1522-7189(199911/12)7:6<311::aid-nt75>3.0.co;2-i
- Ribeiro, S., and Amorim, A. (2008). Environmental drivers of temporal succession in recent dinoflagellate cyst assemblages from a coastal site in the North-East Atlantic (Lisbon Bay, Portugal). *Mar. Micropaleontol.* 68, 156–178. doi: 10.1016/j.marmicro.2008.01.013
- Ribeiro, S., Amorim, A., Andersen, T. J., Abrantes, F., and Ellegaard, M. (2012). Reconstructing the history of an invasion: the toxic phytoplankton species *Gymnodinium catenatum* in the Northeast Atlantic. *Biol. Invasions* 14, 969–985. doi: 10.1007/s10530-011-0132-6

- Rochon, A., Vernal, A. de, Turon, J.-L., Matthießen, J., and Head, M. J. (1999). Distribution of recent dinoflagellate cysts in surface sediments from the North Atlantic Ocean and adjacent seas in relation to sea-surface parameters. *American Association of Stratigraphic Palynologists Contribution Series* 35, 1–146. Available at: <https://epic.awi.de/3706/>
- Rodríguez, S., Cuevas, E., Prospero, J. M., Alastuey, A., Querol, X., López-Solano, J., et al. (2015). Modulation of Saharan dust export by the North African dipole. *Atmos. Chem. Phys.* 15, 7471–7486. doi: 10.5194/acp-15-7471-2015
- Rodríguez-Villegas, C., Díaz, P. A., Salgado, P., Tomasetti, S. J., Díaz, M., Marín, S. L., et al. (2022). The role of physico-chemical interactions in the seasonality of toxic dinoflagellate cyst assemblages: The case of the NW Patagonian fjords system. *Environ. Pollut.* 311, 119901. doi: 10.1016/j.envpol.2022.119901
- Rollwagen-Bollens, G., and Bollens, S. (2020). Biotic vs. abiotic forcing on plankton assemblages varies with season and size class in a large temperate estuary. *J. Plankton Res.* 42, 221–237. doi: 10.1093/plankt/fbaa010
- Romero, O. E., Baumann, K.-H., Zonneveld, K. A. F., Donner, B., Hefter, J., Hamady, B., et al. (2020). Flux variability of phyto- and zooplankton communities in the Mauritanian coastal upwelling between 2003 and 2008. *Biogeosciences* 17, 187–214. doi: 10.5194/bg-17-187-2020
- Romero, O. E., and Fischer, G. (2017). Shift in the species composition of the diatom community in the eutrophic Mauritanian coastal upwelling: Results from a multi-year sediment trap experiment (2003–2010). *Prog. Oceanogr.* 159, 31–44. doi: 10.1016/j.pocean.2017.09.010
- Romero, O. E., and Ramondenc, S. (2022). A 17-year time-series of diatom populations ‘flux and composition in the Mauritanian coastal upwelling. *Frontiers in Marine Science* 9. doi: 10.3389/fmars.2022.1006345
- Romero, O. E., Ramondenc, S., and Fischer, G. (2021). A 2-decade (1988–2009) record of diatom fluxes in the Mauritanian coastal upwelling: impact of low-frequency forcing and a two-step shift in the species composition. *Biogeosciences* 18, 1873–1891. doi: 10.5194/bg-18-1873-2021
- Roza, S. E. V., Versteegh, G. J. M., Pospelova, V., and Zonneveld, K. A. F. (2024). Environmental control of interannual and seasonal variability in dinoflagellate cyst export flux over 18 years in the Cape Blanc upwelling region (Mauritania). *Frontiers in Marine Science* 11. doi: 10.3389/fmars.2024.1284425
- Sala-Pérez, M., Lattuada, M., Flecker, R., Anesio, A., and Leroy, S. A. G. (2020). Dinoflagellate cyst assemblages as indicators of environmental conditions and shipping activities in coastal areas of the Black and Caspian Seas. *Reg. Stud. Mar. Sci.* 39, 101472. doi: 10.1016/j.rsma.2020.101472
- Saraswati, P. K., and Srinivasan, M. S. (2016). “Taphonomy and Quality of the Fossil Record,” in *Micropaleontology: Principles and Applications*, eds. P. K. Saraswati and M. S. Srinivasan (Cham: Springer International Publishing), 19–33. doi: 10.1007/978-3-319-14574-7\_2
- Sarmiento, J. L., Gruber, N., Brzezinski, M. A., and Dunne, J. P. (2004). High-latitude controls of thermocline nutrients and low latitude biological productivity. *Nature* 427, 56–60. doi: 10.1038/nature02127
- Schneider, T., Bischoff, T., and Haug, G. H. (2014). Migrations and dynamics of the intertropical convergence zone. *Nature* 513, 45–53. doi: 10.1038/nature13636
- Schnepf, E., and Elbrächter, M. (1992). Nutritional strategies in dinoflagellates: A review with emphasis on cell biological aspects. *Eur. J. Protistol.* 28, 3–24. doi: 10.1016/S0932-4739(11)80315-9

- Seibold, E., and Fütterer, D. (1982). "Sediment dynamics on the Northwest African continental margin," in *The Ocean Floor: Bruce Heezen commemorative volume*, eds. R. A. Scrutton and M. Talwani (Chichester: Wiley), 147–163. Available at: <https://epic.awi.de/id/eprint/35543/>
- Skonieczny, C., Bory, A., Bout-Roumazeilles, V., Abouchami, W., Galer, S. J. G., Crosta, X., et al. (2013). A three-year time series of mineral dust deposits on the West African margin: Sedimentological and geochemical signatures and implications for interpretation of marine paleo-dust records. *Earth and Planetary Science Letters* 364, 145–156. doi: 10.1016/j.epsl.2012.12.039
- Skovgaard, A., Karpov, S. A., and Guillou, L. (2012). The parasitic dinoflagellates *Blastodinium* spp. inhabiting the gut of marine, planktonic copepods: Morphology, ecology, and unrecognized species diversity. *Front. Microbiol.* 3, 305. doi: 10.3389/fmicb.2012.00305
- Smayda, T. J. (2002). Adaptive ecology, growth strategies and the global bloom expansion of dinoflagellates. *J. Oceanogr.* 58, 281–294. doi: 10.1023/a:1015861725470
- Smayda, T. J., and Reynolds, C. S. (2003). Strategies of marine dinoflagellate survival and some rules of assembly. *J. Sea Res.* 49, 95–106. doi: 10.1016/S1385-1101(02)00219-8
- Smayda, T. J., and Trainer, V. L. (2010). Dinoflagellate blooms in upwelling systems: Seeding, variability, and contrasts with diatom bloom behaviour. *Prog. Oceanogr.* 85, 92–107. doi: 10.1016/j.pocean.2010.02.006
- Šmilauer, P., and Lepš, J. (2014). *Multivariate Analysis of Ecological Data using CANOCO 5*. Cambridge University Press Available at: <https://play.google.com/store/books/details?id=3hkmAwwAAQBAJ>
- Sprangers, M., Dammers, N., Brinkhuis, H., van Weering, T. C. E., and Lotter, A. F. (2004). Modern organic-walled dinoflagellate cyst distribution offshore NW Iberia; tracing the upwelling system. *Rev. Palaeobot. Palynol.* 128, 97–106. doi: 10.1016/S0034-6667(03)00114-3
- Starr, M., Lair, S., Michaud, S., Scarratt, M., Quilliam, M., Lefaivre, D., et al. (2017). Multispecies mass mortality of marine fauna linked to a toxic dinoflagellate bloom. *PLoS One* 12, e0176299. doi: 10.1371/journal.pone.0176299
- Stat, M., Morris, E., and Gates, R. D. (2008). Functional diversity in coral–dinoflagellate symbiosis. *Proceedings of the National Academy of Sciences* 105, 9256–9261. doi: 10.1073/pnas.0801328105
- Stuut, J. B., Zabel, M., Ratmeyer, V., Helmke, P., Schefuß, E., Lavik, G., et al. (2005). Provenance of present-day eolian dust collected off NW Africa. *Journal of Geophysical Research* 110. doi: 10.1029/2004JD005161
- Sultan, B., and Janicot, S. (2000). Abrupt shift of the ITCZ over West Africa and intra-seasonal variability. *Geophys. Res. Lett.* 27, 3353–3356. doi: 10.1029/1999gl011285
- Susek, E., Zonneveld, K. A. F., Fischer, G., Versteegh, G. J. M., and Willems, H. (2005). Organic-walled dinoflagellate cyst production in relation to upwelling intensity and lithogenic influx in the Cape Blanc region (off north-west Africa). *Phycological Res.* 53, 97–112. doi: 10.1111/j.1440-183.2005.00377.x
- Sylla, A., Mignot, J., Capet, X., and Gaye, A. T. (2019). Weakening of the Senegalo–Mauritanian upwelling system under climate change. *Clim. Dyn.* 53, 4447–4473. doi: 10.1007/s00382-019-04797-y
- Taleb, H., Vale, P., and Blaghen, M. (2003). Spatial and temporal evolution of PSP toxins along the Atlantic shore of Morocco. *Toxicon* 41, 199–205. doi: 10.1016/s0041-0101(02)00277-5
- Tanaka, T. Y., and Chiba, M. (2006). A numerical study of the contributions of dust source regions to the global dust budget. *Glob. Planet. Change* 52, 88–104. doi: 10.1016/j.gloplacha.2006.02.002

- Taylor, F. J. R. (1987). *The Biology of Dinoflagellates.*, ed. F. J. R. Taylor. Oxford, UK: Blackwell Scientific Publications.
- Taylor, F. J. R., Hoppenrath, M., and Saldarriaga, J. F. (2008). Dinoflagellate diversity and distribution. *Biodivers. Conserv.* 17, 407–418. doi: 10.1007/s10531-007-9258-3
- Taylor, F. J. R., and Pollinger, U. (1987). “The ecology of dinoflagellates,” in *The Biology of Dinoflagellates*, ed. F. J. R. Taylor (Oxford, UK: Blackwell Scientific Publications), 398–502. Available at: <https://cir.nii.ac.jp/crid/1574231875508804096>
- Telesh, I., Schubert, H., and Skarlato, S. (2021). Abiotic stability promotes dinoflagellate blooms in marine coastal ecosystems. *Estuar. Coast. Shelf Sci.* 251, 107239. doi: 10.1016/j.ecss.2021.107239
- ter Braak, C. J. F., and Prentice, I. C. (1988). A Theory of Gradient Analysis, in *Advances in Ecological Research*, eds. M. Begon, A. H. Fitter, E. D. Ford, and A. Macfadyen (Academic Press), 271–317. doi: 10.1016/S0065-2504(08)60183-X
- ter Braak, C. J. F., and Šmilauer, P. (2002). CANOCO Reference Manual and CanoDraw for Windows User’s Guide: Software for Canonical Community Ordination (version 4.5). Itacha, NY, USA: Microcomputer Power. Available at: <https://play.google.com/store/books/details?id=0ZhoGwAACAAJ>
- Terenko, G., and Krakhmalnyi, A. (2021). Red tide of *Lingulodinium polyedrum* (Dinophyceae) in Odesa Bay (Black Sea). *Turkish Journal of Fisheries and Aquatic Sciences* 22. doi: 10.4194/TRJFAS20312
- Torrence, C., and Compo, G. P. (1998). A practical guide to wavelet analysis. *Bulletin of the American Meteorological Society* 79, 61–78. doi: 10.1175/1520-0477(1998)079<0061:APGTWA>2.0.CO;2
- van Camp, L., Nykjaer, L., Mittelstaedt, E., and Schlittenhardt, P. (1991). Upwelling and boundary circulation off Northwest Africa as depicted by infrared and visible satellite observations. *Prog. Oceanogr.* 26, 357–402. doi: 10.1016/0079-6611(91)90012-B
- van der Does, M., Brummer, G.-J. A., Korte, L. F., and Stuut, J.-B. W. (2021). Seasonality in Saharan dust across the Atlantic Ocean: From atmospheric transport to seafloor deposition. *J. Geophys. Res.* 126. doi: 10.1029/2021jd034614
- van der Does, M., Korte, L. F., Munday, C. I., Brummer, G.-J. A., and Stuut, J.-B. W. (2016). Particle size traces modern Saharan dust transport and deposition across the equatorial North Atlantic. *Atmos. Chem. Phys.* 16, 13697–13710. doi: 10.5194/acp-16-13697-2016
- van Nieuwenhove, N., Head, M. J., Limoges, A., Pospelova, V., Mertens, K. N., Matthiessen, J., et al. (2020). An overview and brief description of common marine organic-walled dinoflagellate cyst taxa occurring in surface sediments of the Northern Hemisphere. *Mar. Micropaleontol.* 159, 101814. doi: 10.1016/j.marmicro.2019.101814
- Versteegh, G. J. M., and Zonneveld, K. A. F. (2022). Micro-Fourier transform infrared spectroscopy of degradation-resistant organic microfossils; Influence of preservation environment and phylogeny. *Frontiers in Marine Science* 9. doi: 10.3389/fmars.2022.1040543
- Vindel, J. M., Valenzuela, R. X., Navarro, A. A., and Polo, J. (2020). Temporal and spatial variability analysis of the solar radiation in a region affected by the intertropical convergence zone. *Meteorol. Appl.* 27. doi: 10.1002/met.1824
- Vink, A., Zonneveld, K. A. F., and Willems, H. (2000). Organic-walled dinoflagellate cysts in western equatorial Atlantic surface sediments: distributions and their relation to environment. *Rev. Palaeobot. Palynol.* 112, 247–286. doi: 10.1016/s0034-6667(00)00046-4



- Visbeck, M. (2018). Ocean science research is key for a sustainable future. *Nature Communications* 9. doi: 10.1038/s41467-018-03158-3
- Wall, D., and Dale, B. (1968). Modern dinoflagellate cysts and evolution of the Peridinales. *Micropaleontology* 14, 265–304. doi: 10.2307/1484690
- Wang, X., Wang, Q., Prass, M., Pöhlker, C., Moran-Zuloaga, D., Artaxo, P., et al. (2023). The export of African mineral dust across the Atlantic and its impact over the Amazon Basin. *Atmos. Chem. Phys.* 23, 9993–10014. doi: 10.5194/acp-23-9993-2023
- Winther, J.-G., Dai, M., Rist, T., Hoel, A. H., Li, Y., Trice, A., et al. (2020). Integrated ocean management for a sustainable ocean economy. *Nat Ecol Evol* 4, 1451–1458. doi: 10.1038/s41559-020-1259-6
- Worden, A. Z., Follows, M. J., Giovannoni, S. J., Wilken, S., Zimmerman, A. E., and Keeling, P. J. (2015). Rethinking the marine carbon cycle: factoring in the multifarious lifestyles of microbes. *Science* 347, 1257594. doi: 10.1126/science.1257594
- Wyatt, N. J., Birchill, A., Ussher, S., Milne, A., Bouman, H. A., Shoenfelt Troein, E., et al. (2023). Phytoplankton responses to dust addition in the Fe-Mn co-limited eastern Pacific sub-Antarctic differ by source region. *Proc. Natl. Acad. Sci. U. S. A.* 120, e2220111120. doi: 10.1073/pnas.2220111120
- Wynn, R. B., Masson, D. G., Stow, D. A. v., and Weaver, P. P. e. (2000). The Northwest African slope apron: a modern analogue for deep-water systems with complex seafloor topography. *Mar. Pet. Geol.* 17, 253–265. doi: 10.1016/S0264-8172(99)00014-8
- Yang, T., Chen, Y., Zhou, S., and Li, H. (2019). Impacts of aerosol copper on marine phytoplankton: a review. *Atmosphere* 10, 414. doi: 10.3390/atmos10070414
- Yu, H., Tan, Q., Chin, M., Remer, L. A., Kahn, R. A., Bian, H., et al. (2019). Estimates of African dust deposition along the trans-Atlantic transit using the decade-long record of aerosol measurements from CALIOP, MODIS, MISR, and IASI. *J. Geophys. Res.* 124, 7975–7996. doi: 10.1029/2019JD030574
- Zenk, W., Klein, B., and Schroder, M. (1991). Cape Verde Frontal Zone. *Deep Sea Res. A* 38, S505–S530. doi: 10.1016/S0198-0149(12)80022-7
- Zhou, W., Li, Q. P., and Wu, Z. (2021). Coastal phytoplankton responses to atmospheric deposition during summer. *Limnol. Oceanogr.* 66, 1298–1315. doi: 10.1002/lno.11683
- Zonneveld K. A. F., Albert M., Boom L., Donner B., Ebersbach F., Friese C., et al. (2016) Aerobic degradation of particulate organic matter and benthic microbial turnover rates reflecting ocean redox conditions off NW Africa (ADOMIS). *Maria S. Merian MSM* 48, pp. 65.
- Zonneveld K. A. F., Baumann K.-H., Boersen B., Bösche J., Decker C., de J.-D., et al. (2019a). A deglacial record of carbon release from thawing permafrost of the European tundra (EUROTHAW) - Marine Carbon Production, Export, relocation and degradation under varying ocean redox conditions off NW Africa (MACPEI). *Maria S. Merian MSM* 79, pp 64.
- Zonneveld, K. A. F., Bockelmann, F., and Holzwarth, U. (2007). Selective preservation of organic-walled dinoflagellate cysts as a tool to quantify past net primary production and bottom water oxygen concentrations. *Mar. Geol.* 237, 109–126. doi: 10.1016/j.margeo.2006.10.023
- Zonneveld, K. A. F., and Brummer, G. A. (2000). (Palaeo-)ecological significance, transport and preservation of organic-walled dinoflagellate cysts in the Somali Basin, NW Arabian Sea. *Deep Sea Res. Part 2 Top. Stud. Oceanogr.* 47, 2229–2256. doi: 10.1016/S0967-0645(00)00023-0

- Zonneveld, K.A.F., Coulibaly, O., Flintrop, C., Grotheer, H., Klann, M., Knoke, M., et al. (2020). Marine Particles off NW Africa, from source to sink. Cruise report R.V. Meteor M165, pp. 49.
- Zonneveld, K. A. F., Ebersbach, F., Maeke, M., and Versteegh, G. J. M. (2018). Transport of organic-walled dinoflagellate cysts in nepheloid layers off Cape Blanc (N-W Africa). *Deep Sea Res. Part I* 139, 55–67. doi: 10.1016/j.dsr.2018.06.003
- Zonneveld, K. A. F., Gray, D. D., Kuhn, G., and Versteegh, G. J. M. (2019b). Postdepositional aerobic and anaerobic particulate organic matter degradation succession reflected by dinoflagellate cysts: The Madeira Abyssal Plain revisited. *Mar. Geol.* 408, 87–109. doi: 10.1016/j.margeo.2018.11.010
- Zonneveld, K. A. F., Grotheer, H., and Versteegh, G. J. M. (2022a). Dinoflagellate cysts production, excystment and transport in the upwelling off Cape Blanc (NW Africa). *Frontiers in Marine Science* 9. doi: 10.3389/fmars.2022.915755
- Zonneveld, K. A. F., Harper, K., Klügel, A., Chen, L., De Lange, G., and Versteegh, G. J. M. (2024). Climate change, society, and pandemic disease in Roman Italy between 200 BCE and 600 CE. *Sci Adv* 10, eadk1033. doi: 10.1126/sciadv.adk1033
- Zonneveld, K. A. F., and Jurkschat, T. (1999). *Bitectatodinium spongium* (Zonneveld, 1997) Zonneveld et Jurkschat, comb. nov. from modern sediments and sediment trap samples of the Arabian Sea (Northwestern Indian Ocean): taxonomy and ecological affinity. *Rev. Palaeobot. Palynol.* 106, 153–169. doi: 10.1016/S0034-6667(99)00007-X
- Zonneveld, K. A. F., Marret, F., Versteegh, G. J. M., Bogus, K., Bonnet, S., Bouimetarhan, I., et al. (2013). Atlas of modern dinoflagellate cyst distribution based on 2405 data points. *Rev. Palaeobot. Palynol.* 191, 1–197. doi: 10.1016/j.revpalbo.2012.08.003
- Zonneveld, K. A. F., Meilland, J., Donner, B., and Versteegh, G. J. M. (2022b). Export flux succession of dinoflagellate cysts and planktonic foraminifera in an active upwelling cell off Cape Blanc (NW Africa). *Eur. J. Phycol.* 57, 29–47. doi: 10.1080/09670262.2021.1885066
- Zonneveld, K.A.F., Mundanatt, A. A., Bolte, A., Eldering, D., de Visser, J.-D., Gottwald, J., et al. (2022c). Sinking Particles, their production, transfer and preservation. Cruise Report R.V. Maria S. Merian MSM 104, pp. 51.
- Zonneveld, K. A. F., and Pospelova, V. (2015). A determination key for modern dinoflagellate cysts. *Palynology* 39, 387–409. doi: 10.1080/01916122.2014.990115
- Zonneveld, K. A. F., Sebastian Meier, K. J., Esper, O., Siggelkow, D., Wendler, I., and Willems, H. (2005). The (palaeo) environmental significance of modern calcareous dinoflagellate cysts: a review. *Paläontologische Zeitschrift* 79, 61–77. doi: 10.1007/BF03021754
- Zonneveld, K. A. F., Susek, E., and Fischer, G. (2010). Seasonal variability of the organic-walled dinoflagellate cyst production in the coastal upwelling region off Cape Blanc (Mauritania): A five-year survey. *J. Phycol.* 46, 202–215. doi: 10.1111/j.1529-8817.2009.00799.x
- Zonneveld, K. A. F., Versteegh, G., and Kodrans-Nsiah, M. (2008). Preservation and organic chemistry of Late Cenozoic organic-walled dinoflagellate cysts: A review. *Mar. Micropaleontol.* 68, 179–197. doi: 10.1016/j.marmicro.2008.01.015
- Zumaque, J., Eynaud, F., and de Vernal, A. (2017). Holocene paleoceanography of the Bay of Biscay: Evidence for west-east linkages in the North Atlantic based on dinocyst data. *Palaeogeography, Palaeoclimatology, Palaeoecology* 468, 403–413. doi: 10.1016/j.palaeo.2016.12.031

## Appendix

Besides conducting research and writing scientific publications, a doctoral candidate was also advised to participate in scientific meetings such as conferences and workshops and present the results of their doctoral projects. This activity aims to build a discussion regarding the projects with scientists outside the candidate working group. Moreover, scientific meetings can expand the knowledge and network of the candidate within or outside of their research topics. In this chapter, I enlisted abstracts submitted to multiple scientific meetings on internal and international scales.

### *Status Conference for Research Vessels 2022*

#### **18 years of dinoflagellate cyst export flux and benthic foraminifera deposition recovered from a sediment trap in the upwelling region off Cape Blanc (NW. Africa)**

Surya Eldo V. Roza, Gerard G. J. Versteegh, and Karin A. F. Zonneveld

The upwelling system off Cape Blanc (NW Africa) is one of the most productive areas in the world. Year-round upwelling and frequent input of Sahara dust results high nutrient concentrations throughout the year. Although upwelling is a permanent feature in the region, upwelling intensity and dynamics are highly diverse depending on seasonal variability as well as dynamics of local weather, notably wind strength and direction. Here we present results from an 18-years study (2002 - 2020) on the dynamics of the particulate organic export flux formed by dinoflagellate cysts and benthic foraminifera. Material has been collected by trap CBeu at ca 1260 m depth, which is deployed as part of the long-term MARUM/GeoB sediment trap monitoring program at 20°50' N/18°44' W (off Cape Blanc). The trap is located just offshore the active upwelling cell locations below the track of offshore drifting surface water upwelling filaments. We document a long-term trend in changing the phyto- and zooplankton export flux composition with major association shifts recorded during the years 2005 and 2009. The record also shows multiannual cyclic plankton association changes. Multiannual and interannual dynamics of the system are very high with each upwelling event having a different plankton export flux association. We furthermore show that the export flux in the region is not only formed by particulate organic matter formed in the upper waters near the trap location but consist for a considerable part of reworked shelf material that most probably has been transported offshore by subsurface nepheloid layers.

### *12th International Conference on Modern and Fossil Dinoflagellates*

#### **Seasonal, annual, and multi-annual variability of dinoflagellate cyst export production in the upwelling region off Cap Blanc based on a 18 years sediment trap time series**

Surya Eldo V. Roza, Gerard J. M. Versteegh, and Karin A. F. Zonneveld

Dinoflagellate resting cysts in marine sediments archives form a useful tool to reconstruct past changes in marine environments. Embedded in the sediments they can be vital for time intervals up to a century. Especially sedimentary “seed banks” of cysts of harmful algal bloom species form a potential risk for future hazards. An adequate paleo-environmental interpretation of fossil assemblages depends on our knowledge of their ecology and factors that influence their production on seasonal to multi-annual resolution. The same holds for studies on the production and bloom dynamics of harmful cyst producing dinoflagellates. Here, we aim to enhance the ecological knowledge of organic-walled cyst forming dinoflagellates and provide information of factors that influence the cyst export production on

seasonal, annual and multi-annual scales based on a study of 18 years sediment trap record obtained from the Cape Blanc upwelling system. This upwelling system is one of the Eastern Boundary Upwelling Ecosystems (EBUEs), known as one of the most productive regions in the world. Surface waters are characterized by year-round upwelling of intermediate waters into the photic zone, as well as frequent input of Sahara dust, both fertilizing the surface ocean. The upwelled waters can be laterally transported offshore in the form of eddies and filaments.

The organic cysts were studied in material collected by a sediment trap located under the filament track of the main upwelling cell at the depth around 1300m. The trap collected sinking particles since 2003 until 2020, with the range of 1-3 weeks sampling intervals. A 1/125th split of each sample was sieved over 20  $\mu\text{m}$  high precision sieve (Storck-Verco) with tap water. A known aliquot of every sample was embedded in glycerin gelatin and sealed with a cover slip on a palynological slide. The quantification and identification of dinoflagellate organic-walled cysts was performed under light microscopy and referred to the determination of. Both variability in export flux (cysts/m<sup>2</sup>/day) and relative abundances of cysts were compared with seasonal, annual, and multi-annual variability in local environmental parameters that influence the Cap Blanc oceanographic environments. The parameters include: sea surface temperature (SST) difference between the trap site and an open ocean location 200nm west of the trap location (SSTa), Chlorophyll-a concentrations at the trap site, local wind speed, local wind direction and dust-storm events. Information about the local wind system and dust events were obtained from the meteorological report of Nouadibhou airport (Cap Blanc). Data of SST and Chlorophyll-a were extracted from ERDAPP satellite observation (<https://coastwatch.pfeg.noaa.gov/erddap/griddap/ncdcOisst2Agg.html>). Correlation has been performed using the multivariate ordination method of Canonical Correspondence Analysis (Jongman et al., 1995).

The organic-walled cysts association is dominated by the heterotrophic dinoflagellates with photo-/mixotrophic species forming only around 6% of the total cyst. Maximum cyst export production was observed at times of high upwelling intensity in spring-summer. During these intervals, the cyst association was dominated by cysts of *Brigantidinium* spp. and *Echinidinium* species. Both cyst export production and relative abundance of cysts of the photo-/mixotrophic species slightly increased at times of upwelling relaxation (weak upwelling intensity). *Lingulodinium machaerophorum* and cysts of *Gymnodinium* species are specifically observed at times of weakening upwelling. Our long-time record shows large signal of annual and inter-annual variability. We observed that the cysts associations composition of individual upwelling episode was variable. Although the occurrence of several species was bound to intensive upwelling and can be characterized as typical upwelling species, they were not present in every upwelling event. Additionally, *Lingulodinium machaerophorum* and cysts of *Gymnodinium* were typically observed at times of upwelling relaxation, they were not present at the end of every upwelling event and only sporadically showed largely enhanced absolute and relative abundances. We assume this to be the result of interspecies competition. These results also clearly show that the studied system is highly variable and information about the ecology of cyst forming species can only be achieved when long time series are being studied.

On a multi-annual scale, we observe a consisting association change around 2009. Upwelling events prior to 2009 were dominated by *Brigantidinium* spp. with a varying number of cysts of *Protoperidinium americanum*, *P. monospinum*, and *Stelladinium stellatum*. After 2009 the cyst associating to upwelling events was characterized by *Echnidinium* species, notably the species *Echinidinium aculeatum*, *E. delicatum*, *E. granulatum*, *E. transparentum*, and *E. zonnaveldiae*. This change in association is contemporaneous with an increase of dust input into the coastal region. Whereas dust input in the region occurred seasonally during winter - spring, it became a more permanent character with maxima both in winter and summer from 2011. From this year an increase in Chlorophyll-a in surface waters at the trap site can be observed. Within the dinoflagellate cyst assemblage, we observed higher export production and relative abundances of species that in several regions of the world could be linked to the presence of anthropogenic induced pollution. We assume that these species; *Polykrikos*

*kofoidii*, *P. schwartzii*, *Quinquecuspis concretum*, and *Votadinium calvum* reflect a eutrophication of the Cape Blanc upwelling ecosystem.

### ***12th International Conference on Modern and Fossil Dinoflagellates***

#### **New ecological insight of calcareous dinoflagellate cyst export production based on 18 years sediment trap study in the Cap Blanc upwelling area (NW. Africa)**

Surya Eldo V. Roza, Gerard J. M. Versteegh, and Karin A. F. Zonneveld

Some phototrophic species of dinoflagellates are known to form calcareous cysts. Downcore calcareous dinoflagellate cyst associations are useful to reconstruct changes in past ecosystems, notably in the open ocean. For an adequate establishment of such reconstructions, detailed ecological information with respect to factors that influence cyst production is essential. Compared to organic-walled dinoflagellate cysts the ecology of calcareous cysts is much less studied. Here, we enrich the ecological information of calcareous dinoflagellate cysts by providing results from an 18 years sediment trap study executed in the Mauritanian upwelling area. For this we compared the cyst export flux with changes in oceanographic conditions at times of deposition. Cape Blanc region is one of the most productive regions in the world, as a result of upwelling of deep nutrient rich waters into the photic zone and mineral dust input from the Sahara. Permanent upwelling occurs along a small band near the shelf edge. Nutrient rich upwelled waters are being transported offshore in the form of large filaments. Although upwelling is present throughout the year, maximal intensity is observed in winter and spring.

Calcareous dinocysts were collected by a sediment trap at about 1300m from 2003 to 2020 with sampling intervals of 1 to 3 weeks. From every sample, 1/125th split material was sieved over 20 µm precession sieve (Storck-Verco) with tap water, concentrated to 0,5 ml solution, and transferred to an eppendorf tube. A known aliquot of the material was embedded in glycerin gelatin and sealed with a cover slip on a palynological slide. The calcareous cysts were counted and identified under polarized-light microscopy. Cysts accumulation rates and relative abundances have been compared with environmental conditions at times of deposition notably sea surface temperature (SST), sea surface temperature difference between the trap site and an open ocean location 200km west of the trap location (SSTA), Chlorophyll-a concentrations at the trap site, local wind speed, local wind direction and dust input. Correlation has been performed using the multivariate ordination method Redundancy Analysis (RDA). Information about the local wind system and dust events are derived from the meteorological report of Nouadibhou airport (Cape Blanc). Data of SST, SSTA and Chlor-a are obtained from ERDAPP satellite observation (<https://coastwatch.pfeg.noaa.gov/erddap/griddap/ncdc/Oisst2Agg.html>).

The calcareous-walled cyst association is dominated by *Thoracosphaera heimii*, followed by *Calciadinellum albatrosianum*, and *Leonella granifera*. Total cysts flux appeared to be increased at times of low upwelling intensity (upwelling relaxation). This is in line with previous findings that generally documented enhanced cyst concentrations in oligotrophic environments with stratified upper water column. Based on visual examination of the data and the RDA ordination, we could arrange 4 groups of species with comparable relationship to environmental parameters. Group 1 consist of one species; *T. heimii* that is ordinated in the negative side of the first RDA axis and positive side of the second RDA axis. The axis of this species is heading to the same direction of the wind direction but opposite to the upwelling indices parameters (wind velocity and SSTA). The abundance of *T. heimii* increases at the time of stratified upper water, linked to the result of mentioned publications above. Group 2 consists of *C. albatrosianum*, *C. operosum*, and *Pernambugia tuberosa*, and other rarer species. These species are ordinated at the negative side of the first RDA axis. They show high relative abundances at times of low wind speed with winds blowing from the northeast, slow wind speed, and relative high surface water temperatures. This suggest that these species have highest relative

abundances at times of minimal upwelling intensity. Group 3 consist of *L. granifera*, *Lebbessphaera urania*, *Scripsiella trifida*, and *S. trochoidea* ordinated at the positive side of the first RDA axis and negative side of the second RDA axis. It is positively related to one of upwelling indices (SSTa) and dust-storm events. but negatively to SST and wind direction. In line with previous findings, *L. granifera* species is most abundant at times of enhanced dust input in the region. Group 4 consist of *Bicarinellum tricarinelloides*, *Praecalcionellum schizoseptum*, *Rhabdothorax sp.*, *S. precaria*, and *S. regalis*. These species are ordinated at the positive side of the first and second RDA axes in the same direction as wind speed (the main driven-factor of upwelling in the region), SSTa, and Chl-a. The ordination of group 3 and 4 (except for *L. granifera*) suggest that these species are more abundant at times of enhanced upwelling intensity. So far, only high abundance of *S. trochoidea* have been reported to be linked to nutrient rich environments. Therefore, we assume species of group 3 and 4 are more tolerable to the upwelling conditions and eutrophic surface waters compared to the other calcareous dinoflagellate cysts species. This finding can improve the knowledge of calcareous cyst ecology, since previous studies often relate the enhanced production of calcareous cysts as indication of limited nutrient environment.

### ***Ocean Floor Symposium 2022 “Understanding element fluxes – processes and budgets”***

#### **Particulate organic matter export flux and ecosystem change in the Cape Blanc upwelling region during the last 18 years reflected by dinoflagellate cysts: a sediment trap study**

Surya Eldo V. Roza, Gerard J. M. Versteegh, Gerhard Fischer, and Karin A. F. Zonneveld

For understanding of the natural and human-induced changes in ocean carbon flux it is essential to obtain insight into the variability in particulate organic matter (POM) export flux to the deep ocean during the last decades. Here we present the export flux of dinoflagellate cysts on a sub-monthly resolution over the last 18 years collected by a sediment trap located in the Cape Blanc upwelling system. The location is characterized by year-round upwelling with maximal intensity in winter/spring and frequent input of Sahara dust, both fertilizing the surface ocean. Dinoflagellate cysts are produced by phototrophic and heterotrophic dinoflagellates living in the upper waters and form one of the key-group organisms in marine ecosystems. They can be used as representative for both the phyto- and zooplankton POM export signal as well as indicators for ecosystem change. We show that export flux composition in both trophic levels is highly variable with different association composition in each year at maximum upwelling intensity. Nevertheless, we observed a clear change in association composition at the year 2008 related to the enhanced input of dust in the region. The cyst association suggests that after this time a gradual increase in trophic state of the surface waters occurred. The strong intra- and inter-annual variabilities subscribe the importance of a long-term monitoring in order to determine natural and human induced ecosystem change.

### ***15th Bremen PhD days in Marine Sciences***

#### **Dinoflagellate cysts: A journey from the upper water column to the ocean floor**

Surya Eldo V. Roza, Gerard J. M. Versteegh, and Karin A. F. Zonneveld

Anthropogenic carbon has been polluting the earth's atmosphere for at least 300 years causing a warming climate. This pollutant pressurizes all kinds of environmental niches on earth, including the marine ecosystem. Phytoplankton is the agent capable of turning atmospheric carbon into energy and biomass through photosynthesis. These biomasses are the key to the sustainability of marine organisms at higher trophic levels such as; zooplankton and fishes. The deceased organisms will sink and embedded

in the sediment carrying information about the upper ocean production and the environmental condition. One of many useful plankton as a climate proxy is dinoflagellates, which are formed by photo- and heterotrophic species. Throughout their life cycle, dinoflagellates produce a cyst that is made of organic carbon or calcareous walls. Cysts are biodegraded-resistant which makes them fossilisable in the paleo-archive. This knowledge raised some crucial questions: (1) How much carbon (cysts) was represented in the bottom sediment? and (2) What could influence cysts accumulation rate and composition in the sediment archive? Therefore, we are inspired to compare the export flux of cysts obtained by a sediment trap with the upper part of a sediment core in the same location.

### ***International Conference for Young Marine Researchers 2023***

#### **Environmental factors influencing the dinoflagellate cysts production and their preservation in the bottom sediment in the upwelling region off Cape Blanc, Mauritania: a comparison of sediment trap with down-core sediment cyst record**

Surya Eldo V. Roza, Gerard J. M. Versteegh, Karin A. F. Zonneveld, Hendrik Wolschke, Iria García-Moreiras, Fangzhu Wu, and Gunner Gerdts

Dinoflagellates are one of the most important primary producers in marine ecosystems. Many living dinoflagellate species produce organic-walled cysts during their sexual reproduction. Dinoflagellate cysts are well-preserved in the sediment leading to their common usage as a proxy to investigate past marine ecosystems. Understanding the environmental factors that drive cyst production is essential to interpret the cyst record from the sediment archive. One question of interest in paleoceanography is how well the sediment cyst record reflects the local productivity and upper water conditions. To answer this question, we have conducted a comparison study at the upwelling region off Cape Blanc, Mauritania where the primary producers are supported by nutrients coming mainly from the coastal upwelling and the Saharan dust. We have collected 18 years (2003 - 2020) of dinoflagellate cysts' export flux using a sediment trap, which was compared with an undisturbed sediment core from the vicinity area of the trap. The core was subsampled per 3 mm to produce a high-resolution cyst record. The selected samples were dated with  $^{210}\text{Pb}$  and the result indicated a sedimentation rate of ca. 3 years per sample, therefore, the upper 1.8 cm of the sediment core coincided with the period covered by the sediment trap. The cyst associations recorded in the sediment trap and sediment core were dominated by heterotrophic cyst taxa with *Brigantedinium spp.* as the most common species. However, its relative abundance fell by almost half in the sediment cyst association. Consequently, other species increased their relative abundance, particularly phototrophic cyst taxa whose relative abundance doubled in the down-core record. Our preliminary results indicated that certain alterations occurred in the cyst association after being deposited in the bottom sediment. Further investigation of the core features (e.g., oxygen concentration and bioturbation) will be applied to identify the cause of this alteration.

### ***20th International Conference on Harmful Algae***

#### **Time series analysis of the cyst production of toxic dinoflagellates in the Cape Blanc upwelling region, NW Africa between 2003 and 2020**

Surya Eldo V. Roza, Runat Reuter, Gerard J. M. Versteegh, and Karin A. F. Zonneveld

The pressure of the recent climate change on marine ecosystems affects the bloom dynamics of toxic dinoflagellates. Cysts of toxic bloom-forming dinoflagellates can form a seed bank in the sediments. To gain a better knowledge of how climate change might affect the cyst

production of these species, it is essential to have a long and precise record of their cyst production over time. Here, we present an 18 years-record of dinoflagellate cysts export flux in the upwelling region off Cape Blanc, Mauritania collected by a moored sediment trap. In this region that belongs to the world's most productive marine ecosystems, 73 dinocysts taxa were identified of which 3 were potentially produced by toxic species. Cyst production of these species; *Gymnodinium* spp., *Lingulodinium polyedra*, and *Protoceratium reticulatum* occurred relatively continuous throughout the time series. By applying a time series analysis, we gained insight into the periodicity and variation of their export fluxes in the studied time interval that is characterized by rapid global warming. By comparing the cyst export flux with atmospheric and hydrographic changes in the research area, we could obtain insight into the driving factors of cyst production. For instance; irregular peaks of *Gymnodinium* spp. export flux were observed in 2004 and 2007, which coincided with the coldest sea surface summer temperatures of our time series.

### *International Seminar Series on dinophytes*

#### **Unveiling the recent climate change in the Northwest African Coast using time series analysis on dinocyst export production**

Surya Eldo V. Roza, Karin A. F. Zonneveld, Gerard J. M. Versteegh, Vera Pospelova, Runa Reuter, and Jan-Berend Stuut

The anthropogenic carbon contribution and consistent changes in nature have put a huge pressure on the sustainability of all ecosystems, and the ocean is no exception. Investigating high-resolution proxies for environmental reconstruction, such as marine plankton, is crucial to gaining better knowledge about the climate change. Therefore, we deliver a recent record of dinoflagellate cysts (dinocysts) from the coastal upwelling near Cape Blanc (Northwest Africa). Herein, the high plankton production (including dinoflagellates) is accommodated by the annual permanent upwelling and is supported by Saharan dust. Dinocysts were collected by a sediment trap from 2003 until 2020 with a resolution of one to three weeks. This data type is limited, and published studies focus more on the interannual production and ecology of the dinocyst taxa. Under the recent climate change scenario, we want to test the potential of the dinocyst record as a climate proxy. We executed dinocysts record and abiotic factors in this area, such as upwelling wind, dust emission, and sea surface temperature, with wavelet time series analysis to distinguish half-year and annual cycles in each dataset. Moreover, we observed three phases in the upwelling wind and dust emission cycles that also occurred in the dinocyst record. The annual cycle variations suggest a shift in the position of the Inter Tropical Convergence Zone (ITCZ), indicating changes in Northern/Southern hemisphere's temperature.

### *International workshop on dinoflagellate cysts*

#### **Do fossils of dinoflagellate cysts show us the truth?**

Surya Eldo V. Roza, Karin A. F. Zonneveld, Gerard J. M. Versteegh, Vera Pospelova, Runa Reuter, Jan-Berend Stuut, and Hendrik Wolschke

Dinoflagellate cyst is often used for past environment reconstruction, due to its high preservation rate. However, dinoflagellate cysts are still susceptible to post-depositional alterations, challenging its usage as a paleoenvironmental proxy. Therefore, we aim to compare the organic-walled cysts from the



---

upper water column with those embedded in the ocean floor offshore Cape Blanc, Northwest Africa. Sunked cysts between 2003 and 2020 were collected by a sediment trap, and a core was obtained in 2020 at the same location. The core was sliced every 3.11 mm, equal to a resolution of  $1.5 \pm 0.9$  years  $\text{mm}^{-1}$  based on the  $^{210}\text{Pb}$  core dating method. The cyst taxa composition was relatively similar, with a few rare species absent in the core. The heterotrophic taxa remained dominant, with *Brigantedinium* spp. as the most abundant. However, this taxon's mean relative abundance dropped in the core (from 56% to 32%), which was also observed in other heterotrophic taxa. In the core, the heterotroph production trends altered more than the photo-/mixotrophs, particularly at depths under oxic conditions, whilst some taxa (e.g., *P. monospinum* and *P. stellatum*) depicted a significant increase, hinting at a potential allochthonous material. Despite the alteration, the taxa composition change in the sediment trap could still be determined in the core samples, and it occurred around the same year. Our results suggested that the knowledge of the post-depositional effect is also important to enhance the interpretation quality of dinoflagellate cyst fossils.